Analysis of the Barley Cereal Cyst Nematode Resistance Locus *Rha2*

Bart Van Gansbeke

Thesis submitted in fulfilment of the requirements

for the degree of Doctor of Philosophy

School of Agriculture, Food and Wine

Faculty of Sciences

The University of Adelaide

April 2019

Table of contents

Abstract

Cereal cyst nematodes (CCN, *Heterodera avenae*) are obligate soil-borne pathogens of cereal crops such as barley (*Hordeum vulgare*) that can reduce plant vigour and crop yield. Juvenile nematodes infect roots, establish feeding sites in root vascular tissue and become sedentary. Female nematodes mature into egg-filled cysts, which remain in the soil. Production of susceptible cultivars allows the numbers of cysts to increase, increasing the risk of damage to future crops. Some barley cultivars are resistant. Their roots can be infected, but few nematodes mature and form cysts. The focus of this thesis is the resistance conferred by the *Rha2* locus on chromosome 2H of barley.

By undertaking genotyping-by-sequencing of the resistant cultivars Sloop SA and Sloop VIC, their susceptible progenitor Sloop and other material, new DNA sequence polymorphisms were discovered on chromosome 2H. Marker assays were designed for these polymorphisms and assayed on two populations (Clipper/Sahara 3771 and Chebec/Harrrington) in which *Rha2* had been previously mapped. An initial candidate region of 5,077 kbp was defined on the barley genome assembly. In order to obtain new recombinants and develop near-isogenic lines, Sloop SA was backcrossed to Sloop. Over 9,000 BC_2F_2 seeds were genotyped. A detailed genetic map of the candidate region was made by genotyping and phenotyping 64 selected BC_2F_3 families. The candidate region was narrowed to 978 kbp. That region of the genome assembly has 19 predicted genes. Markers in the region were evaluated on a range of barley germplasm and two markers were found to be diagnostic of CCN resistance.

An RNA-seq experiment was conducted with root tissue sampled over a period of 28 days. The samples comprise non-inoculated control plants of the susceptible cultivar Sloop and inoculated plants of Sloop and its resistant derivatives Sloop SA and Sloop VIC. Of the 19 predicted genes in the candidate region, one gene (HORVU2Hr1G097780), which is

annotated as encoding a tonoplast intrinsic protein, exhibited differential expression between the inoculated resistant cultivars and the susceptible cultivar. Further research is required for the functional characterisation of this gene.

Interaction between cereal cyst nematodes and barley roots was also investigated by using laser ablation tomography to scan infected segments. On average, feeding sites in the roots of susceptible plants were smaller than those in the roots of resistant plants. The feeding sites in the roots of susceptible plants were surrounded by multiple dense layers of small cells. In contrast, the feeding sites in the roots of resistant plants were surrounded by layers of larger cells.

This work presents a detailed genetic map of the *Rha2* region of chromosome 2H, including two markers that appear to be diagnostic of resistance, the results of a transcriptomic experiment to explore differentially regulated genes, including candidate resistance genes. Laser ablation tomography was conducted on infected root tissue. Feeding site structure differed between a susceptible cultivar and its resistant derivative, including a smaller volume for the latter. The outcomes of this thesis research may lead to identification of the causal *Rha2* resistance gene against cereal cyst nematode pathotype Ha13.

Thesis declaration

I certify that this work contains no material which has been accepted for the award of any other degree or diploma in my name in any university or other tertiary institution and, to the best of my knowledge and belief, contains no material previously published or written by another person, except where due reference has been made in the text. In addition, I certify that no part of this work will, in the future, be used in a submission in my name for any other degree or diploma in any university or other tertiary institution without the prior approval of the University of Adelaide and where applicable, any partner institution responsible for the joint award of this degree.

The author acknowledges that copyright of published works contained within this thesis resides with the copyright holders of those works.

I give permission for the digital version of my thesis to be made available on the web, via the University's digital research repository, the Library Search and also through web search engines, unless permission has been granted by the University to restrict access for a period of time.

I acknowledge the support I have received for my research through the provision of a Beacon Enlightenment Scholarship by the University of Adelaide.

Bart Van Gansbeke 12/04/2019

Acknowledgments

Thanks to my thesis supervisors Prof. Diane Mather, A/Prof. Kenneth Chalmers, and Dr. Kelvin Khoo for their support from day one. I am grateful for their continued help and feedback throughout my candidature. I am also very appreciative that the supervisors provided me emotional support and kindness when I experienced hardships.

None of this would have been possible without the initial assistance from Dr. Abhishek Dutta, a researcher at the KU Leuven. He always believed in me and pursuit the initial work about almonds and marzipan, leading towards my first publication. He provided me with such incredible guidance in setting the first stone towards my PhD.

This acknowledgement section is too short to thank everyone that I have met during this journey, but special thanks to my Australian friend Nicholas Sitlington Hansen and my French friends Allan Kouidri and Pauline Thomelin. In the past four years, I have met people from over the whole world, including all my close colleagues in the lab and the Plant Genomics Centre, staff members and other PhD students at the Waite campus and people that I have met during my year as president of the student community AgPOGS. Throughout my PhD, I was also a member of the Dutch SA club and the president of Vlamingen In de Wereld; clubs that me bring closer to home. Having so many social activities was a great addition to my life down under.

I owe special thanks to my parents and brother. They always believed in me and encouraged me to proceed. During my PhD, I spent many hours in the glasshouse and the following song by Edith Piaf summarises my PhD experience very well:

Non, rien de rien, non, je ne regrette rien

Ni le bien qu'on m'a fait, ni le mal

Tout ça m'est bien égal

Non, rien de rien, non, je ne regrette rien

C'est payé, balayé, oublié, je me fous du passé

Avec mes souvenirs j'ai allumé le feu

Mes chagrins, mes plaisirs

Je n'ai plus besoin d'eux

Balayé les amours avec leurs trémolos

Balayé pour toujours

Je reparts à zéro

Non, rien de rien, non, je ne regrette rien

Ni le bien qu'on m'a fait, ni le mal

Tout ça m'est bien égal

Non, rien de rien, non, je ne regrette rien

Car ma vie, car mes joies

Aujourd'hui ça commence avec toi

Lastly, "Aujourd'hui ça commence avec toi" (today starts with you) is a reference to my dearly beloved darling, Laurence Cobbaert. She was tremendously supportive in the final year and she was able to support me to the last words of this thesis. Indeed, a new chapter of my life is waiting and I need to let this thesis go. It is a fascinating topic and this research has filled gaps in the knowledge in regards to plant resistance against cereal cyst nematodes.

List of abbreviations

BC	backcross
BC_x-F_y	backcross X of F_y generation
CCN	cereal cyst nematode
cM	centiMorgan
C/H	doubled haploid population Chebec/Harrington
C/S	doubled haploid population Clipper/Sahara 3771
DAMP	damage-associated molecular pattern
DH	doubled haploid
Gb	giga base pairs
GBS	genotyping-by-sequencing
HC	high confidence
JA	jasmonic acid
KASP	Kompetitive allele-specific PCR™
kbp	kilo base pairs
LAT	laser ablation tomography
LC	low confidence
MAPK	mitogen-associated protein kinase
Mbp	mega base pairs
NBS-LRR	nucleotide-binding site leucine-rich repeat
PC	principal component
PCA	principal component analysis
RFLP	restriction fragment length polymorphism
ROS	reactive oxygen species
rlog	regularised-logarithm transformation
SA	salicylic acid

SCAR	sequence characterised amplified region
SHMT	serine hydroxymethyltransferase
SNP	single nucleotide polymorphism
SSR	simple sequence repeat
TIP	tonoplast intrinsic protein
TPM	transcripts per million
qPCR	quantitative real-time polymerase chain reaction
VST	variance stabilising transformation

List of figures

List of tables

List of appendices

Chapter 1 Introduction

Cyst nematodes (*Heterodera* and *Globodera* spp) are soil-borne endoparasites which can cause severe damage to plant roots. The life cycle of cyst nematodes has been thoroughly described by Bohlmann and Sobczak (2014), Lilley et al. (2005), Perry and Moens (2006), and Siddique and Grundler (2015). In short, juvenile cyst nematodes enter roots and migrate through cortical cells. When a nematode reaches the vascular bundle, it begins to feed from an initial feeding cell and it injects effectors into that cell. This results in significant changes to plant biochemical and molecular pathways. The initial cell merges with other plant cells, forming a syncytial feeding site from which the developing nematode extracts nutrients. Female nematodes form white egg-filled cysts that protrude from the root surface. These cysts later darken and harden, forming brown cysts that protect the eggs, also enabling them to persist in the soil.

Cyst nematodes affect many hosts, including potato, soybean, beet and cereals. Cereal cyst nematodes infect barley, oat, wheat and some other grasses. They can cause substantial yield losses. For a long time, the presence of CCN was a major concern in the main cereal growing regions of southern Australia. The CCN population in Australia is generally considered to consist of a single pathotype, which has been classified as the Ha13 pathotype of *Heterodera avenae* (Andersen and Andersen 1982b) but also as a separate species (*H. australis*) within the *Avenae* group of the *Heterodera* genus (Subbotin et al. 2002).

The above-ground symptoms of CCN infection include abnormal yellowing of leaves and reduced growth. Given that CCN has been estimated to be present in almost 75 % of the southern Australian cereal growing areas, annual potential yield loss in barley could be as high as 20 % which would represent a yearly loss of 148 million AUD (Murray and Brennan 2010). Fortunately, current control methods relying on crop rotation and the use of resistant cultivars are highly effective in Australia. Effective control involves reduction of the nematode population density in the soil. Growers can diminish CCN populations the

following season by alternating between host crops (the cereals) and non-host crops, such as legumes (Andersson 1982; Meagher 1982; Rovira and Simon 1982). In seasons when host plants are not present, nematodes still hatch in the soil but fail to find a suitable host. Early sowing of cereals can also contribute to CCN control, with plants developing good root systems before soil conditions become optimal for nematode infection (Andersson 1982; Meagher 1982). Nematicides were once widely applied in southern Australia (reviewed by Brown (1984)) to kill infective larvae, but are no longer used because of the high cost and awareness of environmental and human health dangers, such as a potential link to increased occurrence of cancers (Kim et al. 2017). The use of cereal varieties with resistance contributes to effective control (Andersen and Andersen 1982a; Andersson 1982; Brown 1982; Cook 1982). Consistent use of resistant cereal cultivars was demonstrated to reduce the numbers of nematodes in the soil (Brown 1982; Cook and York 1982), and widespread deployment of resistant cereal cultivars reduced CCN below detectable levels within Australian cereal growing areas (Riley and McKay 2009). Reliable detection methods for the occurrence and quantification of CCN in the soil were developed to enable ongoing monitoring for CCN (Ophel-Keller et al. 2008).

In Australia, cereal breeding for CCN resistance has delivered good results. The development and adoption of resistant cereal cultivars has substantially reduced CCN populations in agricultural soils. In barley, two resistance loci have been found to confer resistance against the Ha13 pathotype: *Rha2* on chromosome 2H and *Rha4* on chromosome 5H.

Prior to the research reported in this thesis, the *Rha2* locus had been mapped on chromosome 2H relative to RFLP markers (Kretschmer et al. 1997), but not fine mapped using current marker technologies. The causal gene had not been identified and there had been no investigations of differential gene expression between resistant and susceptible plants.

Infected root regions had been examined with microscopy, providing two-dimensional images of nematode feeding sites within roots (Aditya et al. 2015; Seah et al. 2000) but there had been little investigation of the three-dimensional structure of CCN feeding sites.

The main objectives of the research conducted for this thesis were: 1) to fine map the CCN resistance locus *Rha2*; 2) to identify and develop diagnostic molecular markers for use in barley breeding; 3) to identify differentially expressed genes between susceptible and resistant cultivars; 4) to visualise feeding sites with a high-throughput scanning method.

The thesis consists of six chapters:

Chapter 1 (Introduction): A general background to the research topic, introducing the parasite (cereal cyst nematode) and its host (barley), and stating research objectives.

Chapter 2 (Literature review): A comprehensive literature review to present background information for the research.

Chapter 3 (Fine mapping of *Rha2* in barley reveals candidate genes for resistance against cereal cyst nematode): This chapter was published in Theoretical and Applied Genetics on the 18th of January 2019. This manuscript reports on the fine mapping of the *Rha2* locus on the 2H chromosome to a 978 kbp candidate region, development of diagnostic molecular markers and discusses three potential resistance candidate genes. The thesis chapter is the same as the published paper, except for minor changes have been made to provide consistent format throughout the thesis. These changes include renumbering of tables and figures, placement of the supplementary materials into thesis appendices and consolidation of references into a single list at the end of the thesis.

Chapter 4 (Transcriptomic responses to cereal cyst nematode infection of susceptible and resistant barley cultivars): This chapter presents results from an exploratory transcriptomic analysis of genes that are differentially expressed between inoculated susceptible plants and non-inoculated controls, and between inoculated susceptible and resistant cultivars. Particular attention is paid to genes that are located in the candidate region defined in Chapter 3, and qPCR results are presented for one of those genes.

Chapter 5 (Use of laser ablation tomography to compare the roots of susceptible and resistant barley cultivars after infection with cereal cyst nematode): This chapter presents results from the use of laser ablation tomography to examine whole root segments which include CCN feeding sites in susceptible and resistant barley cultivars.

Chapter 6 (General conclusion): A conclusion of the significance of the research reported in this thesis, with suggestions for improvements and future research directions.

This thesis includes 17 appendices. A full list of the appendices is included at the beginning thesis, on page 17.

Chapter 2 Literature review

2.1 Life cycle of cyst nematodes

Cyst nematodes are plant parasites that feed from the roots of many crops, including potato, maize, rice, sugar beet, soybean, forage grasses, wheat, oat and barley. Regardless of their host specificity, cyst nematodes have similar life cycles (Heinrich et al. 1998; Jones 1981; Lilley et al. 2005; Perry and Moens 2006; Siddique and Grundler 2015; Sobczak et al. 2011; Toumi et al. 2018).

The eggs of cyst nematodes are enclosed in lemon-shaped cysts, which protect the eggs from extreme environmental conditions such as drought, heat or frost. Dormant eggs inside the cysts may be in a diapause stage (unable to hatch regardless of environmental conditions) or a quiescent stage (able to hatch under favourable conditions). In Australia, these favourable conditions include decreasing temperature, increasing soil moisture and exposure to root exudates (Ellenby and Perry 1976). The hatching process in cyst nematodes has been extensively reviewed by Perry (2002). Inside the cyst, the water permeability of the egg changes and the larvae (stage 1 or J1 juvenile) moult within the quiescent dormant eggs to the infective J2 stage (Ellenby and Perry 1976). The J2 nematodes leave the cyst and migrate to host plant roots. They penetrate roots in the elongation zone using their stylets to break cell walls. They also secrete cell wall degrading enzymes to facilitate this process. Transcripts for carbohydrate active enzymes have been detected in transcriptomes of J2 *H. avenae* and other cyst nematodes (Fosu-Nyarko et al. 2016; Kumar et al. 2014; Rai et al. 2015; Yang et al. 2017). Other cell wall degrading enzymes such as β-1,4-endoglucanases have been detected from both the potato cyst nematode *Globodera rostochiensis* and the soybean cyst nematode *Heterodera glycines* (Smant et al. 1998). A pectate lyase has been reported from *G. rostochiensis* (Popeijus et al. 2000). For *H. avenae*, there is transcriptomic evidence for the expression of both β-1,4-endoglucanase and pectate lyase genes (Kumar et al. 2014; Zheng et al. 2015).

The larvae select initial feeding cells and secrete effectors into those cells, subsequently forming feeding plugs in the cell walls of feeding cells (Golinowski et al. 1999). The larvae pierce through these feeding plugs with their stylets, invaginating the plasmalemma (Golinowski et al. 1999; Jones and Dropkin 1975). While the stylet is in the cytoplasm, nematode secretions form a feeding tube through the feeding plug (Golinowski et al. 1999; Nvyss et al. 1984; Wyss and Grundler 1992). Once an initial feeding cell is established, the nematode injects further effectors and complex interactions appear to occur between the nematode and the plant cell to enlarge the initial feeding cell (Wyss and Grundler 1992). The results of transcriptomic experiments have indicated that juvenile cyst nematodes facilitate parasitism by expressing and secreting effector proteins such as defense suppressors, cell wall degrading enzymes, CLAVATA3(CLV3)/endosperm surrounding region-related effector genes, expansins, calreticulin, and fatty-acid and retinol-binding proteins (Chronis et al. 2013; Cotton et al. 2014; Kumar et al. 2014; Moffett et al. 2015; Yang et al. 2017; Zheng et al. 2015).

Larvae inject effectors that induce partial degradation of plant cell walls, providing access to nutrients beyond what can be provided by the one plant cell (Wyss and Zunke 1986). The individual initial feeding cell is modified into a multinucleate syncytium. In Arabidopsis, Hewezi et al. (2008) demonstrated a direct link between the release of cyst nematode proteins in the syncytium, a cellulose binding protein, and interaction with a pectin methylesterase protein that helps the nematode to establish the feeding site via dissolution of plant cell walls.

The reproductive biology of cyst nematodes has been thoroughly described in several review articles (Lilley et al. 2005; Perry et al. 2018; Siddique and Grundler 2018). During the expansion of the feeding site, the larva develops further and its gender is determined. Male juveniles grow until their reproductive organs are developed. They then enter the J4 stage, disconnect from their feeding sites, regain motility and leave the roots. In contrast, female

juveniles stay connected to the syncytia in the vascular cylinder. Their posterior ends expand through the cortex and protrude from the root. Adult males are attracted and mating occurs. Fertilised eggs are retained within the bodies of adult female nematodes, which become white cysts protruding from the root. When the female nematodes die, they morph into brown cysts. The eggs within these cysts are protected by the cuticle.

2.2 Classification of CCN species and pathotypes

Cereal cyst nematodes belong to the genus *Heterodera* Schmidt, which has been further subdivided into *H. latipons*, *H. hordecalis* and a *H. avenae* complex with multiple species. Within the *H. avenae* complex, it is difficult to distinguish among species based on the morphology of nematodes and cysts. Up to 10 species have been proposed based on examination of sequence variation for an internal transcribed spacer rDNA sequence and the mitochondrial cytochrome c oxidase I gene (Fu et al. 2011; Subbotin et al. 2002, 2003, 2018). Subbotin et al. (2002) proposed that the cereal cyst nematode encountered in Australia be classified as *H. australis*, but this has not been universally accepted (Riley and McKay 2009; Smiley et al. 2017; Vanstone et al. 2008). This is partly due to the lack of type cultures for this proposed species.

Another way of classifying nematode populations is to expose them to differential panels of host plant lines. The exposure to panels allows for the classification of nematodes into pathotypes based on differential reactions. An International Cereal Cyst Nematode Test Assortment panel was initially proposed by Andersen and Andersen (1982b). Based on reviews of available data, cereal cyst nematodes in Australia have been classified as pathotype 13 (Ha13) (Andersen and Andersen 1982b; Cook and Noel 2002; Cook and Rivoal 1998; Cui et al. 2015; Rivoal and Cook 1993; Smiley et al. 2011). According to Andersen and Andersen (1982b) and Cui et al. (2015), the barley lines Morocco, Martin 403-2 and Marocaine C.I.8341 (probably a descendant of Morocco) are resistant against Ha13.

There are disagreements regarding the origin of CCN in Australia. CCN may have been introduced by early European settlers, along with livestock transported from Spain (Lewis et al. 2009). An alternative hypothesis was elaborated by Subbotin et al. (2018). Given the molecular similarity with some cereal cyst nematode populations in China, they argued that CCN may have originated from China (Subbotin et al. 2018).[1]

2.3 Interaction of cyst nematodes with the roots of host plants

The host plant interaction with cyst nematodes has been described for several pathosystems (e.g. Hofmann and Grundler (2007), Lilley et al. (2005) and Siddique and Grundler (2018)). Growing roots produce exudates, some of which are detected by nematode chemoreception organs (Curtis 2008; Fioretti et al. 2002). Specifically, plant ethylene production plays a role in the chemotaxis of cyst nematodes. Enhanced production of ethylene or ethylene concentration in the roots increased the attraction of *H. schachtii* towards Arabidopsis roots (Kammerhofer et al. 2015; Wubben et al. 2001). In contrast, ethylene has been reported to inhibit attraction of *H. glycines* towards Arabidopsis roots (Hu et al. 2017). However, it is not known whether ethylene plays a role in the attraction of *H. avenae* to barley roots. Once inside the roots, cyst nematodes leave a path of destruction in the cortex by mechanically damaging cells (Andres et al. 2001; Grymaszewska and Golinowski 1987). Damage to cortical cells has sometimes been observed as cell necrosis (Grymaszewska and Golinowski 1987). Plant cells have the capacity to recognise local damage with receptors of damage-associated molecular patterns (DAMPs), which activates their plant defense mechanisms (Chen et al. 2017). This defense mechanism triggered by DAMPs starts a cascade of responses along defense-related pathways such as those involving reactive oxygen species

[1] As far as I am aware, the nematodes used for this thesis research are the same as accessions from Australia that have previously been classified as *H. avenae* pathotype 13 and/or *H. australis*. In this thesis, they will be referred to as *H. avenae*

(ROS), jasmonic acid (JA) and salicylic acid (SA) signalling, and mitogen-associated protein kinase (MAPK) signalling (reviewed by Choi and Klessig (2016)).

The nematodes move along the vascular bundle in the root cortex. The nematode becomes sedentary once it has selected an individual cell of the vascular bundle as an initial feeding cell. This process significantly affects plant root morphology. Cell walls of adjacent cells start to degrade (Grundler et al. 1998; Williams and Fisher 1993). Those cells merge with the initial feeding cell to become a multinucleate syncytium. The change of the normal function into a feeding cell is associated with a change in a range of molecular functions and enzymes. Based on transcriptomic analysis, some of the enzymes have been identified as enzymes of the lipoxygenase family, enzymes with molecular functions such as cell wall degrading and heme binding proteins, and enzymes with ammonia-lyase binding and oxidoreductase activity (Hosseini and Matthews 2014; Ithal et al. 2007a, b; Kong et al. 2015; Zheng et al. 2015). The feeding site, which is the only nutrient source of the nematode, acts as a transfer cell (Jones and Northcote 1972; Jones and Dropkin 1975). The drawing out for nutrients creates flow streams in the cytoplasm and possible pressure on the cell walls around the feeding tube. Callose deposition may strengthen the connection between the nematode and the feeding site (Williams and Fisher 1993).

Further development of the feeding site includes merging of additional adjacent cells. Syncytia can appear to be very active, with hypertrophied nuclei and dense cytoplasm (Aditya et al. 2015; Endo 1965, 1991; Grymaszewska and Golinowski 1987, 1991; Seah et al. 2000; Williams and Fisher 1993). The formation and maintenance of syncytia causes an upregulation of pathways related to plant defense (Chen et al. 2017; Goverse and Smant 2014; Sobczak et al. 2005; Wan et al. 2015). The establishment and maintenance of a feeding site is crucial for completion of the nematode's life cycle. The maintenance and expansion in the feeding site are regulated by plant pathways mainly affect catabolic processes such as

carbohydrate metabolism, energy metabolism, nucleotide metabolism, and amino acid metabolism (Hosseini and Matthews 2014; Kang et al. 2018; Kong et al. 2015; Zheng et al. 2015). For example, specific metabolic pathways have been found to be differentially expressed between inoculated and non-inoculated roots during the development of a feeding site in a susceptible soybean cultivar (Kang et al. 2018). These included pathways related to the metabolism of vitamin B6, taurine, hypotaurine and seleno compounds. Therefore, these pathways might be essential for the continued development of the feeding site.

Syncytia have been reported to contain many vacuoles filled with amorphous material (Aditya et al. 2015; Jones and Northcote 1972). However, the content of these organelles remains unknown. Metabolic pathways related to cell organelles and vacuoles have been reported to be enhanced during interaction with cereal cyst nematodes (Xu et al. 2012).

The syncytia induced by cyst nematodes are much larger than surrounding cells and need support to resist high turgor pressure (Böckenhoff and Grundler 2009). The usage of monoclonal antibodies showed that cell walls of syncytia in infected wheat consist predominantly of highly substituted heteroxylans (Zhang et al. 2017). Similarly, cell walls of barley feeding sites contained β-linked-glucose polymers, with significant differences in (1,3;1,4)-β-glucan between barley cultivars (Aditya et al. 2015). In soybean, it has been shown that remnants of cell walls within syncytia form “pillars” or “columns” that provide structural support (Andres et al. 2001; Ohtsu et al. 2017).

2.4 Host plant resistance

In plant-nematode pathosystems, host resistance impedes the reproduction of the nematode. For cereal cyst nematodes, attraction to roots, invasion of roots, and migration through the root cortex occurs regardless of the resistance status of the host cereal plant itself (Cui et al. 2017; Soetopo 1986; Williams and Fisher 1993). Differences between resistant and

susceptible plants only become evident during the sedentary stage. Contrary to the small vacuoles observed in the syncytia of susceptible plants, enlarged vacuoles have been observed within the syncytia of resistant wheat (Williams and Fisher 1993) and barley (Aditya et al. 2015; Seah et al. 2000) cultivars. The enlarged vacuoles occupy a large proportion of the syncytia, pressing cytoplasm and other cellular components against the inner side of cell walls (Aditya et al. 2015; Seah et al. 2000; Williams and Fisher 1993).

A recent study has investigated differences in transcriptional responses between resistant and susceptible wheat cultivars (Chen et al. 2017). In the roots of susceptible plants, differential expression was detected for many genes in the following domains: biological process, cellular component, and molecular function. The phenolpropanoid/phenylpropanoid pathway was differentially expressed, leading to increased biosynthesis of lignin and other secondary metabolites (Klink et al. 2009, 2010; Kong et al. 2015; Wan et al. 2015). Parts of this specific pathway were more upregulated in the roots of resistant plants than in the roots of susceptible plants, potentially leading to lignification of cell walls in resistant plants (Chen et al. 2017). Lignification is a primary defense mechanism in response to various biotic and abiotic stresses (Moura et al. 2010). In wheat plants with *Cre2* CCN resistance, increases in peroxidase enzymatic activity and lignification were observed (Andres et al. 2001). Peroxidase activity is part of the ROS activity, potentially leading to an increase in lignification of the cell walls (as reviewed by Barros et al. (2015)). Extra lignin makes cell walls stiff and non-permeable (Francoz et al. 2015). Therefore, increased cell wall lignin might contribute to sealing off the feeding site. As has been observed for abiotic stress responses, lignin deposition may lead to avoidance of symplastic transport (Le Gall et al. 2015).

In plant-nematode interactions, plant defense enzymes such as serine protease inhibitors and disease resistance proteins have often been indicated as significant elicitors in plant immune

responses that lead towards the activation of auxin and jasmonic acid pathways (Klink et al. 2010; Kong et al. 2015; Mazarei et al. 2011; Sobczak et al. 2005; Uehara et al. 2010).

Thus far, no causal genes for cyst nematode resistance have been isolated from monocots. Cyst nematode resistance genes have, however, been isolated from sugar beet, soybean, tomato and potato. The sugar beet gene $Hs1^{pro-1}$ confers resistance against *H. schachtii* (Cai et al. 1997). The $Hs1^{pro-1}$ gene is expressed in response to nematode contact and feeding site expansion (Thurau et al. 2003), possibly affecting WRKY transcription factors and eliciting a defense response (Murray et al. 2007). In potato, *Gro1-4* and *Gpa2* confer resistance against the potato cyst nematode. Both are members of the nucleotide binding leucine-rich repeat resistance class which elicits plant cell death (Paal et al. 2004; van der Vossen et al. 2000). In soybean, four genes related to the resistance against soybean cyst nematode have been isolated, three at the *Rhg1* locus and one at the *Rhg4* locus. *Rhg1* resistance is conferred by copy number variation that increases the expression of three genes. These three genes encode respectively an amino acid transporter, an α-SNAP protein and a wound-inducible protein (Cook et al. 2012). *Rhg4* encodes a serine hydroxymethyltransferase (SHMT) (Liu et al. 2012) which is non-functional in susceptible varieties. SHMT enzymes are present in different parts of the plant cell such as mitochondria, plastid, and cytosol (Hanson et al. 1995; Herbig et al. 2002; Naydenov et al. 2012; Wei et al. 2013; Zhang et al. 2010). The exploration of the phylogenetic relationship between *Rhg4* and Arabidopsis SHM1 might indicate that the SHMT enzyme is present and active in the cytosol (Wu et al. 2016). The SHMT enzyme in the cytoplasm cleaves the hydroxymethyl group of a serine amino acid (Mouillon et al. 1999).

Although no causal genes for nematode resistance have been cloned in wheat or barley, there has been extensive genetic mapping in these crops. For wheat, at least nine CCN resistance loci have been mapped, including some for which the resistance alleles were introgressed from other grass species (Delibes et al. 1993; Eastwood et al. 1994; Jahier et al. 1996, 2001;

Jayatilake et al. 2015; Ogbonnaya et al. 2001; Slootmaker et al. 1974; Taylor et al. 1998; Williams et al. 1994, 2003, 2006).

In barley, four loci have been reported for resistance against CCN: *Rha1*, *Rha2*, *Rha3,* and *Rha4* (Andersen and Andersen 1968; Andersen and Andersen 1973; Barr et al. 1998; Cotten and Hayes 1969; Kretschmer et al. 1997). Of these, *Rha2* and *Rha4* are known to be effective against the Ha13 pathotype of *H. avenae*.

The resistance locus *Rha2* was first mapped on chromosome 2H by Cotten and Hayes (1969). Kretschmer et al. (1997) constructed restriction fragment length polymorphism (RFLP) linkage maps for the barley populations Chebec/Harrington and Clipper/Sahara 3771, both of which segregate for *Rha2*. The *Rha2* locus was positioned between 6.1 and 4.0 centiMorgans (cM) distal to the RFLP marker awbma21 (Kretschmer et al. 1997).

The focus of the research conducted for this thesis is mainly on materials that derived their CCN resistance from Chebec or Sahara 3771. Chebec was used as a parent in the development of the CCN-resistant varieties Sloop SA (Chebec/3*Sloop) and Sloop VIC (Sahara 3771/WI2723//Chebec/2*Sloop). Given that Sloop is susceptible, Sloop SA must have inherited its resistance from Chebec, but Sloop VIC could have inherited its resistance from either Sahara 3771, Chebec or WI2723 (a Chebec derivate).

During the course of this research, a reference assembly became available for the barley genome (Mascher et al. 2017), making it possible to anchor the *Rha2* region of chromosome 2H to the 2H pseudomolecule. The available sequence represents 95 % of the entire barley genome with 4.54 Gb out of 4.79 Gb assigned to chromosomal locations. Predicted genes have been annotated on the genome assembly and information is known about the expression profiles of those genes (Colmsee et al. 2015). Currently, no studies have been undertaken to

investigate transcriptomic differences between susceptible and resistant barley cultivars after infection by cereal cyst nematode.

2.5 Research gaps

The main aim of this study was to gain a better understanding of the *Rha2* resistance mechanism in barley against the cereal cyst nematode *H. avenae* Ha13. Based on evaluation of knowledge gaps in the literature reviewed here, the following research objectives were established:

- To define and refine the *Rha2* candidate region with recombinant individuals that leads to the identification of a list of candidate genes possibly conferring *Rha2* resistance.
- To identify genes and/or pathways which are differentially expressed between inoculated and non-inoculated plants, between inoculated susceptible and resistant cultivars, and particularly to investigate whether candidate genes are differentially expressed in response to nematode infection.
- To visualise feeding sites in resistant and susceptible cultivars to provide a spatial understanding of plant-nematode interactions.

Chapter 3 Fine mapping of *Rha2* in barley reveals candidate genes for resistance against cereal cyst nematode

Statement of authorship

Statement of Authorship

Title of Paper	Fine mapping of *Rha2* in barley reveals candidate genes for resistance against cereal cyst nematode
Publication Status	☑ Published ☐ Accepted for Publication ☐ Submitted for Publication ☐ Unpublished and Unsubmitted w ork w ritten in manuscript style
Publication Details	Van Gansbeke, B., Khoo, K. H. P., Lewis, J. G., Chalmers, K. J., & Mather, D. E. (2019). Fine mapping of *Rha2* in barley reveals candidate genes for resistance against cereal cyst nematode. Theoretical and Applied Genetics.

Principal Author

Name of Principal Author (Candidate)	Bart VAN GANSBEKE		
Contribution to the Paper	Developed plant materials, conducted phenotyping, designed markers, conducted genotyping, analysed data and wrote manuscript.		
Overall percentage (%)	65		
Certification:	This paper reports on original research I conducted during the period of my Higher Degree by Research candidature and is not subject to any obligations or contractual agreements with a third party that would constrain its inclusion in this thesis. I am the primary author of this paper.		
Signature		Date	5/4/2019

Co-Author Contributions

By signing the Statement of Authorship, each author certifies that:

i. the candidate's stated contribution to the publication is accurate (as detailed above);
ii. permission is granted for the candidate in include the publication in the thesis; and
iii. the sum of all co-author contributions is equal to 100% less the candidate's stated contribution.

Name of Co-Author	Kelvin H. P. KHOO		
Contribution to the Paper	Designed the GBS experiment, contributed to design markers, the analysis and interpretation of the results. Read the manuscript and suggested revisions.		
Signature		Date	3/4/2019

Name of Co-Author	John G. LEWIS		
Contribution to the Paper	Maintained nematode cultures and conducted phenotyping. Read the manuscript and suggested revisions.		
Signature		Date	3/4/2019

Name of Co-Author	Kenneth J. CHALMERS
Contribution to the Paper	Designed the GBS experiment, contributed to analysis and interpretation of the results. Read the manuscript and suggested revisions.
Signature	Date 3/4/19

Name of Co-Author	Diane E. MATHER
Contribution to the Paper	Provided overall supervision of the research. Contributed to analysis and interpretation of the results. Supervised the revision of the manuscript.
Signature	Date 5/04/2019

Title

Fine mapping of *Rha2* in barley reveals candidate genes for resistance against cereal cyst nematode

Bart Van Gansbeke[1], Kelvin H.P. Khoo[1], John G. Lewis[2], Kenneth J. Chalmers[1] and Diane E. Mather[1]

[1]School of Agriculture, Food and Wine, Waite Research Institute, The University of Adelaide, PMB 1, Glen Osmond, SA 5064, Australia

[2]South Australian Research and Development Institute, GPO Box 397, Adelaide, SA 5001, Australia

Corresponding author: Diane E. Mather, diane.mather@adelaide.edu.au, +61 8 8313 7156

ORCID IDs:

0000-0001-5627-0227 (BVG)

0000-0002-7405-8518 (KHPK)

0000-0001-5838-0235 (JGL)

0000-0002-9687-8680 (KJC)

0000-0001-7506-2589 (DEM)

Author contribution statement

KHPK, KJC and DEM designed the GBS experiment. BVG developed plant materials. JGL maintained nematode cultures. BVG, KHPK and JGL conducted phenotyping. BVG and KHPK designed markers, conducted genotyping, and analysed data. BVG and DEM wrote the manuscript. All authors contributed to the interpretation of the results and to the revision of the manuscript.

Acknowledgements

The research was conducted with financial support from the Grains Research and Development Corporation (Projects UA000127, UA00143 and UA00157). We thank David Moody, Stewart Coventry, Amanda Box, Jason Eglinton, and Andrew Barr for information, encouragement and advice and Elysia Vassos, Rebecca Fox and Allan Binney for technical advice and assistance.

Conflict of interest statement

On behalf of all authors, the corresponding author states that there is no conflict of interest.

Keywords

Heterodera avenae, *Hordeum vulgare*, *Rha2*, plant defense, KASP assays

Key message

The cereal cyst nematode resistance locus *Rha2* was mapped to a 978 kbp region on the long arm of barley chromosome 2H. Three candidate genes are discussed.

3.1 Abstract

The cereal cyst nematode (CCN) *Heterodera avenae* is a soil-borne obligate parasite that can cause severe damage to cereals. This research involved fine mapping of *Rha2*, a CCN resistance locus on chromosome 2H of barley. *Rha2* was previously mapped relative to restriction fragment length polymorphisms (RFLPs) in two mapping populations. Anchoring of flanking RFLP clone sequences to the barley genome assembly defined an interval of 5,077 kbp. Genotyping-by-sequencing of resistant and susceptible materials led to the discovery of potentially useful single nucleotide polymorphisms (SNPs). Assays were designed for these SNPs and applied to mapping populations. This narrowed the region of interest to 3,966 kbp. Further fine mapping was pursued by crossing and backcrossing the resistant cultivar Sloop SA to its susceptible ancestor Sloop. Evaluation of F_2 progeny confirmed that the resistance segregates as a single dominant gene. Genotyping of 9,003 BC_2F_2 progeny identified recombinants. Evaluation of recombinant BC_2F_3 progeny narrowed the region of interest to 978 kbp. Two of the SNPs within this region proved to be diagnostic of CCN resistance across a wide range of barley germplasm. Fluorescence-based and gel-based assays were developed for these SNPs for use in marker-assisted selection. Within the candidate region of the reference genome, there are nine high-confidence predicted genes. Three of these, one that encodes RAR1 (a cysteine- and histidine-rich domain-containing protein), one that is predicted to encode an acetylglutamate kinase and one that is predicted to encode a tonoplast intrinsic protein, are discussed as candidate genes for CCN resistance.

3.2 Introduction

The cereal cyst nematode (CCN) *Heterodera avenae* is a soil-borne parasite that infects the roots of many grass species and can cause significant yield losses in cereal crops including barley (*Hordeum vulgare* L.), wheat (*Triticum aestivum* L.) and oat (*Avena sativa* L.). Like other cyst nematodes, it is a sedentary endoparasite. Motile J2-stage larvae enter the elongation zones of roots and migrate intracellularly through the root cortex. Upon reaching the vascular cylinder, they establish feeding sites. Initially each feeding site consists of a single plant cell, but the nematode induces the dissolution of cell walls and adjacent cells are 'recruited', resulting in the formation of a multinuclear syncytium. Once the nematodes differentiate into males and females, the males detach from their feeding sites and leave the roots. The females remain within the root, growing and maturing, until their bodies become egg-filled white cysts that protrude from the roots and finally hard brown cysts within which the eggs can withstand unfavourable conditions in the soil.

Within host plant species that are affected by cyst nematodes, there is genetic variation for resistance (the ability to reduce nematode populations in the soil). Genes for resistance against cyst nematodes have been isolated from dicot species (Cai et al. 1997; Liu et al. 2012, 2017; Paal et al. 2004; van der Vossen et al. 2000), but not from any monocot species. In barley (reviewed below) and in wheat (reviewed by Jayatilake et al. (2015)), resistance loci have been genetically mapped and resistance alleles have been used in cereal breeding. In Australia, where there is thought to be only one pathotype (Ha13) of *H. avenae,* consistent use of resistant cereal cultivars and cultural management practices has been very effective in reducing nematode populations in agricultural soils and preventing yield losses (Murray and Brennan 2010).

In barley, the inheritance of CCN resistance was first investigated by Nilsson-Ehle (1920), who reported results indicating segregation of a single unit of inheritance, for which

resistance was dominant. Subsequent research established that there are up to three CCN resistance loci on chromosome 2H (Andersen and Andersen 1968; Andersen and Andersen 1973; Cotten and Hayes 1969; Kretschmer et al. 1997). Of these, two (originally called *Ha2* and *Ha3* but now called *Rha2* and *Rha3*) are very closely linked with each other (or may even be the same locus). The other locus, *Rha1* (formerly *Ha* or *Ha1*) is not closely linked with *Rha2* and *Rha3.* There is also a CCN resistance locus (*Ha4*, now *Rha4*) on chromosome 5H (Barr et al. 1998).

The research reported here focuses on a locus that Kretschmer et al. (1997) mapped relative to molecular markers using two populations of doubled haploid (DH) barley lines: one derived from a cross between Chebec (a resistant cultivar that inherited its resistance from the Algerian cultivar Orge Martin) and Harrington (a susceptible cultivar) and one derived from a cross between Sahara 3771 (a resistant North African landrace) and Clipper (a susceptible cultivar). When these materials were inoculated with juvenile nematodes of the Ha13 pathotype of *H. avenae,* most individual lines could be unambiguously classified as resistant or susceptible. In each population, a resistance locus was mapped on the long arm of chromosome 2H, in the interval between the restriction fragment length polymorphism (RFLP) markers awbma21 and mwg694. Kretschmer et al. (1997) considered this locus to be the same as the one that confers resistance in *Hordeum pallidum* var. 191 and called it '*Ha 2'*. Here, we refer to it as *Rha2*. Using marker-assisted selection, breeding programs in Australia developed two CCN-resistant derivatives of the CCN-susceptible malting barley cultivar Sloop: Sloop SA (Chebec/3*Sloop) and Sloop VIC (Sahara 3771/WI2723//Chebec///2*Sloop) (Andrew Barr and David Moody, personal communication). Simple sequence repeat (SSR) markers were added to genetic maps (Barr et al. 2003; Karakousis et al. 2003; Williams et al. 2006). While some of these markers were used for selection, they were not entirely diagnostic of resistance. To overcome some of the limitations of RFLP and SSR markers for use in marker-assisted selection, Dayteg et al. (2008) developed a co-dominant sequence

characterised amplified region (SCAR) marker, Ha2S18. Using a population derived from a cross between the cultivars SW Buddy and SW Cecilia, they mapped this marker on chromosome 2H and reported it to be 4.3 cM distal to *Ha2*.

With the availability of a reference assembly of the barley genome (Mascher et al. 2017), many markers that are associated with known sequences can now be anchored to specific physical positions on pseudomolecule sequences. Further, with current technologies for DNA sequencing and marker genotyping, new DNA polymorphisms can be readily discovered and mapped. In the research reported here, *Rha2*-linked markers were anchored to the 2H pseudomolecule sequence, genotyping-by-sequencing (GBS) was applied to discover informative single nucleotide polymorphisms (SNPs) and Kompetitive Allele Specific PCR™ (KASP) technology was used for fine mapping.

3.3 Materials and methods

3.3.1 Barley materials

The plant materials used here included two populations of doubled haploid lines (Chebec/Harrington (C/H) and Clipper/Sahara 3771 (C/S)), their parents (Chebec, Harrington, Clipper and Sahara 3771), the susceptible cultivar Schooner, accessions of 17 barley lines that had previously been used to discriminate among pathotypes of *H. avenae* (Appendix 1) (Andersen and Andersen 1982b; Kort et al. 1964; O'Brien and Fisher 1977, 1979; Smiley et al. 2011) and 175 other cultivars of barley (Appendix 2). The C/H and C/S populations were the same as those used by Kretschmer et al. (1997).

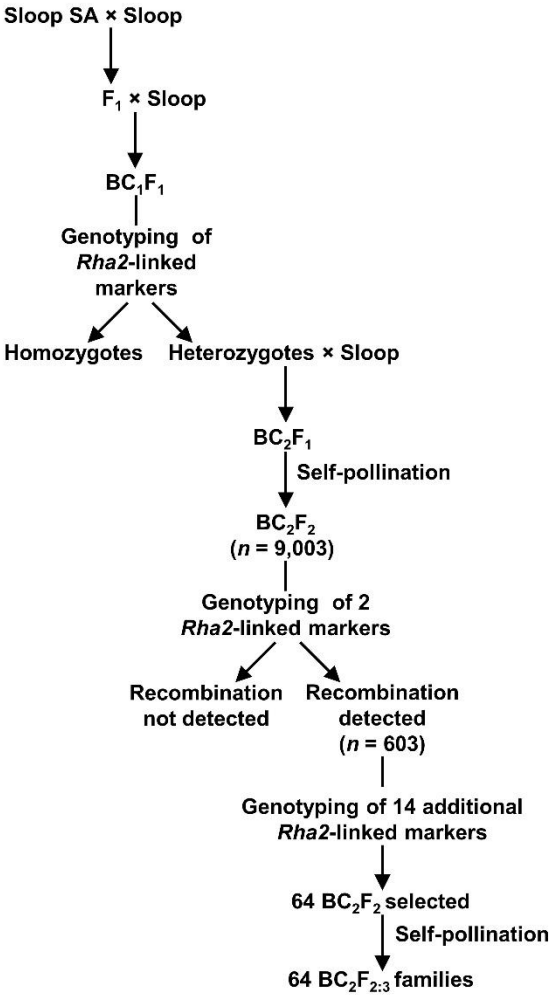

Figure 3-1: Marker-assisted backcrossing scheme used to generate $BC_2F_{2:3}$ families segregating for recombinant haplotypes in the *Rha2* region of chromosome 2H

To develop additional materials for this research, Sloop SA was crossed with Sloop, F_1 plants were grown and allowed to self-pollinate and F_2 seeds were harvested at maturity. Some Sloop SA/Sloop F_1 plants were backcrossed to Sloop, providing BC_1F_1 progeny (Figure 3-1). Selected BC_1F_1 progeny were backcrossed to Sloop, providing BC_2F_1 progeny. These plants were grown to maturity, providing 9,003 BC_2F_2 seeds.

3.3.2 Methods for evaluation of resistance against cereal cyst nematode

Two methods were used to evaluate the resistance of barley plants against CCN: 'tube tests' and 'pots tests' (Lewis et al. 2009) (Appendix 3 and Appendix 4). For tube tests (Fisher 1982; O'Brien and Fisher 1977), opaque plastic tubes (2.5 cm internal diameter and 13 cm deep) were filled with pre-sterilised sandy loam soil and set upright in a base of potting mixture. One pre-germinated seed was sown in each tube and the tubes were transferred to a controlled environment room that was maintained at a constant temperature of 15 °C with a 12 h light/dark cycle. At 1, 4, 7, 11 and 14 d after sowing, 1 mL of inoculum (a suspension of 100 J2-stage *H. avenae* larvae per mL water) was pipetted onto the soil surface around each seedling. At 70 d after the final inoculation, the soil was washed off the roots and white *H. avenae* females (white cysts) were counted. For pots tests (Lewis et al. 2009), pots (5 cm in diameter and 10 cm deep) were filled with a mixture of sandy loam soil and Osmocote Plus 8-9 Month slow release fertiliser (ICL – Specialty Fertilizers, The Netherlands) that was infested with mature *H. avenae* cysts to provide approximately 25 eggs per g of soil. Pots were arranged in wire mesh crates (50 pots per crate in a 5 × 10 array). One seed was sown in each pot. The crates were placed outdoors in autumn, on well-drained terraces in Urrbrae, South Australia (34°58′9.5″S 138°38′25.0″). Supplementary irrigation was provided as needed. At 84 d after sowing, the root balls were removed from the pots. The number of white cysts on the surface of each root ball was counted.

While tube tests can be conducted at any time of year, and they are generally considered to be more reliable and precise than pots tests, they are more expensive to conduct and their throughput is limited by the size and availability of controlled environment facilities. In Australia, tube tests are used for official classification of varieties for CCN resistance, while pots tests have been used for preliminary screening of breeding lines. In our experience, the resistance conferred by *Rha2* can be readily detected in either type of test. The research described here involved evaluation of resistance in successive generations over several years. At each stage, the choice to use tube tests or pots tests was made based on practical considerations including time of year, availability of facilities, cost and the numbers of plants to be evaluated. In both types of test, white cysts are counted for each individual plant. If the count is high, that plant can be unambiguously scored as susceptible. However if the count is low, it is not possible to be sure that the plant is resistant, as it could be a susceptible plant that 'escaped' infection. Therefore, it is important to use replication. For evaluation of the resistance status of cultivars and other accessions, between four and ten replicates (plants) of each accession were included in tube tests. For fine-mapping, replication was achieved by evaluating multiple progeny of recombinant plants, with at least 16 plants evaluated for each recombinant haplotype.

3.3.3 Determination of the physical positions of RFLP and SCAR markers

Clone sequences for five RFLP markers (mwg892, mwg865, psr901, awbma21 and mwg694) that had been mapped by Kretschmer et al. (1997) and the sequence for which Dayteg et al. (2008) had developed the SCAR marker Ha2S18 were subjected to a BLASTn analysis (Altschul et al. 1990) against the International Barley Genome Sequencing Consortium 2H pseudomolecule (150831_barley_pseudomolecules_chr2H.fasta, downloaded from http://webblast.ipk-gatersleben.de/barley_ibsc/downloads/) (Mascher et al. 2017).

3.3.4 Evaluation of mapping data

For the C/H and C/S populations, genotypic and phenotypic data that had been used by Kretschmer et al. (1997) were examined. Subsets of lines with parental haplotypes in the region of interest and for which the existing phenotypic data were consistent with the observed haplotype (i.e. few or no white cysts for lines with the Chebec or Sahara 3771 haplotype; high numbers of white cysts for lines with the Harrington or Clipper haplotype) were selected for use in genotyping-by-sequencing to discover DNA polymorphisms. Lines that had recombinant haplotypes in the region of interest but for which the existing phenotypic data were missing or inconclusive were evaluated in tube tests to confirm their resistance status.

3.3.5 Genotyping-by-sequencing

The genomic DNA used for GBS analysis included samples isolated from leaf tissue sampled from one plant of each of Chebec, Harrington, Clipper, Sahara 3771, selected C/H and C/S DH lines (some resistant and some susceptible), the resistant barley cultivars Sloop SA and Sloop VIC and 13 susceptible barley cultivars (Baudin, Buloke, Cowabbie, Fitzroy, Gairdner, Hamelin, Malloy, Oxford, Skiff, Schooner, Sloop, Tantangara and Vlamingh). For these samples, DNA was isolated from milled leaf samples using a phenol chloroform method (Rogowsky et al. 1991) with modifications as described by Pallotta et al. (2000). Five pooled DNA samples were formed by mixing equal quantities of DNA of each member of five sets of lines: 66 resistant C/H lines with the Chebec haplotype in the region of interest on chromosome 2H; 22 susceptible C/H lines with the Harrington haplotype in the region of interest; 71 resistant C/S lines with the Sahara 3771 haplotype in the region of interest; 71 susceptible C/S lines with the Clipper haplotype in the region of interest on chromosome 2H; and 12 of the 13 susceptible cultivars (all except Sloop). One aliquot for each of Sloop, Sloop SA, Sloop VIC, Chebec, Harrington, Clipper and Sahara 3771 and one aliquot of each pooled

sample were sent to Diversity Arrays Technology (Bruce, ACT, Australia) for analysis with its DArTseq GBS platform (www.diversityarrays.com/dart-application-dartseq).

The GBS sequence data were analysed by Diversity Arrays Technology using its proprietary software pipeline. Tag sequences that were reported as including SNPs were used in BLASTn analysis (Altschul et al. 1990) against the 2H pseudomolecule of the barley reference genome (Mascher et al. 2017). Tags with a BLAST hit alignment (minimum e-value = $1e^{-5}$) were selected.

To select SNPs that segregate in the C/H and/or C/S populations and that would map in the region of interest, results for contrasting (resistant and susceptible) pools were compared with each other and with the results for their resistant and susceptible parents. To identify SNPs that could be widely applicable in marker-assisted selection for CCN resistance, the selected tag pairs were filtered to retain only those for which Sahara 3771, Chebec and both pools of resistant lines exhibited only one tag and for which Clipper, Harrington and all pools of susceptible lines or cultivars exhibited only the alternate tag.

3.3.6 Development and application of marker assays

Primers for KASP marker assays (Appendix 5) were designed for selected SNPs using Kraken™ software (LGC Genomics Limited, Hoddlesdon, UK). The resulting assays were applied using an automated SNPLine™ system (LGC Genomics Limited, Hoddlesdon, UK) according to the manufacturer's instructions. Some of the DNA samples used for this were isolated from leaf tissue sampled from young seedlings. Other DNA samples were isolated from endosperm tissue, so that individual seeds could be genotyped to select those to be germinated for evaluation of resistance. Endosperm tissue samples were obtained by dissecting individual barley grains into two parts: one containing the embryo and the other

consisting mostly of endosperm. Detailed protocols for tissue sampling, tissue preparation and DNA extraction are given in Appendix 6.

To provide gel-based assays for two SNPs that were determined to be very closely linked to *Rha2,* temperature-switch PCR primer sets (Table 3-1) were designed using the methods described by Tabone et al. (2009). Briefly, primers were designed with Primer3 release 2.3.7 (Rozen and Skaletsky 2000) by using genomic sequence retrieved from the 2H pseudomolecule. Each assay consists of a locus-specific primer pair and a nested allele-specific primer. The assays were performed with a QIAGEN *Taq* DNA polymerase kit in a 10 µL reaction mixture containing 2 µL template DNA (10 ng/µL), 0.1 µL polymerase, 1 µL 10× buffer, 1.6 µL dNTPs (1.25 mM), 2 µL 5× Q solution, 0.1 µL locus-specific forward primer (10 µM), 0.1 µL locus specific reverse primer (10 µM), 0.5 µL nested allele-specific primer (10 µM) and 2.6 µL sterile nuclease-free water. The amplification protocol was as follows: (1) an initial denaturation step of 10 min at 95 °C, (2) 15 cycles of 30 s at 94 °C, 30 s at 58 °C and 60 s at 72 °C, (3) 8 cycles of 10 s at 94 °C and 30 s at 45 °C, (4) 15 cycles of 30 s at 94 °C, 30 s at 53 °C and 30 s at 72 °C. Finally, the samples were cooled to 20 °C. The reactions were run on DNA Engine Dyad Peltier Thermal Cycler (Bio-Rad Laboratories, Hercules, California, USA). The PCR products were separated on a 1.5 % (w/v) agarose gel containing SYBR™ Safe gel stain (Life Technologies Australia Pty Ltd., Mulgrave, VIC, Australia) for 45 min at 110 V and were visualised with a UV transilluminator.

Table 3-1: Primer sequences for temperature-switch PCR assays wri328 and wri329, which were designed to assay the same SNPs as KASP assays wri321 and wri297, respectively

Primer	wri328	wri329
LSF_1	AGGTGATCACGATCTCCATCACCAC	GCGGATGCAATGGAGGTCTA
LSR_1	CTTCTTGTGCAGGGCAACTGAC	ACGGAATGCTCCCCTAGGAA
ASF_1	GGAAACTGCAGGAGGAA	GTGAGATGCAATTGAAATCG

3.4 Results

Phenotypic evaluation of a small panel of accessions in a tube test showed that Athinais, Bajo Aragon, Barley 191, Martin 403-2, Morocco, Morocco (Early), Nile, Orge Martin, Orge Martin 839, Sabarlis and Siri are all resistant to the *H. avenae* pathotype that was used here, with mean numbers of white cysts ranging from 0 to 1.1 per plant (Appendix 1) while Alfa, Drost, Herta, Ortolan, Schooner and Varde are all susceptible to that pathotype, with mean numbers of white cysts ranging from 5.4 to 10.7 per plant. Phenotypic results for the available accessions of Marocaine 079 and Quinn were inconclusive.

Sequences associated with five RFLP markers that Kretschmer et al. (1997) had mapped near the resistance locus were anchored to the pseudomolecule sequence for chromosome 2H at positions between 654,782 (mwg865) and 684,123 kbp (mwg694) (Appendix 7). The sequence for which Dayteg et al. (2008) had developed a SCAR marker (Ha2S18) was anchored just distal to these positions, at 685,898 kbp.

With examination of RFLP data for the C/H and C/S populations, four DH lines were identified as having recombination events between mwg892 (677,498 kbp) and awbma21 (682,575 kbp): C/S DH5, C/S DH6, C/S DH27 and C/H DH69. Phenotypic and genotypic data for two of these lines (C/S DH5 and C/S DH6) indicate that the resistance locus is distal to mwg892, while the data for the other two lines (C/S DH27 and C/H DH69) indicate that the resistance locus is proximal to awbma21 (Figure 3-2 a). Based on these observations, the 5,077 kbp region between mwg892 and awbma21 was considered as the candidate region for *Rha2*.

Analysis of the GBS data yielded 8,923 SNP-bearing tag pairs, of which 1,937 could be anchored to the pseudomolecule sequence for chromosome 2H (Appendix 8). Of these, 38 were anchored within the candidate region (677,498 to 682,575 kbp). KASP assays were

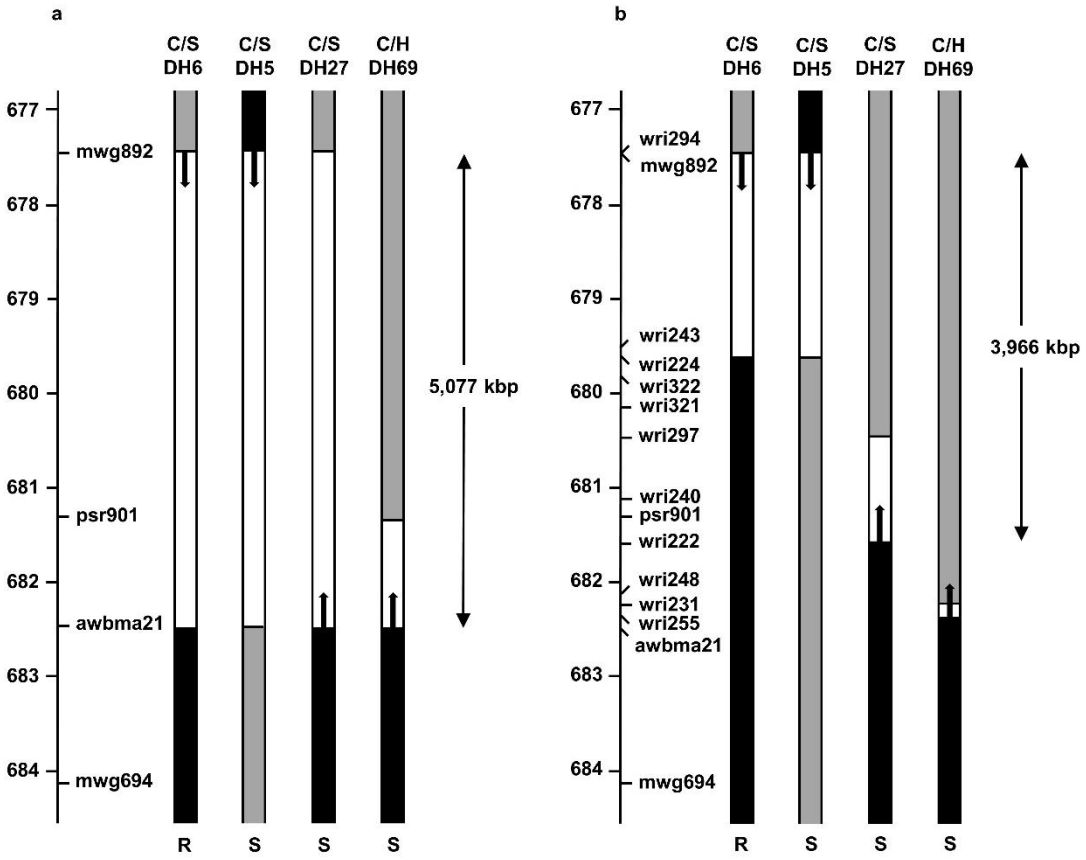

Figure 3-2: Graphical representation of *Rha2*-region genotypes of three Clipper/Sahara 3771 (C/S) doubled haploid lines and one Chebec/Harrington (C/H) doubled haploid line. In each case, the axis to the left of the graphical genotypes shows the physical positions of markers (in Mbp) on the 2H pseudomolecule of the barley genome assembly. (a) Graphical genotypes based on pre-existing RFLP marker information. (b) Graphical genotypes based on both pre-existing RFLP marker information and new KASP marker information. In each graphical genotype, the region shaded in black was inherited from the resistant parent (Sahara 3771 or Chebec), the region shaded in grey was inherited from the susceptible parent (Harrington or Clipper) and the unshaded region is the region within which recombination occurred. The cereal cyst nematode resistance status of each line is indicated by the letter R (resistant) or S (susceptible) at the bottom of the figure. Single-headed arrows point in the direction towards which the resistance locus can be deduced to lie based on the genotype and phenotype of each individual line. Double-headed arrows define the candidate intervals for *Rha2* based on this information

designed for 106 SNPs, including 24 in the candidate region. With application of 11 KASP assays to the four recombinant DH lines (C/S DH5, C/S DH6, C/S DH27 and C/H DH69), the candidate region for *Rha2* was narrowed to the 3,966 kbp region between mwg892 (677,498 kbp) and wri222 (681,464 kbp) (Figure 3-2 b). Consistent with this, application of KASP assays to Sloop, Sloop VIC and Sloop SA, indicated that Sloop VIC and Sloop SA each differ from Sloop in the candidate region (Figure 3-3). For six consecutive markers (wri243, wri224, wr322, wri321, wri297 and wri326) there were no genotype differences detected between Sloop VIC and Sloop SA, indicating that the region from 679,677 to 680,443 kbp could be identical-by-descent in these two resistant cultivars.

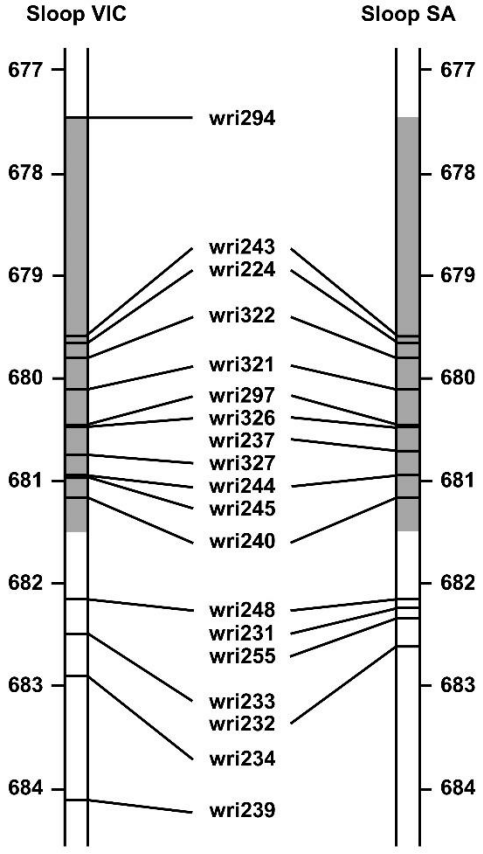

Figure 3-3: A candidate region (shaded) for *Rha2* on barley chromosome 2H, showing the physical positions (in Mbp on the 2H pseudomolecule of the barley genome assembly) at which KASP marker assays revealed single nucleotide polymorphisms between the susceptible cultivar Sloop and one or both of its resistant derivatives Sloop VIC (left) and Sloop SA (right)

KASP assays for wri243 (679,677 kbp) and wri256 (685,490 kbp) were applied to 9,003 BC_2F_2 progeny of Sloop and Sloop SA. Based on the results obtained, 603 plants carrying recombinant haplotypes were selected for use in fine mapping. KASP assays for 14 additional co-dominant KASP assays were applied to the 603 selected plants. The results provided a genetic order that was consistent with the physical order of the markers on the 2H pseudomolecule, with only two exceptions: (1) wri240 (681,155 kbp) did not map in the region and (2) wri255 (682,309 kbp) was found to be proximal to wri231 (682,242 kbp). Sixty-four plants with recombination events between wri243 (679,677 kbp) and wri232 (682,572 kbp) were grown and allowed to self-pollinate to provide BC_2F_3 families. Members of 53 BC_2F_3 families were evaluated for CCN resistance and were genotyped (Appendix 9). With comparison of the phenotypic and genotypic results the region of interest was narrowed to the 978 kbp interval between wri224 (679,727 kbp) and wri237 (680,705 kbp) (Figure 3-4). This interval coincides with the region in which Sloop VIC and Sloop SA could not be distinguished from each other. Within that region, nine genes have been predicted with high confidence (Table 3-2, Figure 3-5) (Mascher et al. 2017).

Among all progeny to which the assays for wri322 (679,878 kbp), wri321 (680,107 kbp), wri297 (680,441 kbp) and wri326 (680,443 kbp) were applied, no recombination was observed among these markers. Among 101 Sloop SA/Sloop F_2 plants that were evaluated in a pot test, the segregation ratio observed for these markers was 20:52:29 (Sloop SA homozygotes: heterozygotes: Sloop homozygotes), which does not deviate significantly from the expected 1:2:1 ratio (chi-square: 1.69; $p = 0.43$; df = 2). Of the 72 plants with Sloop SA alleles in either the homozygous or heterozygous state, none had more than three white cysts (Appendix 10). Similar results were obtained for Sloop SA control plants. Among the other 29 plants (Sloop homozygotes), numbers of white cysts ranged from 0 to 22. A wide range (0 to 34 white cysts) was also observed among Sloop control plants. Overall, these results are

consistent with the resistance of Sloop SA being conferred by a single dominant gene that is closely linked with wri322, wri321, wri297 and wri326.

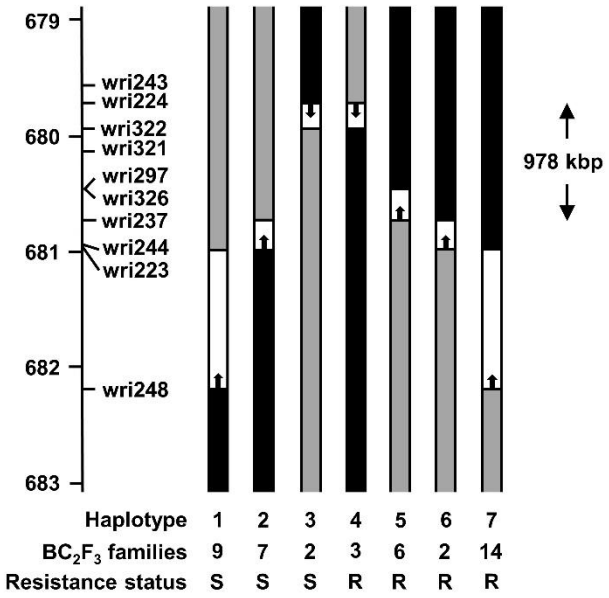

Figure 3-4: Graphical representations of seven recombinant *Rha2*-region haplotypes observed in progeny derived by backcrossing the resistant cultivar Sloop SA to its susceptible parent Sloop. The axis to the left of the graphical genotype shows the physical positions of markers (in Mbp) on the 2H pseudomolecule of the barley genome assembly. In each graphical genotype, the region shaded in black was inherited from the resistant parent (Sloop SA), the region shaded in grey was inherited from the susceptible parent (Sloop) and the unshaded region is the region within which recombination occurred. For each haplotype, the number of BC_2F_3 families assessed is shown and the resistance status of those families is indicated as R (resistant) or S (susceptible). The double-headed arrow defines a candidate interval for *Rha2* based on this information

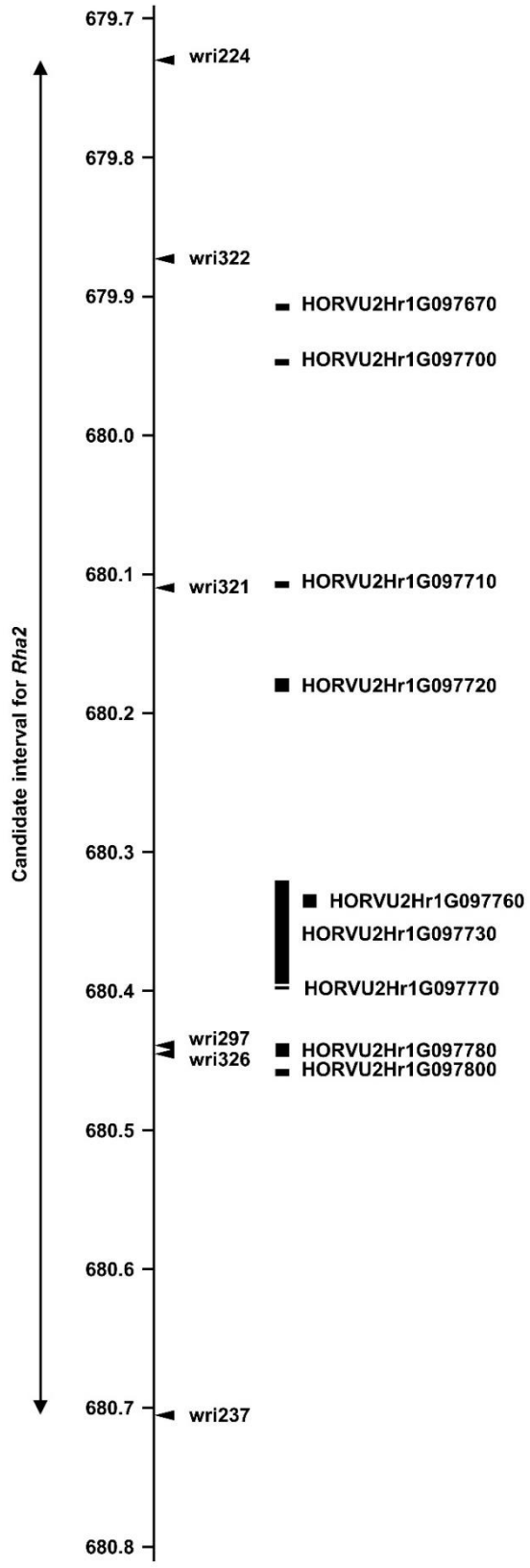

Figure 3-5: Positions of six single nucleotide polymorphisms (indicated by triangles and labelled by the names of KASP marker assays) and nine high-confidence predicted genes (rectangles) relative to a 978 kbp candidate interval for *Rha2* on the 2H pseudomolecule of the barley genome assembly

Table 3-2: High-confidence predicted genes in the candidate region between 679,727 kbp and 680,705 kbp on chromosome 2H (Mascher et al. 2017)

Gene code	Position	Annotation
HORVU2Hr1G097670	679,904,944 - 679,907,205	Plastid-lipid associated protein
HORVU2Hr1G097700	679,946,510 - 679,947,405	Unknown protein
HORVU2Hr1G097710	680,104,708 - 680,108,022	F-box family protein
HORVU2Hr1G097720	680,177,439 - 680,186,077	Acetylglutamate kinase
HORVU2Hr1G097730	680,321,819 - 680,393,065	Acetylglutamate kinase
HORVU2Hr1G097760	680,332,215 - 680,337,187	Uncharacterised conserved protein
HORVU2Hr1G097770	680,394,226 - 680,395,854	Carotenoid cleavage dioxygenase 7
HORVU2Hr1G097780	680,440,771 - 680,446,606	Aquaporin like superfamily protein
HORVU2Hr1G097800	680,457,446 - 680,461,502	Cysteine and histidine rich domain containing protein, RAR1

When the assays for the four genetically co-segregating markers (wri322, wri321, wri297 and wri326) were applied to accessions of barley lines that have previously been used to differentiate among pathotypes of *H. avenae,* five haplotypes were observed (Appendix 1). As expected, the resistance-associated T-A-A-G haplotype that is present in Chebec was also observed for its resistant ancestor Orge Martin. This haplotype was also observed for Bajo Aragon, Barley 191, Morocco, Martin 403-2, Orge Martin 839, Sabarlis and Siri, all of which have been classified as carrying *Rha2* and/or *Rha3* (Andersen and Andersen 1982; Smiley et al. 2011). Four other haplotypes were observed: two in accessions that were found to be resistant (C-G-G-G in Morocco (Early) and Athinais, and C-A-A-G in Nile) and two (C-G-G-A and C-G-G-null) among cultivars that were found to be susceptible (Alfa, Clipper, Drost, Herta, Ortolan, Varde and Schooner). For each of Quinn and Marocaine 079, the two accessions evaluated exhibit different haplotypes: (C-G-G-null and C-G-G-A for Quinn; T-A-A-G and C-G-G-A for Marocaine 079).

Assays for the four co-segregating markers (wri322, wri321, wri297 and wri326) were applied to a large panel of barley cultivars. The results (Appendix 2) indicate that the wri326 assay is neither reliable nor diagnostic of resistance. With this assay, some samples were readily called as G:G homozygotes (predominantly HEX fluorescence) or A:A homozygotes (predominantly FAM fluorescence). Others were called as 'nulls' because little fluorescence of either type was detected. Still others could not be called because their results were intermediate (between the null and A:A clusters or between the G:G and A:A clusters). With the susceptible cultivars Brindabella, Clipper and Harrington all exhibiting the resistance-associated G:G genotype, wri326 is clearly not diagnostic of resistance. This marker was therefore excluded from further consideration for use in barley breeding. With assays wri322, wri321 and wri297, four haplotypes were observed: T-A-A, C-G-G, null-G-G and T-G-G. The resistance-associated T-A-A haplotype was detected for the resistant parents Chebec and Sahara 3771, their resistant derivatives Sloop SA and Sloop VIC, two other resistant cultivars (Dash and Hindmarsh) and seven cultivars of unknown resistance status (Albacete, Alf, Fractal, GrangeR, Harbin, Optic and SY Rattler). The opposite (C-G-G) haplotype was detected for 31 susceptible cultivars, 16 resistant cultivars whose resistance is due to the *Rha4* locus that Barr et al. (1998) mapped on chromosome 5H (Barque, Capstan, Commander, Doolup, Dhow, Fathom, Flagship, Fleet Australia, Galleon, Keel, Maritime, Navigator, Skipper, Torrens and Yarra) and 112 cultivars of unknown resistance status. The T-G-G haplotype was observed for Brindabella and Haruna Nijo (both known to be susceptible) and for Digger, Kearney and Prior Early (all with unknown resistance status). The null-G-G haplotype was detected for Azumamugi, Kikkaihadaka and Zavilla (all with unknown resistance status). When the T-A-A, T-G-G and null-G-G cultivars of unknown resistance status were compared to Chebec (resistant; T-A-A) and Schooner (susceptible; C-G-G) in a tube test, all seven T-A-A cultivars were classified as resistant (with mean numbers of white cysts between 0 and 4.5 per plant) and all T-G-G and null-G-G cultivars were classified as

susceptible (with mean numbers of white cysts between 32.8 and 54.3 per plant) (Appendix 11).

For the A>G SNPs assayed by wri297 and wri321, additional assays (wri328 and wri329, respectively), were developed to make it possible to assay the target SNPs using temperature-switch PCR (Tabone et al. 2009) and gel electrophoresis. With each of these assays (Table 3-1), one product (457 bp for wri328 and 335 bp for wri329) was amplified when the susceptibility-associated nucleotide G was present and a product of a different length (250 bp for wri328; 514 bp for wri329) was amplified when the resistance-associated nucleotide A was present (Appendix 12). For heterozygous samples, both products were visible for each assay.

3.5 Discussion

It is generally accepted that Ha13 is the prevalent pathotype of *H. avenae* in Australia (Brown 1982) and it is known that CCN resistance derived from either Chebec or Sahara 3771 is effective in Australia. Kretschmer et al. (1997) attributed the resistance of both Chebec and Sahara 3771 to the *Rha2* locus on chromosome 2H. According to Smiley et al. (2011), *Rha3* confers resistance against the Ha13 pathotype. This led us to question whether Chebec and Sahara 3771 might carry *Rha3* rather than *Rha2*. To investigate this, we evaluated materials that had previously been reported to carry *Rha2* and/or *Rha3* resistance. They all exhibited resistance against the pathotype used in this research. As we could not differentiate between *Rha2* and *Rha3* materials either phenotypically or genotypically, we retained the designation *Rha2* for the locus mapped by Kretschmer et al. (1997), even though we could not unequivocally demonstrate that this resistance is identical-by-descent with that of Barley 191 (the original source of *Rha2* that was investigated by Andersen and Andersen (1968)).

The analysis conducted here for two mapping populations demonstrates that the use of pre-existing data in combination with current genome sequence information (Mascher et al. 2017) can help define the physical position of a locus that was previously only roughly mapped relative to RFLP markers. With this approach, it was possible to define a 5,077 kbp region of the chromosome 2H pseudomolecule as the candidate region for *Rha2*. With the application of DArTseq GBS technology to bulks of resistant and susceptible mapping lines and with the anchoring of GBS tag sequences to the barley genome assembly, informative SNPs were discovered in that region. With KASP genotyping of SNPs on recombinant lines from the mapping populations, the region of interest was narrowed to 3,966 kbp. Consistent with this, the resistant cultivars Sloop VIC and Sloop SA were both found to differ from their susceptible ancestor Sloop at markers within the region of interest. For Sloop SA, Chebec is the only possible source of resistance. For Sloop VIC, the source of resistance is a less clear, given that Sloop VIC has both Sahara 3771 and Chebec in its pedigree. Based on results

obtained using the wri294 assay for a SNP at 677,483,533 kbp (A for Sloop, Chebec and Sloop SA; G for Sahara 3771 and Sloop VIC) and the wri327 assay for a SNP at 680,719,172 (G for Sloop, Chebec and Sloop SA; C for Sahara 3771 and Sloop VIC), it seems likely that the Sloop VIC *Rha2* segment originated from Sahara 3771.

Further narrowing of the region required new progeny with recombinant haplotypes in the region and new molecular markers to distinguish among haplotypes. Therefore, a large set of BC_2F_2 progeny was generated and screened with KASP assays for SNPs that had been discovered by GBS. With genotypic and phenotypic analysis of BC_2F_3 progeny, the region of interest was narrowed to 978 kbp. In the BC_2F_2 fine map, the candidate region consists of a proximal flanking marker (wri224, 679,727 kbp), a distal flanking marker (wri237, 680,705 kbp) and four co-segregating markers: wri322 (679,878 kbp), wri321 (680,107 kbp), wri297 (680,441 kbp) and wri326 (680,443 kbp). Within the 978-kbp region between the flanking markers, nine genes have been predicted with high confidence.

According to information in the BARLEX database (Colmsee et al. 2015), four of the nine high-confidence predicted genes between 679,727 and 680,705 kbp on the 2H pseudomolecule (Figure 3-5), are expressed in young roots of barley. One of these (HORVU2Hr1G097760) is annotated as encoding an 'uncharacterised conserved protein' and conserved domain analysis for the predicted protein product did not identify any characterised functional domains. The other three (HORVU2Hr1G097800; HORVU2Hr1G097720 and HORVU2Hr1G097780) will be discussed here as possible candidates for *Rha2*.

HORVU2Hr1G097800 encodes a zinc-binding protein (RAR1; required for *Mla12* resistance) containing a highly conserved cysteine and histidine rich domain (CHORD, PF04968). The RAR1 protein is known to contribute to hypersensitive responses of barley against powdery mildew (*Blumeria graminis* f. sp *hordei*) (Shirasu et al. 1999). In hypersensitive responses

against fungal pathogens, entry of the pathogen into resistant plants is halted at the infection site by rapid death of infected cells (Hückelhoven et al. 1999, 2000; Hückelhoven and Kogel 1998; Shirasu et al. 1999). This differs from the interactions of cyst nematodes with their hosts, in that juvenile cyst nematodes can readily invade the roots of resistant plants, migrate through cortical cells and establish feeding sites (Grymaszewska and Golinowski 1991; Holtmann et al. 2000; Seah et al. 2000; Williams and Fisher 1993; Wyss and Zunke 1986). However, shortly after the establishment of feeding sites, the affected plant cells can begin to deteriorate in resistant plants but not in susceptible plants (Endo 1991; Rice et al. 1985; Sobczak et al. 2005). The reaction observed in resistant plants has been described as a hypersensitive response resulting in a necrotic layer around the feeding site (Grymaszewska and Golinowski 1991; Kim et al. 1987; Mahalingam and Skorupska 1996; Rice et al. 1985, 1987; Yu and Steele 1981). Consistent with this, some genes that confer cyst-nematode resistance in dicot species (Cai et al. 1997; Liu et al. 2012, 2017; Paal et al. 2004; van der Vossen et al. 2000) are known to encode nucleotide-binding site leucine-rich repeat (NBS-LRR) proteins that contribute to hypersensitive responses and Lagudah et al. (1997) suggested NBS-LRR-encoding genes as candidates for the wheat *Cre3* CCN resistance locus. Thus HORVU2Hr1G097800 seems worthy of investigation as a plausible candidate for *Rha2*.

HORVU2Hr1G097720 is annotated as encoding an acetylglutamate kinase. Acetylglutamate kinases are required for synthesis of L-arginine, which is in turn required for production of L-orthinine and the polyamines putrescine, spermidine and spermine. These polyamines have been detected at elevated levels in barley leaf tissue infected with leaf rust (*Puccinia hordei*) (Greenland and Lewis 1984) or powdery mildew (Walters et al. 1985). Research conducted with other plant species has demonstrated that spermidine and spermine play roles in plant defense. Spermidine contributes to the formation of pyrrolizidine alkaloid defense compounds (reviewed by Takahashi and Kakehi (2009); Ober and Hartmann (1999)). Spermine induces accumulation of acidic pathogenesis-related (PR) proteins that are associated with

hypersensitive responses (Yamakawa et al. 1998). Thus HORVU2Hr1G097720 also seems worthy of investigation as a plausible candidate for *Rha2*.

HORVU2Hr1G097780 is annotated as encoding an aquaporin-like protein (Mascher et al. 2017). According to information in the BARLEX database (Colmsee et al. 2015), this gene exhibits root-specific expression. With comparison of the HORVU2Hr1G097780 sequence with the barley aquaporin gene family, HORVU2Hr1G097780 was identified as tonoplast intrinsic protein 2;2 (HvTIP2;2 GenBank accession number AB540223) (Hove et al. 2015). In a phylogenetic study based on major intrinsic protein sequences of the monocots barley, maize (*Zea mays*) and rice (*Oryza sativa*) and the dicot Arabidopsis (*Arabidopsis thaliana*), the most similar protein to HvTIP2;2 was the maize protein ZmTIP2-3 (Besse et al. 2011). Several other monocot TIPs were present in the same clade: the maize TIPs ZmTIP2-1 and ZmTIP2-2, the rice TIP OsTIP2;1 and the barley TIP HvTIP2;1 (Besse et al. 2011). The genes encoding these TIPs are all mainly or solely expressed in roots (Chaumont et al. 2001; Lopez et al. 2004; Sakurai et al. 2005; Walley et al. 2016), with OsTIP2;1 known to be localised mainly in the stele and endodermis (Sakurai et al. 2008). Among the Arabidopsis TIPs, AtTIP2;2 and AtTIP2;3, were the most similar to HvTIP2;2 (Besse et al. 2011). The genes encoding AtTIP2; and AtTIP2;3 have both been shown to be expressed in the tonoplasts and central vacuoles of pericycle cells (Gattolin et al. 2009).

Although no aquaporin genes have been demonstrated to confer resistance against parasites or pathogens, there are reports of the involvement of TIPs in plant-nematode interactions. Transcriptomic analysis has shown that inoculation of Arabidopsis plants with either the beet cyst nematode *H. schachtii* or the root knot nematode *Meloidogyne incognita* affects TIP expression (Barcala et al. 2010; Szakasits et al. 2009). Similarly, a root-specific aquaporin, RB7, has been found to be upregulated during infection of transgenic tobacco plants with root-knot nematodes *(M. incognita*, *M. arenaria* and *M. javanica)* (Opperman et al. 1994).

Furthermore, a tomato TIP has been shown to interact with the *M. incognita* effector protein 8D05 until up to 24 days after inoculation (Xue et al. 2013).

While the main function of aquaporins is to facilitate water transport through membranes, an Arabidopsis TIP (AtTIP2;3) and a wheat TIP (TaTIP2;2) have also been found to transport NH_3 (Bertl and Kaldenhoff 2007; Loqué et al. 2005). In Arabidopsis roots, the presence of ammonia increased the expression of AtTIP2;3 (Loqué et al. 2005). If the ability of HvTIP2;2 to transport water, NH_3 or other compounds is enhanced in CCN-resistant barley plants, this might help explain the enlargement of vacuoles that has been observed in the syncytia of CCN-infected resistant plants (e.g. Aditya et al. 2015).

In the course of the fine-mapping research that is reported here, many new SNPs were discovered and assayed on resistant and susceptible materials. For any of these SNPs to be useful in marker-assisted breeding for CCN resistance, they should be diagnostic across a broad range of germplasm. Often, markers that are closely associated with traits in individual mapping populations prove to not be suitable for marker-assisted selection in other cross combinations because marker alleles associated with the favourable trait are common even among materials that do not exhibit the desired trait. This is particularly true when mapping is conducted using arrays of previously discovered polymorphisms, given that common variants are generally preferred for the construction of such arrays. Here, the use of GBS for *de novo* SNP discovery provided an opportunity to discover new variants that might be specific to resistant materials. The inclusion of a range of susceptible cultivars in the GBS experiment provided an opportunity for early selection of potentially diagnostic SNPs. From the GBS data alone, four SNPs stood out because they distinguished the parents and progeny with *Rha2* resistance from susceptible parents and progeny and from cultivars with *Rha4* resistance. As fine mapping continued, KASP assays designed for these SNPs (wri297, wri321, wri322 and wri326) proved to be valuable in selecting resistant progeny for

backcrossing. Across a larger panel of barley cultivars, assays wri321 and wri297 were both diagnostic of *Rha2*-based resistance. These markers have been readily adopted in commercial barley breeding in Australia, reducing reliance on costly phenotyping. Given that these two markers are particularly useful for marker-assisted selection, gel-based assays (wri328 and wri329) were developed to provide alternative ways to assay the same SNPs. These assays use temperature-switch PCR technology (Tabone et al. 2009), with which length polymorphisms can be generated from SNPs.

In conclusion, the research reported here narrowed the candidate region for the *Rha2* resistance gene to just 978 kbp and provided KASP and gel-based assays for each of two apparently diagnostic SNPs within that region. Evaluation of predicted genes within the candidate region revealed four genes that are known to be expressed in young roots. While three of these are discussed here as plausible candidates for *Rha2*, other possibilities cannot be excluded. Given that the barley reference genome sequenced was assembled based on sequences from non-*Rha2* materials, it is also possible that the causal gene is not represented in the assembly. Further, if the expression of the causal gene is induced by infection, its expression would not be reflected in the BARLEX database and the gene itself might not be annotated as a high-confidence gene.

Chapter 4 Transcriptomic responses to cereal cyst nematode infection of susceptible and resistant barley cultivars

4.1 Summary

A time-course transcriptomic experiment was performed on barley roots infected with cereal cyst nematodes using a susceptible cultivar, Sloop, and two resistant cultivars, Sloop SA and Sloop VIC. A whole transcriptome approach was applied for detection of differentially expressed genes. Comparisons were made between inoculated Sloop and non-inoculated Sloop, between inoculated Sloop SA and inoculated Sloop, and between inoculated Sloop VIC and inoculated Sloop. The two latter comparisons are of particular interest because they could provide insights about resistance. There were two genes that were differentially expressed in both of those comparisons and at all time periods after inoculation: one (HORVU3Hr1G009340) that is annotated as encoding an ENTH/ANTH/VHS superfamily protein and one (HORVU4Hr1G001830) that is annotated as encoding an undescribed protein. Predicted genes in the *Rha2* region of chromosome 2H were examined for differential expression. In root samples from the susceptible cultivar Sloop, HORVU2Hr1G097780, which is annotated as encoding the TIP2;2 tonoplast intrinsic protein exhibited more than twofold upregulation after inoculation. This provides further support for considering HORVU2Hr1G097780 as a candidate gene for *Rha2*.

4.2 Introduction

Infection by parasitic nematodes affects gene expression in host plants (Fernandez et al. 2015; Holbein et al. 2016; Juvale and Baum 2018; Perry et al. 2018; Siddique and Grundler 2018). The interaction between nematode effector proteins and plant host cells leads to host responses that have been observed at a microscopic level. The key plant host responses include cell wall degradation, very active cytoplasm, and an abundance of small vacuoles. Morphological changes reflect the changes in gene expression that have been observed with transcriptomic approaches such as RNA-seq (Cotton et al. 2014; Li et al. 2014, 2018; Palomares-Rius et al. 2012; Xu et al. 2012).

The formation of feeding sites in the roots of susceptible plants leads to dysregulation of the plant cell metabolism compared to non-infected roots. In soybean roots infected with soybean cyst nematode, transcriptomic analysis has shown a delineation between the migratory and sedentary phases of infection by soybean cyst nematode (Klink et al. 2009, 2010). During the sedentary phase, plant metabolic pathways are affected and initial feeding cells are induced to develop into syncytial feeding sites (Chronis et al. 2013; Cotton et al. 2014; Kumar et al. 2014; Moffett et al. 2015; Zheng et al. 2015). In various hosts during the early stages of the infection, pathways involved in plant cell wall degradation have been found to be upregulated while pathways involved in host plant resistance have been found to be downregulated (Cotton et al. 2014; Tucker et al. 2007; Wan et al. 2015). Other metabolic processes that have been reported to be enhanced in roots upon cyst nematode infection of susceptible soybean and wheat include those that involve transporter proteins which transport sugars, amino acids, peptides and lipids (Li et al. 2014, 2018; Qiao et al. 2019). These genes, pathways and processes may be targets of suppression by the nematode.

Comparisons between resistant and susceptible plants have revealed differential responses in pathways that are known to be involved in plant defense against other biotic stresses.

Resistant soybean, common bean and wheat hosts have shown upregulation of NBS-LRR genes or transcription factors (e.g. WRKY transcription factors, zinc fingers) as a reaction to the cyst nematode infection (Jain et al. 2016; Klink et al. 2009, 2010; Kong et al. 2015; Wan et al. 2015). Other defense pathways, such as ROS scavenging and MAPK pathways, have been reported to be differentially expressed in susceptible soybean during interaction with soybean cyst nematode (Klink et al. 2009, 2010; Li et al. 2014; Wan et al. 2015). The ROS scavenging and MAPK pathways are well-known for eliciting resistance reactions (extensively reviewed in Mittler (2017) and Bigeard and Hirt (2018)). The expressed genes annotated as plant hormone activity were identified in reports for soybean roots inoculated with soybean cyst nematode at early infection stage. The identified plant hormones reported in these studies, play an essential role in the resistance reactions including in the ethylene, jasmonic acid, salicylic acid, and cytokinin - auxin pathway (Klink et al. 2009; Li et al. 2014; Wan et al. 2015; Xu et al. 2012). The aforementioned pathways and genes are part of the plant immune system, which involves eliciting resistance reactions against pathogens (Berens et al. 2017).

Beside the defense response pathways, consistent differential gene expression is observed, consistent with differential morphological changes between susceptible and resistant infected plant roots. Gene members of the general cell wall modification processes were differentially expressed in inoculated resistant versus susceptible soybean cultivars (Wan et al. 2015). Genes encoding structural cell wall proteins have been reported to be differentially expressed in infected roots of resistant versus susceptible cultivars of common bean and wheat (Jain et al. 2016; Kong et al. 2015). Structural cell wall proteins, such as hydroxyproline-rich glycoproteins are thought to enforce and stiffen cell walls. The cinnamic acid metabolic pathway was upregulated in infected roots of resistant wheat and soybean (Kong et al. 2015; Li et al. 2014). The cinnamic acid metabolic pathway leads to lignification of the cell wall which stiffens the cell wall as well. Beside cell wall modification, plant degradation

ubiquitins have been reported to be differentially expressed upon cereal cyst nematode contact in wheat (Qiao et al. 2019). The plant ubiquitins might influence the cell degradation.

Since there are no reports of transcriptomic analysis of CCN-infected barley roots and a lack of understanding regarding the resistance mechanism of *Rha2* in barley, a transcriptomic experiment was performed as part of this research. RNA-seq analysis was performed on root tissue from CCN-inoculated and non-inoculated plants of a susceptible barley cultivar (Sloop) and CCN-inoculated plants of two resistant barley cultivars (Sloop SA and Sloop VIC).

4.3 Materials and methods

4.3.1 Plant material and sampling

The plant materials used in this study were the cultivars Sloop (susceptible) and Sloop SA and Sloop VIC (the latter two cultivars carry the *Rha2* resistance allele). Seeds were placed on moistened filter paper in Petri dishes and incubated overnight at 4 °C. The following day, the Petri dishes were placed in a controlled environment room at a constant temperature of 15 °C with a 12 h light/dark cycle. The seedlings were grown in a tube test (as described in Appendix 3). In short, polyvinyl chloride (PVC) tubes were filled with sterile sandy loam soil and one seedling was transplanted per tube. Root samples were taken from all cultivars and considered as samples at 0 days after inoculation (DAI). Plants were inoculated once with approximately 150 nematodes on the day of transplanting. Swollen regions of inoculated roots in the upper root region were sampled for all cultivars at 4, 8, 12, 16, 20, 24 and 28 DAI. The corresponding regions of non-inoculated roots were sampled from Sloop to be used as control samples. Three biological replicates were collected at each of 4, 8, 12, 16 and 20 DAI, and two replicates at 24 and 28 DAI. Each biological replicate consisted of several swollen regions from three or four individual plants. The samples were snap-frozen in liquid nitrogen.

4.3.2 RNA extraction and sequencing

Total RNA was extracted using the Spectrum™ Plant Total RNA Kit (Merck, New Jersey, United States) with a modified version of the manufacturer's extraction protocol. The lysis buffer was added in two steps of 250 µL. In the first step, 250 µL of lysis buffer was used to bring the roots into suspension and facilitate manual grinding with a pestle in an Eppendorf tube. The remaining liquid was used to rinse the pestle and ensure that all plant material remained in the tube. At the end of the extraction protocol, the column was eluted once with 30 µL elution buffer. The samples were treated with an Ambion TURBO DNA-free™ kit (Life Technologies, California, United States) to remove remaining DNA, DNase and reagents.

RNA integrity was assessed using a LabChip GX (PerkinElmer, Massachusetts, United States) and quantity was measured by Qubit Fluorometric Quantification (ThermoFisher Scientific, Massachusetts, United States). For each treatment combination (i.e. cultivar and time point), the sample with the best RNA quality and concentration was chosen for sequencing. In total 31 samples were sequenced, three (non-inoculated Sloop, Sloop SA and Sloop VIC) sampled at 0 DAI, and four (a non-inoculated Sloop control and inoculated Sloop, Sloop SA and Sloop VIC) for each of the remaining seven sampling times. RNA from each selected sample was used to prepare a sequencing library according to the Illumina (California, United States) manufacturer's protocol and sequenced on an Illumina NextSeq instrument.

4.3.3 RNA transcriptome analysis

4.3.3.1 Exploratory analysis

The reads were aligned to the *H. avenae* transcriptome (Kumar et al. 2014) and *H. vulgare* genome (Mascher et al. 2017) using the software CLC Genomics Workbench v8.0. The reads per gene were counted to provide a count table. Further analysis was performed in R with the DESEQ2 package (Love et al. 2014). Objects were loaded into the main function as described in the vignette (Love et al. 2015). An exploratory analysis was conducted with the parameters "sample type" and "time point" in the design formula. There were four sample types: non-inoculated Sloop (which will be referred to here as Control) and inoculated Sloop, Sloop SA and Sloop VIC. The raw read data were transformed in three ways: $\log_2$ transformation, variance stabilising transformation (VST) (Anders and Huber 2010), and regularised-logarithm log (rlog). The transformed data were compared according to the intended comparisons: Control versus Sloop, Sloop versus Sloop SA and Sloop versus Sloop VIC at each time point. The appropriate transformation was selected and a principal component analysis was performed.

4.3.3.2 Analysis of differential expression

For the analysis of differential expression, the samples collected at 0 and 28 DAI were excluded, while samples that were obtained from 4 and 8 DAI, 12 and 16 DAI, and 20 and 24 DAI were combined to provide 'early', 'middle', and 'late' groups, respectively, that could be statistically compared. The investigation of the combined data was performed in R with the DESEQ2 package, using the same design formula as the exploratory analysis, except that 'time point' was replaced by 'time period' (Love et al. 2015). The comparisons performed were: Control versus Sloop, Sloop SA versus Sloop and Sloop VIC versus Sloop for each time period. All genes with an adjusted *p*-value below 0.05 were selected for further consideration.

4.3.4 qPCR analysis

4.3.4.1 cDNA preparation

The samples used for the qPCR experiment were the same as for the RNA-seq experiment, but with additional replicates for Sloop SA and Sloop VIC. For each RNA sample, a cDNA library was generated using the SuperScript III (50U) (ThermoFisher Scientific, Massachusetts, United States) kit following the manufacturer's protocol with minor modifications to accommodate the low RNA concentrations of some samples. The concentration of the RNA samples was not increased with evaporation techniques due to the fragile nature of the samples. Therefore, the maximum RNA volume allowance was used. A mixture of 11.75 µL RNA, 2 µL dNTP mixture (1.25 mM of each nucleotide), 1 µL oligo dT primer (50 µM) was incubated at 65 °C for 5 min. The samples were placed on ice and an additional 4 µL 5× First strand Buffer, 1 µL DTT and 0.25 µL Superscript (50U) were added. The mixture was incubated at 50 °C for 70 min and the Superscript enzyme was inactivated by raising the temperature to 70 °C for 15 min. The integrity of the cDNA libraries was checked by amplifying the GAPDH gene with primer pair 5′ GTGAGGCTGGTGCTGATTACG 3′ (forward primer) and 5′

TGGTGCAGCTAGCATTTGAGAC 3′ (reverse primer). The PCR mixture contained: 1 µL template cDNA, 2.5 µL 10× PCR buffer (contains 15 mM $MgCl_2$), 4 µL 1.25 mM dNTP, 1.4 µL 25 mM $MgCl_2$, 5 µL of mixture of forward and reverse primer (5 µM of each primer), 0.15 µL *Taq* polymerase and 10.95 µL water to obtain a total reaction volume of 25 µL. The PCR protocol was as follows: 2 min at 94 °C, followed by 25 cycles of 20 s at 94 °C, 20 s at 55 °C, and 20 s at 72 °C. Finally, the mixture was heated to 72 °C for 5 min. The PCR products were checked on an agarose gel.

4.3.4.2 qPCR experiment

For one candidate gene (HORVU2Hr1G097780) qPCR was performed, using four housekeeping genes for normalisation: HvGAP (HORVU7Hr1G074690), HvCyclophilin (HORVU6Hr1G012570), HvTubulin (HORVU1Hr1G081280) and HvHSP70 (HORVU5Hr1G113180). The qPCR was performed as described by Burton et al. (2008). Data analysis and processing were done as described by Vandesompele et al. (2002) and Hellemans et al. (2007).

4.4 Results

4.4.1 Transcriptome analysis

4.4.1.1 Exploratory analysis

The total RNA read number per sample ranged between 8.0 and 14.5 million reads, except for 'Control at 0 DAI' for which the total read number was just 3.4 million (Figure 4-1 and Appendix 13). Most reads could be mapped onto the barley genome. Of the reads from control samples from 0 to 24 DAI, between 95 and 97 % of the reads could be mapped on the barley genome. In contrast, only 83 % of the reads from 28 DAI sample were mapped on the barley genome. Inoculated samples showed more variation, with between 24 and 97 % of the total RNA reads mapped on the barley genome. In samples taken from inoculated plants at 12 DAI or later, some reads were mapped onto the *H. avenae* transcriptome. Moreover, in samples taken at 28 DAI from inoculated plants, the numbers of reads mapped to the *H. avenae* transcriptome were almost as high as the numbers mapped to the barley genome. Some reads could not be mapped to either assembly, and the proportion of these tended to increase over time, reaching 28 % at 28 DAI for Sloop.

Comparisons of transformed read counts between inoculated and non-inoculated Sloop (Figure 4-2), between inoculated Sloop SA and Sloop (Figure 4-3), and between inoculated Sloop VIC and Sloop (Figure 4-4) indicated that the rlog transformation provided a consistently better fit to the assumption of homoscedasticity than either the $\log_2$ or VST transformation.

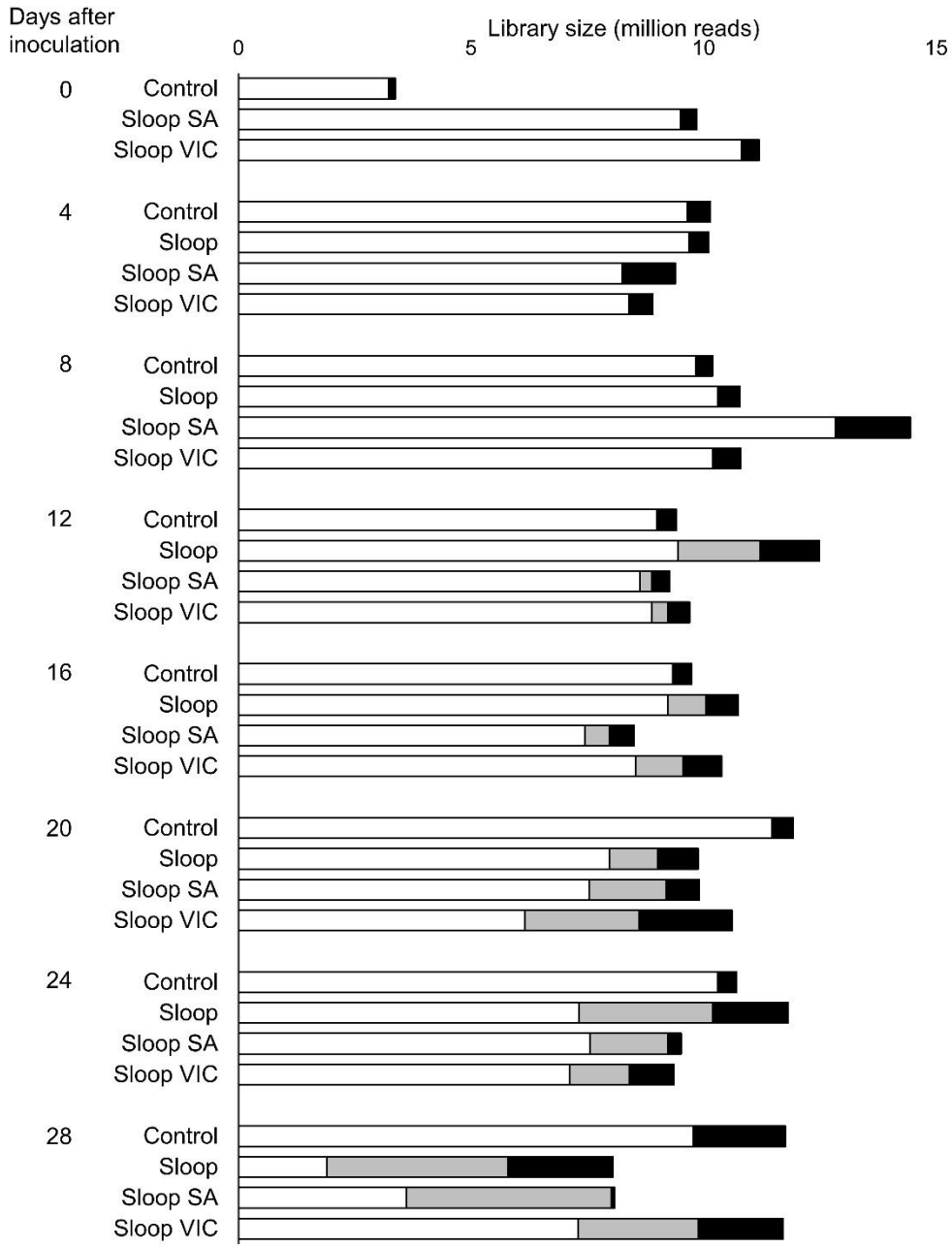

Figure 4-1: Total numbers of RNA reads in samples taken from plants of the cultivars Sloop (control), Sloop SA and Sloop VIC prior to inoculation (day 0) and from non-inoculated plants of Sloop (control) and inoculated plants of Sloop, Sloop SA and Sloop VIC between 4 and 28 days after inoculation. Within each bar, the white part represents reads that were mapped onto the *Hordeum vulgare* reference genome; the grey part represents reads that were mapped onto the *Heterodera avenae* transcriptome; and the black part represents reads that could not be mapped onto either the *H. vulgare* reference genome or the *H. avenae* transcriptome

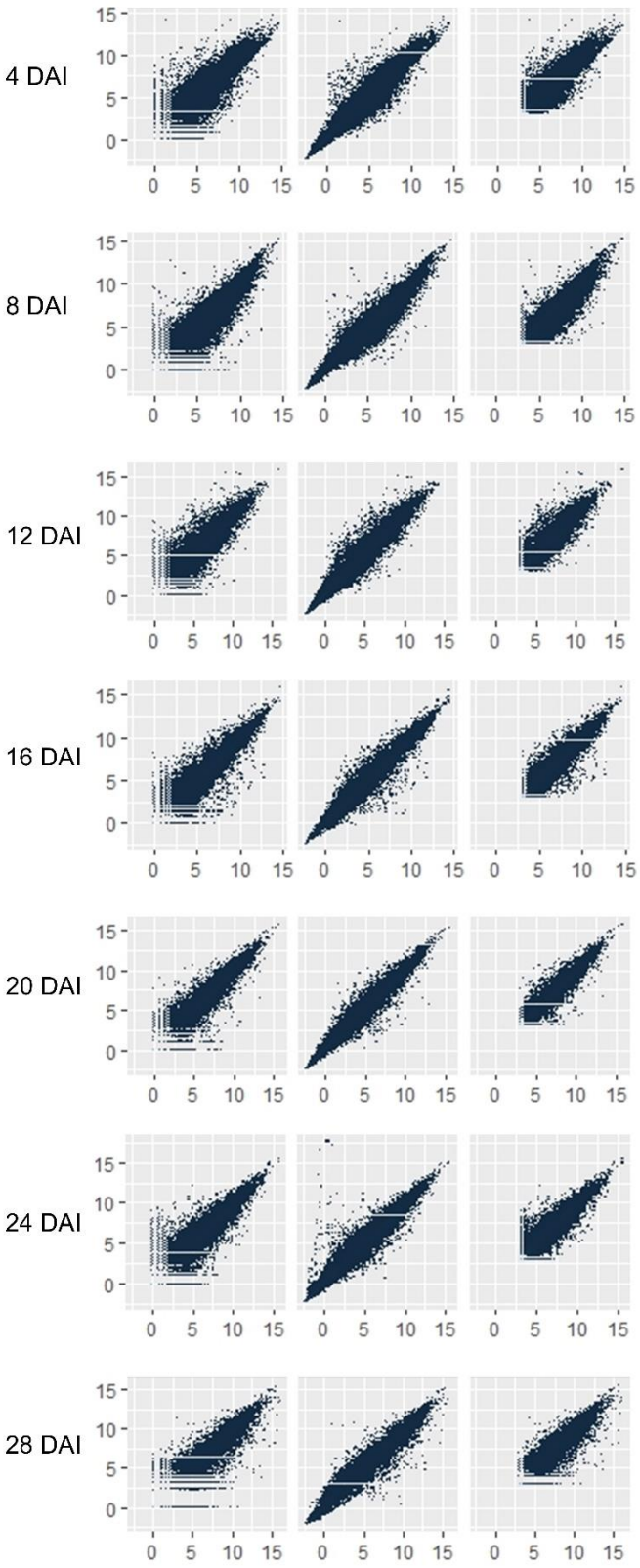

Figure 4-2: Comparison of read counts between inoculated plants of Sloop (vertical axis) and non-inoculated control plants of Sloop (horizontal axis) at 4, 8, 12, 16, 20, 24 and 28 days after inoculation (DAI) with read counts transformed using three methods: $\log_2(x+1)$ (left), rlog (middle), and VST (right)

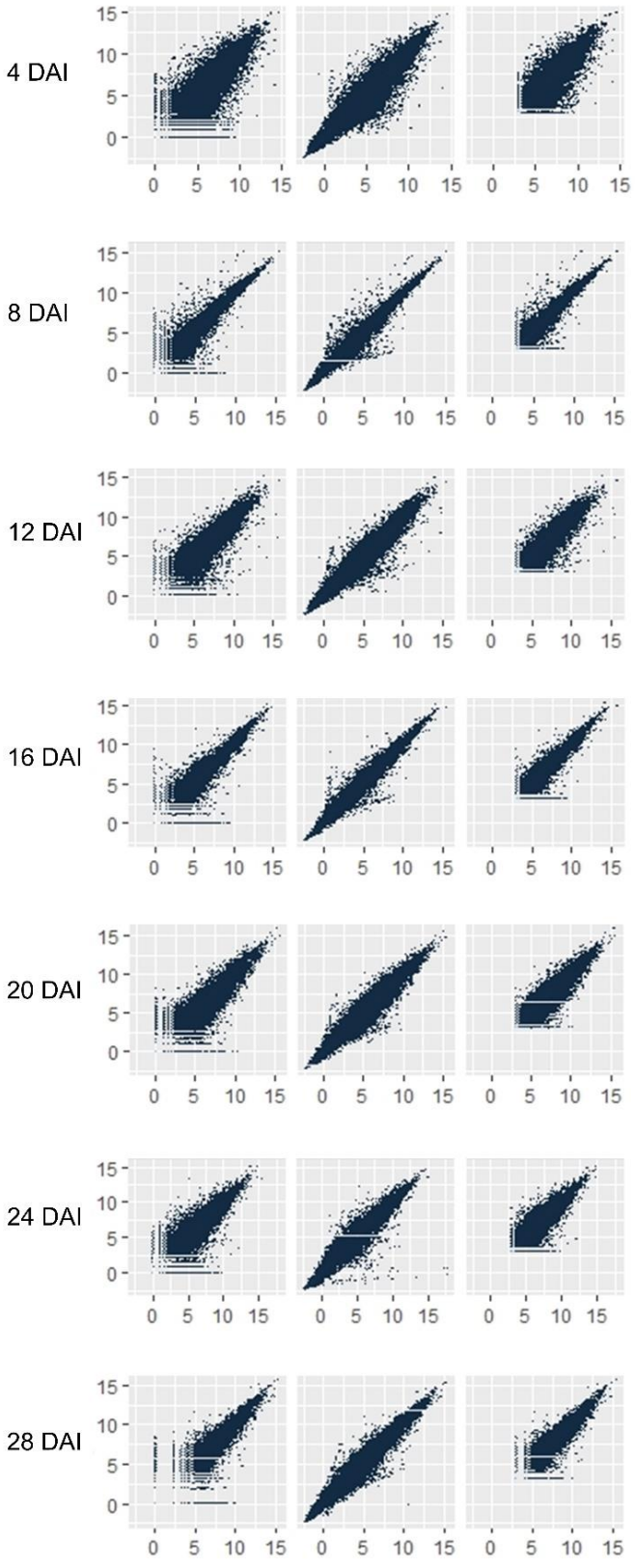

Figure 4-3: Comparison of read counts between inoculated plants of Sloop SA (vertical axis) and Sloop (horizontal axis) at 4, 8, 12, 16, 20, 24 and 28 days after inoculation (DAI) with read counts transformed using three methods: $\log_2(x+1)$ (left), rlog (middle), and VST (right)

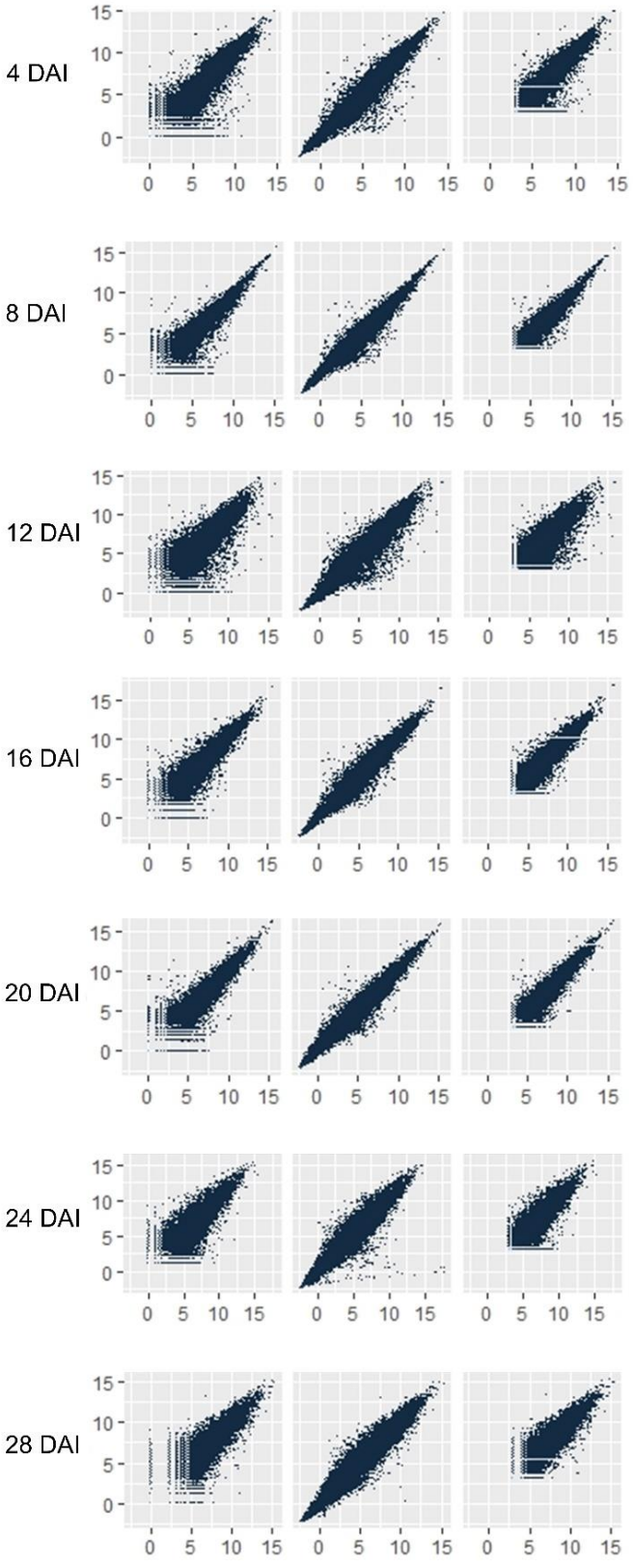

Figure 4-4: Comparison of read counts between inoculated plants of Sloop VIC (vertical axis) and Sloop (horizontal axis) at 4, 8, 12, 16, 20, 24 and 28 days after inoculation (DAI) with read counts transformed using three methods: $\log_2(x+1)$ (left), rlog (middle), and VST (right)

In a principal component analysis (PCA) using rlog-transformed read data, the first and second principal components explained 40 % and 12 % of the variance, respectively. In an orthogonal graph of these two components (Figure 4-5), the samples could be separated into three clusters according to sampling times: 0, 4 and 8 DAI; 12 and 16 DAI; and 20, 24 and 28 DAI.

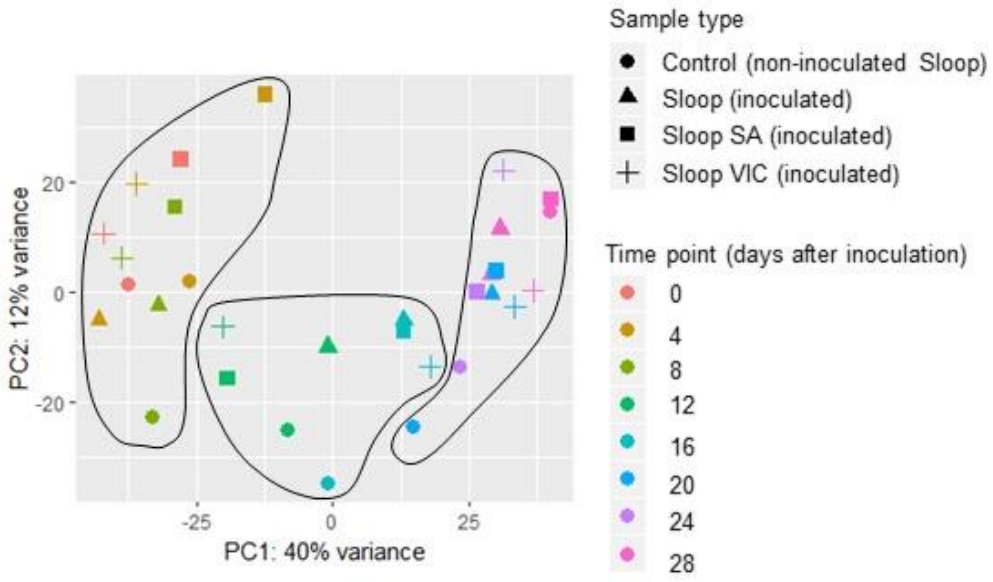

Figure 4-5: Principal component analysis of gene expression. Values for the first and second principal components (PC1 and PC2) are shown for each of 31 samples. The black lines separate the values into clusters corresponding to three time periods

4.4.1.2 Differential expression analysis

Significant differences in transcript abundance were detected for 466 barley genes (Appendix 14). Comparisons of transcript abundance between inoculated and non-inoculated plants of Sloop showed significant differences for only a few genes in the early time period (Figure 4-6 a and Table A14-1 of Appendix 14) with more detected in the middle and late periods while 17 genes exhibited significant differences in both the middle and late sampling periods. In comparisons between inoculated plants of resistant cultivars (Sloop SA or Sloop VIC) and the

susceptible cultivar Sloop, significant differences were detected for many genes in the early time period (Figure 4-6 b and c; Table A14-2 and Table A14-3 of Appendix 14).

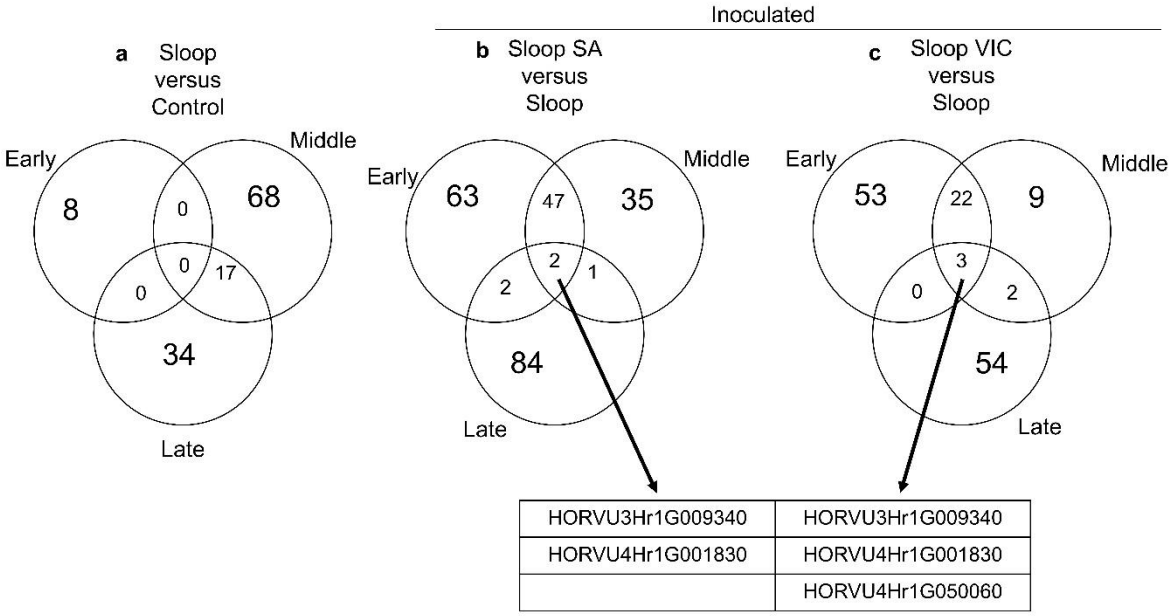

Figure 4-6: Venn diagrams showing the numbers of differentially expressed genes for three treatment comparisons: (a) inoculated Sloop versus non-inoculated Sloop (Control), (b) inoculated Sloop SA versus inoculated Sloop and (c) inoculated Sloop VIC versus inoculated Sloop, all at early (combination of 4 and 8 days after inoculation (DAI)), middle (combination of 12 and 16 DAI), and late (combination of 20 and 24 DAI) sampling periods. The common genes in the intersection are listed below the Venn diagrams

Table 4-1: Predicted genes commonly expressed among all time periods for inoculated samples Sloop SA versus Sloop, and Sloop VIC versus Sloop (Mascher et al. 2017)

Gene code	Annotation
HORVU3Hr1G009340	ENTH/ANTH/VHS superfamily protein
HORVU4Hr1G001830	Undescribed protein
HORVU4Hr1G050060	Patatin-like protein 4

Table 4-2: Predicted genes with significant (p <0.05) differential expression between inoculated and non-inoculated barley plants of the cultivar Sloop

		Log_2 fold change[a]		
Gene code	Annotation	Early	Middle	Late
HORVU4Hr1G000870	AT-hook motif nuclear-localized protein 20	-3.22E+14		
HORVU2Hr1G004600	Cytochrome P450 superfamily protein	6.66E+12		
HORVU6Hr1G014970	Ubiquitin 11		-2.93E+06	-2.83E+06
HORVU6Hr1G026200	Polyubiquitin 3		-1.81E+06	-2.18E+06
HORVU7Hr1G109650	Ubiquitin 4		3.36E+06	6.15E+06
HORVU2Hr1G027270	Disease resistance-responsive (dirigent-like protein) family protein		-5.17E+06	
HORVU2Hr1G116740	Wound-responsive family protein		4.23E+06	
HORVU5Hr1G087090	Leucine-rich receptor-like protein kinase family protein		6.09E+06	
HORVU0Hr1G001750	Ethylene receptor 2		2.57E+14	
HORVU0Hr1G034160	NADH-ubiquinone oxidoreductase chain 5		4.17E+14	
HORVU1Hr1G058940	Ethylene-responsive transcription factor 1		5.09E+14	
HORVU7Hr1G002910	NBS-LRR resistance-like protein			-4.58E+06
HORVU2Hr1G104390	Ubiquitin 11			5.89E+06
HORVU0Hr1G038500	Polyubiquitin			-2.39E+14
HORVU2Hr1G097940	Homeobox-leucine zipper protein 4			3.81E+06
HORVU5Hr1G078400	Heat shock 70 kDa protein C			7.18E+06

[a]Positive values indicate higher expression in the inoculated plants. Negative values indicate higher expression in the non-inoculated plants.

Comparisons between samples from inoculated and non-inoculated Sloop plants showed a peak in the number of differentially expressed genes at the middle time period (Figure 4-6 a), with most of the differentially expressed genes (Appendix 14) related to metabolic processes of cell maintenance and cell growth. Some differentially expressed genes are related to plant immunity, including genes annotated as encoding ethylene-receptors, ubiquitins, disease-response proteins and NBS-LRR proteins (Table 4-2).

In the comparisons of inoculated plants of Sloop SA and Sloop VIC with inoculated plants of Sloop, two genes were detected as being down-regulated in both cultivars in all three time periods (Figure 4-6). One of these genes, HORVU3Hr1G009340, is annotated as encoding a member of the ENTH/ANTH /VHS superfamily. ENTH/ANTH/VHS proteins have either an epsin N-terminal (ENTH), an AP180 N-terminal homology (ANTH) or Vps27, Hrs and STAM (VHS) domain at their N-terminus. Their main functions are in endosomal trafficking in vesicles. The other gene (HORVU4Hr1G001830) is annotated as encoding an undescribed protein. A third gene (HORVU4Hr1G050060, annotated as encoding a patatin-like protein) was upregulated in all three time periods, but only in the comparison between Sloop VIC and Sloop. Patatin-like proteins have phospholipase activity.

Another way to approach the RNA-seq data was to identify the genes that were differentially expressed in both Sloop SA and Sloop VIC in each time period. There were fifteen such genes (Figure 4-7 and Appendix 15). Two of them (HORVU3Hr1G009340 and HORVU4Hr1G001830) were mentioned in the previous paragraph as exhibiting differential expression in all three time periods. Another two genes were differentially expressed in both the early and middle periods; HORVU6Hr1G087410 (annotated as encoding an RWP-RK plant regulator) was upregulated in the resistant cultivars, while HORVU7Hr1G051900 (with unknown function) was downregulated in the resistant cultivars. One gene (HORVU0Hr1G017400, annotated as encoding haloacid dehalogenase-like hydrolase

superfamily protein) was downregulated in the middle and late time periods in both resistant cultivars. The remaining 10 genes were differentially expressed in only one time period (two early, one middle and seven late).

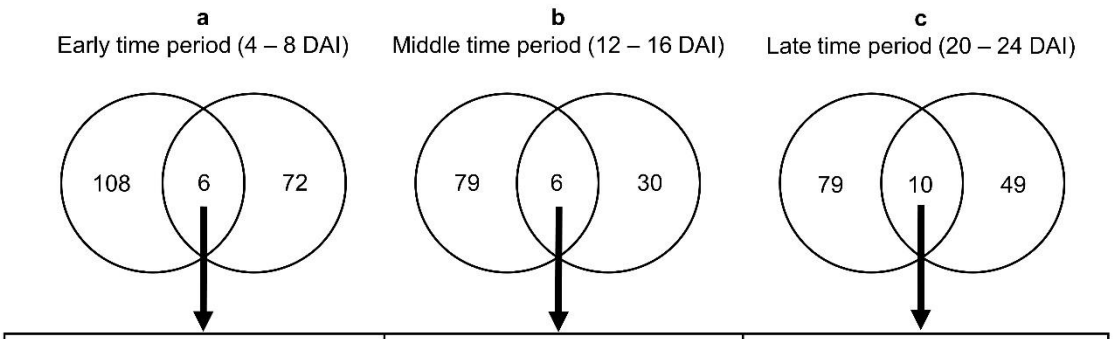

HORVU3Hr1G009340	HORVU3Hr1G009340	HORVU3Hr1G009340
HORVU4Hr1G001830	HORVU4Hr1G001830	HORVU4Hr1G001830
HORVU7Hr1G051900	HORVU7Hr1G051900	
HORVU6Hr1G087410	HORVU6Hr1G087410	
	HORVU0Hr1G017400	HORVU0Hr1G017400
HORVU7Hr1G117800		
HORVU6Hr1G047560		
	HORVU2Hr1G110900	
		HORVU0Hr1G040120
		HORVU3Hr1G033230
		HORVU1Hr1G068790
		HORVU1Hr1G068640
		HORVU2Hr1G003640
		HORVU7Hr1G045290
		HORVU7Hr1G114000

Figure 4-7: Venn diagrams showing the numbers of genes that were differentially expressed between inoculated plants of resistant cultivars (Sloop SA or Sloop VIC) and inoculated plants of the susceptible cultivar Sloop at (a) early (combination of 4 and 8 days after inoculation (DAI)), (b) middle (combination of 12 and 16 days DAI) and (c) late (combination of 20 and 24 (DAI)) sampling periods. The common genes in the intersections are listed below the Venn diagrams

Table 4-3: Predicted genes that were differentially expressed between inoculated plants of resistant cultivars (Sloop SA and Sloop VIC) and an inoculated susceptible cultivar (Sloop) in at least one time period

Gene number	Annotation
HORVU0Hr1G017400	Haloacid dehalogenase-like hydrolase (HAD) superfamily protein
HORVU0Hr1G040120	Undescribed protein
HORVU1Hr1G068640	60S ribosomal protein L30
HORVU1Hr1G068790	ADP-ribosylation factor 1
HORVU2Hr1G003640	Cysteine-rich receptor-like protein kinase 41
HORVU2Hr1G110900	Protein kinase superfamily protein
HORVU3Hr1G009340	ENTH/ANTH/VHS superfamily protein
HORVU3Hr1G033230	Centromere-associated protein E
HORVU4Hr1G001830	Undescribed protein
HORVU6Hr1G047560	Calcium-dependent lipid-binding family protein
HORVU6Hr1G087410	Plant regulator RWP-RK family protein
HORVU7Hr1G045290	Aluminium-activated malate transporter 9
HORVU7Hr1G051900	Unknown function
HORVU7Hr1G114000	Aldehyde oxidase 2
HORVU7Hr1G117800	BURP domain-containing protein 11

As reported in Chapter 3, the *Rha2* region was fine-mapped to a 978 kbp region on the 2H pseudomolecule. The region is flanked by markers wri224 (679,727 kbp) and wri237 (680,705 kbp). The genomic region between these two markers contains 19 predicted genes (Mascher et al. 2017). Those predicted genes are listed in Table 4-4.

Among the 19 predicted genes in the region of interest, 9 were predicted with high confidence and 10 with low confidence. For each of these predicted genes, the total number of reads per million (TPM) for each sample was extracted from the RNA-seq data. Only five genes had TPM values above 5 for any sample: HORVU2Hr1G097730, HORVU2Hr1G097760, HORVU2Hr1G097780, HORVU2Hr1G097800 and HORVU2Hr1G097830. Three of these

Table 4-4: High-confidence (HC) and low-confidence (LC) predicted genes in the candidate region between 679,727 kbp and 680,705 kbp on the 2H pseudomolecule of the barley genome assembly (Mascher et al. 2017)

Gene code	Position	Confidence level	Annotation
HORVU2Hr1G097650	679,828,647 - 679,831,265	LC	Unknown protein
HORVU2Hr1G097660	679,904,879 - 679,905,053	LC	Unknown protein
HORVU2Hr1G097670	679,904,944 - 679,907,205	HC	Plastid-lipid associated protein
HORVU2Hr1G097680	679,908,004 - 679,908,531	LC	Unknown protein
HORVU2Hr1G097690	679,925,725 - 679,925,913	LC	Unknown protein
HORVU2Hr1G097700	679,946,510 - 679,947,405	HC	Unknown protein
HORVU2Hr1G097710	680,104,708 - 680,108,022	HC	F-box family protein
HORVU2Hr1G097720	680,177,439 - 680,186,077	HC	Acetylglutamate kinase
HORVU2Hr1G097730	680,321,819 - 680,393,065	HC	Acetylglutamate kinase
HORVU2Hr1G097740	680,326,824 - 680,327,037	LC	Unknown protein
HORVU2Hr1G097750	680,330,430 - 680,332,797	LC	Unknown protein
HORVU2Hr1G097760	680,332,215 - 680,337,187	HC	Uncharacterised conserved protein
HORVU2Hr1G097770	680,394,226 - 680,395,854	HC	Carotenoid cleavage dioxygenase 7
HORVU2Hr1G097780	680,440,771 - 680,446,606	HC	Aquaporin like superfamily protein
HORVU2Hr1G097790	680,453,236 - 680,453,754	LC	Putative retrotransposon protein
HORVU2Hr1G097800	680,457,446 - 680,461,502	HC	Cysteine and histidine rich domain containing protein, RAR1

Table 4-4 continued

Gene code	Position	C	Annotation
HORVU2Hr1G097810	680,459,706 - 680,459,907	LC	Unknown protein
HORVU2Hr1G097820	680,462,570 - 680,462,785	LC	Unknown protein
HORVU2Hr1G097830	680,705,042 - 680,706,064	LC	Unknown protein

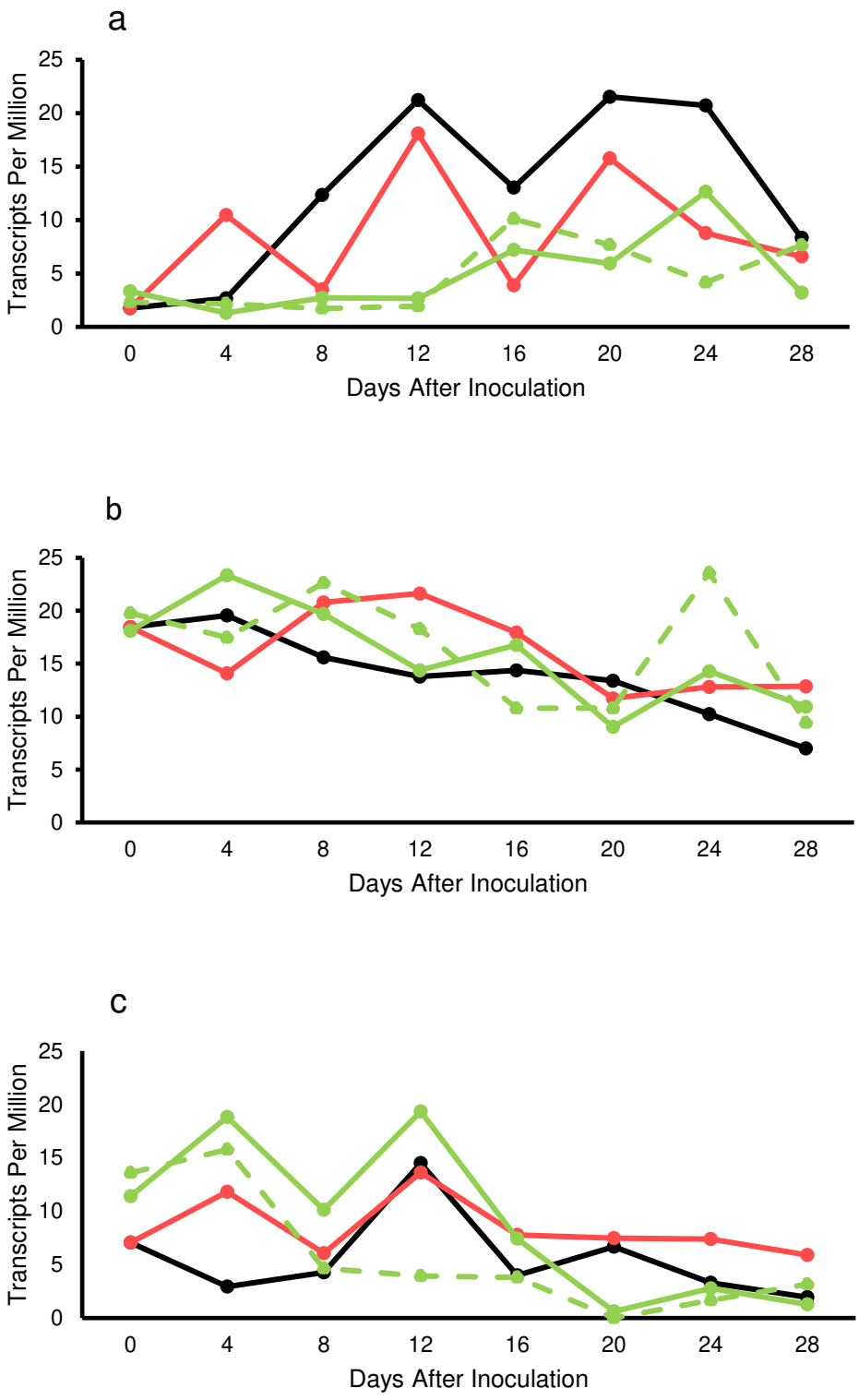

Figure 4-8: Expression values (transcripts per million) for three predicted barley genes (HORVU2Hr1G097760 (a), HORVU2Hr1G097800 (b) and HORVU2Hr1G097830 (c)) in samples of root tissue from non-inoculated plants of Sloop (black line) and inoculated plants of Sloop (red line), Sloop SA (solid green line), and Sloop VIC (dashed green line) between 0 and 28 days after inoculation

(HORVU2Hr1G097760, HORVU2Hr1G097800 and HORVU2Hr1G097830) had quite low TPM values (Figure 4-8). One (HORVU2Hr1G097730) had somewhat higher TPM values (up to 50) (Figure 4-9), with the inoculated samples of Sloop SA and Sloop VIC having slightly lower values than either the inoculated or control samples of Sloop. One (HORVU2Hr1G097780) had high TPM values (ranging from 36 to 175) at 0 and 4 DAI for all samples (Figure 4-10). Prior to inoculation (i.e. 0 DAI), HORVU2Hr1G097780 transcripts seemed more abundant for the susceptible cultivar Sloop than for the resistant cultivars Sloop SA and Sloop VIC. At 4 DAI, the sample of inoculated Sloop had a much higher TPM value than any of the other samples.

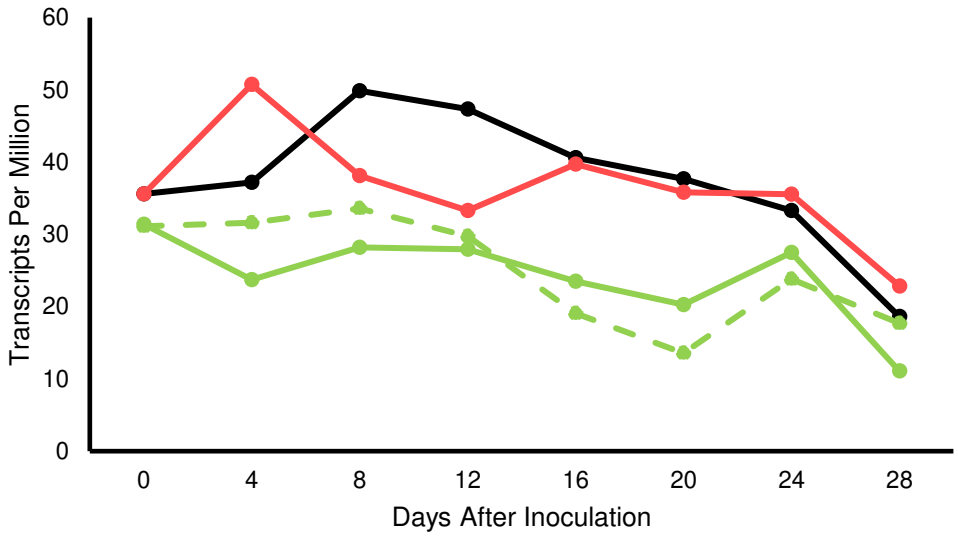

Figure 4-9: Expression values (transcripts per million) for predicted barley gene HORVU2Hr1G097730 in samples of root tissue from non-inoculated plants of Sloop (black line) and inoculated plants of Sloop (red line), Sloop SA (solid green line), and Sloop VIC (dashed green line) between 0 and 28 days after inoculation

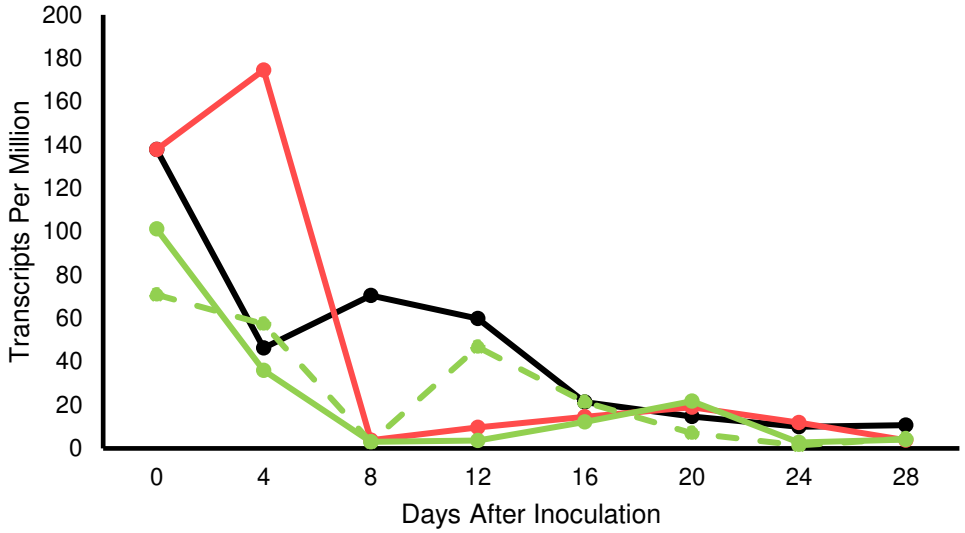

Figure 4-10: Expression values (transcripts per million) for the predicted barley gene HORVU2Hr1G097780 in samples of root tissue from non-inoculated plants of Sloop (black line) and inoculated plants of Sloop (red line), Sloop SA (solid green line), and Sloop VIC (dashed green line) between 0 and 28 days after inoculation

4.4.2 qPCR experiment

The early differential expression of the gene annotated as encoding an aquaporin-like protein (HORVU2Hr1G097780) was confirmed by qPCR (Figure 4-11). Prior to inoculation (0 DAI), the transcript abundance was much higher for the susceptible cultivar Sloop than for the resistant cultivars Sloop SA and Sloop VIC. At 4 DAI, only the inoculated samples of Sloop maintained high transcript abundance. At later sampling dates, the transcript abundance was low for all samples, except for the inoculated samples of Sloop at 24 DAI.

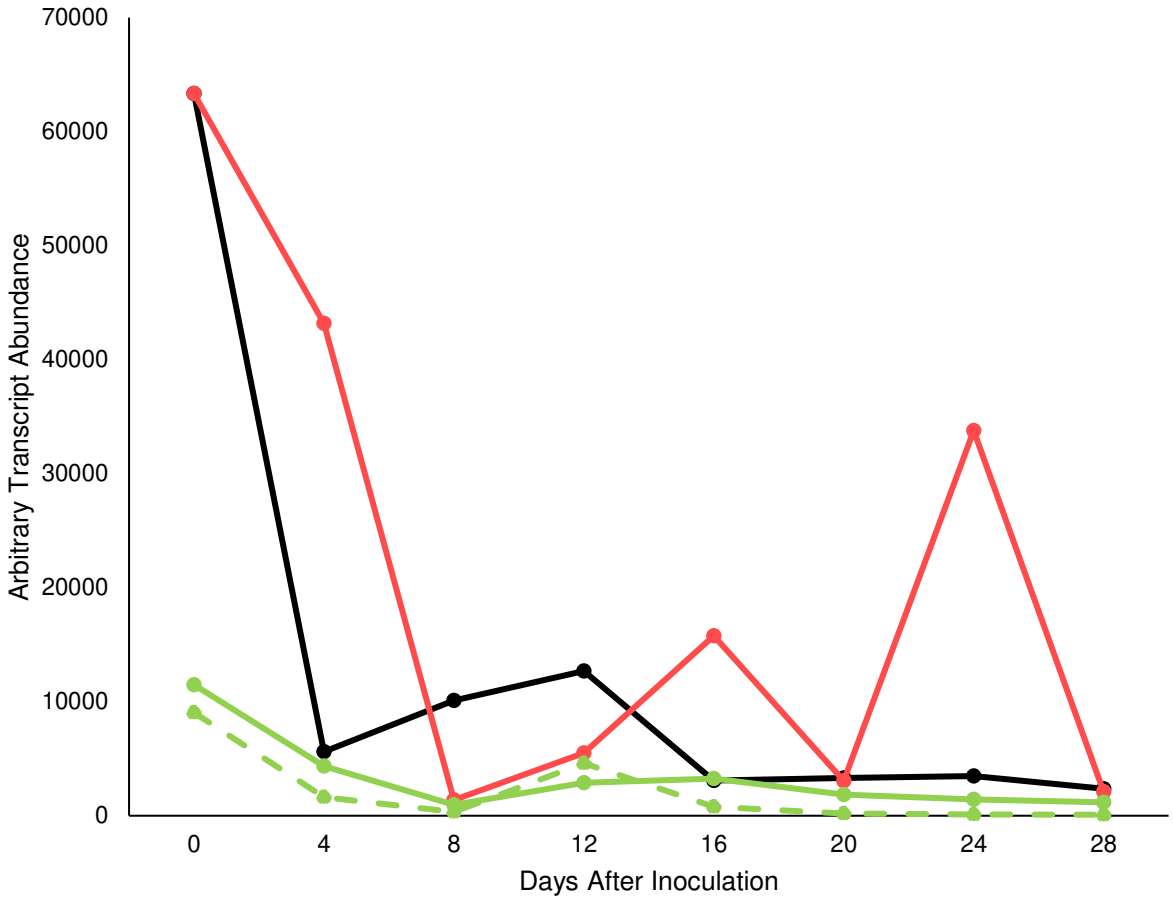

Figure 4-11: Expression values (arbitrary expression unit) from the qPCR experiment for a predicted barley aquaporin gene (HORVU2Hr1G097780) in samples taken from non-inoculated plants of Sloop (black line) and inoculated plants of Sloop (red line), Sloop SA (solid green line) and Sloop VIC (dashed green line) between 0 and 28 days after inoculation (DAI). As some error bars are too short to be visible, standard error values are not shown in this graph but provided in Appendix 16

4.5 Discussion

The aim of the research conducted for this chapter was to examine changes in barley gene expression after infection by cereal cyst nematode as well as identifying differentially expressed genes between resistant and susceptible plants. This was addressed using RNA-seq analysis as this method is able to provide expression data for many genes simultaneously. However, some issues were encountered in obtaining sufficient high-quality RNA from each sample. This limitation was partly because mature samples were difficult to grind. After taking into account the quantity and quality of the RNA samples as well as the high cost of sequencing, it was decided that only one biological replicate of each treatment would be sequenced for each sampling date.

The PCA analysis helped categorise the samples into groups of three periods: early (4 and 8 DAI), middle (12 and 16 DAI), and late (20 and 24 DAI). This grouping provided a basis for statistical analysis of the results, with the two sampling dates within each period considered as replicates. The analysis was based on the read numbers, without considering the genomic location of the genes.

Comparisons between inoculated plants and non-inoculated control plants of Sloop indicated that the number of differentially expressed genes peaked at the middle time period (Figure 4-6). Genes that were differentially expressed between inoculated and non-inoculated Sloop included some that could be expected to be involved in the plant immune system. Many of these were downregulated in response to inoculation, which might reflect suppression of plant defense responses. Examples include genes annotated as a disease responsive protein (HORVU2Hr1G027270, downregulated in the middle time period), an NBS-LRR resistance-like protein (HORVU7Hr1G002910, downregulated in the late time period). Genes encoding NBS-LRR proteins are typically differentially expressed upon contact with plant pathogens, including cyst nematodes (Jain et al. 2016; Klink et al. 2009; Klink et al. 2010; Kong et al.

2015; Wan et al. 2015). Many NBS-LRR genes have been reported to be downregulated upon contact of a resistant wheat cultivar with *H. avenae* (Qiao et al. 2019).

On the other hand, some immune response genes were upregulated such as genes annotated as an ethylene receptor 2 (HORVU0Hr1G001750, upregulated in the middle time period), and an ethylene-responsive transcription factor 1 (HORVU1Hr1G008780, upregulated in the middle time period). Ethylene receptors and ethylene-responsive transcription factors are both involved in the ethylene triggering pathway. It is not clear to what extent the ethylene pathway contributes to the responses against cereal cyst nematode. Nonetheless, it has been shown in Arabidopsis roots that ethylene plays a role in the chemotaxis of cyst nematodes. In Arabidopsis, increased concentration of ethylene in roots has been reported to increase the attraction of *H. schachtii* (Kammerhofer et al. 2015; Wubben et al. 2001), but to diminish attraction of *H. glycines* (Hu et al. 2017). Further, loss-of-function mutations in an Arabidopsis gene encoding ethylene receptor 1 (ETR1) of Arabidopsis plants decreased susceptibility to *H. glycines* (Piya et al. 2019).

Comparisons between inoculated plants of the susceptible cultivar Sloop with inoculated plants of its resistant derivatives, Sloop SA and Sloop VIC, showed more differentially expressed genes than comparisons between control and inoculated plants of Sloop (Figure 4-6 a). At all three time periods, two genes were differentially expressed between Sloop SA and Sloop, and three between Sloop VIC and Sloop. Both comparisons share the common downregulation of genes encoding an ENTH/ANTH/VHS superfamily (HORVU3Hr1G009340) and an undescribed gene (HORVU4Hr1G001830). Proteins in the ENTH/ANTH/VHS superfamily have functions such as cytoskeleton strengthening and cargo recruitment (see extensive review by Zouhar and Sauer (2014)). While it is not clear whether this gene plays a role in resistance, cytoskeleton strength has been considered to be important in the development of *H. schachtii* feeding sites in Arabidopsis roots (de Almeida Engler et

al. 2004, 2010). Additionally, a third differentially expressed gene was upregulated Sloop VIC compared to Sloop in all three time periods: HORVU4Hr1G050060, which encodes a patatin-like protein. These proteins are known to be abundant in potato tubers (Rocha-Sosa et al. 1989) and are associated with plant responses to fungi and bacteria (La Camera et al. 2005). Expression of patatin-like genes elicits expression of JA-dependent genes and the JA reaction results in a strong necrotic reaction (Cheng et al. 2018). In addition to this synergistic regulatory effect, patatin-like proteins exhibit phospholipase activity (Jimenez-Atienzar et al. 2003). Phospholipases have also been differentially expressed in resistance reactions (Kong et al. 2015). Hence, phosholipases might play an important role as a regulator mechanism for wheat against CCN.

Based on the evidence presented in Chapter 3, it seems likely that Sloop SA and Sloop VIC share the same *Rha2* allele. Therefore, genes that exhibited similar differential expression in both Sloop SA and Sloop VIC could be of interest for investigation of a common resistance mechanism. Several genes were identified in the intersections as shown in Figure 4-7. These genes have been annotated but their functions remain unknown in barley or in relation to nematode resistance.

None of the genes that were found to be differentially regulated in the RNA-seq analysis are known to be located within the candidate region of chromosome 2H within which *Rha2* has been mapped. Further analysis was undertaken to specifically examine the expression profiles of the 19 predicted genes in that region. Of these, five were confirmed to be expressed in infected roots. Three genes have already been discussed in Chapter 3 on the basis of their location within the candidate region and expression in root tissue according to the BARLEX expression atlas (Colmsee et al. 2015): HORVU2Hr1G097780, HORVU2Hr1G097800, and HORVU2Hr1G097730 which encode an aquaporin-like protein, the zinc-binding protein RAR1 and an acetylglutamate kinase, respectively. The other two differentially expressed

genes located in that region (the high-confidence gene HORVU2Hr1G097760 and the low-confidence gene HORVU2Hr1G097830) are annotated as encoding unknown proteins.

Two of the genes for which differential expression was detected (HORVU2Hr1G097720 and HORVU2Hr1G097730) have been annotated as encoding acetylglutamate kinases (Mascher et al. 2017). Both of these genes were classified as 'high confidence genes' yet examination of their sequences raises questions about whether they represent distinct genes. The genomic sequences of these both genes include repeated regions, some of which are also repeated elsewhere in the *Rha2* region or elsewhere in the genome. HORVU2Hr1G097720 has more repeat regions than HORVU2Hr1G097730 and also has a large 'gap' of unknown sequence. For each of these predicted genes, several transcript splice variants have been predicted: six for HORVU2Hr1G097720 and five for HORVU2Hr1G097730 (Mascher et al. 2017). The barley expression atlas (Colmsee et al. 2015) includes expression data for the splice variants HORVU2Hr1G097720.4 and HORVU2Hr1G097730.3. Aligning the RNA-seq sequences from this experiment on the entire candidate region resulted in sequences being mapped on HORVU2Hr1G097720.4 and on HORVU2Hr1G097730.3. However, a consensus RNA transcript constructed as a contig of overlapping RNA sequence tags extended beyond the predicted first exon of HORVU2Hr1G097730 and did not match any of the splice variants of HORVU2Hr1G097730. Future work would be required to determine whether HORVU2Hr1G097720 and HORVU2Hr1G097730 are indeed two separate genes or whether there is a sequence misassembly within the current version of the 2H pseudomolecule.

Among the five possibly differentially expressed genes from the candidate region, one (HORVU2Hr1G097780, which encodes the aquaporin-like protein TIP 2;2) showed significant $\log_2$ differential upregulation between the susceptible cultivar and the two resistant cultivars at two time points (4 and 12 DAI). For this gene, differential expression was confirmed with qPCR. Differential expression of TIP-encoding genes has previously been

reported in response to various osmotic conditions such as waterlogging (Rodrigues et al. 2013; Wang et al. 2011). To my knowledge, this is the first investigation of differential expression of a TIP-encoding gene in the context of biotic stress responses.

In conclusion, the analyses of transcript abundance reported in this chapter confirmed that the expression of many barley genes responds to CCN infection. Among these genes, some responded similarly in both susceptible and resistant cultivars, while others exhibited differential expression between susceptible and resistant cultivars. Among genes that are located within the candidate region for *Rha2*, one that encodes the TIP2;2 aquaporin, exhibited the highest expression in root tissue and the strongest differential response between the susceptible cultivar Sloop and its resistant derivatives Sloop SA and Sloop VIC. This observation, which was confirmed with qPCR, is consistent with the idea that TIP2;2 may play a pivotal role in CCN resistance.

Chapter 5 Use of laser ablation tomography to compare the roots of susceptible and resistant barley cultivars after infection with cereal cyst nematode

5.1 Summary

Laser ablation tomography (LAT) was applied to obtain images of barley roots infected with cereal cyst nematodes. The utilisation of laser ablation tomography support imaging relative large root segments (1 cm) in high resolution for qualitative and quantitative determination of feeding sites. Nematodes and their feeding sites could be observed at 10 days after inoculation. Feeding sites were compared in a susceptible cultivar and its resistant derivative. In susceptible plants, feeding sites were compact, and most internal cell walls were dissolved. In addition, cortex cells surrounding the feeding site were also found to be distorted. The feeding sites in roots of resistant plants were significantly larger, with more remnants of internal cell walls.

5.2 Introduction

It was necessary to obtain three-dimensional views of infected barley roots in order to learn more about the effects of cereal cyst nematodes on the roots they invade. Professor Jonathan Lynch's group at Pennsylvania State University had previously developed methods for laser ablation tomography (LAT) and applied them to plant roots (Chimungu et al. 2014, 2015 a and b; Saengwilai et al. 2014; York et al. 2015). Briefly, LAT involves ablating a sample layer by layer with a laser and recording the removal of each laser-illuminated section with a digital high-definition camera. These recordings are processed and converted into single images. The red, green and blue spectra of stacks of these images can subsequently be analysed with software such as MIPAR^{TM} (Sosa et al. 2014). Laser ablation tomography has been used to investigate the cell walls and structural features of maize (*Zea mays* L.) roots (Chimungu et al. 2014, 2015 a and b; Saengwilai et al. 2014; York et al. 2015). However, LAT had not been used to investigate any plant-parasite interactions. A collaborative arrangement with the Lynch group was established in order to gain further information on the interactions of cyst nematodes with host plants and particularly on any differences between roots of resistant and susceptible barley cultivars. Samples of inoculated and non-inoculated barley roots were prepared at the University of Adelaide and sent to Pennsylvania State University, where PhD candidate Christopher Strock scanned them with LAT. Moreover, the Lynch lab obtained and scanned samples of plant roots containing other edaphic organisms: maize roots colonised by an arbuscular mycorrhizal fungus, maize roots infected by insect larvae, and common bean roots infected by a fungal pathogen. This work led to the publication of a manuscript to the Journal of Experimental Botany (Strock et al. (2019), see abstract in Appendix 17). That manuscript includes results for one CCN infected segment of a root from Sloop barley. The manuscript is not included as part of this thesis given that (1) its focus is the application of LAT methodology to a range of organisms and not differences between resistant and susceptible barley lines and it includes results for only one CCN-infected barley root segment; (2) my contribution to the manuscript (sample preparation and

assistance with interpretation of the images) was less than the 50 % required by the University of Adelaide for inclusion in a PhD thesis.

The current chapter reports on LAT data generated from 42 root segments. The analysis of these data focuses on comparison of infected root segments between susceptible and resistant cultivars. This chapter also presents some comparisons of LAT imaging with confocal laser scanning microscopy of similar samples.

5.3 Materials and methods

Two barley cultivars were used in this research; Sloop and Sloop SA. Sloop is susceptible to CCN. Sloop SA, a backcross derivative of Sloop, is resistant to CCN due to the introgression of the *Rha2* resistance gene from the cultivar Chebec. Seeds of Sloop and Sloop SA were surface-sterilised in 10 % sodium hypochlorite (NaOCl) for 10 min on a shaker, before being rinsed three times with sterilised water for 5 min. The seeds were placed on moistened filter paper in a Petri dish and incubated overnight at 4 °C. The following day, the seeds were transferred to sterile 2 % agar plates and placed in a controlled environment room at a constant temperature of 15 °C with a 12 h light/dark cycle. Seedlings were inoculated when roots were 2-3 cm long (approximately 3 d old).

Stage-2 juvenile (J2) nematodes were collected from 'nematode farms' and inoculum was prepared as described in Appendix 3 Figure A3-1. One drop of inoculum was pipetted onto each root tip. Small blocks of agar were placed on top of the roots to prevent desiccation and to maintain the roots in close contact with the agar surface.

At 10 DAI, root segments approximately 5 cm in length, each with a swollen region in the middle indicating infection, were excised. In total, 42 segments were collected from 5 seedlings for each cultivar; 22 segments for the susceptible cultivar and 20 segments for the resistant cultivar. Each segment was assigned at random to one of four fixation treatments: 1) fixation in 75 % ethanol for at least 7 d; 2) staining with acid fuchsin; 3) fixation in paraformaldehyde (4 % paraformaldehyde in phosphate buffer saline, pH 7.4); and 4) fixation in paraformaldehyde followed by staining in acid fuchsin. At least five segments from each cultivar were assigned to each fixation treatment. Acid fuchsin staining was carried out as described by Bybd et al. (1983). Briefly, the root segments were cleared for 15 minutes in 10 % NaOCl and heated in staining solution (33 % glycerol, 33 % lactic acid, 33 % water, 1 % acid fuchsin) just to boiling point. The samples were rinsed with water and placed in

destaining solution (49.5 % glycerol, 49.5 % water, 1 % lactic acid). The destaining solution containing the root sample was heated to just under boiling point. Acid-fuchsin-stained root segments were checked for the presence of nematodes with a Leica stereomicroscope (Leica Microsystems, Wetzlar, Germany).

All preserved samples were transferred to water and transported from the University of Adelaide (Australia) to the Pennsylvania State University (USA) for LAT scanning. Upon arrival, the samples were transferred to 75 % (ethanol:water, v/v) and further processed. Briefly, this involved preserving the sample using a Leica EM CPD300 critical point dryer (Leica Microsystems, Wetzlar, Germany). The root segments were mounted on a movable stage and ablated with an Avia 7000, 355 nm pulsed laser. The laser ablated layer by layer and simultaneously imaged each layer with a digital single lens reflex camera 5×. Each sample was scanned and the data returned as videos. The videos consisted of one frame per µm of the root, with each frame representing an ablated layer of the root. The images were used for three-dimensional reconstruction by using Avizo 9 Lite software (VSG Inc., Burlington, MA, USA). More information regarding the LAT technology is available in Saengwilai (2013); Saengwilai et al. (2014) and Strock et al. (submitted).

Following examination of the videos and selecting regions in which one or more nematodes and feeding sites were observed, one out of every five frames was sampled (1 frame per 5 µm). These frames were loaded into ImageJ viewer (Abramoff et al. 2004) and individually assessed. The images were assessed qualitatively because a scale bar was lacking.

In addition to a two-dimensional assessment, the stack of frames was visualised using the 5Dviewer plugin (http://www.nanoimaging.de/View5D/View5D.html). The 5Dviewer projected the stack of images simultaneously into three planes: XY, XZ and YZ. Within each plane, feeding sites appeared as distinct dark ‘gaps’. The outline of each feeding site was

manually traced in each dimensional plane, and the pixel volume was calculated for each feeding. These measurements and calculations were carried out three times for each of the 45 feeding sites within Sloop root segments as well as each of 44 feeding sites within Sloop SA root segments.

Prior to statistical analysis, the estimated volume for each of the feeding site was log transformed. The log volume values were used as the response variable in a linear mixed model:

$$\boldsymbol{y} = \boldsymbol{X\tau} + \boldsymbol{Zu} + \boldsymbol{e}$$

in which $\boldsymbol{y}$ is the log-transformed volume of the feeding sites, $\boldsymbol{X\tau}$ is the fixed component of the model consisting of terms to estimate the main effects for the treatment, and the two cultivars as well as a term to estimate the their interaction effects, $\boldsymbol{Zu}$ is the random component of the model consisting of a term to account for additional variation due to measuring volumes between plants of the same variety as well as term to capture the variation between replicate volume measurements within each of the plants. The error term of the model was assumed to be distributed $\boldsymbol{e} \sim \boldsymbol{N}(\boldsymbol{0}, \sigma^2)$, where σ^2 is the residual variance. Differences in log volume between cultivars were tested using a Wald statistic (Cox and Hinkley 1974), and best linear unbiased estimators of the log volume for each cultivar were extracted from the model.

For confocal microscopy, swollen regions were excised from roots at 10 d after inoculation, embedded in 4 % agarose (Ultrapure Agarose, Invitrogen) and sectioned using a vibratome Leica VT1200 (Leica Microsystems, Wetzlar, Germany) to provide series of 70-µm transverse sections. Each section was placed in one of three wells (12 mm in diameter) on a Teflon®-coated slide. Sections were stained for 20 min with calcofluor white (0.1 % calcofluor white in 20 % ethanol), rinsed twice with water, stained for 5 min with propidium iodide (10 µg/ mL in water) and rinsed twice with water again. A drop of 50 % glycerol in

water was added, and a cover slip was placed on top. The slides were kept overnight in a humid box at 4 °C. Digital images were captured with a Nikon A1R Laser Scanning Confocal microscope (excitation wavelengths 405 and 514 nm and detection wavelengths 450 and 595 nm, respectively).

5.4 Results

5.4.1 Laser ablation tomography of non-infected barley root sections

Laser ablation tomography provided transverse-section images of barley roots (Figure 5-1 a) in which it was possible to distinguish the main features of root anatomy: root hairs, the epidermis, the cortex, the endodermis, one central metaxylem vessel and between 8 and 10 peripheral metaxylem vessels. The image resolution obtained was less than that obtained using confocal microscopy (Figure 5-1 b), where it was possible to adjust the focus for each image. Similar levels of detail were obtained regardless of which fixation technique had been used prior to LAT (Figure 5-2).

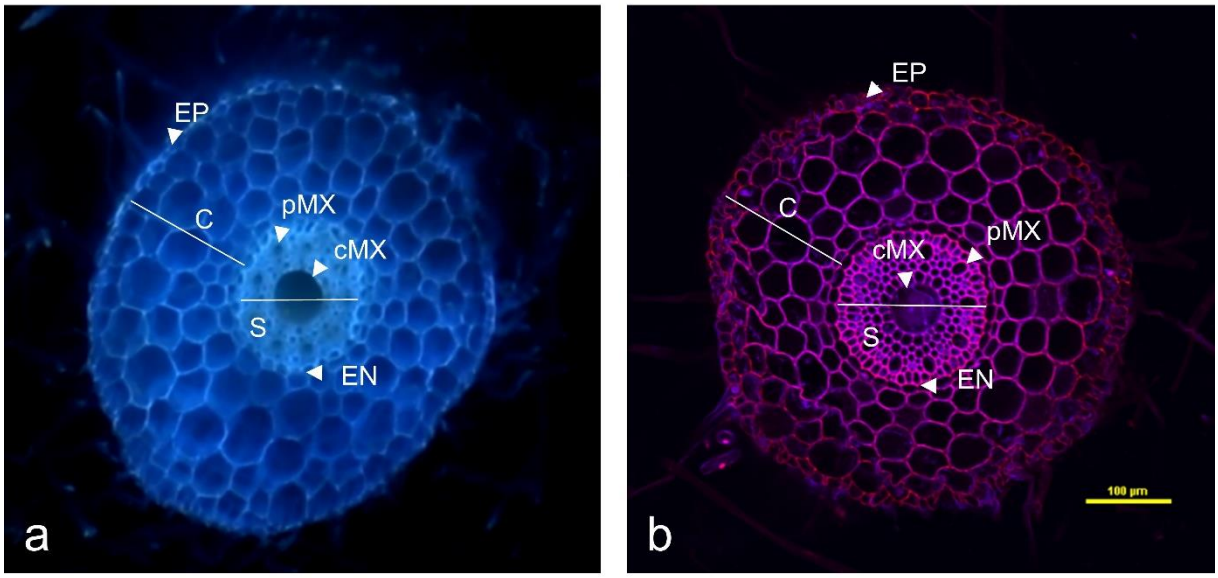

Figure 5-1: Transverse sections of non-infected segments of barley roots imaged with (a) laser ablation tomography and (b) laser scanning confocal microscopy. Tissues are labelled as follows: epidermis (EP), cortex (C), endodermis (EN), stele (S), central metaxylem (cMX), and peripheral metaxylem (pMX). The scale bar is 100 µm

5.4.2 Laser ablation tomography of infected susceptible barley cultivar sections

The examination of multiple LAT images of transverse planes through feeding sites in samples from the susceptible cultivar Sloop (Figure 5-3) shows the following features: a

central metaxylem vessel, several peripheral metaxylem vessels, xylem parenchyma cells and, in some planes, one or more feeding sites. In regions with no visible feeding site, the stele anatomy was similar to the one of a non-infected root. In regions containing feeding sites, it was not systematically possible to clearly distinguish all peripheral metaxylem vessels with either LAT (Figure 5-3) or confocal microscopy (Figure 5-4). With LAT, feeding sites generally appeared like black voids. However, in some cases, thin remnants of inner cell walls were visible (Figure 5-3 c and d). Remnants of inner cell walls could also be seen with confocal microscopy (Figure 5-4). In the LAT images, feeding sites were often surrounded by

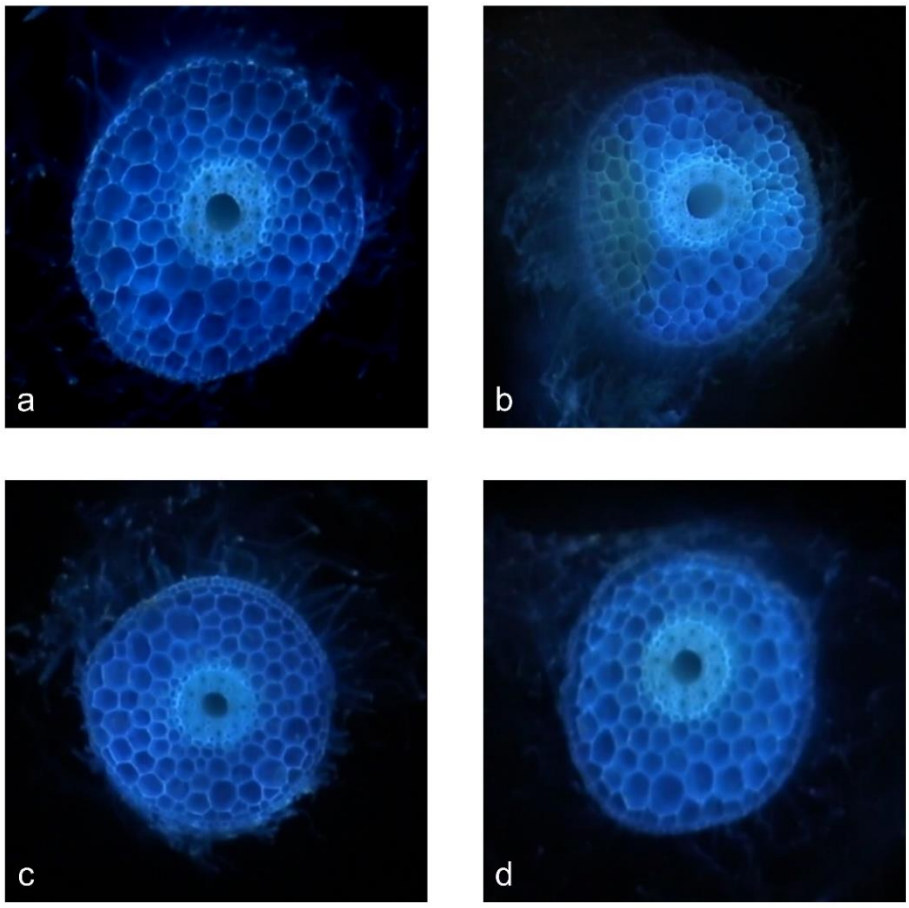

Figure 5-2: Transverse sections of non-infected segments of barley roots imaged with laser ablation tomography after (a) fixation with 70 % ethanol, (b) staining with acid fuchsin, (c) fixation with paraformaldehyde and (d) fixation with paraformaldehyde followed by staining with acid fuchsin

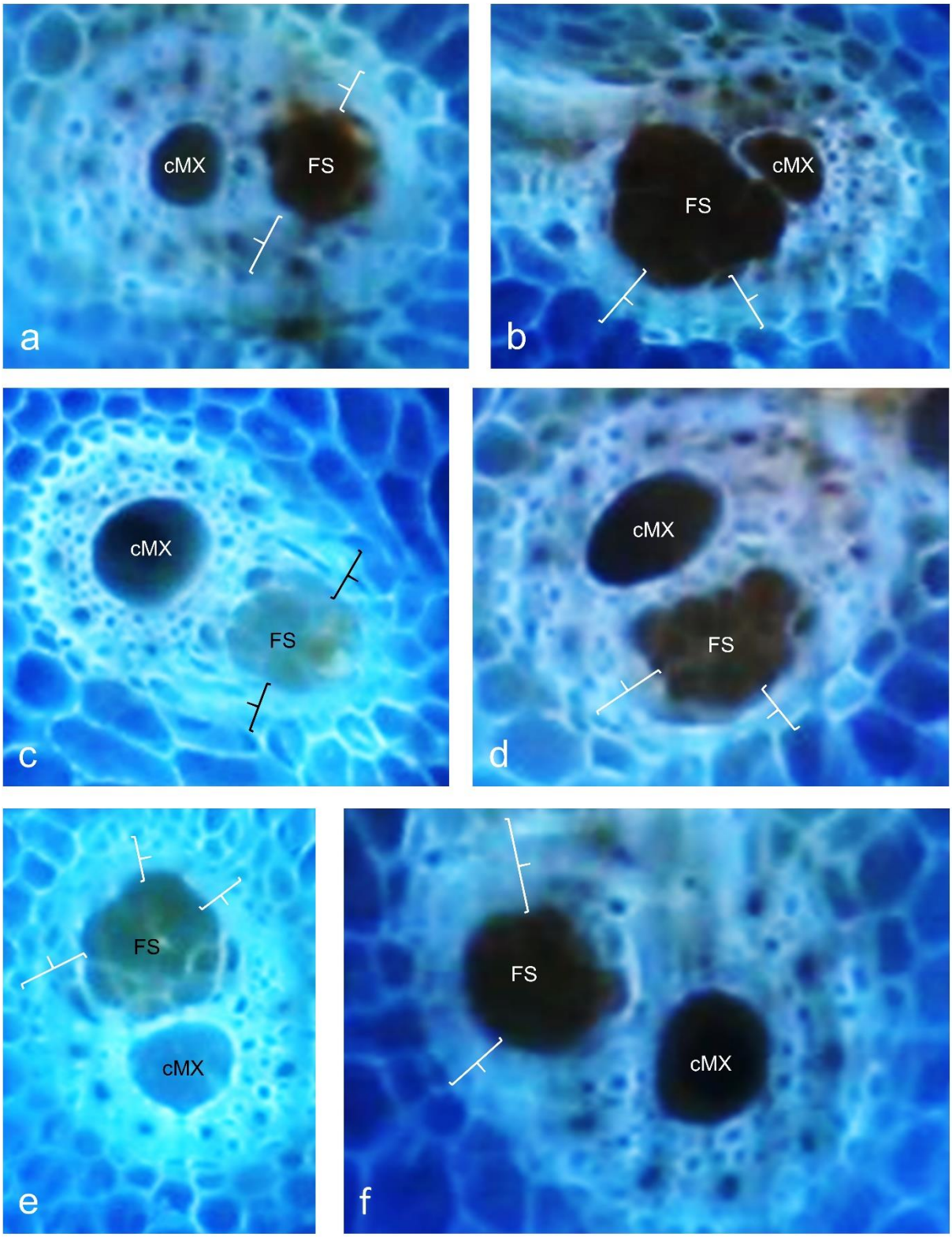

Figure 5-3: Transverse images of the stele region in six root segments (a-f) of the susceptible barley cultivar Sloop. Images were obtained with laser ablation tomography. Each image shows the central metaxylem (cMX) and a feeding site (FS). White and black brackets indicate layers of apparently compressed cells around the feeding sites

diffuse light blue bands. The diffuse light blue bands may represent autofluorescence from many tightly packed cell walls of small compressed cells, such as those that can be seen with confocal microscopy (Figure 5-4).

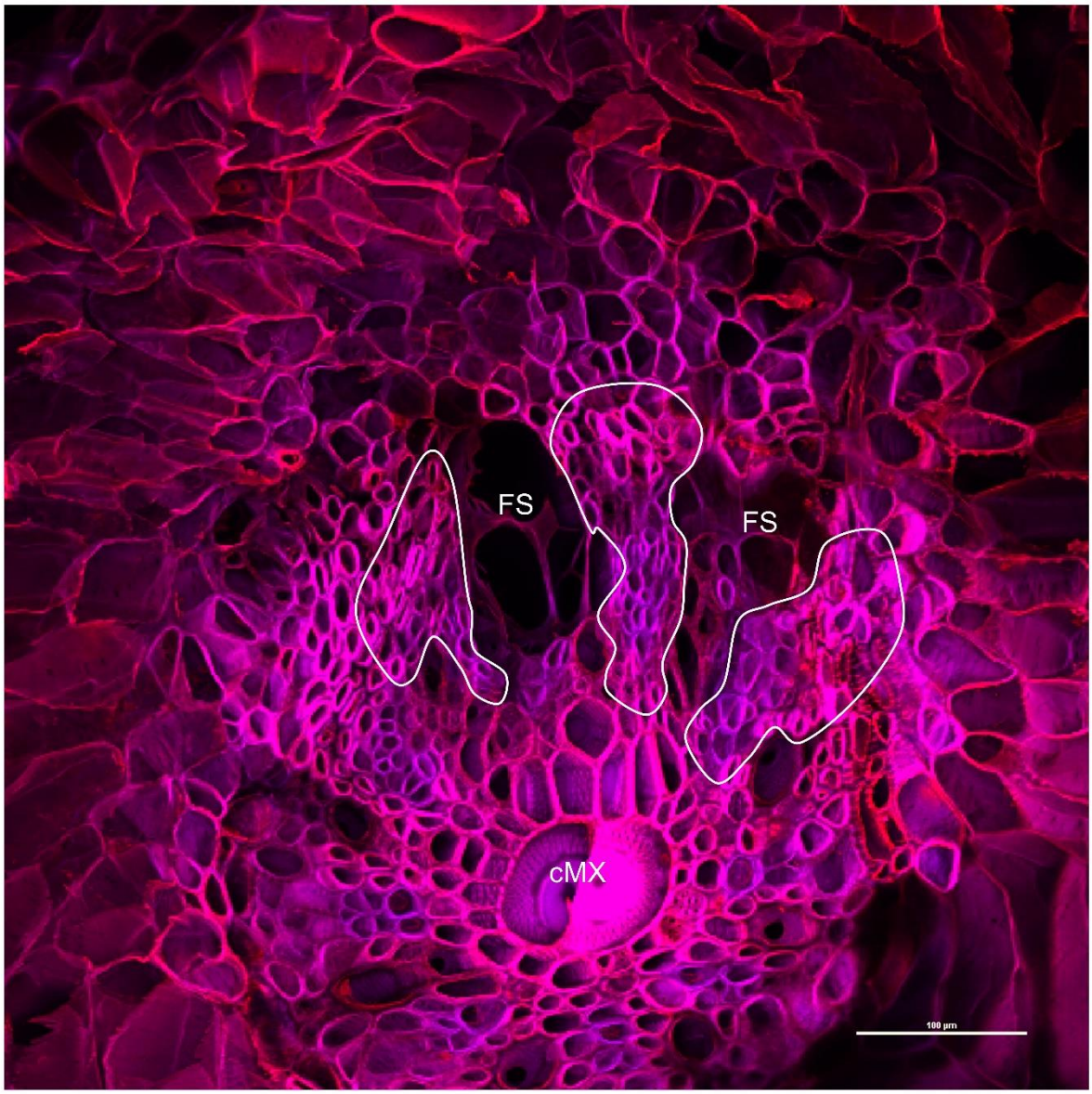

Figure 5-4: Transverse section of infected root tissue from the susceptible barley cultivar, Sloop, stained with calcofluor white and propidium iodide and imaged with laser scanning confocal microscopy. Tissues are labelled as follows: feeding site (FS), central metaxylem (cMX). Compressed stele cells around feeding site are encircled (white lines). The scale bar is 100 µm

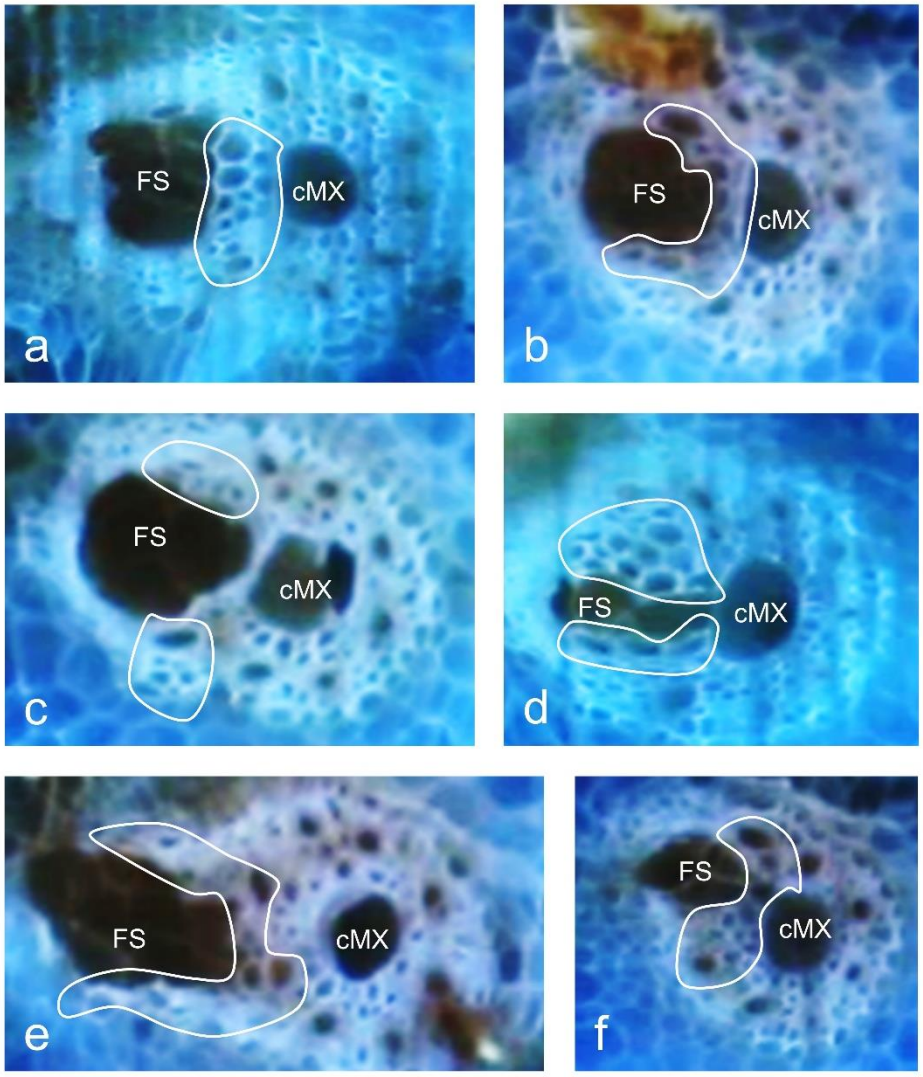

Figure 5-5: Transverse images of the stele region of six root segments (a-f) of the resistant barley cultivar Sloop SA. Images were obtained with laser ablation tomography. Each image shows the central metaxylem (cMX) and a feeding site (FS). Some of the regions surrounding the feeding site (encircled by white lines) contain large stele cells

5.4.3 Laser ablation tomography of infected resistant barley cultivar sections

Transverse sections from roots of the resistant barley cultivar Sloop SA showed similar core anatomical features as in the susceptible cultivar (Figure 5-5 and Figure 5-6). There were, however, some differences in and around the feeding site. Adjacent to the feeding site, and often between the feeding site and the central metaxylem, xylem parenchyma cells seemed

enlarged. In some images, it was difficult to define the exact boundary between the enlarged surrounding cells and the feeding site (Figure 5-5 c and e, and Figure 5-6).

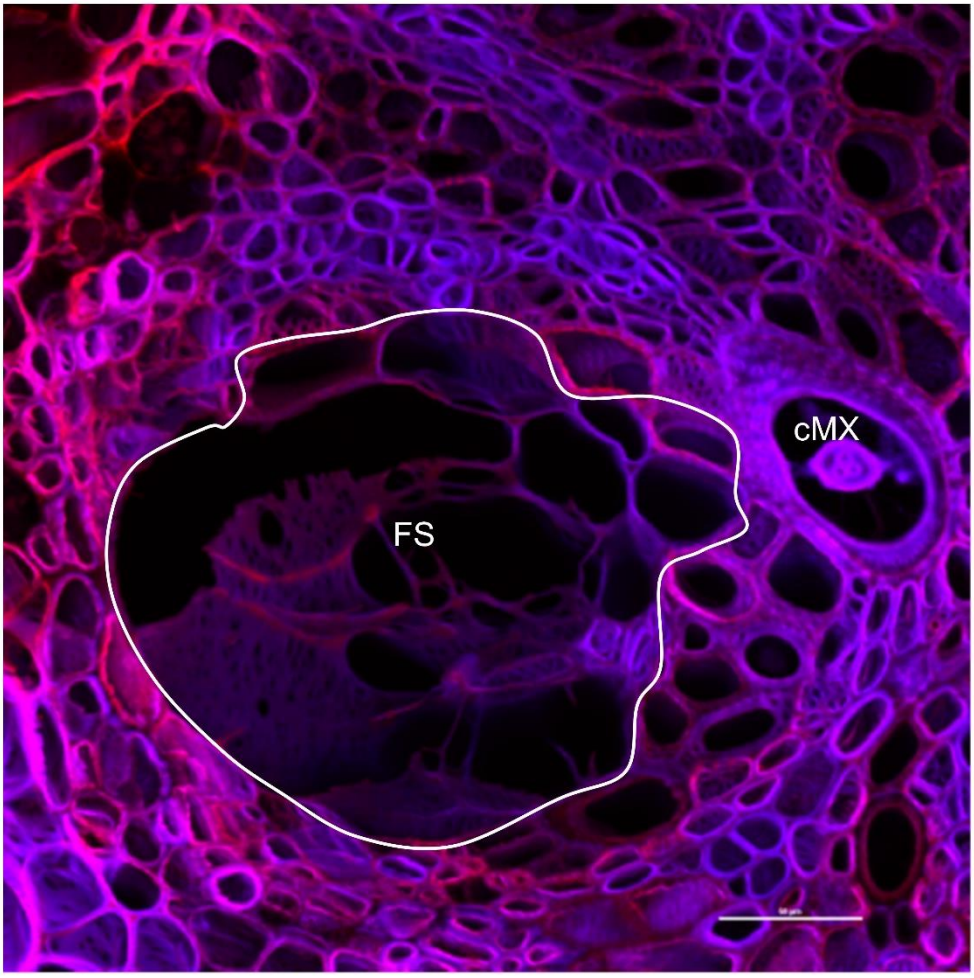

Figure 5-6: Transverse section of infected root tissue from resistant barley cultivar Sloop SA, stained with calcofluor white and propidium iodide and imaged using laser scanning confocal microscopy. The white line represents the boundary of the feeding site. Other tissues are labelled as follows: feeding site (FS) and central metaxylem (cMX). The scale bar is 50 µm

5.4.4 Laser ablation tomography of the entire infected barley root segment

Laser ablation tomography allowed for visualisation of an entire infected barley root segment. In several of the LAT images of barley roots infected with *H. avenae*,

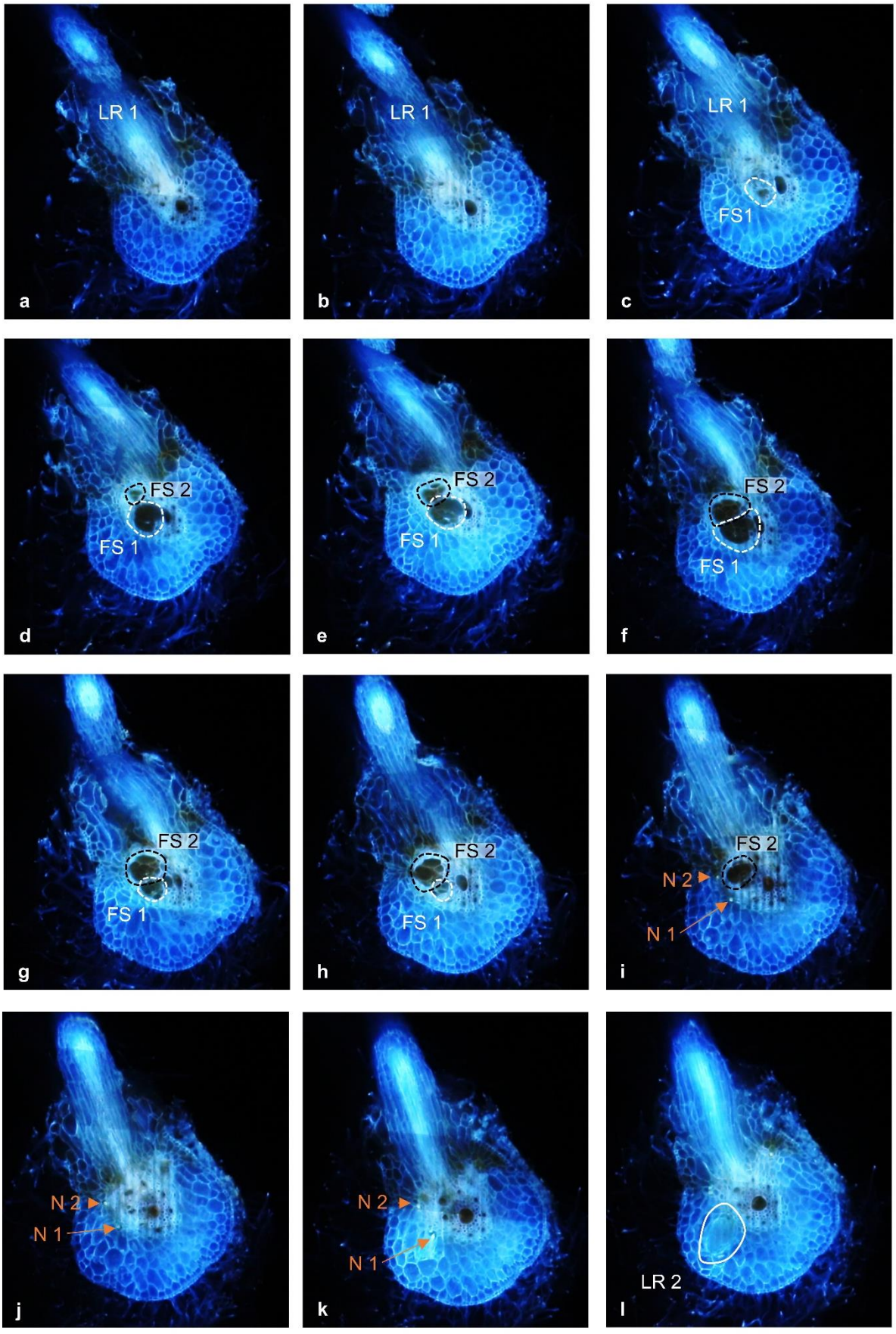

Figure 5-7: Laser ablation tomography images at a 25-µm intervals through a segment of a barley root containing two cereal cyst nematodes and two feeding sites. One feeding site, FS1

caption Figure 5-7 continued: (c-h), is contained within the white dotted lines while black dotted lines contained the second feeding site, FS2 (d-i). Orange arrows indicate nematodes N1 and N2 respectively (i-k). The main lateral root, LR1, is indicated in a-c and present in each figure (a-l). The white circle indicates a second, emerging lateral root labelled as LR2 (l)

nematodes or their feeding sites were visible. In each of 12 transverse images sampled at 25 µm intervals through an infected root segment (Figure 5-7) that contains two adjacent feeding sites, a lateral root can be seen, as well the other major features of the root: the epidermis, cortex, stele, and central metaxylem. No signs of altered morphology are observed in the initial sections (Figure 5-7 a and b) or the final section (Figure 5-7 l), all which are similar to the non-infected tissues. In the final section (Figure 5-7 l), a part of a second lateral root is visible. In the other images (Figure 5-7 c-k), one or both feeding sites and nematodes are visible. One feeding site is visible in Figure 5-7 c-h (50 to 175 µm) and the other is visible in Figure 5-7 d-i (75 to 200 µm). The first feeding site is directly adjacent to the central metaxylem walls (Figure 5-7 d-g). The second feeding site is directly adjacent to the first one (Figure 5-7 e-h). Nonetheless, the two feeding sites are separated from each other with a common and intact cell wall. Neither feeding site is directly connected to the central metaxylem, but both feeding sites are separated from surrounding tissues by intact cell walls. The central portion of each feeding site appears mostly as a dark 'void', with only thin remnants of inner cell walls remaining (Figure 5-8). Cortical cells near the feeding sites seem larger and less regularly shaped than those on the other side of the root. The presence of the feeding sites appears to have affected the positions of the peripheral metaxylem vessels. However, not all peripheral metaxylem vessels are visible; some may have been displaced by, crushed by, or incorporated into the feeding site (Figure 5-7 e-f and Figure 5-8). Bright circles in the cortex correspond to nematodes. Both nematodes are visible in Figure 5-7 i-k (200 to 250 µm).

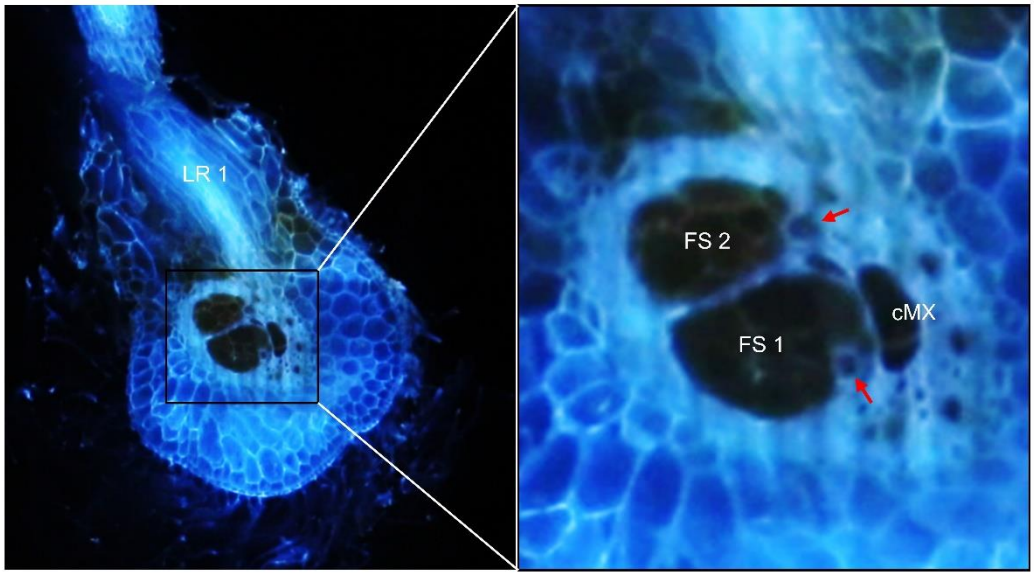

Figure 5-8: Enlargement of part of the image from Figure 5-7 f, showing two adjacent feeding sites (FS 1 and FS 2), each containing remnants of internal cell walls. The two red arrows point to the cells that may be peripheral xylem vessels displaced by the development of the feeding site

5.4.5 Volume assessment

When the image stacks were projected onto each of two orthogonal planes (XZ and YZ), most feeding sites exhibited approximately ellipsoidal shapes (Figure 5-9 b and c). The estimated volumes of individual feeding sites exhibited considerable variation ranging from 7,676 to 118,350 voxels. Sample treatments (ethanol, acid fuchsin, paraformaldehyde, acid fuchsin and paraformaldehyde) had no significant effect on feeding site volume. Across all sample treatments, the mean feeding site volume was significantly greater for the resistant cultivar Sloop SA (35,836 voxels) than for the susceptible cultivar Sloop (29,799 voxels) (p = 0.00533) (Figure 5-10). No consistent morphological differences were observed among sample treatments.

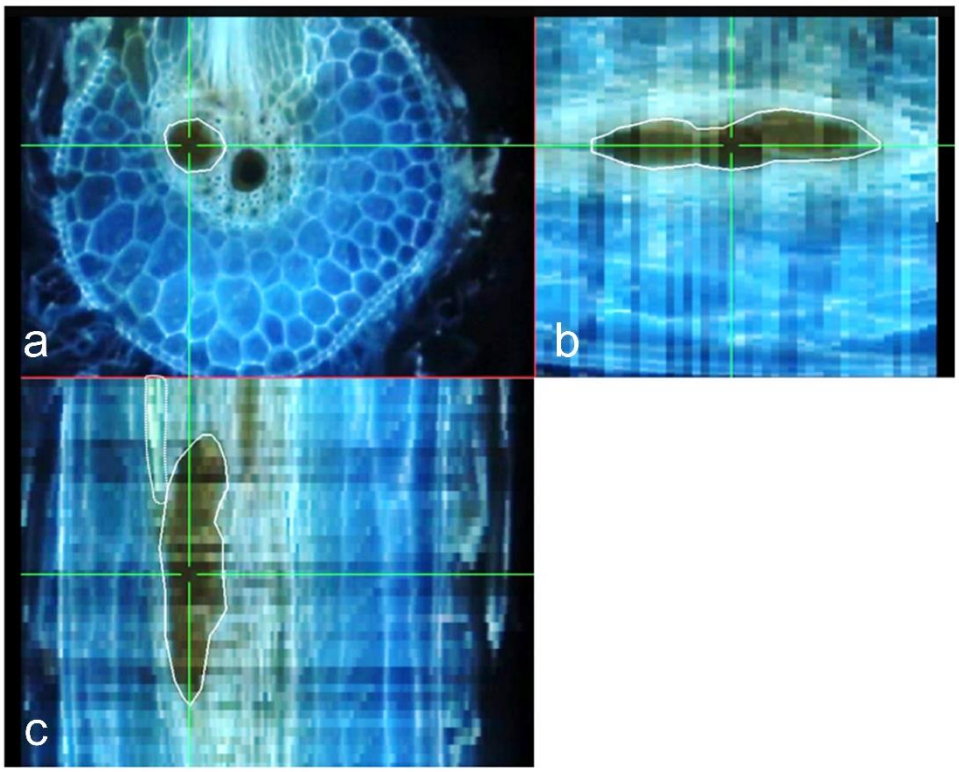

Figure 5-9: Images of a transverse (XY) plane (a), an XY plane (b) and the corresponding YZ plane (c) through a feeding site in a barley root

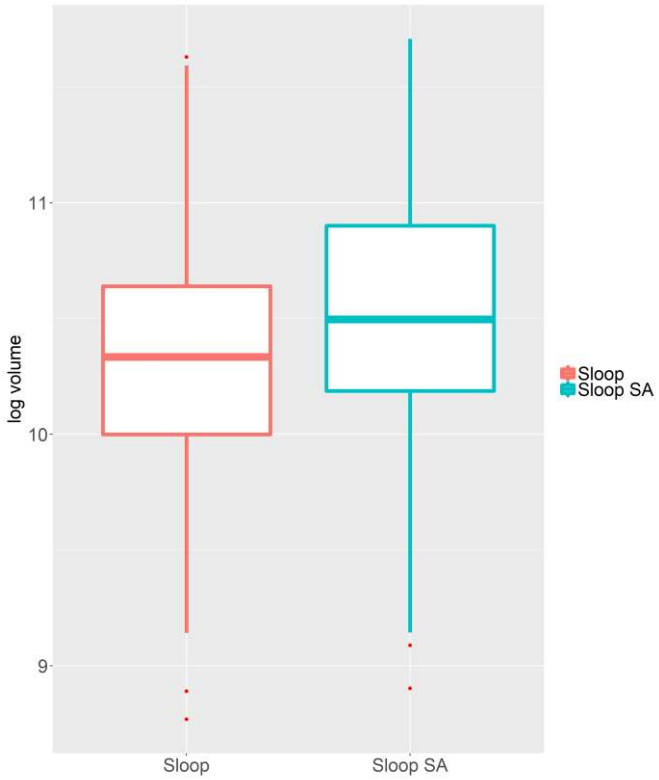

Figure 5-10: Box plots for log transformed volumes of feeding sites in roots of the susceptible cultivar Sloop and the resistant cultivar Sloop SA

5.5 Discussion

The LAT scanning technique was useful for imaging root segments from barley seedlings. A major concern was the thickness of the root, as LAT had previously been applied only to species (maize and common bean) with thicker roots than barley. Although individual transverse images from LAT scan were not as clear as images obtained by laser scanning confocal microscopy of sectioned roots, all main anatomical features could be distinguished. Importantly, LAT provided images at 1-µm intervals throughout each tissue sample, generating much more information than can readily be obtained with conventional sectioning and microscopy. The layer-by-layer data generated with LAT can be used to construct 3D projections that can be virtually sectioned and rotated. Projections of barley root segments sometimes included one or more nematodes and their feeding sites (e.g. Strock et al. submitted).

While confocal imaging required staining with fluorescent dyes, no stains were required for LAT scanning. In LAT scans, the nematodes fluoresced particularly brightly. The observed fluorescence is presumed to have been caused by compositional difference between the tissues of the parasite (mainly proteins) and the cell walls of the host (mainly polysaccharides).

The positions and longitudinal orientation of the nematodes observed in the cortex are consistent with the expectation that, by 10 DAI, nematodes would have migrated through cortex cells and established feeding sites in the stele (Seah et al. 2000). Several fixation and staining techniques were applied here but none of these affected the integrity of the sample or the quality of LAT imaging.

Given that the samples were fixed and critically dried prior to scanning, cytoplasm could not be observed within the feeding sites or other plant cells. Cell walls could be observed, and it

was possible to see differences in cell wall thickness. The main advantage of LAT over microscopy lies in its ability to allow for high-throughput serial optical sectioning through large root segments. LAT scanning made it possible to observe and estimate the volume of multiple feeding sites.

Based on previous research (Aditya et al. 2015; Grymaszewska and Golinowski 1991; Seah et al. 2000; Williams and Fisher 1993), it was expected that, by 10 DAI, the initial feeding cell would have 'recruited' adjacent cells and the interior cell walls of the syncytium would be largely degraded. Consistent with this, the feeding sites appeared as dark 'voids' that were often much larger than surrounding cells. Within some feeding sites, remnants of interior cell walls were observed. In transverse images, the feeding sites were approximately round but in longitudinal images (generated from the volume assessment), they were ellipsoidal. This indicates that the recruitment of cells and early expansion of the feeding site had mainly progressed longitudinally through the stele. Frequently, there were two or more feeding sites in close proximity to each other and this complicated interpretation of individual images. However, it was usually possible to resolve uncertainties by exploring multiple sequential images to determine whether neighbouring features represented two distinct feeding sites or different parts of the same feeding site.

The primary motivation for undertaking this work was to better understand host resistance by comparing the feeding sites in a resistant barley cultivar, Sloop SA, with those in a related susceptible cultivar, Sloop. Some differences that had been reported in cereals (in number and size of vacuoles; in density, apparent metabolic activity and position of the cytoplasm within feeding sites; Aditya et al. (2015); Andres et al. (2001); Grymaszewska and Golinowski (1991); Seah et al. (2000); Williams and Fisher (1993)) could not be investigated here given that plant cell contents are not visible in LAT scans. In contrast, cell walls were clearly visible. This high visibility made it possible to confirm the greater persistence of interior cell

walls within the feeding sites in the roots of a resistant cultivar (Sloop SA) than in the roots of its susceptible parent (Sloop). This finding is consistent with differences that had been noted by Seah et al. (2000) and Aditya et al. (2015) based on microscopic analysis of feeding sites in resistant and susceptible barley cultivars. Another difference that had been observed with microscopy was a tendency for feeding sites to be larger in resistant cultivars (Jones and Dropkin 1975). Nonetheless, this had never been quantified due to limited sampling and to limitations of two-dimensional imaging. With LAT, sufficient data were readily obtained to estimate the volumes of over 40 individual feeding sites from each of the two cultivars. The results indicated that the mean feeding site volume was significantly larger in the resistant cultivar (Sloop SA) than in the susceptible cultivar (Sloop). This result is opposite to what might have been expected, indicating that feeding site volume is not a good indicator of feeding site success. Relative to the large feeding sites, the compact feeding sites in Sloop may be better able to maintain turgor pressure and viability, and/or to deliver a sufficient concentration of nutrients to nematodes. Alternatively, perhaps the large feeding sites in Sloop SA simply expanded more quickly than the nematodes could inject effectors what could cause fatigue.

The cell wall structure inside cyst nematode feeding sites degrades over time. Scanning electron microscopy of feeding sites of potato roots and 3D images of the potato cell walls has shown the progression from cell wall openings through to almost entirely degraded cell walls with only a few remaining ‘pillars’ (Jones and Dropkin 1975). A similar pillar structure has been observed in 3D images of syncytia induced by soybean cyst nematode in *Astragalus sinicus* (Ohtsu et al. 2017). Here, some feeding sites in the roots of susceptible cultivar Sloop had remnants of internal cell walls (Figure 5-3), but there was no evidence of ‘pillars’.

With LAT scanning of root segments, it was possible to investigate the spatial structure of cells near feeding sites: in the stele, cortex, and developing lateral roots. In the susceptible

cultivar, the stele cells around feeding sites were smaller, and the cells seemed to be compressed on the boundaries of the feeding site. In contrast, in the resistant cultivar, the cells around feeding sites were larger than in other parts of the stele. Consistent with the observations made by Williams and Fisher (1993), the cells in the cortex were distorted. In cereal roots infected with cereal cyst nematodes, there is often a proliferation of lateral roots (Aditya et al. 2015; Seah et al. 2000). Consistent with this, the feeding sites observed here were often located near the base of lateral roots. Further, new lateral root initials were observed and their development may have been triggered by nematode infection. New lateral roots may be important in ensuring adequate water and nutrient supply to both the plant and the nematode.

In conclusion, the results presented here demonstrate both the potential and the limitations of LAT for the investigation of plant-nematode interactions in roots. Like many other methods that have been used to observe these interactions, LAT is destructive. As implemented here, it allowed for the observations of plant cell walls but not plant cell contents. Its strength, relative to manual sectioning followed by two-dimensional microscopy, lies in its ability to quickly and automatically generate images at 1-µm intervals throughout a tissue sample. The data acquired in this manner can subsequently be used to generate three-dimensional projections. For the biological system investigated here, this technique made it possible to quantitatively determine that at 10 DAI after inoculation with *H. avenae*, feeding sites in resistant plants were significantly larger than their counterparts in susceptible plants.

Chapter 6 General conclusion

The work presented in this thesis involved several approaches to explore the differential responses to CCN infection between susceptible and resistant barley plants.

One objective was to visualise entire root segments, including feeding sites and nematodes. This was achieved using laser ablation tomography, making it possible to compare feeding sites between resistant and susceptible cultivars. Previous literature had shown that nematode's attraction, penetration, and initial feeding site establishment in the roots of cereal plants occurs in a similar manner regardless of the resistance status (Aditya et al. 2015; Andres et al. 2001; Grymaszewska and Golinowski 1987, 1991; Seah et al. 2000; Williams and Fisher 1993). It has also been shown that further feeding site development slows down in the resistant cultivar. However, the development continues in the susceptible cereal cultivar. My work has quantified differences in feeding site volume at ten days after inoculation between resistant and susceptible barley cultivars. Feeding sites in the susceptible cultivar were significantly smaller than those in the resistant cultivar. This finding seems counter-intuitive, especially if it is expected that large feeding sites have recruited more cells and are more effective in supporting the nematode than small feeding sites. With closer examination of cells surrounding the feeding sites, I noticed that feeding sites in the susceptible cultivar were typically surrounded by compact cell layers of small cells. These cell layers may stabilise the structure of the feeding site, providing the resistance needed to support the high turgor pressure of a large syncytium. In contrast, feeding sites in the resistant cultivars were typically surrounded by less compact layers of larger cells. These feeding sites may lack the support needed for ongoing viability.

Another objective was to gain more information about the cause and effects of resistance in barley roots infected with cereal cyst nematode. Time-course analysis was conducted to detect genes that were differentially expressed in a time-course experiment between inoculated and non-inoculated barley roots, and between the *Rha2* resistant cultivars Sloop SA and Sloop

VIC and the susceptible cultivar, Sloop. Five key genes were identified to have common expression among several time periods for the inoculated resistant cultivars. These expressed genes among all time periods are a gene encoding an ENTH/ANTH/VHS superfamily protein (HORVU3Hr1G009340) and a predicted gene (HORVU4Hr1G001830). The early and middle time periods have two genes in common; a gene encoding a plant regulator RWP-RK family protein (HORVU6Hr1G087410), and a predicted gene (HORVU4Hr1G051900). The middle and late time point have only one gene in common which encodes a haloacid dehalogenease-like hydrolase (HAD) superfamily protein (HORVU0Hr1G017400). Lastly, one gene, encoding a patatin-like protein 4 (HORVU4Hr1G050060) is only expressed in Sloop VIC. Based on the evidence provided above, these selected genes might be involved in the plant resistance reaction against cereal cyst nematode due to the presence in multiple samples and time periods. As none of these genes is in the *Rha2* region, they cannot be the causal gene for resistance. Instead, their differential expression may reflect downstream effects of the resistance mechanism.

A third objective was to understand the genetic cause of resistance. This objective was addressed by fine mapping *Rha2* and exploring of the genes within the *Rha2* region. This investigation started with the use of GBS to discover SNPs in the *Rha2* region. Development of marker assays for those SNPs made it possible to fine map the *Rha2* region. This work started with the existing with DH populations Chebec/Harrington and Clipper/Sahara 3771 and was continued using new progeny obtained by backcrossing *Rha2* from Sloop SA into Sloop. The fine mapping significantly narrowed the candidate region of Kretschmer et al. (1997) to a region of only 978 kbp on the 2H pseudomolecule. That region contains 19 predicted genes, which can be considered as candidate genes for *Rha2*.

Further, the expression of the genes in the candidate region were taken into consideration. Of the 19 predicted genes, only five appear to be expressed in the examined barley roots. A

predicted gene for an aquaporin-like superfamily protein (HORVU2Hr1G097780) showed substantial differential expression within the qPCR experiments reported here. For this gene, the differential expression was confirmed at the early stages of the infection. Consequently, HORVU2Hr1G097780 appears to be a prime candidate gene for *Rha2*. One of the SNPs used for fine-mapping (a G > A SNP assayed by KASP marker wri297) is located within the second exon of this gene. The susceptible cultivar Sloop carries the G allele, as do the reference cultivars Morex, Barke, and Bowman. Resistant cultivars, including Sloop SA and Sloop VIC, carry the A allele. This SNP, which is the only non-synonymous SNP between the HORVU2Hr1G097780 alleles of Sloop and its resistant derivatives (data not shown; personal communication Dr K. Khoo), causes an amino-acid difference (leucine>phenylalanine) at protein position 117. The effect of this difference is not obvious from the sequence alone. In follow-up research conducted recently using *Xenopus* oocytes, the TIP2;2 protein encoded by the Sloop SA had slightly higher water permeability and significantly higher ionic conductance than the TIP2;2 protein encoded by the Sloop allele (personal communication Prof. S. Tyerman). TIP proteins are localised in the tonoplast (vacuolar membrane). Therefore, a difference in permeability of a TIP could affect the vacuolar contents. Aditya et al. (2015) reported significantly larger vacuoles in *Rha2* resistant cultivars compared to susceptible cultivars, which might be influenced by differential transport characteristics.

Based on the comments above, my recommendations for further research are as follows:

1) Further fine mapping with remaining plant material

   Additional selfed progeny from the materials that I developed can be genotyped to potentially discover additional recombinants that could be assessed for resistance in order to further narrow the candidate region.

2) Analysis of additional sequence for the candidate region

   The current length of the candidate region is 978 kbp based on the barley genome assembly. The region includes some repeat sequences and unknown sequences (see

discussion of acetylglutamate kinase sequences in Chapter 4). As new genomic sequences are generated in an international barley pan-genome project (Monat et al. 2019), the *Rha2* region could be further analysed. The additional sequence will probably resolve the current sequence inconsistencies and sequence breaks of unknown sequence. The pan-genome project will include some barley accessions that carry the *Rha2* resistance allele (personal communication A/Prof. K. Chalmers and Prof. D. Mather). Further investigation can be done by comparing the genomic sequence between barley cultivars with and without the *Rha2* resistance allele.

3) Further exploration on the TIP2;2 sequence and expression difference

   The TIP2;2 gene has a non-synonymous SNP and differential expression between resistant and susceptible barley cultivars as shown in this research. Given that preliminary results indicate that the TIP2;2 proteins of susceptible and resistant cultivars have differential transport properties, it is recommended to investigate further these transport properties. Further, the TIP2;2-encoding gene is differential expressed between the resistant and susceptible cultivars, thus further genomic sequence exploration could be done to identify the promotor upstream of this gene and could help explain the differential expression.

4) Laser-assisted microdissection of feeding site for expression analysis

   To extend transcriptomic analysis beyond the exploratory work presented in this thesis, I recommend application of laser-assisted microdissection to dissect specific cell types (Kerk et al. 2003). Subsequent to the isolation of the feeding site, RNA extraction and expression analysis could be done only from feeding sites (e.g. Anjam et al. (2016) and Ithal and Mitchum (2011)).

5) *In situ* hybridisation of potential candidate genes

   This technique could be used to hybridise labelled probes with transcripts of interest on preserved root sections. The purpose of this approach would be used to localise the expression of candidate genes in the feeding site or surrounding cells.

6) Proof of gene function in transgenic plants

   Transgenic barley plants with loss-of-function and/or gain-of-function of the gene might provide proof of function. For example consider the gene that encodes TIP2;2. It was upregulated in the inoculated susceptible cultivar compared to the inoculated resistant cultivars. A knock-out or silencing of the aquaporin in a susceptible cultivar may result in the absence of TIP2;2 expression. Plants without TIP2;2 expression could be evaluated for a gain of nematode resistance. There are several transgenic techniques for barley that could be used to knock-out or silence a gene of interest, such as CRISPR/Cas9, RNAi knockdown and a virus-induced transient transformation (Cheuk and Houde 2018; Gasparis et al. 2018; Hinchliffe and Harwood 2019; Kis et al. 2019; Lawrenson and Harwood 2019; Lee et al. 2012; Lightfoot et al. 2017; Zalewski et al. 2012). These techniques have been already applied on barley, but further investigation is required to select the appropriate transgenic technique for the potential candidate gene or genes following from additional sequence analysis.

This research has identified several candidate genes for *Rha2*. A gene that encodes the TIP2;2 tonoplastic intrinsic protein is of particular interest for functional analysis to determine whether differences in its expression and/or sequence affect resistance of barley against cereal cyst nematode (pathotype Ha13).

References

Abramoff M, Magalhaes P, Ram S (2004) Image processing with ImageJ. Biotphotonics Int 11:36-42

Aditya J, Lewis J, Shirley NJ, Tan H-T, Henderson M, Fincher GB, Burton RA, Mather DE, Tucker MR (2015) The dynamics of cereal cyst nematode infection differ between susceptible and resistant barley cultivars and lead to changes in (1,3;1,4)-β-glucan levels and *HvCslF* gene transcript abundance. New Phytol 207:135-147

Altschul SF, Gish W, Miller W, Myers EW, Lipman DJ (1990) Basic local alignment search tool. J Mol Biol 215:403-410

Anders S, Huber W (2010) Differential expression analysis for sequence count data. Genome Biol 11:R106

Andersen K, Andersen S (1968) Inheritance of resistance to *Heterodera avenae* in barley. Nematologica 14:128-130

Andersen S, Andersen K (1973) Linkage between marker genes on barley chromosome 2 and a gene for resistance to *Heterodera avenae*. Hereditas 73:271-276

Andersen K, Andersen S (1982a) Classification of plants resistant to *Heterodera avenae*. EPPO Bull 12:435-437

Andersen S, Andersen K (1982b) Suggestions for determination and terminology of pathotypes and genes for resistance in cyst-forming nematodes, especially *Heterodera avenae*. EPPO Bull 12:379-386

Andersson S (1982) Population dynamics and control of *Heterodera avenae* - A review with some original results. EPPO Bull 12:463-475

Andres MF, Melillo MT, Delibes A, Romero MD, Bleve-Zacheo T (2001) Changes in wheat root enzymes correlated with resistance to cereal cyst nematodes. New Phytol 152:343-354

Anjam MS, Ludwig Y, Hochholdinger F, Miyaura C, Inada M, Siddique S, Grundler FM (2016) An improved procedure for isolation of high-quality RNA from nematode-

infected Arabidopsis roots through laser capture microdissection. Plant Methods 26:12-25

Barcala M, García A, Cabrera J, Casson S, Lindsey K, Favery B, García-Casado G, Solano R, Fenoll C, Escobar C (2010) Early transcriptomic events in microdissected Arabidopsis nematode-induced giant cells. Plant J 61:698-712

Barr AR, Chalmers KJ, Karakousis A, Kretschmer JM, Manning S, Lance RCM, Lewis J, Jeffries SP, Langridge P (1998) RFLP mapping of a new cereal cyst nematode resistance locus in barley. Plant Breed 117:185-187

Barr AR, Karakousis A, Lance RCM, Logue SJ, Manning S, Chalmers KJ, Kretschmer JM, Boyd WJR, Collins HM, Roumeliotis S, Coventry SJ, Moody DB, Read BJ, Poulsen D, Li CD, Platz GJ, Inkerman PA, Panozzo JF, Cullis BR, Smith AB, Lim P, Langridge P (2003) Mapping and QTL analysis of the barley population Chebec × Harrington. Aust J Agric Res 54:1125-1130

Barros J, Serk H, Granlund I, Pesquet E (2015) The cell biology of lignification in higher plants. Ann Bot 115:1053-1074

Berens ML, Berry HM, Mine A, Argueso CT, Tsuda K (2017) Evolution of hormone signaling networks in plant defense. Annu Rev Phytopathol 55:401-425

Bertl A, Kaldenhoff R (2007) Function of a separate NH_3-pore in aquaporin TIP2;2 from wheat. FEBS Lett 581:5413-5417

Besse M, Knipfer T, Miller AJ, Verdeil J-L, Jahn TP, Fricke W (2011) Developmental pattern of aquaporin expression in barley (*Hordeum vulgare* L.) leaves. J Exp Bot 62:4127-4142

Bigeard J, Hirt H (2018) Nuclear signaling of plant MAPKs. Front Plant Sci 9 (469):469

Böckenhoff A, Grundler FMW (2009) Studies on the nutrient uptake by the beet cyst nematode *Heterodera schachtii* by *in situ* microinjection of fluorescent probes into the feeding structures in *Arabidopsis thaliana*. Parasitology 109:249-255

Brown RH (1982) Studies on the Australian pathotype of *Heterodera avenae*. EPPO Bull 12:413-416

Brown RH (1984) Ecology and control of cereal cyst nematode (*Heterodera avenae*) in southern Australia. J Nematol 16:216-222

Bybd DW, Kirkpatrick T, Barker KR (1983) An improved technique for clearing and staining plant tissues for detection of nematodes. J Nematol 15:142-143

Cai D, Kleine M, Kifle S, Harloff HJ, Sandal NN, Marcker KA, Klein-Lankhorst RM, Salentijn EM, Lange W, Stiekema WJ, Wyss U, Grundler FM, Jung C (1997) Positional cloning of a gene for nematode resistance in sugar beet. Science 275:832-834

Caparrós-Martin JA, McCarthy-Suárez I, Culiáñez-Macià FA (2013) HAD hydrolase function unveiled by substrate screening: enzymatic characterization of *Arabidopsis thaliana* subclass I phosphosugar phosphatase AtSgpp. Planta 237:943-954

Caparrós-Martin JA, McCarthy-Suárez I, Culiáñez-Macià FA (2014) The kinetic analysis of the substrate specificity of motif 5 in a HAD hydrolase-type phosphosugar phosphatase of *Arabidopsis thaliana*. Planta 240:479-487

Chardin C, Meyer C, Girin T, Krapp A, Roudier F (2014) The plant RWP-RK transcription factors: key regulators of nitrogen responses and of gametophyte development. J Exp Bot 65:5577-5587

Chaumont F, Barrieu F, Wojcik E, Chrispeels MJ, Jung R (2001) Aquaporins constitute a large and highly divergent protein family in maize. Plant Physiol 125:1206-1215

Chen C, Cui L, Chen Y, Zhang H, Liu P, Wu P, Qiu D, Zou J, Yang D, Yang L, Liu H, Zhou Y, Li H (2017) Transcriptional responses of wheat and the cereal cyst nematode *Heterodera avenae* during their early contact stage. Sci Rep 7:14471

Cheng J, Song N, Wu J (2018) A patatin-like protein synergistically regulated by jasmonate and ethylene signaling pathways plays a negative role in *Nicotiana attenuata* resistance to *Alternaria alternata*. Plant Diversity 41:7-12

Cheuk A, Houde M (2018) A new barley stripe mosaic virus allows large protein overexpression for rapid function analysis. Plant Physiol 176:1919-1931

Chimungu JG, Brown KM, Lynch JP (2014) Reduced root cortical cell file number improves drought tolerance in maize. Plant Physiol 166:1943-1955

Chimungu JG, Loades KW, Lynch JP (2015a) Root anatomical phenes predict root penetration ability and biomechanical properties in maize (*Zea Mays*). J Exp Bot 66:3151-3162

Chimungu JG, Maliro MFA, Nalivata PC, Kanyama-Phiri G, Brown KM, Lynch JP (2015b) Utility of root cortical aerenchyma under water limited conditions in tropical maize (*Zea mays* L.). Field Crops Res 171:86-98

Choi HW, Klessig DF (2016) DAMPs, MAMPs, and NAMPs in plant innate immunity. BMC Plant Biol 16:232

Chronis D, Chen S, Lu S, Hewezi T, Carpenter SCD, Loria R, Baum TJ, Wang X (2013) A ubiquitin carboxyl extension protein secreted from a plant-parasitic nematode *Globodera rostochiensis* is cleaved *in planta* to promote plant parasitism. Plant J 74:185-196

Colmsee C, Beier S, Himmelbach A, Schmutzer T, Stein N, Scholz U, Mascher M (2015) BARLEX – the barley draft genome explorer. Mol Plant 8:964-966

Cook DE, Lee TG, Guo X, Melito S, Wang K, Bayless AM, Wang J, Hughes TJ, Willis DK, Clemente TE, Diers BW, Jiang J, Hudson ME, Bent AF (2012) Copy number variation of multiple genes at *Rhg1* mediates nematode resistance in soybean. Science 338:1206-1209

Cook R (1982) Cereal and grass hosts of some gramineous cyst nematodes. EPPO Bulletin 12:399-411

Cook R, Noel GR (2002) Resistance to plant-parasitic nematodes: Cyst Nematodes: *Globodera* and *Heterodera*. CABI Publishing, Wallingford, pp 71- 105

Cook R, Rivoal R (1998) Genetics of resistance and parasitism. In: Sharma SB (ed) The cyst nematodes. Springer Netherlands, Dordrecht, pp 322-352

Cook R, York PA (1982) Resistance of cereals to *Heterodera avenae*: methods of investigation, sources and inheritance of resistance. EPPO Bull 12:423-434

Cotten J, Hayes JD (1969) Genetic resistance to the cereal cyst nematode (*Heterodera avenae*). Heredity 24:593-600

Cotton JA, Lilley CJ, Jones LM, Kikuchi T, Reid AJ, Thorpe P, Tsai IJ, Beasley H, Blok V, Cock PJA, den Akker SE-v, Holroyd N, Hunt M, Mantelin S, Naghra H, Pain A, Palomares-Rius JE, Zarowiecki M, Berriman M, Jones JT, Urwin PE (2014) The genome and life-stage specific transcriptomes of *Globodera pallida* elucidate key aspects of plant parasitism by a cyst nematode. Genome Biol 15:R43

Cox DR, Hinkley DV (1974) Theoretical statistics. Chapman and Hall, London

Cui Jk, Huang WK, Peng H, Liu SM, Wang GF, Kong LA, Peng DL (2015) A new pathotype characterization of Daxing and Huangyuan populations of cereal cyst nematode (*Heterodera avenae*) in China. J Integr Agric 14:724-731

Cui JK, Peng H, Huang WK, Liu SM, Wu D, Kong LA, He W, Peng DL (2017) Phenotype and cellular response of wheat lines carrying *Cre* genes to *Heterodera avenae* pathotype Ha91. Plant Dis 101:1885-1894

Curtis RHC (2008) Plant-nematode interactions: environmental signals detected by the nematode's chemosensory organs control changes in the surface cuticle and behaviour. Parasite 15:310-316

Dayteg C, Rasmussen M, Tuvesson S, Merker A, Jahoor A (2008) Development of an ISSR-derived PCR marker linked to nematode resistance (*Ha2*) in spring barley. Plant Breed 127:24-27

de Almeida Engler J, Rodiuc N, Smertenko A, Abad P (2010) Plant actin cytoskeleton re-modeling by plant parasitic nematodes. Plant Signal Behav 5:213-217

de Almeida Engler J, Van Poucke K, Karimi M, De Groodt R, Gheysen G, Engler G, Gheysen G (2004) Dynamic cytoskeleton rearrangements in giant cells and syncytia of nematode-infected roots. Plant J 38:12-26

Delibes A, Romero D, Aguaded S, Duce A, Mena M, Lopez-Braña I, Andrés M-F, Martin-Sanchez J-A, García-Olmedo F (1993) Resistance to the cereal cyst nematode (*Heterodera avenae* Woll.) transferred from the wild grass *Aegilops ventricosa* to hexaploid wheat by a "stepping-stone" procedure. Theor Appl Genet 87:402-408

Eastwood RF, Lagudah ES, Appels R (1994) A directed search for DNA sequences tightly linked to cereal cyst nematode resistance genes in *Triticum tauschii*. Genome 37:311-319

Ellenby C, Perry RN (1976) The influence of the hatching factor on the water uptake of the second stage larva of the potato cyst nematode *Heterodera rostochiensis*. J Exp Bio 64:141-147

Endo BY (1965) Histological responses of resistant and susceptible soybean varieties and backcross progeny to entry and development of *Heterodera glycines*. Phytopathology 55:375-381

Endo BY (1991) Ultrastructure of initial responses of susceptible and resistant soybean roots to infection by *Heterodera glycines*. Revue de Nématologie 14:73-94

Fernandez D, Petitot A-S, Grossi de Sá M, Nguyen VP, de Almeida Engler J, Kyndt T (2015) Chapter Eight - Recent Advances in Understanding Plant–Nematode Interactions in Monocots. In: Escobar C, Fenoll C (eds) Advances in Botanical Research. Academic Press, pp 189-219

Fioretti L, Porter A, Haydock PJ, Curtis RHC (2002) Monoclonal antibodies reactive with secreted–excreted products from the amphids and the cuticle surface of *Globodera pallida* affect nematode movement and delay invasion of potato roots. Int J Parasitol 32:1709-1718

Fisher JM (1982) Towards a consistent laboratory assay for resistance to *Heterodera avenae*. EPPO Bull 12:445-449

Fosu-Nyarko J, Nicol P, Naz F, Gill R, Jones MGK (2016) Analysis of the transcriptome of the infective stage of the beet cyst nematode, *H. schachtii*. PLoS ONE 11:e0147511

Francoz E, Ranocha P, Nguyen-Kim H, Jamet E, Burlat V, Dunand C (2015) Roles of cell wall peroxidases in plant development. Phytochemistry 112:15-21

Gasparis S, Kała M, Przyborowski M, Łyżnik LA, Orczyk W, Nadolska-Orczyk A (2018) A simple and efficient CRISPR/Cas9 platform for induction of single and multiple, heritable mutations in barley (*Hordeum vulgare* L.). Plant Methods 14:111

Gattolin S, Sorieul M, Hunter PR, Khonsari RH, Frigerio L (2009) *In vivo* imaging of the tonoplast intrinsic protein family in Arabidopsis roots. BMC Plant Biol 9:133

Golinowski W, Grundler F, Sobczak M (1999) Ultrastructure of feeding plugs and feeding tubes formed by *Heterodera schachtii*. Nematology 1:363

Goverse A, Smant G (2014) The activation and suppression of plant innate immunity by parasitic nematodes. Annu Rev Phytopathol 52:243-265

Greenland AJ, Lewis DH (1984) Amines in barley leaves infected by brown rust and their possible relevance to formation of 'green islands'. New Phytol 96:283-291

Grundler FMW, Sobczak M, Golinowski W (1998) Formation of wall openings in root cells of *Arabidopsis thaliana* following infection by the plant-parasitic nematode *Heterodera schachtii*. Eur J Plant Pathol 104:545-551

Grymaszewska G, Golinowski W (1987) Changes in the structure of wheat (*Triticum aestivum* L.) roots in varieties susceptible and resistant to infestation by *Heterodera avenae* Woll. Acta Soc Bot Pol 56:381-389

Grymaszewska G, Golinowski W (1991) Structure of syncytia induced by *Heterodera avenae* Woll. in roots of susceptible and resistant wheat (*Triticum aestivum L.*). J Phytopathol 133:307-319

Hanson PI, Otto H, Barton N, Jahn R (1995) The N-ethylmaleimide-sensitive fusion protein and α-SNAP induce a conformational change in syntaxin. J Biol Chem 270:16955-16961

Heinrich T, Bartlem D, Jones MGK (1998) Molecular aspects of plant-nematode interactions and their exploitation for resistance strategies. Australas Plant Pathol 27:59-72

Hellemans J, Mortier G, De Paepe A, Speleman F, Vandesompele J (2007) qBase relative quantification framework and software for management and automated analysis of real-time quantitative PCR data. Genome Biol 8:R19

Herbig K, Chiang EP, Lee LR, Hills J, Shane B, Stover PJ (2002) Cytoplasmic serine hydroxymethyltransferase mediates competition between folate-dependent deoxyribonucleotide and S-adenosylmethionine biosyntheses. J Biol Chem 277:38381-38389

Hewezi T, Howe P, Maier TR, Hussey RS, Mitchum MG, Davis EL, Baum TJ (2008) Cellulose binding protein from the parasitic nematode *Heterodera schachtii* interacts with Arabidopsis pectin methylesterase: cooperative cell wall modification during parasitism. Plant Cell 20:3080-3093

Hinchliffe A, Harwood WA (2019) Agrobacterium-Mediated Transformation of Barley Immature Embryos. In: Harwood WA (ed) Barley: Methods and protocols. Springer New York, New York, NY, pp 115-126

Hofmann J, Grundler F (2007) How do nematodes get their sweets? Solute supply to sedentary plant-parasitic nematodes. Nematology 9:451-458

Holbein J, Grundler FMW, Siddique S (2016) Plant basal resistance to nematodes: an update. J Exp Bot 67:2049-2061

Holtmann B, Kleine M, Grundler FMW (2000) Ultrastructure and anatomy of nematode-induced syncytia in roots of susceptible and resistant sugar beet. Protoplasma 211:39-50

Hosseini P, Matthews BF (2014) Regulatory interplay between soybean root and soybean cyst nematode during a resistant and susceptible reaction. BMC Plant Biol 14:300

Hove RM, Ziemann M, Bhave M (2015) Identification and expression analysis of the barley (*Hordeum vulgare* L.) aquaporin gene family. PLoS ONE 10:e0128025

Hu Y, You J, Li C, Williamson VM, Wang C (2017) Ethylene response pathway modulates attractiveness of plant roots to soybean cyst nematode *Heterodera glycines*. Sci Rep 7:41282-41282

Hückelhoven R, Fodor J, Preis C, Kogel K-H (1999) Hypersensitive cell death and papilla formation in barley attacked by the powdery mildew fungus are associated with hydrogen peroxide but not with salicylic acid accumulation. Plant Physiol 119:1251-1260

Hückelhoven R, Fodor J, Trujillo M, Kogel KH (2000) Barley *Mla* and *Rar* mutants compromised in the hypersensitive cell death response against *Blumeria graminis* f.sp. *hordei* are modified in their ability to accumulate reactive oxygen intermediates at sites of fungal invasion. Planta 212:16-24

Hückelhoven R, Kogel K-H (1998) Tissue-specific superoxide generation at interaction sites in resistant and susceptible near-isogenic barley lines attacked by the powdery mildew fungus (*Erysiphe graminis* f. sp. *hordei*). Mol Plant Microbe Interact 11:292-300

Ithal N, Mitchum MG (2011) Laser capture microdissection of nematode feeding cells. Methods Mol Biol 712:227-240

Ithal N, Recknor J, Nettleton D, Hearne L, Maier T, Baum TJ, Mitchum MG (2007) Parallel genome-wide expression profiling of host and pathogen during soybean cyst nematode infection of soybean. Mol Plant Microbe Interact 20:293-305

Jahier J, Abelard P, Tanguy M, Dedryver F, Rivoal R, Khatkar S, Bariana HS, Koebner R (2001) The *Aegilops ventricosa* segment on chromosome 2AS of the wheat cultivar 'VPM1' carries the cereal cyst nematode resistance gene *Cre5*. Plant Breed 120:125-128

Jahier J, Tanguy AM, Abelard P, Rivoal R (1996) Utilization of deletions to localize a gene for resistance to the cereal cyst nematode, *Heterodera avenue*, on an *Aegilops ventricosa* chromosome. Plant Breed 115:282-284

Jain S, Chittem K, Brueggeman R, Osorno JM, Richards J, Nelson BD, Jr. (2016) Comparative transcriptome analysis of resistant and susceptible common bean genotypes in response to soybean cyst nematode infection. PLoS ONE 11:e0159338

Jayatilake DV, Tucker EJ, Brueggemann J, Lewis J, Garcia M, Dreisigacker S, Hayden MJ, Chalmers K, Mather DE (2015) Genetic mapping of the *Cre8* locus for resistance against cereal cyst nematode (*Heterodera avenae* Woll.) in wheat. Mol Breed 35:66

Jimenez-Atienzar M, Cabanes J, Gandia-Herrero F, Escribano J, Garcia-Carmona F, Perez-Gilabert M (2003) Determination of the phospholipase activity of patatin by a continuous spectrophotometric assay. Lipids 38:677-682

Jones MG, Northcote DH (1972) Nematode-induced syncytium: a multinucleate transfer cell. J Cell Sci 10:789-809

Jones MGK (1981) Host cell responses to endoparasitic nematode attack: structure and function of giant cells and syncytia. Ann Appl Biol 97:353-372

Jones MGK, Dropkin VH (1975) Scanning electron microscopy of syncytial transfer cells induced in roots by cyst nematodes. Physiol Plant Pathol 7:259-263

Juvale PS, Baum TJ (2018) “Cyst-ained” research into *Heterodera* parasitism. PLOS Pathogens 14:e1006791

Kammerhofer N, Radakovic Z, Regis JMA, Dobrev P, Vankova R, Grundler FMW, Siddique S, Hofmann J, Wieczorek K (2015) Role of stress-related hormones in plant defence during early infection of the cyst nematode *Heterodera schachtii* in Arabidopsis. New Phytol 207:778-789

Kang W, Zhu X, Wang Y, Chen L, Duan Y (2018) Transcriptomic and metabolomic analyses reveal that bacteria promote plant defense during infection of soybean cyst nematode in soybean. BMC Plant Biol 18:86

Karakousis A, Barr AR, Kretschmer JM, Manning S, Jefferies SP, Chalmers KJ, Islam AKM, Langridge P (2003) Mapping and QTL analysis of the barley population Clipper × Sahara. Aust J Agric Res 54:1137-1140

Kerk NM, Ceserani T, Tausta SL, Sussex IM, Nelson TM (2003) Laser capture microdissection of cells from plant tissues. Plant Physiol 132:27-35

Kim KH, Kabir E, Jahan SA (2017) Exposure to pesticides and the associated human health effects. Sci Total Environ 575:525-535

Kim YH, Riggs RD, Kim KS (1987) Structural changes associated with resistance of soybean to *Heterodera glycines*. J Nematol 19:177-187

Kis A, Hamar É, Tholt G, Bán R, Havelda Z (2019) Creating highly efficient resistance against wheat dwarf virus in barley by employing CRISPR/Cas9 system. Plant Biotechnol J NA

Klink VP, Hosseini P, Matsye P, Alkharouf NW, Matthews BF (2009) A gene expression analysis of syncytia laser microdissected from the roots of the *Glycine max* (soybean) genotype PI 548402 (Peking) undergoing a resistant reaction after infection by *Heterodera glycines* (soybean cyst nematode). Plant Mol Biol 71:525-567

Klink VP, Hosseini P, Matsye PD, Alkharouf NW, Matthews BF (2010) Syncytium gene expression in *Glycine max* [PI 88788] roots undergoing a resistant reaction to the parasitic nematode *Heterodera glycines*. Plant Physiol Biochem 48:176-193

Kong LA, Wu DQ, Huang WK, Peng H, Wang GF, Cui JK, Liu SM, Li ZG, Yang J, Peng DL (2015) Large-scale identification of wheat genes resistant to cereal cyst nematode *Heterodera avenae* using comparative transcriptomic analysis. BMC Genomics 16:801

Kort J, Dantuma G, van Essen A (1964) On biotypes of the cereal-root eelworm (*Heterodera avenae*) and resistance in oats and barley. Neth J Plant Path 70:9-17

Kretschmer JM, Chalmers KJ, Manning S, Karakousis A, Barr AR, Islam A, Logue SJ, Choe YW, Barker SJ, Lance RCM, Langridge P (1997) RFLP mapping of the *Ha2* cereal cyst nematode resistance gene in barley. Theor Appl Genet 94:1060-1064

Kumar M, Gantasala NP, Roychowdhury T, Thakur PK, Banakar P, Shukla RN, Jones MGK, Rao U (2014) *De novo* transcriptome sequencing and analysis of the cereal cyst nematode, *Heterodera avenae*. PLoS ONE 9 (5)

La Camera S, Geoffroy P, Samaha H, Ndiaye A, Rahim G, Legrand M, Heitz T (2005) A pathogen-inducible patatin-like lipid acyl hydrolase facilitates fungal and bacterial host colonization in Arabidopsis. Plant J 44:810-825

Lagudah ES, Moullet O, Appels R (1997) Map-based cloning of a gene sequence encoding a nucleotide binding domain and a leucine-rich region at the *Cre3* nematode resistance locus of wheat. Genome 40:659-665

Lawrenson T, Harwood WA (2019) Creating targeted gene knockouts in barley using CRISPR/Cas9. Barley. Springer, pp 217-232

Le Gall H, Philippe F, Domon J-M, Gillet F, Pelloux J, Rayon C (2015) Cell wall metabolism in response to abiotic stress. Plants 4:112

Lee WS, Hammond-Kosack KE, Kanyuka K (2012) *Barley Stripe Mosaic Viru*s-mediated tools for investigating gene function in cereal plants and their pathogens: virus-induced gene silencing, host-mediated gene silencing, and virus-mediated overexpression of heterologous protein. Plant Physiol 160:582-590

Lewis JG, Matic M, McKay AC (2009) Success of cereal cyst nematode resistance in Australia: history and status of resistance screening systems. Proceedings of the First Workshop of the International Cereal Cyst Nematode Initiative. International Maize and Wheat Improvement Centre (CIMMYT), Addis Ababa, pp 137-142

Li B, Sun J-M, Wang L, Zhao R-J, Wang L-Z (2014) Comparative analysis of gene expression profiling between resistant and susceptible varieties infected with soybean cyst nematode race 4 in *Glycine max*. J Integr Agric 13:2594-2607

Li S, Chen Y, Zhu X, Wang Y, Jung KH, Chen L, Xuan Y, Duan Y (2018) The transcriptomic changes of Huipizhi Heidou (*Glycine max*), a nematode-resistant black soybean during *Heterodera glycines* race 3 infection. J Plant Phy 220:96-104

Lightfoot DJ, Mcgrann GRD, Able AJ (2017) The role of a cytosolic superoxide dismutase in barley–pathogen interactions. Mol Plant Pathol 18:323-335

Lilley CJ, Atkinson HJ, Urwin PE (2005) Molecular aspects of cyst nematodes. Wiley-Blackwell, pp 577-588

Liu S, Kandoth PK, Lakhssassi N, Kang J, Colantonio V, Heinz R, Yeckel G, Zhou Z, Bekal S, Dapprich J, Rotter B, Cianzio S, Mitchum MG, Meksem K (2017) The soybean *GmSNAP18* gene underlies two types of resistance to soybean cyst nematode. Nat Commun 8:14822

Liu S, Kandoth PK, Warren SD, Yeckel G, Heinz R, Alden J, Yang C, Jamai A, El-Mellouki T, Juvale PS, Hill J, Baum TJ, Cianzio S, Whitham SA, Korkin D, Mitchum MG, Meksem K (2012) A soybean cyst nematode resistance gene points to a new mechanism of plant resistance to pathogens. Nature 492:256-260

Lopez F, Bousser A, Sissoëff I, Hoarau J, Mahé A (2004) Characterization in maize of ZmTIP2-3, a root-specific tonoplast intrinsic protein exhibiting aquaporin activity. J Exp Bot 55:539-541

Loqué D, Ludewig U, Yuan L, von Wirén N (2005) Tonoplast intrinsic proteins AtTIP2;1 and AtTIP2;3 facilitate NH_3 transport into the vacuole. Plant Physiol 137:671-680

Love M, Anders S, Kim V, Huber W (2015) RNA-Seq workflow: gene-level exploratory analysis and differential expression. F1000Research 4

Love MI, Huber W, Anders S (2014) Moderated estimation of fold change and dispersion for RNA-seq data with DESeq2. Genome Biol 15:550

Mahalingam R, Skorupska HT (1996) Cytological expression of early response to infection by *Heterodera glycines* Ichinohe in resistant PI 437654 soybean. Genome 39:986-998

Mascher M, Gundlach H, Himmelbach A, Beier S, Twardziok SO, Wicker T, Radchuk V, Dockter C, Hedley PE, Russell J, Bayer M, Ramsay L, Liu H, Haberer G, Zhang X-Q, Zhang Q, Barrero RA, Li L, Taudien S, Groth M, Felder M, Hastie A, Šimková H, Staňková H, Vrána J, Chan S, Muñoz-Amatriaín M, Ounit R, Wanamaker S, Bolser D, Colmsee C, Schmutzer T, Aliyeva-Schnorr L, Grasso S, Tanskanen J, Chailyan A, Sampath D, Heavens D, Clissold L, Cao S, Chapman B, Dai F, Han Y, Li H, Li X, Lin C, McCooke JK, Tan C, Wang P, Wang S, Yin S, Zhou G, Poland JA, Bellgard MI, Borisjuk L, Houben A, Doležel J, Ayling S, Lonardi S, Kersey P, Langridge P, Muehlbauer GJ, Clark MD, Caccamo M, Schulman AH, Mayer KFX, Platzer M, Close TJ, Scholz U, Hansson M, Zhang G, Braumann I, Spannagl M, Li C, Waugh R, Stein N (2017) A chromosome conformation capture ordered sequence of the barley genome. Nature 544:427-433

Mazarei M, Liu W, Al-Ahmad H, Arelli PR, Pantalone VR, Stewart CN (2011) Gene expression profiling of resistant and susceptible soybean lines infected with soybean cyst nematode. Theor Appl Genet 123:1193-1206

Meagher JW (1982) Yield loss caused by *Heterodera avenae* in cereal crops grown in a mediterranean climate. EPPO Bull 12:325-331

Mittler R (2017) ROS are good. Trends Plant Sci 22:11-19

Moffett P, Ali S, Magne M, Chen S, Obradovic N, Jamshaid L, Wang X, Bélair G (2015) Analysis of *Globodera rostochiensis* effectors reveals conserved functions of SPRYSEC proteins in suppressing and eliciting plant immune responses. Front Plant Sci 6 (623)

Monat C, Schreiber M, Stein N, Mascher M (2019) Prospects of pan-genomics in barley. Theor Appl Genet 132:785-796

Mouillon J-M, Aubert S, Bourguignon J, Gout E, Douce R, Rébeillé F (1999) Glycine and serine catabolism in non-photosynthetic higher plant cells: their role in C1 metabolism. Plant J 20:197-205

Moura JCMS, Bonine CAV, De Oliveira Fernandes Viana J, Dornelas MC, Mazzafera P (2010) Abiotic and biotic stresses and changes in the lignin content and composition in plants. J Integr Plant Biol 52:360-376

Murray GM, Brennan JP (2010) Estimating disease losses to the Australian barley industry. Australas Plant Pathol 39:85-96

Murray SL, Ingle RA, Petersen LN, Denby KJ (2007) Basal resistance against *Pseudomonas syringae* in Arabidopsis involves WRKY53 and a protein with homology to a nematode resistance protein. Mol Plant Microbe Interact 20:1431-1438

Naydenov NG, Harris G, Morales V, Ivanov AI (2012) Loss of a membrane trafficking protein αSNAP induces non-canonical autophagy in human epithelia. Cell Cycle 11:4613-4625

Nilsson-Ehle H (1920) Über Resistenz gegen *Heterodera schachtii* bei gewissen Gerstensorten, ihre Vere bungsweise und Bedeutung für die Paxis. Hereditas 1:1-34

Nvyss U, Stender C, Lehmann H (1984) Ultrastructure of feeding sites of the cyst nematode *Heterodera schachtii* Schmidt in roots of susceptible and resistant *Raphanus sativus* L. var. *oleiformis* Pers. cultivars. Physiol Plant Pathol 25:21-37

O'Brien PC, Fisher JM (1977) Development of *Heterodera avenae* on resistant wheat and barley cultivars. Nematologica 23:390-397

O'Brien PC, Fisher JM (1979) Reactions of cereals to populations of *Heterodera avenae* in South Australia. Nematology 25:261-267

Ober D, Hartmann T (1999) Homospermidine synthase, the first pathway-specific enzyme of pyrrolizidine alkaloid biosynthesis, evolved from deoxyhypusine synthase. Proc Natl Acad Sci USA 96:14777-14782

Ogbonnaya FC, Seah S, Delibes A, Jahier J, López-Braña I, Eastwood RF, Lagudah ES (2001) Molecular-genetic characterisation of a new nematode resistance gene in wheat. Theor Appl Genet 102:623-629

Ohtsu M, Sato Y, Kurihara D, Suzaki T, Kawaguchi M, Maruyama D, Higashiyama T (2017) Spatiotemporal deep imaging of syncytium induced by the soybean cyst nematode *Heterodera glycines*. Protoplasma 254:2107-2115

Ophel-Keller K, McKay A, Hartley D, Herdina, Curran J (2008) Development of a routine DNA-based testing service for soilborne diseases in Australia. Australas Plant Pathol 37:243-253

Opperman CH, Taylor CG, Conkling MA (1994) Root-knot nematode — directed expression of a plant root-specific gene. Science 263:221-223

Paal J, Henselewski H, Muth J, Meksem K, Menendez CM, Salamini F, Ballvora A, Gebhardt C (2004) Molecular cloning of the potato *Gro1-4* gene conferring resistance to pathotype *Ro1* of the root cyst nematode *Globodera rostochiensis,* based on a candidate gene approach. Plant J 38:285-297

Pallotta MA, Graham RD, Langridge P, Sparrow DHB, Barker SJ (2000) RFLP mapping of manganese efficiency in barley. Theor Appl Genet 101:1100-1108

Palomares-Rius JE, Hedley PE, Cock PJ, Morris JA, Jones JT, Vovlas N, Blok V (2012) Comparison of transcript profiles in different life stages of the nematode *Globodera pallida* under different host potato genotypes. Mol Plant Pathol 13:1120-1134

Perry RN (2002) Chapter 6: Hatching. The biology of nematodes. Baton Rouge: Chapman and Hall/CRC, Baton Rouge

Perry RN, Moens M (2006) Plant nematology. CAB International, Wallingford

Perry RN, Moens M, Jones JT (2018) Cyst nematodes. CAB International, Wallingford

Piya S, Binder BM, Hewezi T (2019) Canonical and noncanonical ethylene signaling pathways that regulate Arabidopsis susceptibility to the cyst nematode *Heterodera schachtii*. New Phytol 221:946-959

Popeijus H, Overmars H, Jones J, Blok V, Goverse A, Helder J, Schots A, Bakker J, Smant G (2000) Degradation of plant cell walls by a nematode. Nature 406:36

Qiao F, Kong LA, Peng H, Huang WK, Wu DQ, Liu SM, Clarke JL, Qiu DW, Peng DL (2019) Transcriptional profiling of wheat (*Triticum aestivum* L.) during a compatible interaction with the cereal cyst nematode *Heterodera avenae*. Sci Rep 9:2184

Rai KM, Balasubramanian VK, Welker CM, Pang M, Hii MM, Mendu V (2015) Genome wide comprehensive analysis and web resource development on cell wall degrading enzymes from phyto-parasitic nematodes. BMC Plant Biol 15:187

Rice SL, Leadbeater BSC, Stone AR (1985) Changes in cell structure in roots of resistant potatoes parasitized by potato cyst-nematodes. 1. Potatoes with resistance gene H1 derived from *Solanum tuberosum* ssp. *andigena*. Physiol Plant Pathol 27:219-234

Rice SL, Stone AR, leadbeater BSC (1987) Changes in cell structure in roots of resistant potatoes parasitized by potato cyst nematodes. 2. Potatoes with resistance derived from *Solanum vernei*. Physiol Mol Plant Pathol 31:1-14

Riley IT, McKay AC (2009) Cereal cyst nematode in Australia: biography of a biological invader. Proceedings of the First Workshop of the International Cereal Cyst Nematode Initiative. International Maize and Wheat Improvement Centre (CIMMYT), Addis Ababa, pp 23-28

Rivoal R, Cook R (1993) Nematode pests of cereals. CAB International, Wallingford, pp 259-303

Rocha-Sosa M, Sonnewald U, Frommer W, Stratmann M, Schell J, Willmitzer L (1989) Both developmental and metabolic signals activate the promoter of a class I patatin gene. EMBO J 8:23-29

Rodrigues MI, Bravo JP, Sassaki FT, Severino FE, Maia IG (2013) The tonoplast intrinsic aquaporin (TIP) subfamily of Eucalyptus grandis: Characterization of EgTIP2, a root-specific and osmotic stress-responsive gene. Plant Science 213:106-113

Rogowsky PM, Guidet FLY, Langridge P, Shepherd KW, Koebner RMD (1991) Isolation and characterization of wheat-rye recombinants involving chromosome arm 1DS of wheat. Theor Appl Genet 82:537-544

Rovira AD, Simon A (1982) Integrated control of *Heterodera avenae*. EPPO Bull 12:517-523

Rozen S, Skaletsky H (2000) Primer3 on the WWW for general users and for biologist programmers. Methods Mol Biol 132:365-386

Saengwilai P (2013) Root traits for efficient nitrogen acquisition and genome-wide association study of root anatomical traits in maize (*Zea mays* L.). Pennsylvania State University, p 172

Saengwilai P, Nord EA, Chimungu JG, Brown KM, Lynch JP (2014) Root cortical aerenchyma enhances nitrogen acquisition from low-nitrogen soils in maize. Plant Physiol 166:726-735

Sakurai J, Ahamed A, Murai M, Maeshima M, Uemura M (2008) Tissue and cell-specific localization of rice aquaporins and their water transport activities. Plant Cell Physiol 49:30-39

Sakurai J, Ishikawa F, Yamaguchi T, Uemura M, Maeshima M (2005) Identification of 33 rice aquaporin genes and analysis of their expression and function. Plant Cell Physiol 46:1568-1577

Seah S, Miller C, Sivasithamparam K, Lagudah ES (2000) Root responses to cereal cyst nematode (*Heterodera avenae*) in hosts with different resistance genes. New Phytol 146:527-533

Shirasu K, Lahaye T, Tan M-W, Zhou F, Azevedo C, Schulze-Lefert P (1999) A novel class of eukaryotic zinc-binding proteins is required for disease resistance signaling in barley and development in *C. elegans*. Cell 99:355-366

Siddique S, Grundler FMW (2015) Chapter Five - Metabolism in nematode feeding sites. In: Escobar C, Fenoll C (eds) Advances in Botanical Research. Academic Press, pp 119-138

Siddique S, Grundler FMW (2018) Parasitic nematodes manipulate plant development to establish feeding sites. Curr Opin Microbiol 46:102-108

Slootmaker LAJ, Lange W, Jochemsen G, Schepers J (1974) Monosomic analysis in bread wheat of resistance to cereal root eelworm. Euphytica 23:497-503

Smant G, Stokkermans JP, Yan Y, de Boer JM, Baum TJ, Wang X, Hussey RS, Gommers FJ, Henrissat B, Davis EL, Helder J, Schots A, Bakker J (1998) Endogenous cellulases in animals: isolation of β-1, 4-endoglucanase genes from two species of plant-parasitic cyst nematodes. Proc Natl Acad Sci USA 95:4906-4911

Smiley R, Yan G, N. Pinkerton J (2011) Resistance of wheat, barley and oat to *Heterodera avenae* in the Pacific Northwest, USA. Nematology 13:539-552

Smiley RW, Dababat AA, Iqbal S, Jones MGK, Maafi ZT, Peng D, Subbotin SA, Waeyenberge L (2017) Cereal cyst nematodes: a complex and destructive group of *Heterodera* species. Plant Dis 101:1692-1720

Sobczak M, Avrova A, Jupowicz J, Phillips MS, Ernst K, Kumar A (2005) Characterization of susceptibility and resistance responses to potato cyst nematode (*Globodera* spp.) infection of tomato lines in the absence and presence of the broad-spectrum nematode resistance *Hero* gene. Mol Plant Microbe Interact 18:158-168

Sobczak M, Fudali-Alves S, Wieczorek K (2011) Cell sall modifications induced by nematodes. Genomics and molecular genetics of plant-nematode interactions. Springer, Dordrecht, pp 395-422

Soetopo L (1986) Resistance to cereal cyst nematode (*Heterodera avenae* Woll.) in barley. Dept of Agronomy, Waite Agricultural Research Institute. The University of Adelaide, p 156

Sosa JM, Huber DE, Welk B, Fraser HL (2014) Development and application of MIPAR™: a novel software package for two- and three-dimensional microstructural characterization. Integr Mater Manuf Innov 3:10

Strock CF, Schneider H, Galindo-Castañeda T, Hall B, Van Gansbeke B, Mather DE, Roth MG, Chilvers MI, Guo X, Brown K, Lynch J (2019) Laser ablation tomography is a novel method for rapid quantitave and qualitative analysis of root anatomy, providing

new opportunities to investigate interactions between roots and edaphic organisms. J Exp Bot erz271

Subbotin SA, Sturhan D, Rumpenhorst HJ, Moens M (2002) Description of the Australian cereal cyst nematode *Heterodera australis* sp. n. (Tylenchida: *Heteroderidae*). Russ J Nematol 10:139-148

Subbotin SA, Toumi F, Elekçioğlu IH, Waeyenberge L, Tanha Maafi Z (2018) DNA barcoding, phylogeny and phylogeography of the cyst nematode species of the group from the genus (Tylenchida: *Heteroderidae*). Nematology 20:671-702

Szakasits D, Heinen P, Wieczorek K, Hofmann J, Wagner F, Kreil DP, Sykacek P, Grundler FMW, Bohlmann H (2009) The transcriptome of syncytia induced by the cyst nematode *Heterodera schachtii* in Arabidopsis roots. Plant J 57:771-784

Tabone T, Mather DE, Hayden MJ (2009) Temperature Switch PCR (TSP): Robust assay design for reliable amplification and genotyping of SNPs. BMC Genomics 10:580

Takahashi T, Kakehi J-I (2009) Polyamines: ubiquitous polycations with unique roles in growth and stress responses. Ann Bot 105:1-6

Taylor C, Shepherd KW, Langridge P (1998) A molecular genetic map of the long arm of chromosome 6R of rye incorporating the cereal cyst nematode resistance gene, *CreR*. Theor Appl Genet 97:1000-1012

Tedeschi F, Rizzo P, Rutten T, Altschmied L, Baumlein H (2017) RWP-RK domain-containing transcription factors control cell differentiation during female gametophyte development in Arabidopsis. New Phytol 213:1909-1924

Thurau T, Kifle S, Jung C, Cai D (2003) The promoter of the nematode resistance gene $Hs1^{pro-1}$ activates a nematode-responsive and feeding site-specific gene expression in sugar beet (*Beta vulgaris* L.) and *Arabidopsis thaliana*. Plant Mol Biol 52:643-660

Toumi F, Waeyenberge L, Viaene N, Dababat AA, Nicol JM, Ogbonnaya F, Moens M (2018) Cereal cyst nematodes: importance, distribution, identification, quantification, and control. Eur J Plant Pathol 150:1-20

Tucker ML, Burke A, Murphy CA, Thai VK, Ehrenfried ML (2007) Gene expression profiles for cell wall-modifying proteins associated with soybean cyst nematode infection, petiole abscission, root tips, flowers, apical buds, and leaves. J Exp Bot 58:3395-3406

Uehara T, Sugiyama S, Matsuura H, Arie T, Masuta C (2010) Resistant and susceptible responses in tomato to cyst nematode are differentially regulated by salicylic acid. Plant Cell Physiol 51:1524-1536

van der Vossen EA, van der Voort JN, Kanyuka K, Bendahmane A, Sandbrink H, Baulcombe DC, Bakker J, Stiekema WJ, Klein-Lankhorst RM (2000) Homologues of a single resistance-gene cluster in potato confer resistance to distinct pathogens: a virus and a nematode. Plant J 23:567-576

Van Gansbeke B, Khoo KHP, Lewis JG, Chalmers KJ, Mather DE (2019) Fine mapping of *Rha2* in barley reveals candidate genes for resistance against cereal cyst nematode. Theor Appl Genet 132:1309-1320

Vandesompele J, De Preter K, Pattyn F, Poppe B, Van Roy N, De Paepe A, Speleman F (2002) Accurate normalization of real-time quantitative RT-PCR data by geometric averaging of multiple internal control genes. Genome Biol 3:research0034.0031 - 0011

Vanstone VA, Hollaway GJ, Stirling GR (2008) Managing nematode pests in the southern and western regions of the Australian cereal industry: continuing progress in a challenging environment. Australas Plant Pathol 37:220-234

Walley JW, Sartor RC, Shen Z, Schmitz RJ, Wu KJ, Urich MA, Nery JR, Smith LG, Schnable JC, Ecker JR, Briggs SP (2016) Integration of omic networks in a developmental atlas of maize. Science 353:814-818

Walters DR, Wilson PWF, Shuttleton MA (1985) Relative changes in levels of polyamines and activities of their biosynthetic enzymes in barley infected with the powdery mildew fungus, *Erysiphe graminis* D.C. ex Merat f. sp. *hordei* Marchal. New Phytol 101:695-705

Wan J, Vuong T, Jiao Y, Joshi T, Zhang H, Xu D, Nguyen HT (2015) Whole-genome gene expression profiling revealed genes and pathways potentially involved in regulating interactions of soybean with cyst nematode (*Heterodera glycines* Ichinohe). BMC Genomics 16:148

Wang X, Li Y, Ji W, Bai X, Cai H, Zhu D, Sun XL, Chen LJ, Zhu YM (2011) A novel *Glycine soja* tonoplast intrinsic protein gene responds to abiotic stress and depresses salt and dehydration tolerance in transgenic *Arabidopsis thaliana*. J Plant Physiol 168:1241-1248

Wei Z, Sun K, Sandoval FJ, Cross JM, Gordon C, Kang C, Roje S (2013) Folate polyglutamylation eliminates dependence of activity on enzyme concentration in mitochondrial serine hydroxymethyltransferases from *Arabidopsis thaliana*. Arch Biochem Biophys 536:87-96

Williams KJ, Fisher JM (1993) Development of *Heterodera avenae* Woll. and host cellular responses in susceptible and resistant wheat. Fundam Appl Nematol 16:417-423

Williams KJ, Fisher JM, Langridge P (1994) Identification of RFLP markers linked to the cereal cyst nematode resistance gene (*Cre*) in wheat. Theor Appl Genet 89:927-930

Williams KJ, Lewis JG, Bogacki P, Pallotta MA, Willsmore KL, Kuchel H, Wallwork H (2003) Mapping of a QTL contributing to cereal cyst nematode tolerance and resistance in wheat. Aust J Agric Res 54:731-737

Williams KJ, Willsmore KL, Olson S, Matic M, Kuchel H (2006) Mapping of a novel QTL for resistance to cereal cyst nematode in wheat. Theor Appl Genet 112:1480-1486

Wu XY, Zhou GC, Chen YX, Wu P, Liu LW, Ma FF, Wu M, Liu CC, Zeng YJ, Chu AE, Hang YY, Chen JQ, Wang B (2016) Soybean cyst nematode resistance emerged via artificial selection of duplicated serine hydroxymethyltransferase genes. Front Plant Sci 7 (998)

Wubben MJE, Su H, Rodermel SR, Baum TJ (2001) Susceptibility to the sugar beet cyst nematode is modulated by ethylene signal transduction in *Arabidopsis thaliana*. Mol Plant Microbe Interact 14:1206-1212

Wyss U, Grundler FMW (1992) Feeding behavior of sedentary plant parasitic nematodes. Neth J Plant Path 98:165-173

Wyss U, Zunke U (1986) Observations on the behaviour of second stage juveniles of *Heterodera schachtii* inside host roots. Revue de Nématologie 9:153-165

Xu DL, Long H, Liang JJ, Zhang J, Chen X, Li JL, Pan ZF, Deng GB, Yu MQ (2012) *De novo* assembly and characterization of the root transcriptome of *Aegilops variabilis* during an interaction with the cereal cyst nematode. BMC Genomics 13:133

Xue B, Hamamouch N, Li C, Huang G, Hussey RS, Baum TJ, Davis EL (2013) The *8D05* parasitism gene of *Meloidogyne incognita* is required for successful infection of host roots. Phytopathology 103:175-181

Yamakawa H, Kamada H, Satoh M, Ohashi Y (1998) Spermine is a salicylate-independent endogenous inducer for both tobacco acidic pathogenesis-related proteins and resistance against tobacco mosaic virus infection. Plant Physiol 118:1213-1222

Yang D, Chen C, Liu Q, Jian H (2017) Comparative analysis of pre- and post-parasitic transcriptomes and mining pioneer effectors of *Heterodera avenae*. Cell & Bioscience 7:11

York LM, Galindo-Castañeda T, Schussler JR, Lynch JP (2015) Evolution of US maize (*Zea mays* L.) root architectural and anatomical phenes over the past 100 years corresponds to increased tolerance of nitrogen stress. J Exp Bot 66:2347-2358

Yu MH, Steele AE (1981) Host-parasite interaction of resistant sugarbeet and *Heterodera schachtii*. J Nematol 13:206-212

Zalewski W, Orczyk W, Gasparis S, Nadolska-Orczyk A (2012) *HvCKX2* gene silencing by biolistic or *Agrobacterium*-mediated transformation in barley leads to different phenotypes. BMC Plant Biol 12:206-206

Zhang L, Lilley CJ, Imren M, Knox JP, Urwin PE (2017) The complex cell wall composition of syncytia induced by plant parasitic cyst nematodes reflects both function and host plant. Front Plant Sci 8 (1087)

Zhang Y, Sun K, Sandoval FJ, Santiago K, Roje S (2010) One-carbon metabolism in plants: characterization of a plastid serine hydroxymethyltransferase. Biochem J 430:97-105

Zheng M, Long H, Zhao Y, Li L, Xu D, Zhang H, Liu F, Deng G, Pan Z, Yu M (2015) RNA-seq based identification of candidate parasitism genes of cereal cyst nematode (*Heterodera avenae*) during incompatible infection to *Aegilops variabilis*. PLoS ONE 10:e0141095

Zouhar J, Sauer M (2014) Helping hands for budding prospects: ENTH/ANTH/VHS accessory proteins in endocytosis, vacuolar transport, and secretion. Plant Cell 26:4232-4244

Appendices

Appendix 1. Genotypic and phenotypic data for 20 barley lines

Genotypic data, cyst counts and resistance status for accessions of 20 barley lines that were evaluated for cereal cyst nematode resistance in a tube test

Accession name	Accession number	Genotypes obtained with KASP assays[a]				Number of plants evaluated	Number of white cysts per plant		Resistance status
		wri322	wri321	wri297	wri326		Mean	Standard error	
Barley 191	AUS400381	T:T	A:A	A:A	G:G	10	0.9	0.35	Resistant
Orge Martin	AUS402640	T:T	A:A	A:A	G:G	10	0.0	0.00	Resistant
	AUS401665	T:T	A:A	A:A	G:G	10	0.1	0.10	
	AUS401666	T:T	A:A	A:A	G:G	10	0.0	0.00	
Orge Martin 839	AUS401667	T:T	A:A	A:A	G:G	10	0.8	0.80	Resistant
Martin 403-2	AUS401380	T:T	A:A	A:A	G:G	10	0.0	0.00	Resistant
Bajo Aragon	AUS405928	T:T	A:A	A:A	G:G	10	0.0	0.00	Resistant
	AUS495235	T:T	A:A	A:A	G:G	10	0.0	0.10	
Sabarlis	AUS401881	T:T	A:A	A:A	G:G	10	0.5	0.22	Resistant
Siri	AUS401958	T:T	A:A	A:A	G:G	10	1.1	0.43	Resistant
	AUS495232	T:T	A:A	A:A	null[b]	10	0.8	0.47	
Morocco	AUS401480	T:T	A:A	A:A	G:G	10	0.0	0.00	Resistant
	AUS411152	T:T	A:A	A:A	G:G	10	0.0	0.00	
	AUS490064	T:T	A:A	A:A	G:G	10	0.0	0.00	
Morocco (Early)	AUS401481	C:C	G:G	G:G	G:G	10	0.5	0.22	Resistant
Athinais	AUS400316	C:C	G:G	G:G	G:G	10	0.2	0.13	Resistant
Nile	AUS401544	C:C	A:A	A:A	G:G	9	0.1	0.11	Resistant
Alfa	AUS400254	C:C	G:G	G:G	A:A	10	8.4	2.37	Susceptible
Clipper	AUS400190	C:C	G:G	G:G	A:A	10	8.1	1.22	Susceptible
	AUS400624	C:C	G:G	G:G	A:A	10	7.2	1.82	

Appendix 1 continued

Accession name	Accession number	Genotypes obtained with KASP assays[a]				Number of plants evaluated	Number of white cysts per plant		Resistance status
Drost	AUS400746	C:C	G:G	null	A:A	9	7.3	2.60	Susceptible
Herta	AUS401011	C:C	G:G	G:G	A:A	10	10.7	2.11	Susceptible
	AUS495226	C:C	G:G	G:G	A:A	10	9.0	1.83	
Ortolan	AUS401673	C:C	G:G	G:G	A:A	10	7.2	1.31	Susceptible
	AUS495233	C:C	G:G	G:G	A:A	10	6.3	1.72	
	AUS411267	C:C	G:G	G:G	null	10	6.8	1.18	
Schooner	AUS499011	C:C	G:G	G:G	null	9	5.6	0.97	Susceptible
	AUS400187	C:C	G:G	G:G	null	9	7.5	1.72	
Varde	AUS402192	C:C	G:G	G:G	A:A	9	5.4	1.42	Susceptible
	AUS495231	C:C	G:G	G:G	A:A	9	8.3	1.84	
	AUS495225	C:C	G:G	G:G	A:A	10	8.5	1.28	
Quinn	AUS401810	C:C	G:G	G:G	null	10	5.2	1.32	Uncertain
	AUS401809	C:C	G:G	G:G	A:A	10	2.0	0.60	
Marocaine 079	AUS401374	T:T	A:A	A:A	G:G	10	0.0	0.00	Uncertain
	AUS401375	C:C	G:G	G:G	A:A	9	12.1	2.18	

[a] Dark shading indicates marker alleles that are the same as those of *Rha2* cultivars. Light shading indicates marker alleles that differ from those of *Rha2* cultivars.
[b] Neither HEX nor FAM fluorescence detected

The information in this appendix was presented in Table S1 in Online Resource 1 of Van Gansbeke et al. (2019).

Appendix 2. Genotypic data for 180 barley cultivars

Expected resistance status	Cultivar	Resistance allele (and its source, if known)	Genotypes obtained with KASP assays[a]			
			wri322	wri321	wri297	wri326
Resistant	Sahara 3771	*Rha2*	T:T	A:A	A:A	G:G
	Chebec	*Rha2* (Orge Martin)	T:T	A:A	A:A	G:G
	Sloop SA	*Rha2* (Chebec)	T:T	A:A	A:A	G:G
	Sloop VIC	*Rha2* (Sahara 3771 or Chebec)	T:T	A:A	A:A	G:G
	Dash	*Rha2*	T:T	A:A	A:A	G:G
	Hindmarsh	*Rha2* (Dash)	T:T	A:A	A:A	G:G
	Galleon	*Rha4* (CI3576)	C:C	G:G	G:G	A:A
	Keel	*Rha4* (possibly CPI18197)	C:C	G:G	G:G	null[b]
	Finniss	*Rha4* (Galleon)	C:C	G:G	G:G	null
	Torrens	*Rha4* (Galleon)	C:C	G:G	G:G	G:G
	Yarra	*Rha4* (Galleon)	C:C	G:G	G:G	A:A
	Barque	*Rha4* (Galleon)	C:C	G:G	G:G	A:A
	Flagship	*Rha4* (Barque)	C:C	G:G	G:G	A:A
	Fathom	*Rha4* (Barque or Keel)	C:C	G:G	G:G	A:A
	Fleet Australia	*Rha4* (Barque or Keel)	C:C	G:G	G:G	null
	Navigator	*Rha4* (Keel)	C:C	G:G	G:G	A:A
	Commander	*Rha4* (Keel)	C:C	G:G	G:G	A:A
	Skipper	*Rha4* (Commander)	C:C	G:G	G:G	null
	Capstan	*Rha4*	C:C	G:G	G:G	A:A
	Dhow	*Rha4*	C:C	G:G	G:G	null
	Doolup	*Rha4*	C:C	G:G	G:G	A:A
	Maritime	*Rha4*	C:C	G:G	G:G	A:A
	GrangeR	Unknown	T:T	A:A	A:A	G:G
Susceptible	Arapiles		C:C	G:G	G:G	A:A
	Bass		C:C	G:G	G:G	-[c]
	Baudin		C:C	G:G	G:G	-
	Brindabella		T:T	G:G	G:G	G:G
	Buloke		C:C	G:G	G:G	-
	Clipper		C:C	G:G	G:G	G:G
	Cowabbie		C:C	G:G	G:G	A:A
	Fitzroy		C:C	G:G	G:G	null
	Flinders		C:C	G:G	G:G	A:A
	Forrest		C:C	G:G	G:G	A:A
	Franklin		C:C	G:G	G:G	null
	Gairdner		C:C	G:G	G:G	A:A
	Galaxy		C:C	G:G	G:G	null
	Hamelin		C:C	G:G	G:G	A:A
	Harrington		C:C	G:G	G:G	G:G
	Haruna Nijo		T:T	G:G	G:G	null
	Henley		C:C	G:G	G:G	A:A

Appendix 2 continued

Expected resistance status	Cultivar	Resistance allele (and its source, if known)	Genotypes obtained with KASP assays[a]			
			wri322	wri321	wri297	wri326
Susceptible	Molloy		C:C	G:G	G:G	-
	Mundah		C:C	G:G	G:G	A:A
	O'Connor		C:C	G:G	G:G	null
	Onslow		C:C	G:G	G:G	null
	Oxford		C:C	G:G	G:G	A:A
	Schooner		C:C	G:G	G:G	null
	Scope		C:C	G:G	G:G	A:A
	Skiff		C:C	G:G	G:G	null
	Sloop		C:C	G:G	G:G	null
	Stirling		C:C	G:G	G:G	A:A
	Tallon		C:C	G:G	G:G	G:G
	Tantangara		C:C	G:G	G:G	null
	Vlamingh		C:C	G:G	G:G	A:A
	Weeah		C:C	G:G	G:G	G:G
	Wimmera		C:C	G:G	G:G	A:A
	Yagan		C:C	G:G	G:G	A:A
Unknown	AC Metcalfe		C:C	G:G	G:G	A:A
	Albacete		T:T	A:A	A:A	G:G
	Alexis		C:C	G:G	G:G	A:A
	Alf		T:T	A:A	A:A	G:G
	Alfor		C:C	G:G	G:G	A:A
	Amaji Nijo		C:C	G:G	G:G	G:G
	Apex		C:C	G:G	G:G	A:A
	Armelle		C:C	G:G	G:G	A:A
	Arta		C:C	G:G	G:G	A:A
	Atahualpa		C:C	G:G	G:G	G:G
	Azumamugi		null	G:G	G:G	G:G
	Azure		C:C	G:G	G:G	G:G
	Barke		C:C	G:G	G:G	A:A
	Baronesse		C:C	G:G	G:G	A:A
	Beecher		C:C	G:G	G:G	A:A
	Beka		C:C	G:G	G:G	null
	Betzes		C:C	G:G	G:G	G:G
	Binalong		C:C	G:G	G:G	A:A
	Blenheim		C:C	G:G	G:G	A:A
	Bomi		C:C	G:G	G:G	G:G
	Bowman		C:C	G:G	G:G	A:A
	Brenda		C:C	G:G	G:G	A:A
	Calicuchima		C:C	G:G	G:G	null
	Canela		C:C	G:G	G:G	A:A
	CDC Bold		C:C	G:G	G:G	-
	CDC Copeland		C:C	G:G	G:G	null
	CDC Dolly		C:C	G:G	G:G	A:A

Appendix 2 continued

Expected resistance status	Cultivar	Resistance allele (and its source, if known)	Genotypes obtained with KASP assays[a]			
			wri322	wri321	wri297	wri326
Unknown	CDC Fleet		C:C	G:G	G:G	A:A
	Cebada Capa		C:C	G:G	G:G	-
	Chevron		C:C	G:G	G:G	A:A
	Chieftain		C:C	G:G	G:G	null
	Chime		C:C	G:G	G:G	A:A
	Clark		C:C	G:G	G:G	A:A
	Colter		C:C	G:G	G:G	G:G
	Cutter		C:C	G:G	G:G	A:A
	Dairokakku		C:C	G:G	G:G	G:G
	Danilo		C:C	G:G	G:G	null
	Denar		C:C	G:G	G:G	null
	Derkado		C:C	G:G	G:G	null
	Diamant		C:C	G:G	G:G	null
	Dicktoo		C:C	G:G	G:G	A:A
	Digger		T:T	G:G	G:G	G:G
	Dobla		C:C	G:G	G:G	-
	Excel		C:C	G:G	G:G	null
	Fairview		C:C	G:G	G:G	A:A
	Foster		C:C	G:G	G:G	null
	Fractal		T:T	A:A	A:A	G:G
	Franka		C:C	G:G	G:G	A:A
	Galena		C:C	G:G	G:G	A:A
	Gerbel		C:C	G:G	G:G	A:A
	Gobernadora		C:C	G:G	G:G	A:A
	Golden Promise		C:C	G:G	G:G	A:A
	Goldmarker		C:C	G:G	G:G	A:A
	Grimmett		C:C	G:G	G:G	A:A
	Grout		C:C	G:G	G:G	A:A
	Gustoe		C:C	G:G	G:G	A:A
	Halcyon		C:C	G:G	G:G	A:A
	Hanacky Moravian		C:C	G:G	G:G	G:G
	Hannan		C:C	G:G	G:G	G:G
	Harbin		T:T	A:A	A:A	G:G
	Harry		C:C	G:G	G:G	A:A
	Hart		C:C	G:G	G:G	A:A
	Igri		C:C	G:G	G:G	A:A
	Kaputar		C:C	G:G	G:G	A:A
	Kearney		T:T	G:G	G:G	G:G
	Kikaihadaka		null	G:G	G:G	G:G
	Kold		C:C	G:G	G:G	A:A
	Krona		C:C	G:G	G:G	A:A
	Lewis		C:C	G:G	G:G	A:A
	Lina		C:C	G:G	G:G	A:A

Appendix 2 continued

Expected resistance status	Cultivar	Resistance allele (and its source, if known)	Genotypes obtained with KASP assays[a]			
			wri322	wri321	wri297	wri326
Unknown	Livet		C:C	G:G	G:G	A:A
	Lockyer		C:C	G:G	G:G	null
	Logan		C:C	G:G	G:G	G:G
	Mackay		C:C	G:G	G:G	A:A
	Macquarie		C:C	G:G	G:G	A:A
	Magnum		C:C	G:G	G:G	null
	Manley		C:C	G:G	G:G	G:G
	Maythorpe		C:C	G:G	G:G	A:A
	Mogador		C:C	G:G	G:G	A:A
	Mona		C:C	G:G	G:G	A:A
	Morex		C:C	G:G	G:G	A:A
	Natasha		C:C	G:G	G:G	null
	Nudinka		C:C	G:G	G:G	G:G
	Nure		C:C	G:G	G:G	A:A
	Optic		T:T	A:A	A:A	G:G
	Patty		C:C	G:G	G:G	A:A
	Plaisant		C:C	G:G	G:G	A:A
	Pompadour		C:C	G:G	G:G	A:A
	Prentice		C:C	G:G	G:G	A:A
	Prior		C:C	G:G	G:G	A:A
	Prior Early		T:T	G:G	G:G	null
	Prisma		C:C	G:G	G:G	null
	Proctor		C:C	G:G	G:G	G:G
	Puffin		C:C	G:G	G:G	A:A
	Regatta		C:C	G:G	G:G	A:A
	Roe		C:C	G:G	G:G	null
	Royal		C:C	G:G	G:G	G:G
	Scarlett		C:C	G:G	G:G	A:A
	Shannon		C:C	G:G	G:G	A:A
	Shepherd		C:C	G:G	G:G	A:A
	Shyri		C:C	G:G	G:G	A:A
	Sonate		C:C	G:G	G:G	A:A
	Stander		C:C	G:G	G:G	G:G
	Steptoe		C:C	G:G	G:G	G:G
	SY Rattler		T:T	A:A	A:A	G:G
	Tadmor		C:C	G:G	G:G	G:G
	Tankard		C:C	G:G	G:G	G:G
	Thuringia		C:C	G:G	G:G	A:A
	Tilga		C:C	G:G	G:G	A:A
	Tremois		C:C	G:G	G:G	A:A
	Triangle		C:C	G:G	G:G	null
	Triumph		C:C	G:G	G:G	G:G
	Tulla		C:C	G:G	G:G	G:G
	Turk		C:C	G:G	G:G	G:G

Appendix 2 continued

Expected resistance status	Cultivar	Resistance allele (and its source, if known)	Genotypes obtained with KASP assays[a]			
			wri322	wri321	wri297	wri326
Unknown	Tystofte Prentice		C:C	G:G	G:G	A:A
	Urambie		C:C	G:G	G:G	A:A
	Vada		C:C	G:G	G:G	A:A
	Valticky		C:C	G:G	G:G	G:G
	Vertess		C:C	G:G	G:G	A:A
	Vogelsanger Gold		C:C	G:G	G:G	A:A
	Westminster		C:C	G:G	G:G	A:A
	Yambla		C:C	G:G	G:G	null
	Yerlong		C:C	G:G	G:G	A:A
	Zavilla		null	G:G	G:G	G:G

[a] Dark shading indicates marker alleles that are the same as those of *Rha2* cultivars. Light shading indicates marker alleles that differ from those of *Rha2* cultivars.
[b] Neither HEX nor FAM fluorescence detected.
[c] Not called due to ambiguous (intermediate) result.

The information in this appendix was presented in Table S2 in Online Resource 1 of Van Gansbeke et al. (2019).

Appendix 3. Tube test

Tube tests for evaluation of resistance of cereal plants against the cereal cyst nematode *Heterodera avenae*

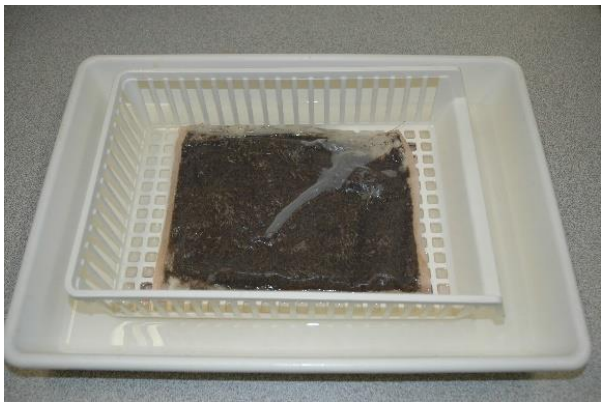

Figure A3-1: A nematode 'farm' used as a source of larvae. A mixture of organic material and cyst-infested soil is packed in silk cloth and submerged in water. The farm is incubated at 5 °C in darkness. Eggs hatch within the cysts and J2-stage larvae emerge. A farm can be maintained for several months and larvae can be collected as needed

Figure A3-2: Plastic tubes are filled with pre-sterilised sandy loam soil. One pre-germinated seed is sown in each tube. Tubes are arranged in a crate (10 rows x 10 columns). Aliquots of inoculum containing approximately 100 J2-stage larvae are pipetted onto the soil surface 1, 4, 7, 11 and 14 d later

Figure A3-3: After the final inoculation, tubes are arranged within a wire grid on a basal layer of cocopeat mixture

Figure A3-4: At 70 d after the final inoculation, shoots are trimmed off and tubes are removed from the grid. Roots and soil are removed from the tube and thoroughly washed with a jet of water over a set of sieves, with the bottom sieve having apertures of 0.25 mm

Figure A3-5: Materials from the bottom sieve are spread out on a black plate and white cysts are counted. The root system is also examined for any white cysts remaining on the roots

The information in this appendix was presented in Figures S1-S5 in Online Resource 2 of Van Gansbeke et al. (2019).

Appendix 4. Pots test

'Pots' tests for evaluation of resistance of cereal plants against the cereal cyst nematode *Heterodera avenae*

Figure A4-1: Pots are filled with soil infested with brown cysts (approximately 25 eggs per g of soil) and arranged in wire mesh crates. One seed is sown per pot

Figure A4-2: Crates containing 50 plants each are placed outdoors in autumn, on well-drained terraces. Sprinkler irrigation is provided three times daily. Nets provide protection against birds

Figure A4-3: After about 3 months, the root ball is removed from each pot. White cysts that are visible on the surface are counted

The information in this appendix was presented in Figures S6-S8 in Online Resource 2 of Van Gansbeke et al. (2019).

Appendix 5. Primer sequences for 106 KASP assays designed for single nucleotide polymorphisms on barley chromosome 2H

KASP assay	Primer sequence (5′-3′)		Common primer sequence (5′-3′)
wri222	FAM	GAAGGTGACCAAGTTCATGCTGAGGAGGCAAAGAATTTATGGGT	TGTGGTTGCTTTGCCTTTGC
	HEX	GAAGGTCGGAGTCAACGGATTGAGGAGGCAAAGAATTTATGGGA	
wri223	FAM	GAAGGTGACCAAGTTCATGCTTCCCCTCTAAATGTCAAGCGGAC	AAACAGGCTGTTGCCGTCCA
	HEX	GAAGGTCGGAGTCAACGGATTTCCCCTCTAAATGTCAAGCGGAG	
wri224	FAM	GAAGGTGACCAAGTTCATGCTGAGTAGTACGTATGAAAGCATATATAACGA	CAGTTGCACACAAACATGAGGTTAG
	HEX	GAAGGTCGGAGTCAACGGATTGAGTAGTACGTATGAAAGCATATATAACGG	
wri225	FAM	GAAGGTGACCAAGTTCATGCTTCTTATCCAAATCCCCTGCCGG	AGCGAAAGTACTCGTAGTAAGCATAG
	HEX	GAAGGTCGGAGTCAACGGATTTCTTATCCAAATCCCCTGCCGA	
wri226	FAM	GAAGGTGACCAAGTTCATGCTGCAAAATTATGGACAACCTGATCATTCT	TTTGTGTAACCCGGATACAACATGAT
	HEX	GAAGGTCGGAGTCAACGGATTGCAAAATTATGGACAACCTGATCATTCC	
wri227	FAM	GAAGGTGACCAAGTTCATGCTACACTGCTGCCTGCAGCAAA	CGGACTTGATTTGTAGGCGGAGG
	HEX	GAAGGTCGGAGTCAACGGATTACACTGCTGCCTGCAGCAAG	
wri228	FAM	GAAGGTGACCAAGTTCATGCTATGCATGAGCGATTCAGACCTGT	GCTCTTCCGATCTCGGCCGT
	HEX	GAAGGTCGGAGTCAACGGATTATGCATGAGCGATTCAGACCTGC	
wri229	FAM	GAAGGTGACCAAGTTCATGCTTGCAGATGCTGCAAATTTCGATTGG	CGATTGTGGCCAGGCAACAC
	HEX	GAAGGTCGGAGTCAACGGATTTGCAGATGCTGCAAATTTCGATTGT	
wri230	FAM	GAAGGTGACCAAGTTCATGCTCTACAGAGACTGCAGTATCAGAAAACAA	CTGATGACATAGAATCCCCCCATTC
	HEX	GAAGGTCGGAGTCAACGGATTCTACAGAGACTGCAGTATCAGAAAACAG	
wri231	FAM	GAAGGTGACCAAGTTCATGCTGACGGTGACCATCGCTGATTTT	CGTGCTTATCCGTGACGTACTTG
	HEX	GAAGGTCGGAGTCAACGGATTGACGGTGACCATCGCTGATTTA	

Appendix 5 continued

KASP assay	Primer sequence (5′-3′)		Common primer sequence (5′-3′)
wri232	FAM	GAAGGTGACCAAGTTCATGCTCATCCCTGCGTCTACAGCGG	TCTTCCGATCTCGGCGCCA
	HEX	GAAGGTCGGAGTCAACGGATTCATCCCTGCGTCTACAGCGC	
wri233	FAM	GAAGGTGACCAAGTTCATGCTCCTTGTTCCTAAAAGGGAGCCAAT	AAGAAAGAAAAATGGAAACCATCTTGTGA
	HEX	GAAGGTCGGAGTCAACGGATTCCTTGTTCCTAAAAGGGAGCCAAC	
wri234	FAM	GAAGGTGACCAAGTTCATGCTTGAGAAATGGAAACTTCACGCTCAA	GCACCGACGGGAATCGAACT
	HEX	GAAGGTCGGAGTCAACGGATTTGAGAAATGGAAACTTCACGCTCAT	
wri235	FAM	GAAGGTGACCAAGTTCATGCTGGGACGAATAGATCTCAAGGGAATTAC	GCGTTGAGTTTAGAATGAAACATTTTGA
	HEX	GAAGGTCGGAGTCAACGGATTGGGACGAATAGATCTCAAGGGAATTAT	
wri236	FAM	GAAGGTGACCAAGTTCATGCTGAGGGACGGATCGTTCAAAATTA	GTTTTCTTCTCTTCTGAGAAACATCGG
	HEX	GAAGGTCGGAGTCAACGGATTGAGGGACGGATCGTTCAAAATTG	
wri237	FAM	GAAGGTGACCAAGTTCATGCTCACCGGGAGGGAAAGCGATT	TCCGCTTTCTCACGCGGCAG
	HEX	GAAGGTCGGAGTCAACGGATTCACCGGGAGGGAAAGCGATG	
wri238	FAM	GAAGGTGACCAAGTTCATGCTCAATAACGAGTTTGTAACAAGCCAATTC	TTTACTGTCTTCTGTACATGCTCGT
	HEX	GAAGGTCGGAGTCAACGGATTCAATAACGAGTTTGTAACAAGCCAATTG	
wri239	FAM	GAAGGTGACCAAGTTCATGCTTCAGTAACTACGGCATCAAGAACA	CGGACTCAGGTATGGTTCATAC
	HEX	GAAGGTCGGAGTCAACGGATTTCAGTAACTACGGCATCAAGAACG	
wri240	FAM	GAAGGTGACCAAGTTCATGCTAGCCGCCGGAGCGGCACC	GTGCATCGTTCCAGTGACGCTCATCTT
	HEX	GAAGGTCGGAGTCAACGGATTAGCCGCCGGAGCGGCACA	
wri241	FAM	GAAGGTGACCAAGTTCATGCTGTCGTAGTAGTCCCTGCCACGG	AGTACGCCGACATCGCGGCCTA
	HEX	GAAGGTCGGAGTCAACGGATTGTCGTAGTAGTCCCTGCCACGA	
wri242	FAM	GAAGGTGACCAAGTTCATGCTCAACTGCAGATGAAAACGGACAACG	CATCGCTTTCTATTCTGGTTTCTTCTAATC
	HEX	GAAGGTCGGAGTCAACGGATTCAACTGCAGATGAAAACGGACAACA	
wri243	FAM	GAAGGTGACCAAGTTCATGCTAATATTTGCTTGTGATTTTTGAAAAATATACTTAT	GGGCATGTTCTTTAAAAAATCAACGAAT
	HEX	GAAGGTCGGAGTCAACGGATTAATATTTGCTTGTGATTTTTGAAAAATATACTTAA	
wri244	FAM	GAAGGTGACCAAGTTCATGCTTTTTTAGTGTACTGCCTGAGCCTCG	AAGATCATCATGCATTATGTCAAAATCAAAG
	HEX	GAAGGTCGGAGTCAACGGATTTTTTAGTGTACTGCCTGAGCCTCA	

Appendix 5 continued

KASP assay	Primer sequence (5′-3′)		Common primer sequence (5′-3′)
wri245	FAM	GAAGGTGACCAAGTTCATGCTAACTGCTGGTAACCATTATATTAGGGT	TCCAACAGCAAATTTTTACGTACCAC
	HEX	GAAGGTCGGAGTCAACGGATTAACTGCTGGTAACCATTATATTAGGGC	
wri246	FAM	GAAGGTGACCAAGTTCATGCTCTCAGGGGATTTATTTCTTAAAATAAACGATA	CTTTTTTATATCTCCTAGTCTGGCATCCA
	HEX	GAAGGTCGGAGTCAACGGATTCTCAGGGGATTTATTTCTTAAAATAAACGATG	
wri247	FAM	GAAGGTGACCAAGTTCATGCTTGCATTTCTAATCTCCCCTTGTGT	GGCAAGATGAATGGAAAACATGTTCTT
	HEX	GAAGGTCGGAGTCAACGGATTTGCATTTCTAATCTCCCCTTGTGC	
wri248	FAM	GAAGGTGACCAAGTTCATGCTCGGTTTCTTTCGAAAGTACAGCTA	GCTAAAAACGGAAGTAATTAAACTGTCAAAG
	HEX	GAAGGTCGGAGTCAACGGATTCGGTTTCTTTCGAAAGTACAGCTG	
wri249	FAM	GAAGGTGACCAAGTTCATGCTCGGCATCCTGTGCTGGAGTATATGCACTC	GCGTGCGTGCGGACACTGGC
	HEX	GAAGGTCGGAGTCAACGGATTCGGCATCCTGTGCTGGAGTATATGCACTG	
wri250	FAM	GAAGGTGACCAAGTTCATGCTTAGCCCTGAGCCTGGTCAACTCA	GTTCAATTCGGCCGTTTGGGGT
	HEX	GAAGGTCGGAGTCAACGGATTTAGCCCTGAGCCTGGTCAACTCT	
wri251	FAM	GAAGGTGACCAAGTTCATGCTCAGCGCGCGGCGGCTTCG	CAAGGTACCAGTTTCTATATTCGGCCGGAGAAA
	HEX	GAAGGTCGGAGTCAACGGATTCAGCGCGCGGCGGCTTCT	
wri252	FAM	GAAGGTGACCAAGTTCATGCTGCGATTTCGGCTGAAAAGCCTG	CCGCTCTTCCGATCTCGGGATTA
	HEX	GAAGGTCGGAGTCAACGGATTGCGATTTCGGCTGAAAAGCCTC	
wri253	FAM	GAAGGTGACCAAGTTCATGCTTGCCATCGCTGATGACACATATG	CCGATCTCGGAGACCGATGTCC
	HEX	GAAGGTCGGAGTCAACGGATTTGCCATCGCTGATGACACATATC	
wri254	FAM	GAAGGTGACCAAGTTCATGCTCAGCAGTGTCACATGATGGGCGTT	TTGTTGTGCAGCATGTGCGGTGA
	HEX	GAAGGTCGGAGTCAACGGATTCAGCAGTGTCACATGATGGGCGTA	
wri255	FAM	GAAGGTGACCAAGTTCATGCTATTATCATCCTTCACCGTTAACATGATAAT	ATCTGAATATAAGACCGGCAGGTTATGA
	HEX	GAAGGTCGGAGTCAACGGATTATTATCATCCTTCACCGTTAACATGATAAC	
wri256	FAM	GAAGGTGACCAAGTTCATGCTCCGATGTTTCTCAGAAGAGAAGAAAACT	GTTTTAGACATTGCAACATTTCACATTTCTT
	HEX	GAAGGTCGGAGTCAACGGATTCCGATGTTTCTCAGAAGAGAAGAAAACG	
wri257	FAM	GAAGGTGACCAAGTTCATGCTAGCTGTGCAGTGCTAGTAACTTTG	GCGTGTTATTGTGTGTTAGCATCTTCTTT
	HEX	GAAGGTCGGAGTCAACGGATTGTAGCTGTGCAGTGCTAGTAACTTTT	

Appendix 5 continued

KASP assay	Primer sequence (5′-3′)		Common primer sequence (5′-3′)
wri258	FAM	GAAGGTGACCAAGTTCATGCTCGAGACGTTTCTTATTATGAAATTCGCAT	GGGATGATCGAAGCAACCTGTAACTT
	HEX	GAAGGTCGGAGTCAACGGATTGAGACGTTTCTTATTATGAAATTCGCAC	
wri259	FAM	GAAGGTGACCAAGTTCATGCTGGACGATGAGGGCCGCAGT	ACCTTCGCACTGGCCTCGCTA
	HEX	GAAGGTCGGAGTCAACGGATTGACGATGAGGGCCGCAGC	
wri260	FAM	GAAGGTGACCAAGTTCATGCTGCCACTCCAATCGAGAAATGGCA	AGATCACCTGCAGAATTACAGAAGTGTT
	HEX	GAAGGTCGGAGTCAACGGATTCCACTCCAATCGAGAAATGGCG	
wri261	FAM	GAAGGTGACCAAGTTCATGCTGAGAATCAGAGTCGTGCGCGA	CTAGTATTGCTGGCCAACCAACCAA
	HEX	GAAGGTCGGAGTCAACGGATTGAGAATCAGAGTCGTGCGCGC	
wri262	FAM	GAAGGTGACCAAGTTCATGCTTCCCCTTGAATGCCTCCGTTC	GCCCCTGCGTGTCCAGGGAA
	HEX	GAAGGTCGGAGTCAACGGATTGTTCCCCTTGAATGCCTCCGTTT	
wri263	FAM	GAAGGTGACCAAGTTCATGCTCGGCGTCTCAATTGCAAATAG	GCTGCACTGCAATGATTCAAGGAGAA
	HEX	GAAGGTCGGAGTCAACGGATTCTCGGCGTCTCAATTGCAAATAC	
wri264	FAM	GAAGGTGACCAAGTTCATGCTTCCTGCAGGAGCATTACTGTTAT	ACCAAGCATCCAAGTATAGAACAGATCAA
	HEX	GAAGGTCGGAGTCAACGGATTCTTCCTGCAGGAGCATTACTGTTAA	
wri265	FAM	GAAGGTGACCAAGTTCATGCTATGTTGAGTAGTTCTGCTGCAGGTA	GACAGAGCTTATCCGGGTGGAGAA
	HEX	GAAGGTCGGAGTCAACGGATTGTTGAGTAGTTCTGCTGCAGGTG	
wri266	FAM	GAAGGTGACCAAGTTCATGCTGATGATGCATTTTCGCCCAGTAATC	AGTCTGCAGCTTCCTGAGATATACTAAT
	HEX	GAAGGTCGGAGTCAACGGATTGGATGATGCATTTTCGCCCAGTAATT	
wri267	FAM	GAAGGTGACCAAGTTCATGCTGATCAGCGGGACAGAACATCTT	GCAGGAACAAGAGCACCCGACTA
	HEX	GAAGGTCGGAGTCAACGGATTGATCAGCGGGACAGAACATCTG	
wri268	FAM	GAAGGTGACCAAGTTCATGCTAAGGAGGATCGAAAGTGAAGC	GTCGCTGTTCCAGTCGTTTATGCTT
	HEX	GAAGGTCGGAGTCAACGGATTGCTAAGGAGGATCGAAAGTGAAGT	
wri269	FAM	GAAGGTGACCAAGTTCATGCTGGTCAGCATATCTCAGAGGACG	GCCGATTATTTTTACGTGCGCTTCTTTTT
	HEX	GAAGGTCGGAGTCAACGGATTCGGTCAGCATATCTCAGAGGACA	
wri270	FAM	GAAGGTGACCAAGTTCATGCTCAACGATCACCGGATTTAGTAAGAC	GATGACTGCAGCCTGCGTGCTT
	HEX	GAAGGTCGGAGTCAACGGATTCAACGATCACCGGATTTAGTAAGAG	

Appendix 5 continued

KASP assay	Primer sequence (5′-3′)		Common primer sequence (5′-3′)
wri271	FAM	GAAGGTGACCAAGTTCATGCTTCCGATGGAACATTCTGCAGC	AGCATGCGTGAGTTCAAGGCCATT
	HEX	GAAGGTCGGAGTCAACGGATTCTTCCGATGGAACATTCTGCAGG	
wri272	FAM	GAAGGTGACCAAGTTCATGCTGCTTTCTTCTCGCACCCGATT	CCTAGGCGTTCCATGTAGAAGCTT
	HEX	GAAGGTCGGAGTCAACGGATTGCTTTCTTCTCGCACCCGATC	
wri273	FAM	GAAGGTGACCAAGTTCATGCTCATAACCGGATCTTCGTGCTGTATA	CTGCAGATTCAAGGGGCAGAAGAAA
	HEX	GAAGGTCGGAGTCAACGGATTATAACCGGATCTTCGTGCTGTATG	
wri274	FAM	GAAGGTGACCAAGTTCATGCTGTAAGCTCAGCCTCTGCAGC	GAGCCTCCCGGATGACCTGTA
	HEX	GAAGGTCGGAGTCAACGGATTCTGTAAGCTCAGCCTCTGCAGT	
wri275	FAM	GAAGGTGACCAAGTTCATGCTCCGCCTTCTTCGGCAAGCTG	CCAGCAGGAGCACCATGTCCAT
	HEX	GAAGGTCGGAGTCAACGGATTCCGCCTTCTTCGGCAAGCTC	
wri276	FAM	GAAGGTGACCAAGTTCATGCTTTCGCGTGCTTTGAGTTTGATCTTTA	CAGCGTCGACGATGTCCAGGTA
	HEX	GAAGGTCGGAGTCAACGGATTCGCGTGCTTTGAGTTTGATCTTTG	
wri277	FAM	GAAGGTGACCAAGTTCATGCTGTGGGTTCTATCGCAGCGATCA	CAACACTTCTGCAGTTCATGCACCAA
	HEX	GAAGGTCGGAGTCAACGGATTGGGTTCTATCGCAGCGATCG	
wri278	FAM	GAAGGTGACCAAGTTCATGCTCCTCCTACTGCAGGAGGGG	CCTTGGTCTGATATTTGTGCTTGAGTATT
	HEX	GAAGGTCGGAGTCAACGGATTCCTCCTACTGCAGGAGGGC	
wri279	FAM	GAAGGTGACCAAGTTCATGCTGTTGACTTGTTGTTGTCATGCCTCT	GCATCTGCAGAGGCCACAACGAA
	HEX	GAAGGTCGGAGTCAACGGATTGACTTGTTGTTGTCATGCCTCC	
wri280	FAM	GAAGGTGACCAAGTTCATGCTAAATCGCCATAGCTGCAGCTTCTA	GAGGACTCTCGGCTTAAAGGCCAT
	HEX	GAAGGTCGGAGTCAACGGATTATCGCCATAGCTGCAGCTTCTG	
wri281	FAM	GAAGGTGACCAAGTTCATGCTAGTACAAGAACATCAGAGTATATTGTACAT	TGACCCTGCAGCTAGCCAATGTATT
	HEX	GAAGGTCGGAGTCAACGGATTGTACAAGAACATCAGAGTATATTGTACAG	
wri282	FAM	GAAGGTGACCAAGTTCATGCTAGCCACAGCCGTGGACCTATT	GATGAGCAGAAAAGGATTATGATCGGTA
	HEX	GAAGGTCGGAGTCAACGGATTAGCCACAGCCGTGGACCTATA	
wri283	FAM	GAAGGTGACCAAGTTCATGCTTCTATCAATCAATAGATAGCTGAGA	TCCTGTTTCATATATTTGTCTTAGCGTCTT
	HEX	GAAGGTCGGAGTCAACGGATTCTTCTATCAATCAATAGATAGCTGAGG	

Appendix 5 continued

KASP assay	Primer sequence (5′-3′)		Common primer sequence (5′-3′)
wri284	FAM	GAAGGTGACCAAGTTCATGCTATCTGAGCTACAGCCGGCCAA	GGATGTATGCATTGTGTACTGTCTAGTTA
	HEX	GAAGGTCGGAGTCAACGGATTCTGAGCTACAGCCGGCCAG	
wri285	FAM	GAAGGTGACCAAGTTCATGCTCGTGCCTTGCTGAAGTGAGAG	ACTCCCTGGCTGCTGGGTACTA
	HEX	GAAGGTCGGAGTCAACGGATTCGTGCCTTGCTGAAGTGAGAC	
wri286	FAM	GAAGGTGACCAAGTTCATGCTTGGATTTCGATGGCGCGCTAAAA	ACCCGACTCCAGAGCGGTTGAT
	HEX	GAAGGTCGGAGTCAACGGATTTCGATGGCGCGCTAAAG	
wri287	FAM	GAAGGTGACCAAGTTCATGCTAGACGGATCAACCTGGACCGA	AATCGCTCCACCTTCCGGCGAA
	HEX	GAAGGTCGGAGTCAACGGATTGACGGATCAACCTGGACCGG	
wri288	FAM	GAAGGTGACCAAGTTCATGCTAACAAGATGGTGGTCAGGTACGTA	CGCCCACCGCCCGCCATTA
	HEX	GAAGGTCGGAGTCAACGGATTCAAGATGGTGGTCAGGTACGTC	
wri289	FAM	GAAGGTGACCAAGTTCATGCTATGTCGGCCTTCTTCGGACCT	CAGTTTCGCCTCTGTGGCAGCTT
	HEX	GAAGGTCGGAGTCAACGGATTGTCGGCCTTCTTCGGACCC	
wri290	FAM	GAAGGTGACCAAGTTCATGCTGAGACAGTTTGTTGGGCTGGCT	AAGCTTTCACCTGCAGCTCACCAAA
	HEX	GAAGGTCGGAGTCAACGGATTGAGACAGTTTGTTGGGCTGGCA	
wri291	FAM	GAAGGTGACCAAGTTCATGCTGGTGTCTGGCCCTGCAGG	TCGTGCGCTCCTTCACCACCAT
	HEX	GAAGGTCGGAGTCAACGGATTCGGTGTCTGGCCCTGCAGA	
wri292	FAM	GAAGGTGACCAAGTTCATGCTATTATGCCTGAATGCGATGTGCTTG	TTAAAGTAGCAAGCGCTGGCTCCAT
	HEX	GAAGGTCGGAGTCAACGGATTATGCCTGAATGCGATGTGCTTC	
wri293	FAM	GAAGGTGACCAAGTTCATGCTAAAGGCAACAGCGAACGGCGAT	GCCACCGAACGTTCCCTGAGAT
	HEX	GAAGGTCGGAGTCAACGGATTGGCAACAGCGAACGGCGAC	
wri294	FAM	GAAGGTGACCAAGTTCATGCTCGATCTCGGGCATTTGTACTAGT	TGGTGGAGTCCCTTTCTTGCCTTTT
	HEX	GAAGGTCGGAGTCAACGGATTCGATCTCGGGCATTTGTACTAGC	
wri295	FAM	GAAGGTGACCAAGTTCATGCTACCTAAGGTGTTCTTCACTATCCG	GTGTCAATTCGCGCGGGAAGTGTA
	HEX	GAAGGTCGGAGTCAACGGATTGACCTAAGGTGTTCTTCACTATCCA	
wri296	FAM	GAAGGTGACCAAGTTCATGCTAACATAATTTGCGTCTGCAGTAGCG	TCGGTGCGTGTTCATGGACTTTCAA
	HEX	GAAGGTCGGAGTCAACGGATTATAACATAATTTGCGTCTGCAGTAGCA	

Appendix 5 continued

KASP assay	Primer sequence (5′-3′)		Common primer sequence (5′-3′)
wri297	FAM	GAAGGTGACCAAGTTCATGCTGGGTGACAAACTGCAGGAGGAA	CTCGGCGCCTCCGTGGCAT
	HEX	GAAGGTCGGAGTCAACGGATTGGTGACAAACTGCAGGAGGAG	
wri298	FAM	GAAGGTGACCAAGTTCATGCTGCATATACTGCAGCAGGAAGCAG	GACGACGAGTTTAATCCTATGATGTTCTT
	HEX	GAAGGTCGGAGTCAACGGATTGCATATACTGCAGCAGGAAGCAC	
wri299	FAM	GAAGGTGACCAAGTTCATGCTGACGTGTAGGCGTAGCAATGGTA	CATCCTTGGTATGATCCGTACACCTA
	HEX	GAAGGTCGGAGTCAACGGATTGACGTGTAGGCGTAGCAATGGTT	
wri300	FAM	GAAGGTGACCAAGTTCATGCTCCTGGACCACGACATAGCAG	ATAGCTGGGTGGACCAACCAACAAA
	HEX	GAAGGTCGGAGTCAACGGATTCCTGGACCACGACATAGCAC	
wri301	FAM	GAAGGTGACCAAGTTCATGCTCATGTGAGCAATAGTTCTCCTTGTCA	ATGTAACCAGGTGTGAATATATCTTCACAT
	HEX	GAAGGTCGGAGTCAACGGATTATGTGAGCAATAGTTCTCCTTGTCG	
wri302	FAM	GAAGGTGACCAAGTTCATGCTATCAACGCTGTGGCTGAGTTCATA	CTGCTAGCTGCCTGTACGGGTA
	HEX	GAAGGTCGGAGTCAACGGATTCAACGCTGTGGCTGAGTTCATG	
wri303	FAM	GAAGGTGACCAAGTTCATGCTCTTGCGCTCCGTGGCCTG	AGGGGCGCCGACTGGGACA
	HEX	GAAGGTCGGAGTCAACGGATTCTTGCGCTCCGTGGCCTC	
wri304	FAM	GAAGGTGACCAAGTTCATGCTTCAGTAGCTCAATTTCTAACAGTACAT	CAATGTTGCTGCAGCACAAAATAAAGAGAT
	HEX	GAAGGTCGGAGTCAACGGATTCAGTAGCTCAATTTCTAACAGTACAC	
wri305	FAM	GAAGGTGACCAAGTTCATGCTCATCGCCGGACTCGATCGAC	GGAGGAAGAAGAGCACGCGGTT
	HEX	GAAGGTCGGAGTCAACGGATTCATCGCCGGACTCGATCGAT	
wri306	FAM	GAAGGTGACCAAGTTCATGCTATTGGTGTCGCGCTTTTTGTGATCT	GCCCTTGCTTCTGGAACCCTCTT
	HEX	GAAGGTCGGAGTCAACGGATTGGTGTCGCGCTTTTTGTGATCC	
wri307	FAM	GAAGGTGACCAAGTTCATGCTATCGTATGCTACTCAACACCGGT	CCGTCGTGTGTGATGCGCCAAT
	HEX	GAAGGTCGGAGTCAACGGATTCGTATGCTACTCAACACCGGC	
wri308	FAM	GAAGGTGACCAAGTTCATGCTCGCTCTTCCGATCTCGGCAC	GAAGAGGGGGTTCCTGTTCTGCAA
	HEX	GAAGGTCGGAGTCAACGGATTCGCTCTTCCGATCTCGGCAG	
wri309	FAM	GAAGGTGACCAAGTTCATGCTTTTTGCTCATATTATTTCCTTGCGTAACA	GGGCATTTTGGCATCGACACCAT
	HEX	GAAGGTCGGAGTCAACGGATTGCTCATATTATTTCCTTGCGTAACG	

Appendix 5 continued

KASP assay	Primer sequence (5′-3′)		Common primer sequence (5′-3′)
wri310	FAM	GAAGGTGACCAAGTTCATGCTGCATGGCGTCGTTGCCGG	CGGCCTCCAAGGTACGTACGTT
	HEX	GAAGGTCGGAGTCAACGGATTAAATGCATGGCGTCGTTGCCGA	
wri311	FAM	GAAGGTGACCAAGTTCATGCTCAGCTCCGCAGCCATGCCTA	TGCAGAGGTACTATTATGGATCTAATTACA
	HEX	GAAGGTCGGAGTCAACGGATTAGCTCCGCAGCCATGCCTG	
wri312	FAM	GAAGGTGACCAAGTTCATGCTGCGGGCTGCAGTTACGACGA	CTCCACCGGCAAGGAGGATCA
	HEX	GAAGGTCGGAGTCAACGGATTCGGGCTGCAGTTACGACGG	
wri313	FAM	GAAGGTGACCAAGTTCATGCTACCATCCTCAACTTTGGACTCTTC	GTGTTGCCGTTGAAGCCGCAGAT
	HEX	GAAGGTCGGAGTCAACGGATTCACCATCCTCAACTTTGGACTCTTA	
wri314	FAM	GAAGGTGACCAAGTTCATGCTATGTAAACAACGTTGAGCTCAAGGC	CCGGGACATGGTGCGGGCT
	HEX	GAAGGTCGGAGTCAACGGATTATGTAAACAACGTTGAGCTCAAGGA	
wri315	FAM	GAAGGTGACCAAGTTCATGCTCAAAAACGGGAACACGGGAGCT	CGCGATGTCCACCTGTCCTTGTA
	HEX	GAAGGTCGGAGTCAACGGATTAAAAACGGGAACACGGGAGCG	
wri316	FAM	GAAGGTGACCAAGTTCATGCTACTGCAGGCTCCTAAATTACTCGT	TCCCATCTAGGAGATTACTTTTCTAACTTT
	HEX	GAAGGTCGGAGTCAACGGATTCTGCAGGCTCCTAAATTACTCGC	
wri317	FAM	GAAGGTGACCAAGTTCATGCTCGGGCTCAGCGCATGGAT	TGCAGTTGGCCGCCAGCCT
	HEX	GAAGGTCGGAGTCAACGGATTCGGGCTCAGCGCATGGAC	
wri318	FAM	GAAGGTGACCAAGTTCATGCTGAGAAAAGCAGGAGATCGTC	CCGCACTTGTACCGGTTGAGCTT
	HEX	GAAGGTCGGAGTCAACGGATTGCTGAGAAAAGCAGGAGATCGTT	
wri319	FAM	GAAGGTGACCAAGTTCATGCTGAGCCAACGAACAAAGTCGGCA	CTGCGGCAGCTTCAAGAACAGGTT
	HEX	GAAGGTCGGAGTCAACGGATTAGCCAACGAACAAAGTCGGCG	
wri320	FAM	GAAGGTGACCAAGTTCATGCTCGGGTCAGTGTGGTGAATTC	TGCAGCATATATGCATGTTGTACTTACTTT
	HEX	GAAGGTCGGAGTCAACGGATTATCTCGGGTCAGTGTGGTGAATTA	
wri321	FAM	GAAGGTGACCAAGTTCATGCTTCGATCTGGACGATAGAGAGTTC	ATGCTGAAAGGACGAGATGCAATTGAAAT
	HEX	GAAGGTCGGAGTCAACGGATTGTTCGATCTGGACGATAGAGAGTTT	
wri322	FAM	GAAGGTGACCAAGTTCATGCTCGGATCTATTGAGCTGGGGCTA	GCCCCATGATGGTCGTGCTGTT
	HEX	GAAGGTCGGAGTCAACGGATTGGATCTATTGAGCTGGGGCTG	

Appendix 5 continued

KASP assay	Primer sequence (5′-3′)		Common primer sequence (5′-3′)
wri323	FAM	GAAGGTGACCAAGTTCATGCTAAAAACGCTGCAGACAGTTGAGCA	GAATCAACAGCTCACACGAGCGAAA
	HEX	GAAGGTCGGAGTCAACGGATTAAAAACGCTGCAGACAGTTGAGCT	
wri324	FAM	GAAGGTGACCAAGTTCATGCTAGCACACCAAAATAATCTGAACGTG	ATCGTTTGTTCCATGTGCCACGGTT
	HEX	GAAGGTCGGAGTCAACGGATTCTAGCACACCAAAATAATCTGAACGTA	
wri325	FAM	GAAGGTGACCAAGTTCATGCTGCAGAGTCTCTCTCCTACGCT	TAAACGCAGACAATAGAGTCAACGCTAA
	HEX	GAAGGTCGGAGTCAACGGATTGCAGAGTCTCTCTCCTACGCA	
wri326	FAM	GAAGGTGACCAAGTTCATGCTACTCCTAGTTATACACCTCAGAGCA	ACCCGGTCATCTCCACAGCGAT
	HEX	GAAGGTCGGAGTCAACGGATTCCTAGTTATACACCTCAGAGCG	
wri327	FAM	GAAGGTGACCAAGTTCATGCTAAAATGGACAAAGAAACCGGCTGG	GAAGTTAACATACGGTTTCGGTTGCTT
	HEX	GAAGGTCGGAGTCAACGGATTAAAATGGACAAAGAAACCGGCTGC	

The information in this appendix was presented in Table S3 in Online Resource 1 of Van Gansbeke et al. (2019).

Appendix 6. Protocol for DNA extraction

Protocol for extraction of DNA from freeze-dried cereal leaf and endosperm tissues

Leaf sample tissue collection and preparation:

- Approximately 2 cm^2 of leaf tissue was harvested from each seedling (at two leaf stage) and placed into 1.1 mL collection mini tubes (Axygen Scientific, California, USA)
- The leaf samples were frozen and stored at -80 °C until freeze-drying commenced

Seed endosperm sample tissue collection and preparation:

- Each seed was cut in two using a scalpel. The embryo-containing portion was stored at 4 °C for future use. The other (endosperm) portion was placed into a 1.1 mL collection mini tube (Axygen Scientific)
- Prior to commencing freeze-drying, 75 µL of sterile water was added to each tube and the samples were kept at room temperature for 4 h
- A 3 mm stainless steel ball bearing was added to each tube and the tubes were capped
- The tissue was milled using a MM300 Retsch mill (Retsch GmbH, Germany) for 1 min at a frequency of 28.5 oscillations per second
- The milled samples were frozen and stored at -80 °C until freeze-drying commenced

Freeze-drying

- Frozen tissue samples were freeze-dried in an Alpha 1-2 LD freeze-dryer (Martin Christ Gefriertrocknungsanlagen GmbH, Germany) for 16 h. Conditions used were -50 °C and 110 mbar.

DNA extraction from freeze-dried leaf and endosperm samples:

- Freeze-dried samples were milled using a MM300 Retsch mill (Retsch GmbH) at a frequency of 28.5 oscillations per second for 1 min
- 600 µL of extraction buffer (0.1 M Tris-HCl, 0.05 M EDTA, 1.25 % SDS (w/v)) was added to each sample. The samples were capped and shaken vigorously to resuspend the crushed tissue. Ball bearings were removed from each tube using a magnet and the samples were incubated at 65 °C for 30 min
- Samples were cooled at 4 °C for 15 min then 300 µL of 6 M ammonium acetate (pre-chilled to 4 °C) was added to each sample. Samples were capped, shaken vigorously to ensure thorough mixing and incubated at to 4 °C for 15 min
- Samples were centrifuged at 2570 rcf for 15 min to pellet down precipitated proteins and cellular debris
- 600 µL of the supernatant from each sample was transferred to a new collection microtube containing 360 µL of isopropanol. Samples were capped, inverted 4-5 times to ensure thorough mixing and incubated at room temperature for 5 min to precipitate the DNA
- Samples were centrifuged at 2570 rcf for 15 min to pellet down the DNA and the supernatant was carefully decanted. Remaining supernatant was allowed to drain off by inverting the sample tubes carefully and standing them on paper towel for 1 min
- 400 µL of 70 % ethanol (v/v) was added to each sample and the DNA pellet was dislodged by gently inverting the capped tubes once
- Samples were centrifuged at 2570 rcf for 15 min and the supernatant was discarded. Samples were then incubated at 50 °C for 5 min to drive off residual ethanol
- The extracted DNA samples were dissolved by resuspending the pellets in 200 µL of RNase A buffer (4µg/mL of RNase A in sterile water)
- Samples were incubated at 4 °C overnight
- The next morning, undissolved debris was pelleted down by centrifuging the samples at 2570 rcf for 20 min
- 200 µL of the supernatant containing the extracted DNA was carefully transferred into fresh tubes and stored at -20 °C until required for downstream experiments

The information in this appendix was presented in Online Resource 3 of Van Gansbeke et al. (2019).

Appendix 7. BLAST queries and hits for RFLP markers and the SCAR marker Ha2S18

This appendix contains query sequences for each of five RFLP markers and the SCAR marker Ha2S18 and information of their best BLAST hits on the International Barley Genome Sequencing Consortium 2H pseudomolecule[a].

Query sequences:

>mwg865

GTAAATATTAAATAACTAGTGTTAATTTGCTTATTATGGCAACAAAAGTCAAGCTTCTGTTCTTTTT
CATGTAGGTAGTATATGGCCCGCTTTCAGTTCTGCCCTGACAGCTGACACTTGCCCCGTTATGGCCA
TCAGGGATTCCGAAATGTTACTGTCAGGCACGTCTAATTCT

> mwg892

CCATAGAAAAAGAAGACTATTTAGAGAATTCAACCGGCCACTAGGTGTAAAGGAAATAAATAGCT
TCCCTTATTAAAGAATGAGGGAGTCTGCTTGCTTGATACATGCAGTAGGAAAGAAGAAACGCAAC
GAACAGTGAGCAGATAAGTAGCGCGAACGAATGTTTACTCACTCGTCTCTGTGAAGGTACCATGGG
ATCTGGATCAATTCGATACCCAGCCCCTGAAATACGTAGCAAAGAACTCCTCATTAGCCTGCGCCT
TGTCCATCTTGGCATCATCTCCCATCTCCTTGGCTTCCTCTATCTCCAATTTTGTCTTTGTGGTTTGG
GATTTCAAGGTACCCTTGTAACTAAGATATCCCATCTGATCCAACTGGGTGCAGAGCTCATCCAGC
CCACTGAAGATTCCATTCAATCCATTGCAATGTATCACCTTGTACTTCACTTTATCCATCCTTTGGA
GCAAACTCTTCACCTCGCTGTACATGTTATCCATGTGGATCTGGACCTCGTCCAAGCTATAGTCGCT
AATCCTCAGCTTCGGCTCCCGTTTCAGCTTCATGGCGTTCTCGGAGATAAGATTGAGCAAGGAGTA
GATCTTAGCCCGAACCGTCTCCGTGCCCGGCCGAGTCTCTGATGTTGTCTCTTCGTGATTCCTCCTC
CTCTGCATCTTTGAAATATACTTGGATATCCGACCATCATCAACGCATCCCTCCCTCGAGATATCCC
GCTTGTCTCGAATAAGCAGGGACCAAGCAACGGTAACCTCCACTTTATAGGGGCCAAGATTACAAA
TGCCTCGACTTATTTTGCATTCCTGAGCTGGGAAGAAAACATGACCACGTGATTTGGAGGCACAGA
TGACGACTTTCAGCTTCCCATTTAACTCTACAGAAACAACGTGCCTTGACAGATCAAGGTAACCAT
CTGAACCATCACCCGTCACTTGATCTTGAAGTACAACCTCCTCTTCAGGTTTAGCTGGCTCAGAAGA
TCCATTGGCAAAGCAGCTAACTCGACCACCATGTTTAAACGGCCATGCCCTCTTCCTCCAATTTGTT
ACACGAACGCTCACAATAGTTGCCTGGACCGTCTTTTCTAATCTTGCACACTGGAACATAATTTTGC
ACAAGTCATTTAACAGAGTGGTATCATCACTGATATAGGTGAAGGTCTGACGCATCAACACTCTAT
CATCCGACTTCCTTCTGCCCTTTACATTCAGTCGAATTTCAAAGTCCACGGGACCTTCAGCGACAAT
TGCGCGAGACGGCCCCGTCAGTTTCAAATAACAATTCTGCATTTGCCAACAATCGTAATCAACAAA
ACAACAAAGATGGACCCATACATGGAAGAAGTAAAGAGAAAACCGTGAGGTCAAAATTGAGTAGT
GGAGTACAACCTTTTGAGTGAGTATTTGGCAGTCACCCCTTTGACGGAGGAAGAGAATGTTGCGGT
TGCGGTCCACGGCATCCCGGGCGGCAACCATGCCGTACACACTCAACGGCCACTTCAACCCAAGAG
CTTCCTCTACTTCTGCGACTTTGAGGGAGCAGAT

> psr901

GTTGGACACATGGGAAGAATAAAGTGGCGAAAATTACCCGAGGAAGATGACACCGACTGATGCTA
TTGAAACCTTTAGAAAGACTTATATTTAGAAACGAAGGAAGTAGAAGATGGAGATAGGATGGAAA
GCAGTTTATGATGCATACAAAGTGTCGTCGAAGAACGCGGTTTTCGGGTAGAAACTTTGGATATAT
GTAGATATATTCATCCGCCTAGAAAAATTTCTTGTGTGGGGTTTTATGGCGTCGTGGCCAGACCCTG
AGAGCAACCCGAAACAAACACCACCTCGAATAAGTGAGGCGCCATTTCCATCAGCGTGGATCTGA
ACTGACATGCACATCTAGTCATCCATGAATAGTATTCATGATCCCGGATCAGTTGCGTCCGTGTGGC
AGTTTGATTGTCCAGTCCACGATCGATCGAATGGTCGGTGGCCGTCCGTGTTTAGTTGTCTATATCC
AAAACCCAAATGATAAGCGGATAACCGAACCACTTAAAATTAGGTATTTATAGGTACATACGTGA
GCAAAAAAAAAAAAAACTATGGAAGAACACTTGCATAGATTAATAGATATATATGCATGCTTTCTG
GAGACACTAATCGCATAAATTAAGCTAAGTAGACCGGCCAGAAGCACACACACACGCGTTAATCA
ATCGCTGGAATTAAGCTTGAGGGACACGGCTGTCCAACAAAACGAACTGAACTGACCTCTCATCAT
CGCCGTCATCATCAGCCAAGCGACAGGACAAACCGCCGTGCCATCCCCTTGCACCCCACCTTCCCT
ACACCCGTATCCCACCATATCCAGCTTTCTCTAGGACCAGCTAAATATTCCCTAAGCTACTGCATGC
TCTTCTACAACACTTGTCACACATTAATACTCGTGTTCCTTCCTGAGAAAGAAAAAA.

> awbma21

AGATCTGGATTTACAAATTTACATACGTATTATTTCCCAGAAAAATATATATTAAAAGTAGCAACA
ACCGAAGAAGAAGAAGAACTAAAGAGTCCCAAACGGAGTCTAGCTAGAAGCCTCAGCCCTCGATC
GAGAAGGCACGCACAACCCGACCACCCAACAGCACAACACACATGCACACAACCCTGCACCGGCC
ACCACCCCTCAAGAAACGGGACAAGACCACGCTAAAGATCAAGCTATAACGGCACGAGCTCGTGG
ATCAGACGACG

> mwg694
AATTCCGCGGCTGCTATCGACGGGCTCTCCCCATTCCCAGGTGATGGGTGGTTCACGTCTGCGCCTA
TGAACATGTAAGGAACACCGTTGTCCAGTGGGAGCTTGTCCTGGAGCTGGGTGTTGATGCCCCCGA
GCTTGCCGTTGATCTTGAGAGCAAGGTTGGACATGTACTGGTCCTGGCCCTGGGTTTTGTTTGCGAG
GTGGCTCAAGAAACACTGGGTTTGGATCCCCAGCTGCGTCTCGCAGATCAGCTTCAGTGTCTTGTA
CCCATGATGCTGCTCAGACATCGGGCAGAAGAGGAGTTGCAGCTTCTGGTTCTTCTTCACCGCAGC
CTGCTTTGCTTTGTTCAGCTCCTCGTGCAGTTGGTGTGGATCCGATAGCACTGACATTTCTGATAAA
TGCACAAAACATGCTGGCTTGTCATCTGAATGCAAGGGCACAGCACTTCCTGAC
>Ha2S18
CACACACACATTCAGAGAGCCCATGAGAATGTCCATGACTTGTGACTAAACTTTCACCCCGAATCC
TTCCTAGCTACTCTAGCCAGTACACAAATCAATAGGCGGCCGGCCGTGTCGCCGTGCACCCATGCC
ACCATGACTTTTCAGGTGCTCATCCCATTATTTGCCTACTAGCTCCTCTACCCTTCTGGAAGGCATG
CATGAACAGTACAGTAGGGACAGAAGCGCCATTTAGCTAGTAGTCTCCACATCTATCTATCCATTG
TGTGGATAAACCCTGTGATGTGCATGAGCCGTGTCAACCAACTCGATCACCATGAGCCGCACGCTA
GCCAGGCCCAGTTCTCCGGTGGGGGTGGGGACACGAGTGACGTGGGTGGTGCAACCCAAACCCAT
GTGTGTGTGTG

BLAST results

Marker	Identity (%)	Length	Mismatch	Gap open	Query start	Query end	Start on 2H (bp)	End on 2H (bp)	E-value	Bitscore
mwg865	100	175	0	0	1	175	654,782,490	654,782,664	3.00E-87	324
mwg892	100	1559	0	0	1	1559	677,498,309	677,499,867	0	2880
psr901	100	914	0	0	1	914	681,289,811	681,290,724	0	1688
awbma21	96.01	276	7	2	1	272	682,575,254	682,575,529	9.00E-124	446
mwg694	98.66	448	4	2	8	453	684,122,590	684,123,037	0	793
Ha2S18	98.06	412	3	3	1	407	685,898,248	685,898,659	0	712

[a] 150831_barley_pseudomolecules_chr2H.fasta downloaded from http://webblast.ipk-gatersleben.de/barley_ibsc/downloads/

The information in this appendix was presented in Table S4 in Online Resource 1 of Van Gansbeke et al. (2019).

Appendix 8. BLAST hits, SNP results and KASP assays for 38 GBS tag pairs

Table S5 in Online Resource 1 of Van Gansbeke et al. (2019) presented sequences for 1937 SNP-containing tag pairs discovered with DArTseq genotyping by sequencing (GBS) of resistant and susceptible barley lines, the best BLAST hits of those sequences on the International Barley Genome Sequencing Consortium 2H pseudomolecule[a] and the names of KASP assays designed for 106 of the SNPs. Due to the very large size of that table, only a subset of the information is presented below. Table A8-1 gives the sequences of SNP-containing tag pairs for which the best BLAST hit was within a 5,077 kbp region between the positions of mwg892 (577,498 kbp) and awbma21 (682,575 kbp). Table A8-2 shows the GBS results for those tag pairs and gives the names of KASP assays.

Table A8-1: GBS tag pairs and query sequences

Tag pair	Query sequence
100019996|F|0--67:G>A	TGCAGTTGCCGCCATGTCCACCACATGTATGGAATAATACACACGATAATGATGTCGGAGAGCAGCGGT
100019280|F|0--17:G>A	TGCAGCTCCATGCCATGGAGGCTGTTTTTGATGGTCACATCAATTATCCCTCCTGTTGCTTCTCACAAA
100001753|F|0--16:A>G	TGCAGACAAAGCATGCATACATTGAGCAAAACTAACCTGTTTTTACATGATAATACAGGACGGCGTTCT
100008069|F|0--14:C>T	TGCAGTTTGTAGTACTAAATTTTGAGTTGAGCATTGCTAGAGGCGACACTTAATGGTTGACTGATCTTT
100017077|F|0--55:C>T	TGCAGTTTCATGTATATGTTTAGTGACATAATAGTTAGGAAGTTCAGTTCCAGTGCACAGAAAATTCAG
100023670|F|0--15:A>G	TGCAGACAGTTCGGCAGCACCAAAACCCTCATCTCTCTCCTTTCGCTCGTGTGAGCTGTTGATTCTTCT
100003923|F|0--48:G>A	TGCAGGACATTTGATCAATTAGCTAGCACACCAAAATAATCTGAACGTGAACCGTGGCACATGGAACAA
100028430|F|0--21:T>A	TGCAGAGTCTCTCTCCTACGCTAGTTAGCGTTGACTCTATTGTCTGCGTTTACATTTGTGCAGCTTCCA
100013992|F|0--40:A>T	TGCAGCAATATTTGCTTGTGATTTTTGAAAAATATACTTAAATTCGTTGATTTTTTAAAGAACATGCCC
100013992|F|0--26:G>A	TGCAGCAATATTTGCTTGTGATTTTTGAAAAATATACTTAAATTCGTTGATTTTTTAAAGAACATGCCC
100019401|F|0--33:G>A	TGCAGAGTAGTACGTATGAAAGCATATATAACGGCTAACCTCATGTTTGTGTGCAACTGTGTATGCTGA
100012977|F|0--68:A>G	TGCAGCAGATCTCTCCTTGTTTCCCGGCGTCAAACCGCTCCACTCTCTCTTATCCAAATCCCCTGCCGA
100031277|F|0--64:T>C	TGCAGTTGTTGATGAAACCGAGATACCCGGGCCCCATGATGGTCGTGCTGTTGGCGCCGCGCGATAGCC
100011037|F|0--50:G>A	TGCAGGCTCCAGCGATACACATGCTGAAAGGACGAGATGCAATTGAAATCGAACTCTCTATCGTCCAGA
100033069|F|0--10:A>G	TGCAGGAGGAAGCATGCCACGGAGGCGCCGAGCAGCTGGGCGACCCAGTAGAAGAGCCCGAGATCGGAA
100014698|F|0--24:T>C	TGCAGCCCCACACACACACACGCATGCTCTGAGGTGTATAACTAGGAGTTGCATGCATGCTTGTGGAAG
100028752|F|0--65:G>T	TGCAGTACCACGACAAGTCTACAATCGCTTGAAAGCTGCGGTGTGCCACCGGGAGGGAAAGCGATGGCT
100008426|F|0--47:C>G	TGCAGGAAAGAAACGTTTTGGAAGTTAACATACGGTTTCGGTTGCTTCCAGCCGAGATCGGAAGAGCGG
100018670|F|0--56:A>G	TGCAGTTGCCGAAAATTATTCCTCCCCCCTGCCTTTTAGTGTACTGCCTGAGCCTCATCTTTGATTTTG

Table A8-1 continued

Tag pair	Query sequence
100007340|F|0--31:T>A	TGCAGTTTCTAGTTTGTGGTCCGTGTTGTTGTGGGTTTCACGCTCAGTCTGAACCCCTGGAAATATGGA
100027857|F|0--66:C>T	TGCAGGAGCGTAGGTAACGTGTGGTTCCTGTAGCTTATACAACTGCTGGTAACCATTATATTAGGGCGG
100017771|F|0--61:G>C	TGCAGTCCTAGTTTATGCTTGCTGTATCTTCTCTTCTGATCCCCTCTAAATGTCAAGCGGAGTGGACGG
100006533|F|0--14:G>T	TGCAGCAGCAACAAGAAGAAGTGAAATATATATCAACCAGGTAAGCACTACCATCCCGAGATCGGAAGA
100031893|F|0--41:A>C	TGCAGCTTGGCCACCAGCAGAACCAGCCGCCGGAGCGGCACAAAGATGAGCGTCACTGGAACGATGCAC
100039867|F|0--56:A>T	TGCAGACTTGGTCGGGAAGCAAGAGCAACACGGAGAGGAGGCAAAGAATTTATGGGAGCAAAGGCAAAG
100036558|F|0--46:T>C	TGCAGGAATAAATCAAAACAAGGAACAAAAGGCGCCGAGGGGGGGATTCGAACCCTGGACCTCTCATCA
100005830|F|0--25:G>C	TGCAGAACAAGCCGCGCTACTGCATGCTACTAAACCGCTGCTAGGGAACAGAGAAGCACGCGCCACGCC
100024591|F|0--42:G>A	TGCAGCCCTGCTACCTGGGCCAGGCTGATCCCCTCCAGCTTTGTGCGAAGCCTCGACACCGCTTCGCAC
100014233|F|0--40:G>T	TGCAGGGTTTGGTGTGTGTGTCAGAGGTGTGCATGTTGGCGTGCATTCACGCGATCCTCCTAAAGAGGC
100038050|F|0--31:C>T	TGCAGGTTAATGCATGAGCGATTCAGACCTGCACGGCCGAGATCGGAAGAGCGGTTCAGCAGGAATGCC
100027260|F|0--60:G>A	TGCAGGTTAATGCATGAGCGATTCAGACCTGCACGGCCGGTTTCTTTCGAAAGTACAGCTGACTTTGAC
100027260|F|0--31:C>T	TGCAGGTTAATGCATGAGCGATTCAGACCTGCACGGCCGGTTTCTTTCGAAAGTACAGCTGACTTTGAC
100001483|F|0--28:T>C	TGCAGGTTCCTGTTCCTGATCGCAGCAATGTACACCCGCAAGATTTCGAGGAGCGCGCTGCTGCCCTGC
100014049|F|0--39:A>T	TGCAGTGCACCGTCGTCAGACGGTGACCATCGCTGATTTAACAAGTACGTCACGGATAAGCACGGGCTC
100003696|F|0--65:C>T	TGCAGGAATATAAGACGGCAGCATAGCTTTGACCTAATTATCATCCTTCACCGTTAACATGATAACATC
100026886|F|0--57:T>A	TGCAGGTCAGGCAAGGTCCAGCAGACCTACGAGGATAGCCCTGAGCCTGGTCAACTCTACCCCAAACGG
100006587|F|0--51:C>T	TGCAGAGATTATCTTCTTTTCCTAATAACCTTGTTCCTAAAAGGGAGCCAACTCACAAGATGGTTTCCA
100014900|F|0--48:C>G	TGCAGTCTTCAGCTTATCGTGCATGGACACATCCCTGCGTCTACAGCGCCTGGCGCCGAGATCGGAAGA

[a] 150831_barley_pseudomolecules_chr2H.fasta downloaded from http://webblast.ipk-gatersleben.de/barley_ibsc/downloads/

Table A8-2: BLAST and GBS results for the respective GBS tags

Tag pair	BLAST results										GBS results											KASP assay
	Identity (%)	Length	Mismatch	Gap open	Query start	Query end	Start on 2H (bp)	End on 2H (bp)	E-value	Bitscore	Chebec (resistant parent)	Resistant C/H lines	Harrington (susceptible parent)	Susceptible C/H lines	Sahara 3771 (resistant parent)	Resistant C/S lines	Clipper (susceptible parent)	Susceptible C/S lines	Sloop (susceptible cultivar)	Sloop SA (resistant cultivar)	Sloop Vic (resistant cultivar)	
100019996|F|0--67:G>A	100.00	67	0	0	1	67	678,270,139	678,270,073	9.00E-28	124	G	G	G	G	A	A	G	G	G	G	A	
100019280|F|0--17:G>A	100.00	69	0	0	1	69	678,294,586	678,294,654	7.00E-29	128	G	G	G	G	A	A	G	G	G	G	A	
100001753|F|0--16:A>G	98.55	69	1	0	1	69	678,621,713	678,621,645	3.00E-27	122	A	A	A	A	A	A	A	A	A	A	A	
100008069|F|0--14:C>T	98.55	69	1	0	1	69	678,958,063	678,958,131	3.00E-27	122	-	C	C	C	-	C	C	C	C	-	-	
100017077|F|0--55:C>T	98.55	69	1	0	1	69	678,958,370	678,958,302	3.00E-27	122	-	C	C	C	-	C	C	C	C	-	-	
100023670|F|0--15:A>G	95.65	69	3	0	1	69	679,062,608	679,062,676	7.00E-24	111	G	G	A	A	A	A	A	A	G	G	G	wri323
100003923|F|0--48:G>A	100.00	69	0	0	1	69	679,425,865	679,425,797	7.00E-29	128	G	G	A	A	G	G	G	G	-	G	G	wri324
100028430|F|0--21:T>A	97.10	69	2	0	1	69	679,641,002	679,641,070	1.00E-25	117	-	-	-	-	-	-	-	-	T	-	-	wri325
100013992|F|0--40:A>T	100.00	69	0	0	1	69	679,676,721	679,676,653	7.00E-29	128	T	T	-	-	T	T	A	A	-	T	T	wri243
100013992|F|0--26:G>A	100.00	69	0	0	1	69	679,676,721	679,676,653	7.00E-29	128	-	A	A	A	-	G	G	G	-	-	-	
100019401|F|0--33:G>A	100.00	69	0	0	1	69	679,727,362	679,727,294	7.00E-29	128	A	A	G	G	A	A	G	G	G	A	A	wri224
100012977|F|0--68:A>G	100.00	68	0	0	1	68	679,830,630	679,830,697	2.00E-28	126	A	A	A	A	A	A	A	A	A	G	A	wri225
100031277|F|0--64:T>C	98.55	69	1	0	1	69	679,877,715	679,877,647	3.00E-27	122	T	T	-	C	T	T	-	C	C	T	T	wri322
100011037|F|0--50:G>A	100.00	69	0	0	1	69	680,107,421	680,107,489	7.00E-29	128	A	A	G	G	A	A	G	G	G	A	A	wri321
100033069|F|0--10:A>G	98.33	60	1	0	1	60	680,441,295	680,441,236	3.00E-22	106	A	A	G	G	A	A	G	G	G	A	A	wri297
100014698|F|0--24:T>C	100.00	69	0	0	1	69	680,442,767	680,442,699	7.00E-29	128	C	C	-	-	C	C	T	T	-	C	C	wri326
100028752|F|0--65:G>T	100.00	69	0	0	1	69	680,705,177	680,705,109	7.00E-29	128	T	T	T	T	G	G	G	G	G	T	G	wri237
100008426|F|0--47:C>G	100.00	54	0	0	1	54	680,719,125	680,719,178	1.00E-20	100	-	C	C	C	C	C	C	C	G	-	C	wri327

Table A8-2 continued

Tag pair	BLAST results										GBS results											KASP assay
	Identity (%)	Length	Mismatch	Gap open	Query start	Query end	Start on 2H (bp)	End on 2H (bp)	E-value	Bitscore	Chebec (resistant parent)	Resistant C/H lines	Harrington (susceptible parent)	Susceptible C/H lines	Sahara 3771 (resistant parent)	Resistant C/S lines	Clipper (susceptible parent)	Susceptible C/S lines	Sloop (susceptible cultivar)	Sloop SA (resistant cultivar)	Sloop Vic (resistant cultivar)	
100018670|F|0--56:A>G	100.00	69	0	0	1	69	680,983,026	680,982,958	7.00E-29	128	-	-	-	-	G	G	A	A	-	-	G	wri244
100007340|F|0--31:T>A	100.00	65	0	0	5	69	680,983,903	680,983,839	1.00E-26	121	T	T	T	T	A	A	-	-	-	T	A	
100027857|F|0--66:C>T	100.00	66	0	0	1	66	680,984,274	680,984,339	3.00E-27	122	T	T	T	T	C	C	T	T	-	T	C	wri245
100017771|F|0--61:G>C	100.00	69	0	0	1	69	680,984,277	680,984,209	7.00E-29	128	G	G	G	G	G	G	G	G	C	G	G	wri223
100006533|F|0--14:G>T	98.28	58	1	0	1	58	681,069,824	681,069,881	4.00E-21	102	G	G	G	G	G	G	G	G	G	G	G	
100031893|F|0--41:A>C	100.00	69	0	0	1	69	681,155,099	681,155,167	7.00E-29	128	-	C	C	C	A	A	-	-	C	-	A	wri240
100039867|F|0--56:A>T	98.55	69	1	0	1	69	681,463,946	681,463,878	3.00E-27	122	-	-	T	T	T	T	-	-	A	-	T	wri222
100036558|F|0--46:T>C	96.36	55	2	0	1	55	681,496,945	681,496,999	9.00E-18	91.6	-	C	C	C	-	-	-	-	-	-	-	
100005830|F|0--25:G>C	97.10	69	2	0	1	69	681,497,261	681,497,329	1.00E-25	117	-	C	-	-	-	-	-	-	-	-	-	
100024591|F|0--42:G>A	88.57	70	6	2	1	69	681,706,632	681,706,564	2.00E-15	84.2	A	G	G	G	A	G	G	G	A	A	A	
100014233|F|0--40:G>T	95.71	70	1	2	1	68	682,159,817	682,159,748	7.00E-24	111	-	-	-	-	T	T	-	T	T	-	T	
100038050|F|0--31:C>T	100.00	39	0	0	1	39	682,177,881	682,177,843	3.00E-12	73.1	C	C	C	C	C	C	C	C	T	C	C	wri228
100027260|F|0--60:G>A	100.00	69	0	0	1	69	682,177,881	682,177,813	7.00E-29	128	A	A	A	A	A	A	G	G	-	A	A	wri248
100027260|F|0--31:C>T	100.00	69	0	0	1	69	682,177,881	682,177,813	7.00E-29	128	-	-	-	-	-	C	C	C	T	-	-	
100001483|F|0--28:T>C	97.10	69	2	0	1	69	682,237,782	682,237,850	1.00E-25	117	T	C	C	T	T	T	T	T	T	T	T	
100014049|F|0--39:A>T	98.55	69	1	0	1	69	682,241,544	682,241,612	3.00E-27	122	A	A	T	T	T	T	T	T	T	A	T	wri231
100003696|F|0--65:C>T	100.00	69	0	0	1	69	682,309,228	682,309,160	7.00E-29	128	C	C	-	C	-	C	C	C	-	C	-	wri255
100026886|F|0--57:T>A	100.00	48	0	0	1	48	682,323,095	682,323,048	3.00E-17	89.8	A	A	A	A	A	A	T	T	A	A	A	wri250

Table A8-2 continued

Tag pair	BLAST results										GBS results											KASP assay
	Identity (%)	Length	Mismatch	Gap open	Query start	Query end	Start on 2H (bp)	End on 2H (bp)	E-value	Bitscore	Chebec (resistant parent)	Resistant C/H lines	Harrington (susceptible parent)	Susceptible C/H lines	Sahara 3771 (resistant parent)	Resistant C/S lines	Clipper (susceptible parent)	Susceptible C/S lines	Sloop (susceptible cultivar)	Sloop SA (resistant cultivar)	Sloop Vic (resistant cultivar)	
100006587|F|0--51:C>T	100.00	69	0	0	1	69	682,420,819	682,420,887	7.00E-29	128	C	C	T	T	T	T	C	C	C	C	T	wri233
100014900|F|0--48:C>G	100.00	58	0	0	1	58	682,572,315	682,572,372	9.00E-23	108	G	G	C	C	C	C	G	G	C	G	C	wri232

The information in this appendix was presented in Table S5 - Online Resource 1 of Van Gansbeke et al. (2019).

Appendix 9. Classification of recombinant haplotypes according to resistance status of recombinant BC_2F_3 plants

BC_2F_2 family or control	Recombinant haplotype[a]																Haplotype number in Figure 3-4	Resistance status of BC_2F_3 progeny with the recombinant haplotype	Phenotypic results supporting the classification of recombinant BC_2F_3 plants as resistant or susceptible								
																			Number of plants evaluated	Number of white cysts per plant							
																				Pots test		Tube test 1		Tube test 2		Tube test 3	
	wri243	wri224	wri322	wri321	wri297	wri326	wri237	wri244	wri223	wri248	wri255	wri231	wri232	wri242	wri235	wri256				Mean	Standard error	Mean	Standard error	Mean	Standard error	Mean	Standard error
BVG3-16-46	T	A	C	G	G	-[b]	G	A	C	G	T	T	C	G	T	G	3	Susceptible	14			19.3	2.9				
BVG3-144-56	T	A	C	G	G	null[c]	G	A	C	-	T	T	C	G	T	-		Susceptible	3					14.7	3.7		
BVG3-31-203	T	A	T	A	A	G	G	A	C	G	T	-	C	G	T	G	5	Resistant	4	0.3	0.2						
BVG3-20-85	T	A	T	A	A	G	G	A	C	G	T	T	C	G	T	G		Resistant	7	0.6	0.4						
BVG3-97-1	T	A	T	A	A	G	G	A	C	G	T	T	C	G	T	G		Resistant	6	0.2	0.2						
BVG3-144-110	T	A	T	A	A	G	G	A	C	G	T	T	C	G	T	-		Resistant	3					3.0	2.0		
BVG3-86-5	T	A	T	A	A	G	G	A	C	G	T	T	C	G	T	G		Resistant	15							4.8	2.1
BVG3-91-29	A	A	T	A	A	G	G	A	C	G	T	T	C	G	T	G		Resistant	9							4.4	1.0
BVG3-41-87	T	A	T	A	A	G	T	A	C	G	T	T	C	G	T	G	6	Resistant	10	0.4	0.2						
BVG3-65-33	T	A	T	A	A	G	T	A	C	G	T	T	C	G	T	G		Resistant	6	0.5	0.3						
BVG3-29-119	T	A	T	A	A	G	T	G	G	G	T	T	C	G	T	G	7	Resistant	7	0.1	0.1						
BVG3-7-1	T	A	T	A	A	G	T	G	G	G	T	T	C	G	T	G		Resistant	6	0.3	0.3						
BVG3-61-80	T	A	T	A	A	G	T	G	G	G	T	T	C	G	T	G		Resistant	4	0.5	0.5						
BVG3-65-106	T	A	T	A	A	G	T	G	G	G	T	T	C	G	T	G		Resistant	8	0.6	0.3						

Appendix 9 continued

BC_2F_2 family or control	Recombinant haplotype[a]																Haplotype number in Figure 3-4	Resistance status of BC_2F_3 progeny with the recombinant haplotype	Phenotypic results supporting the classification of recombinant BC_2F_3 plants as resistant or susceptible								
																			Number of plants evaluated	Number of white cysts per plant							
																				Pots test		Tube test 1		Tube test 2		Tube test 3	
	wri243	wri224	wri322	wri321	wri297	wri326	wri237	wri244	wri223	wri248	wri255	wri231	wri232	wri242	wri235	wri256				Mean	Standard error	Mean	Standard error	Mean	Standard error	Mean	Standard error
BVG3-61-169	T	A	T	A	A	G	T	G	G	G	T	T	C	G	T	G	7	Resistant	7	1.1	0.6						
BVG3-41-68	T	A	T	A	A	G	T	G	G	G	T	T	C	-	T	G		Resistant	8	0.6	0.3						
BVG3-54-163	T	A	T	A	A	G	T	G	G	G	T	T	C	G	T	G		Resistant	3	0.3	0.3						
BVG3-54-123	T	A	T	A	A	G	T	G	G	G	T	T	C	G	T	G		Resistant	7	0.9	0.9						
BVG3-39-1	T	A	T	-	A	G	T	G	G	G	T	T	C	G	T	G		Resistant	4	0.0	0.0						
BVG3-15-258	T	A	T	A	A	G	T	G	G	G	T	T	C	G	T	G		Resistant	7	1.4	0.7						
BVG3-20-192	T	A	T	A	A	G	T	G	G	G	T	T	C	G	T	G		Resistant	4	0.5	0.3						
BVG3-24-69	T	A	T	A	A	G	T	G	G	G	T	T	C	G	T	G		Resistant	6	1.2	0.6						
BVG3-68-91	T	A	T	A	A	G	T	G	G	G	T	T	C	G	T	G		Resistant	8	0.4	0.3						
BVG3-31-63	T	A	T	A	A	G	T	G	G	G	T	T	C	G	T	G		Resistant	6	0.3	0.2						
BVG3-72-67	A	G	T	A	A	G	T	G	G	A	C	A	G	A	C	T	4	Resistant	3			4.3	3.4				
BVG3-42-32	A	G	T	A	A	G	T	G	G	A	C	A	G	A	C	T		Resistant	9			1.0	0.2				
BVG3-116-131	A	G	T	A	A	G	T	G	G	A	C	A	-	A	C	T		Resistant	4					1.3	0.6		
BVG3-84-115	A	G	C	G	G	null	G	G	G	A	C	A	G	A	C	T	2	Susceptible	5					24.8	2.4		
BVG3-90-105	A	G	C	G	G	null	G	G	G	A	C	A	G	A	C	T		Susceptible	4					16.5	2.8		
BVG3-86-12	A	G	C	G	G	null	G	G	G	A	C	A	G	A	C	T		Susceptible	5					32.6	5.0		
BVG3-105-66	A	G	C	G	G	null	G	G	G	A	C	A	G	A	C	T		Susceptible	1					19.0			
BVG3-41-245	A	G	C	G	G	null	G	G	G	A	C	A	G	A	C	T		Susceptible	3	15.3	3.8						
BVG3-24-91	A	G	C	G	G	null	G	G	G	A	C	A	G	A	C	T		Susceptible	4	15.8	3.2						
BVG3-139-110	A	G	C	G	G	null	G	G	G	A	C	A	G	A	C	T		Susceptible	4					24.8	7.5		

Appendix 9 continued

BC_2F_2 family or control	Recombinant haplotype[a]																Haplotype number in Figure 3-4	Resistance status of BC_2F_3 progeny with the recombinant haplotype	Phenotypic results supporting the classification of recombinant BC_2F_3 plants as resistant or susceptible								
																			Number of plants evaluated	Number of white cysts per plant							
																				Pots test		Tube test 1		Tube test 2		Tube test 3	
	wri243	wri224	wri322	wri321	wri297	wri326	wri237	wri244	wri223	wri248	wri255	wri231	wri232	wri242	wri235	wri256				Mean	Standard error	Mean	Standard error	Mean	Standard error	Mean	Standard error
BVG3-16-63	A	G	C	G	G	null	G	A	C	A	C	A	G	A	C	T	1	Susceptible	5	17.2	2.9						
BVG3-24-168	A	G	C	G	G	null	G	A	C	A	C	A	G	A	C	T		Susceptible	8	14.8	2.8						
BVG3-16-215	A	G	C	G	G	null	G	A	C	A	C	A	G	A	C	T		Susceptible	4	7.0	2.0						
BVG3-31-15	A	G	C	G	G	null	G	A	C	A	C	A	G	A	C	T		Susceptible	8	14.0	2.7						
BVG3-46-39	A	G	C	G	G	null	G	A	C	A	C	A	G	A	C	T		Susceptible	6	29.7	0.3						
BVG3-39-109	A	G	C	G	G	null	G	A	C	A	C	A	G	A	C	T		Susceptible	7	16.1	3.2						
BVG3-65-61	A	G	C	G	G	null	G	A	C	A	C	A	G	A	C	T		Susceptible	3	19.7	1.3						
BVG3-72-60	A	G	C	G	G	null	G	A	C	A	C	A	G	A	C	T		Susceptible	6	18.8	1.8						
BVG3-72-131	A	G	C	G	G	null	G	A	C	A	C	A	G	A	C	T		Susceptible	7	15.4	3.1						
BVG3-1-190	A	G	-	G	G	null	G	A	C	G	C	A	G	A	C	T	-[g]	Susceptible	5	21.0	0.0						
BVG3-62-108	A	G	C	G	G	null	G	A	C	G	C	A	G	A	C	T		Susceptible	7	15.7	2.7						
BVG3-118-2	-	G	C	G	G	null	G	A	C	G	C	A	G	A	C	T		Susceptible	5	12.7	3.6						
BVG3-12-66	T	A	T	A	A	G	T	G	G	A	C	T	C	G	T	G	-[g]	Resistant	10	0.7	0.4						
BVG3-62-84	T	A	T	A	A	G	T	G	G	A	C	T	C	G	T	G		Resistant	6	0.3	0.2						
BVG3-72-48	T	A	T	A	A	G	T	G	G	A	T	T	C	G	T	G	-[g]	Resistant	7	1.0	0.7						
BVG3-68-87	T	A	T	A	A	G	T	G	G	A	T	T	C	G	T	G		Resistant	5	0.2	0.2						
BVG3-62-153	T	A	T	A	A	G	T	G	G	A	T	T	C	G	T	G		Resistant	6	0.5	0.3						
BVG3-65-11	T	A	T	A	A	G	T	G	G	A	T	T	C	G	T	G		Resistant	5	0.2	0.2						
BVG3-12-65	T	A	T	A	A	G	T	G	G	A	T	T	C	G	T	G		Resistant	9	0.8	0.4						

Appendix 9 continued

BC_2F_2 family or control	Recombinant haplotype[a]															Haplotype number in Figure 3-4	Resistance status of BC_2F_3 progeny with the recombinant haplotype	Phenotypic results supporting the classification of recombinant BC_2F_3 plants as resistant or susceptible								
																		Number plants of evaluated	Number of white cysts per plant							
																			Pots test		Tube test 1		Tube test 2		Tube test 3	
	wri243	wri224	wri322	wri321	wri297	wri326	wri237	wri244	wri223	wri248	wri255	wri231	wri232	wri242	wri235	wri256				Mean	Standard error	Mean	Standard error	Mean	Standard error	Mean	Standard error
Sloop haplotype																		120[d]	16.2	0.7	23.1	4.2			25.2	5.2
Resistant controls																		60[e]	0.6	0.2	0.1	0.1	1.2	0.3	0.7	0.3
Susceptible controls																		65[f]	15.4	1.1	20.9	3.0	38.8	4.0	34.5	2.5

[a] Shading indicates whether marker alleles are the same as those of Sloop SA (dark) or Sloop (light)
[b] Not called due to ambiguous (intermediate) results
[c] Neither HEX nor FAM fluorescence detected
[d] 105 in the pots test; 9 in tube test 1; 6 in tube test 3
[e] 33 Sloop SA plants in the pot test; 9 Chebec plants in tube test 1; 8 and 10 Sloop SA plants in tube tests 2 and 3, respectively
[f] 31 Sloop plants in the pot test; 10 Schooner plants in tube test 1; 14 and 10 Sloop plants in tube tests 2 and 3, respectively
[g] Not included in Figure 3-4

The information in this appendix was presented in Table S6 in Online Resource 1 of Van Gansbeke et al. (2019).

Appendix 10. Phenotyping of 101 Sloop SA/Sloop F_2 plants

Numbers of plants with between 0 and 34 white cysts, among 23 plants of Sloop, 23 plants of Sloop SA and 101 Sloop SA/Sloop F_2 plants, with each F_2 plant classified as a Sloop homozygote, a Sloop:Sloop SA heterozygote or a Sloop SA homozygote according to genotyping results obtained with KASP assays wri321 and wri297

Number of white cysts	Number of Sloop plants	Number of Sloop SA plants	Number of Sloop/Sloop SA F_2 plants		
			Sloop homozygotes	Sloop:SloopSA heterozygotes	Sloop SA homozygotes
0	3	21	5	44	18
1	2	2	1	5	1
2	3	-	1	2	-
3	-	-	2	1	1
4	3	-	1	-	-
5	1	-	3	-	-
6	2	-	3	-	-
7	-	-	2	-	-
8	-	-	2	-	-
9	-	-	1	-	-
10	-	-	1	-	-
11	-	-	-	-	-
12	-	-	2	-	-
13	-	-	1	-	-
14	2	-	-	-	-
15	1	-	1	-	-
16	-	-	-	-	-
17	-	-	-	-	-
18	1	-	1	-	-
19	-	-	-	-	-
20	2	-	1	-	-
21	-	-	-	-	-
22	1	-	1	-	-
23	-	-	-	-	-
24	-	-	-	-	-
25	1	-	-	-	-
26	-	-	-	-	-
27	-	-	-	-	-
28	-	-	-	-	-
29	-	-	-	-	-
30	-	-	-	-	-
31	-	-	-	-	-
32	-	-	-	-	-
33	-	-	-	-	-
34	1	-	-	-	-
Total	23	23	29	52	20

The information in this appendix was presented in Table S7 in Online Resource 1 of Van Gansbeke et al. (2019).

Appendix 11. Genotypic and phenotypic data for 24 barley cultivars

Genotypic data, number of white cysts and resistance status for 24 barley cultivars that were evaluated for cereal cyst nematode resistance in a tube test

	Genotypes obtained with KASP assays[a]			Number of plants evaluated	Number of white cysts per plant		
Cultivar	**wri322**	**wri321**	**wri297**		**Mean**	**Standard error**	**Resistance status**
Chebec	T:T	A:A	A:A	10	1.0	0.3	Resistant
Albacete	T:T	A:A	A:A	4	0.0	0.0	Resistant
Alf	T:T	A:A	A:A	4	4.5	0.6	Resistant
Fractal	T:T	A:A	A:A	4	3.0	0.7	Resistant
GrangeR	T:T	A:A	A:A	4	0.5	0.3	Resistant
Harbin	T:T	A:A	A:A	4	0.5	0.5	Resistant
Optic	T:T	A:A	A:A	4	2.5	0.6	Resistant
SY Rattler	T:T	A:A	A:A	4	4.3	1.1	Resistant
Digger	T:T	G:G	G:G	4	32.8	7.4	Susceptible
Kearney	T:T	G:G	G:G	4	37.3	8.2	Susceptible
Prior Early	T:T	G:G	G:G	4	36.3	2.3	Susceptible
Azumamugi	null[b]	G:G	G:G	4	51.5	5.2	Susceptible
Kikaihadaka	null	G:G	G:G	4	54.3	2.1	Susceptible
Zavilla	null	G:G	G:G	4	53.3	3.5	Susceptible
Royal	C:C	G:G	G:G	1	6.0	-	Susceptible
AC Metcalfe	C:C	G:G	G:G	4	18.5	10.3	Susceptible
Arta	C:C	G:G	G:G	4	9.8	3.6	Susceptible
Dicktoo	C:C	G:G	G:G	4	11.3	0.9	Susceptible
Krona	C:C	G:G	G:G	4	24.0	10.2	Susceptible
Pompadour	C:C	G:G	G:G	4	4.8	1.4	Susceptible
Sonate	C:C	G:G	G:G	4	4.8	1.5	Susceptible
CDC Fleet	C:C	G:G	G:G	4	8.0	1.6	Susceptible
Roe	C:C	G:G	G:G	4	6.3	2.1	Susceptible
Schooner	C:C	G:G	G:G	10	27.1	4.7	Susceptible

[a] Dark shading indicates marker alleles that are the same as those of *Rha2* cultivars. Light shading indicates marker alleles that differ from those of *Rha2* cultivars

[b] Neither HEX nor FAM fluorescence detected

The information in this appendix was presented in Table S8 in Online Resource 1 of Van Gansbeke et al. (2019).

Appendix 12. Temperature-switch PCR markers

Agarose gel for Temperature Switch PCR markers

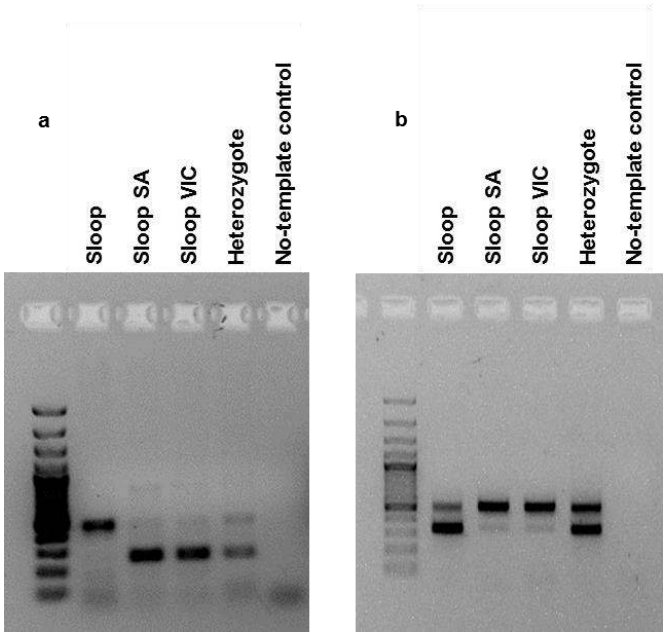

Figure A5-1: Agarose gels showing products amplified by temperature-switch PCR from genomic DNA of Sloop, Sloop SA, Sloop VIC, a Sloop/Sloop SA heterozygote and a water control assessed with (a) the wri328 primer set, which amplifies a 457-bp product from the susceptible cultivar Sloop, a 250-bp product from the resistant cultivars Sloop SA and Sloop VIC and both products from heterozygotes; and (b) the wri329 primer set, which amplifies a 335-bp product from Sloop, a 514-bp product from Sloop SA and Sloop VIC and both products from heterozygotes

The information in this appendix was presented in Figure S9 in Online Resource 2 of Van Gansbeke et al. (2019).

Appendix 13. Total RNA reads

Absolute number of RNA reads in samples taken from plants of cultivar Sloop (Control), Sloop SA and Sloop VIC prior to inoculation (day 0) and from non-inoculated plants of Sloop (Control) and inoculated plants of Sloop, Sloop SA and Sloop VIC between 4 and 28 days after inoculation (DAI). The total read number per sample is divided into mapped reads that were mapped onto the *Hordeum vulgare* reference genome or mapped onto the *Heterodera avenae* transcriptome or not mapped to any of these.

DAI	Sample	Mapped *H. vulgare* reads	Mapped *H. avenae* reads	Not mapped	Total reads
0	Control	3,225,341		150,017	3,375,358
	Sloop SA	9,510,005		345,615	9,855,620
	Sloop VIC	10,812,783		382,707	11,195,490
4	Control	9,651,006		496,153	10,147,159
	Sloop	9,690,290		423,814	10,114,104
	Sloop SA	8,246,639		1,143,620	9,390,259
	Sloop VIC	8,391,452		512,541	8,903,993
8	Control	9,840,289		351,346	10,191,635
	Sloop	10,301,123		479,703	10,780,826
	Sloop SA	12,839,604		1,607,931	14,447,535
	Sloop VIC	10,192,802		602,086	10,794,888
12	Control	8,999,717		419,130	9,418,847
	Sloop	9,453,549	1,767,012	1,273,872	12,494,433
	Sloop SA	8,631,695	252,213	385,237	9,269,145
	Sloop VIC	8,884,061	351,099	463,043	9,698,203
16	Control	9,333,431		411,755	9,745,186
	Sloop	9,236,331	818,971	684,866	10,740,168
	Sloop SA	7,444,362	529,407	528,448	8,502,217
	Sloop VIC	8,543,588	1,011,690	833,083	10,388,361
20	Control	11,473,803		450,786	11,924,589
	Sloop	7,980,612	1,034,022	868,267	9,882,901
	Sloop SA	7,548,505	1,642,058	714,343	9,904,906
	Sloop VIC	6,153,508	2,456,281	2,000,107	10,609,896
24	Control	10,297,338		413,199	10,710,537
	Sloop	7,326,798	2,871,745	1,615,603	11,814,146
	Sloop SA	7,563,987	1,671,971	282,323	9,518,281
	Sloop VIC	7,115,176	1,289,512	959,041	9,363,729
28	Control	9,784,986		1,975,140	11,760,126
	Sloop	1,908,193	3,882,467	2,262,681	8,053,341
	Sloop SA	3,616,187	4,404,522	67,213	8,087,922
	Sloop VIC	7,300,100	2,590,452	1,822,591	11,713,143

Appendix 14. Genes with significant (p <0.05) differential expression for each cultivar comparison

List of all the differentially expressed genes for the nine group comparisons performed on the combined sample analysis with an adjusted p-value < 0.05. The nine comparisons are divided in the respective sample type comparison, e.g. Sloop inoculated versus Sloop non-inoculated (Table A14-1), Sloop SA inoculated versus Sloop inoculated (Table A14-2) and Sloop VIC inoculated versus Sloop inoculated (Table A14-3), and subdivided into the respective time period, e.g. Early, Middle and Late. The numbers represent the $\log_2$ fold change for each individual comparison for the respective genes. The $\log_2$ fold values are in each time period ranked from low to high and shaded from blue (low value) to white to red (high value). The gene list includes the gene code with the respective gene annotation.

Table A14-1: Sloop inoculated versus non-inoculated

		$\log_2$ fold change[a]		
Gene code	Annotation	Early	Middle	Late
HORVU6Hr1G060700	Remorin family protein	-3.53E+14		
HORVU4Hr1G000870	AT-hook motif nuclear-localized protein 20	-3.22E+14		
HORVU4Hr1G089540	Remorin family protein	-2.26E+14		
HORVU3Hr1G003110	Glycosyltransferase	-2.15E+14		
HORVU4Hr1G072320	FAD/NAD(P)-binding oxidoreductase family protein	-2.37E+12		
HORVU2Hr1G004600	Cytochrome P450 superfamily protein	6.66E+12		
HORVU2Hr1G004540	KS protein	6.06E+13		
HORVU6Hr1G008780	Cathepsin B-like cysteine proteinase 5	2.51E+14		
HORVU1Hr1G053670	Bifunctional inhibitor/lipid-transfer protein/seed storage 2S albumin superfamily protein		-4.51E+14	-3.95E+14
HORVU2Hr1G032540	Histone deacetylase 5		-2.03E+06	-1.80E+14
HORVU4Hr1G027320	Undescribed protein		-6.63E+06	-8.31E+06
HORVU2Hr1G046880	Undescribed protein		-7.69E+05	-7.72E+06
HORVU7Hr1G100900	Undescribed protein		-6.59E+06	-6.27E+06
HORVU7Hr1G081580	Undescribed protein		-6.39E+04	-6.15E+06
HORVU7Hr1G117800	BURP domain-containing protein 11		-5.17E+06	-3.78E+06
HORVU6Hr1G014970	Ubiquitin 11		-2.93E+06	-2.83E+06
HORVU6Hr1G026200	Polyubiquitin 3		-1.81E+06	-2.18E+06
HORVU2Hr1G089810	Undescribed protein		4.89E+05	5.59E+05
HORVU6Hr1G029310	Undescribed protein		1.86E+06	1.59E+06
HORVU5Hr1G019580	D. melanogaster polytene		3.10E+06	3.14E+06
HORVU7Hr1G109650	Ubiquitin 4		3.36E+06	6.15E+06
HORVU5Hr1G000180	Actin-11		4.08E+05	6.46E+06
HORVU1Hr1G069840	Novel plant snare 13		2.71E+14	1.75E+14
HORVU1Hr1G006020	Receptor kinase 1		1.86E+14	2.05E+14
HORVU1Hr1G005950	Undescribed protein		5.40E+14	3.48E+14
HORVU1Hr1G029250	Undescribed protein		-7.06E+14	
HORVU0Hr1G028740	Undescribed protein		-5.66E+14	
HORVU1Hr1G078990	Undescribed protein		-5.60E+14	
HORVU2Hr1G007590	Undescribed protein		-7.64E+06	
HORVU3Hr1G053240	Unplaced genomic scaffold PLICRscaffold_102, whole genome shotgun sequence		-6.89E+06	
HORVU7Hr1G057100	Cytochrome P450 superfamily protein		-5.56E+06	
HORVU2Hr1G027270	Disease resistance-responsive (dirigent-like protein) family protein		-5.17E+06	
HORVU5Hr1G073270	Macaca fascicularis brain cDNA clone: QflA-19312, similar to human similar to rRNA intron-encoded homing endonuclease(LOC391446), mRNA, RefSeq: XM_372959.1		-4.88E+06	
HORVU2Hr1G117780	Sulfotransferase 4B		-4.19E+06	
HORVU5Hr1G065660	Sugar transporter protein 7		-4.38E+05	
HORVU5Hr1G079190	RNA binding		6.03E-01	
HORVU1Hr1G038210	Undescribed protein		9.23E-01	
HORVU1Hr1G083480	Mitochondrial protein, putative		3.38E+04	
HORVU5Hr1G023300	Undescribed protein		1.23E+05	
HORVU1Hr1G081550	Malate dehydrogenase		2.33E+05	
HORVU7Hr1G001420	Protein kinase superfamily protein		3.76E+05	
HORVU3Hr1G091320	Acyl-[acyl-carrier-protein] 6-desaturase		4.75E+05	
HORVU3Hr1G048660	Hypoxia-responsive family protein		1.09E+06	
HORVU6Hr1G086220	RING finger protein 13		1.19E+06	
HORVU7Hr1G003460	Glucan synthase-like 8		1.35E+06	
HORVU5Hr1G059870	Undescribed protein		1.38E+06	
HORVU2Hr1G110900	Protein kinase superfamily protein		1.52E+06	
HORVU1Hr1G094970	Mitochondrial outer membrane protein porin 5		1.79E+06	
HORVU4Hr1G005110	HIPL1 protein		1.82E+06	
HORVU7Hr1G094810	Undescribed protein		2.22E+06	

Table A14-1 continued

Gene code	Annotation	Log_2 fold change[a] Early	Middle	Late
HORVU5Hr1G117110	Lipoxygenase 1		2.44E+06	
HORVU5Hr1G070610	Receptor kinase 2		2.57E+06	
HORVU3Hr1G091200	F-box family protein		2.67E+06	
HORVU7Hr1G082490	Unknown function		2.69E+06	
HORVU3Hr1G098360	Methyl esterase 1		3.11E+06	
HORVU5Hr1G089840	Receptor kinase 3		3.12E+06	
HORVU5Hr1G047000	Hypoxia induced protein conserved region containing protein, expressed		3.25E+06	
HORVU2Hr1G099770	Oxygen-dependent coproporphyrinogen-III oxidase		3.37E+06	
HORVU5Hr1G063420	Glutamate receptor 2.8		3.45E+06	
HORVU3Hr1G037350	Undescribed protein		3.51E+06	
HORVU4Hr1G062440	Phosphoenolpyruvate carboxykinase [ATP]		3.53E+06	
HORVU2Hr1G118410	Plant cysteine oxidase 3		3.59E+06	
HORVU3Hr1G037360	Undescribed protein		3.63E+06	
HORVU6Hr1G061690	Undescribed protein		3.73E+06	
HORVU5Hr1G006880	2-aminoethanethiol dioxygenase		3.89E+06	
HORVU5Hr1G108610	Prolyl 4-hydroxylase subunit alpha-1		3.95E+06	
HORVU2Hr1G044520	Receptor kinase 1		4.01E+06	
HORVU2Hr1G116740	Wound-responsive family protein		4.23E+06	
HORVU2Hr1G093910	Undescribed protein		4.29E+06	
HORVU5Hr1G074610	Unknown function		4.40E+06	
HORVU4Hr1G075410	Unknown function		4.49E+06	
HORVU2Hr1G053630	RRNA intron-encoded homing endonuclease		5.09E+06	
HORVU5Hr1G097930	Unknown function		5.13E+06	
HORVU2Hr1G100960	Unknown protein; BEST Arabidopsis thaliana protein match is: unknown protein .		5.46E+06	
HORVU5Hr1G118990	Undescribed protein		5.56E+06	
HORVU5Hr1G087090	Leucine-rich receptor-like protein kinase family protein		6.09E+06	
HORVU7Hr1G020880	Early nodulin-related		7.60E+06	
HORVU1Hr1G013560	Undescribed protein		3.16E+13	
HORVU1Hr1G029290	CCR4-NOT transcription complex subunit 3		1.52E+14	
HORVU1Hr1G014370	Undescribed protein		1.60E+14	
HORVU1Hr1G023930	Undescribed protein		1.90E+14	
HORVU0Hr1G021640	Hemoglobin 3		1.99E+14	
HORVU0Hr1G001750	Ethylene receptor 2		2.57E+14	
HORVU0Hr1G038910	Undescribed protein		3.03E+14	
HORVU0Hr1G019870	Hypothetical protein M:11918-12241 FORWARD		3.13E+14	
HORVU1Hr1G037550	RING finger protein 141		3.40E+14	
HORVU0Hr1G022310	Haloacid dehalogenase-like hydrolase domain-containing protein 3		3.41E+14	
HORVU0Hr1G019860	Hypothetical protein M:11918-12241 FORWARD		3.82E+14	
HORVU0Hr1G017400	Haloacid dehalogenase-like hydrolase (HAD) superfamily protein		3.91E+14	
HORVU0Hr1G034160	NADH-ubiquinone oxidoreductase chain 5		4.17E+14	
HORVU1Hr1G035870	Undescribed protein		4.63E+14	
HORVU1Hr1G029920	Bidirectional sugar transporter N3		4.84E+14	
HORVU1Hr1G058940	Ethylene-responsive transcription factor 1		5.09E+14	
HORVU2Hr1G009950	Receptor-like protein kinase 1			-6.02E+14
HORVU1Hr1G075160	Isoflavone reductase-like protein			-4.04E+14
HORVU1Hr1G072530	laccase 17			-3.74E+14
HORVU0Hr1G038500	Polyubiquitin			-2.39E+14
HORVU1Hr1G064870	Tubulin beta chain 2			-1.50E+14
HORVU0Hr1G014030	PLC-like phosphodiesterases superfamily protein			-2.14E+13
HORVU2Hr1G044620	Undescribed protein			-7.90E+06
HORVU4Hr1G059930	Laccase 17			-6.53E+06
HORVU7Hr1G009580	Undescribed protein			-4.76E+06
HORVU7Hr1G002910	NBS-LRR resistance-like protein			-4.58E+06
HORVU5Hr1G039810	Macaca fascicularis brain cDNA clone: QflA-19312, similar to human similar to rRNA intron-encoded homing endonuclease(LOC391446), mRNA, RefSeq: XM_372959.1			-3.45E+06
HORVU5Hr1G077000	Undescribed protein			-3.13E+06
HORVU6Hr1G016150	Ubiquitin 4			-3.10E+06
HORVU6Hr1G024240	RRNA intron-encoded homing endonuclease			-2.78E+06
HORVU3Hr1G018810	FASCICLIN-like arabinogalactan-protein 11			-2.60E+06
HORVU7Hr1G007220	Sucrose synthase 1			-2.59E+06
HORVU4Hr1G087390	Nicotianamine synthase 3			-1.92E+06
HORVU4Hr1G075840	Pyridoxal 5'-phosphate synthase subunit PdxT			-8.17E-01
HORVU5Hr1G084630	Serine/threonine protein phosphatase 2A 55 kDa Regulatory subunit B' delta isoform			8.98E-01
HORVU7Hr1G100230	Heavy metal transport/detoxification superfamily protein			3.58E+05
HORVU7Hr1G010850	L-tyrosine decarboxylase			3.19E+06
HORVU2Hr1G097940	Homeobox-leucine zipper protein 4			3.81E+06
HORVU5Hr1G067530	1-aminocyclopropane-1-carboxylate oxidase 1			4.27E+06
HORVU5Hr1G067490	1-aminocyclopropane-1-carboxylate oxidase 1			4.61E+06
HORVU7Hr1G085720	Undescribed protein			5.00E+06

Table A14-1 continued

Gene code	Annotation	Log_2 fold change[a] Early	Middle	Late
HORVU7Hr1G109080	Bifunctional inhibitor/lipid-transfer protein/seed storage 2S albumin superfamily protein			5.08E+06
HORVU7Hr1G114030	Protein HASTY 1			5.52E+06
HORVU7Hr1G079380	Alcohol dehydrogenase			5.67E+06
HORVU2Hr1G104390	Ubiquitin 11			5.89E+06
HORVU7Hr1G038960	Undescribed protein			6.14E+06
HORVU5Hr1G078400	Heat shock 70 kDa protein C			7.18E+06
HORVU3Hr1G033230	Centromere-associated protein E, putative isoform 1			8.75E+06
HORVU1Hr1G068640	60S ribosomal protein L30			5.45E+14
HORVU1Hr1G068790	ADP-ribosylation factor 1			6.47E+14

[a]Positive values indicate higher expression in the inoculated plants. Negative values indicate higher expression in the non-inoculated plants.

Table A14-2: Sloop SA inoculated versus Sloop

Gene code	Annotation	Log$_2$ fold change[a] Early	Middle	Late
HORVU4Hr1G001830	Undescribed protein	-9.93E+14	-8.68E+14	-9.02E+14
HORVU3Hr1G009340	ENTH/ANTH/VHS superfamily protein	-7.53E+14	-8.87E+14	-8.52E+14
HORVU6Hr1G084540	Undescribed protein	-9.92E+14	-8.47E+14	
HORVU7Hr1G058630	Protein arginine methyltransferase 10	-9.89E+14	-7.75E+14	
HORVU7Hr1G059690	Undescribed protein	-9.79E+14	-1.17E+14	
HORVU7Hr1G066170	Galactose mutarotase-like superfamily protein	-9.70E+14	-8.36E+13	
HORVU6Hr1G084930	Disease resistance protein	-9.62E+14	-6.83E+14	
HORVU7Hr1G051900	Unknown function	-9.61E+14	-8.88E+14	
HORVU3Hr1G073930	Undescribed protein	-9.54E+14	-8.95E+14	
HORVU6Hr1G082220	Undescribed protein	-8.61E+14	-7.88E+14	
HORVU7Hr1G084640	Phosphoethanolamine N-methyltransferase 1	-8.54E+14	-7.24E+14	
HORVU1Hr1G049000	Subtilisin-like protease	-8.36E+14	-7.80E+14	
HORVU7Hr1G072620	Receptor-like protein kinase 4	-8.24E+14	-8.14E+14	
HORVU7Hr1G050920	Undescribed protein	-8.20E+14	-8.83E+14	
HORVU7Hr1G067200	Undescribed protein	-7.91E+14	-8.00E+14	
HORVU7Hr1G066450	Isopropylmalate dehydrogenase 1	-7.76E+14	-9.62E+13	
HORVU7Hr1G084170	Unknown protein	-7.53E+14	-6.40E+14	
HORVU6Hr1G082230	F-box/RNI-like superfamily protein	-7.17E+14	-6.26E+14	
HORVU3Hr1G069300	Isopropylmalate dehydrogenase 1	-6.92E+14	-7.69E+14	
HORVU7Hr1G066960	Undescribed protein	-6.74E+14	-8.12E+14	
HORVU6Hr1G085270	Unknown function	-6.66E+14	-6.19E+14	
HORVU5Hr1G114960	Pyruvate dehydrogenase E1 component subunit beta	-6.23E+14	-7.54E+13	
HORVU7Hr1G060480	Tubby-like F-box protein 9	-6.07E+14	-3.84E+13	
HORVU7Hr1G054890	B12D protein	-5.91E+14	-6.00E+14	
HORVU1Hr1G067670	Zinc finger protein 830	-5.37E+14	-4.72E+14	
HORVU5Hr1G012710	ABC1 family protein	-5.33E+14	-6.03E+14	
HORVU7Hr1G075160	ATP-dependent DNA helicase PIF1	-3.74E+14	-5.54E+14	
HORVU1Hr1G067590	SOSS complex subunit B homolog	-3.16E+14	-3.07E+14	
HORVU7Hr1G069420	Structural maintenance of omosomes 5	-2.80E+14	-3.02E+14	
HORVU7Hr1G058750	CRIB domain-containing protein RIC1	-2.30E+14	-9.77E+14	
HORVU2Hr1G121320	Cytochrome P450 superfamily protein	-2.28E+14	-5.89E+13	
HORVU7Hr1G082180	Undescribed protein	-2.03E+14	-2.30E+14	
HORVU7Hr1G079220	Undescribed protein	-1.12E+14	-9.04E+14	
HORVU7Hr1G064420	ENTH/ANTH/VHS superfamily protein	-1.06E+14	-8.77E+14	
HORVU7Hr1G050930	Undescribed protein	-1.01E+14	-9.12E+14	
HORVU7Hr1G066970	Cytochrome P450 superfamily protein	-9.37E+13	-9.18E+14	
HORVU7Hr1G074530	Kelch-like protein 20	-8.78E+13	-1.19E+14	
HORVU7Hr1G059430	Undescribed protein	-7.92E+13	-7.85E+13	
HORVU7Hr1G058640	Undescribed protein	-7.87E+13	-7.49E+13	
HORVU7Hr1G074420	BTB-POZ and MATH domain 2	1.67E+14	2.98E+14	
HORVU0Hr1G000650	Hexosyltransferase	2.94E+14	2.59E+14	
HORVU5Hr1G043850	Chromosome 3B, genomic scaffold, cultivar Chinese Spring	4.05E+14	-3.99E+14	
HORVU2Hr1G039250	RRNA intron-encoded homing endonuclease	4.36E+14	-4.51E+14	
HORVU7Hr1G002030	Undescribed protein	5.52E+14	-5.75E+12	
HORVU6Hr1G087410	Plant regulator RWP-RK family protein	5.64E+14	5.80E+14	
HORVU5Hr1G083980	Senescence-associated protein, putative	5.66E+14	-8.54E+14	
HORVU3Hr1G084440	Undescribed protein	5.78E+14	-7.20E+14	
HORVU5Hr1G076970	Senescence-associated protein	5.86E+14	-4.86E+14	
HORVU2Hr1G053620	Senescence-associated protein, putative	7.50E+14	-6.93E+14	
HORVU6Hr1G047560	Calcium-dependent lipid-binding family protein	-1.73E+14		-1.66E+14
HORVU6Hr1G063860	Tripeptidyl peptidase ii	-1.67E+14		-1.65E+14
HORVU5Hr1G089790	Receptor kinase 3	-7.31E+14		
HORVU6Hr1G082240	Transcriptional corepressor LEUNIG	-7.30E+14		
HORVU7Hr1G029190	Histone superfamily protein	-6.61E+14		
HORVU5Hr1G090650	Undescribed protein	-6.58E+14		
HORVU7Hr1G059910	Unknown function	-6.49E+14		
HORVU7Hr1G108530	Peroxidase superfamily protein	-5.66E+14		
HORVU5Hr1G090640	Histone deacetylase HDT1	-5.38E+14		
HORVU7Hr1G098110	Peroxidase superfamily protein	-4.95E+14		
HORVU2Hr1G018520	Peroxidase superfamily protein	-4.83E+14		
HORVU7Hr1G089300	Peroxidase superfamily protein	-4.23E+14		
HORVU5Hr1G009840	RAB GDP dissociation inhibitor 2	-4.10E+14		
HORVU3Hr1G036880	Peroxidase superfamily protein	-4.05E+14		
HORVU7Hr1G117800	BURP domain-containing protein 11	-3.76E+14		
HORVU6Hr1G076270	Unknown function	-3.76E+14		
HORVU2Hr1G082900	Undescribed protein	-3.67E+14		
HORVU2Hr1G099720	Plant protein of unknown function (DUF247)	-3.35E+14		
HORVU2Hr1G099030	F-box family protein	-2.86E+14		
HORVU2Hr1G082910	Undescribed protein	-2.85E+14		
HORVU3Hr1G003110	Glycosyltransferase	-2.82E+14		
HORVU7Hr1G068680	Unknown function	-2.71E+14		
HORVU7Hr1G027520	Flavin-containing monooxygenase family protein	-2.24E+14		
HORVU7Hr1G002370	Glutathione S-transferase family protein	-2.13E+14		
HORVU7Hr1G076680	Non-lysosomal glucosylceramidase	-1.89E+14		
HORVU7Hr1G078170	Protein kinase superfamily protein	-1.30E+14		
HORVU3Hr1G070850	NAD-dependent malic enzyme 2	-5.84E+12		

Table A14-2 continued

Gene code	Annotation	Log$_2$ fold change[a] Early	Middle	Late
HORVU5Hr1G125710	Protein kinase superfamily protein	-9.33E-01		
HORVU1Hr1G050130	Mitochondrial substrate carrier family protein	-9.15E-01		
HORVU7Hr1G075590	Undescribed protein	3.29E+12		
HORVU2Hr1G079040	Unknown function	3.40E+13		
HORVU3Hr1G105930	RNA-binding protein 1	1.00E+14		
HORVU4Hr1G075720	Galactosyltransferase family protein	1.31E+14		
HORVU7Hr1G106810	Undescribed protein	1.49E+14		
HORVU6Hr1G024170	CRIB domain-containing protein RIC1	2.97E+14		
HORVU4Hr1G059470	Undescribed protein	3.31E+14		
HORVU2Hr1G072950	Tar1p	3.37E+14		
HORVU1Hr1G025060	NADH-ubiquinone oxidoreductase chain 1	3.53E+14		
HORVU6Hr1G085710	Leucine-rich receptor-like protein kinase family protein	3.64E+14		
HORVU1Hr1G083480	Mitochondrial protein, putative	3.74E+14		
HORVU2Hr1G072930	RRNA intron-encoded homing endonuclease	3.76E+14		
HORVU4Hr1G051520	Undescribed protein	3.96E+14		
HORVU2Hr1G039210	RRNA intron-encoded homing endonuclease	4.03E+14		
HORVU1Hr1G026050	Undescribed protein	4.05E+14		
HORVU1Hr1G026980	Auxenochlorella protothecoides strain 0710 contig1325, whole genome shotgun sequence	4.23E+14		
HORVU0Hr1G037040	Orf108a	4.27E+14		
HORVU6Hr1G049260	Ribulose bisphosphate carboxylase large chain	4.37E+14		
HORVU7Hr1G020090	Cytochrome C assembly protein	4.41E+14		
HORVU2Hr1G104850	Undescribed protein	4.49E+14		
HORVU0Hr1G000940	Zinc finger protein 830	4.53E+14		
HORVU0Hr1G034160	NADH-ubiquinone oxidoreductase chain 5	4.57E+14		
HORVU2Hr1G121650	S12-like, 30S ribosomal protein S12 subfamily protein	4.67E+14		
HORVU0Hr1G019860	Hypothetical protein M:11918-12241 FORWARD	4.71E+14		
HORVU0Hr1G024560	Ribulose bisphosphate carboxylase large chain	4.74E+14		
HORVU1Hr1G039220	Undescribed protein	4.85E+14		
HORVU4Hr1G016780	Alcohol dehydrogenase 1	4.92E+14		
HORVU0Hr1G023370	Undescribed protein	4.95E+14		
HORVU1Hr1G057550	Undescribed protein	5.14E+14		
HORVU0Hr1G034780	NAD(P)H-quinone oxidoreductase subunit 2 A, chloroplastic	5.28E+14		
HORVU2Hr1G004390	Hypothetical protein M:11918-12241 FORWARD	5.41E+14		
HORVU4Hr1G025470	Senescence-associated protein	5.41E+14		
HORVU2Hr1G082520	DNA, scaffold: scf_mam1_v11112, strain NBRC 6742, whole genome shotgun sequence	5.42E+14		
HORVU0Hr1G023910	Senescence-associated protein	6.00E+14		
HORVU7Hr1G088350	Oxidative stress 3.	6.09E+14		
HORVU1Hr1G073940	Myb-like transcription factor family protein	7.61E+14		
HORVU0Hr1G017400	Haloacid dehalogenase-like hydrolase (HAD) superfamily protein		-3.44E+14	-3.28E+14
HORVU6Hr1G024220	Cytochrome P450 likeTBP		-8.56E+14	
HORVU5Hr1G012990	Protein TAR1		-8.19E+14	
HORVU6Hr1G053140	Senescence-associated protein, putative		-7.74E+14	
HORVU6Hr1G084870	Disease resistance protein RPP13		-7.60E+14	
HORVU0Hr1G033370	Protein TAR1		-7.25E+14	
HORVU5Hr1G058690	RRNA intron-encoded homing endonuclease		-6.98E+14	
HORVU7Hr1G002120	Undescribed protein		-6.46E+14	
HORVU7Hr1G001980	Undescribed protein		-6.19E+14	
HORVU7Hr1G093830	B12D protein		-5.85E+14	
HORVU2Hr1G053630	RRNA intron-encoded homing endonuclease		-5.63E+14	
HORVU7Hr1G053600	RRNA intron-encoded homing endonuclease		-5.46E+14	
HORVU6Hr1G024130	Undescribed protein		-5.44E+14	
HORVU5Hr1G024430	Undescribed protein		-5.02E+14	
HORVU3Hr1G082320	Undescribed protein		-4.98E+14	
HORVU0Hr1G011110	Senescence-associated protein		-4.95E+14	
HORVU2Hr1G072960	Senescence-associated protein		-4.80E+14	
HORVU5Hr1G024420	Senescence-associated protein, putative		-4.56E+14	
HORVU5Hr1G073230	Undescribed protein		-4.50E+14	
HORVU3Hr1G056130	Senescence-associated protein		-4.46E+14	
HORVU0Hr1G011140	Macaca fascicularis brain cDNA clone: QflA-19312, similar to human similar to rRNA intron-encoded homing Endonuclease(LOC391446), mRNA, RefSeq: XM_372959.1		-4.44E+14	
HORVU6Hr1G076410	RRNA intron-encoded homing endonuclease		-4.36E+14	
HORVU1Hr1G050020	Senescence-associated protein, putative		-4.35E+14	
HORVU7Hr1G097520	26S proteasome non-ATPase regulatory subunit 2 homolog B		-3.77E+14	
HORVU0Hr1G019870	Hypothetical protein M:11918-12241 FORWARD		-3.03E+14	
HORVU7Hr1G094810	Undescribed protein		-2.42E+14	
HORVU7Hr1G082200	Leucine-rich receptor-like protein kinase family protein		-2.04E+14	
HORVU2Hr1G110900	Protein kinase superfamily protein		-1.53E+14	
HORVU5Hr1G074880	RRNA intron-encoded homing endonuclease		-1.04E+14	
HORVU7Hr1G053620	Undescribed protein		-9.06E+13	

Table A14-2 continued

Gene code	Annotation	Log$_2$ fold change[a] Early	Middle	Late
HORVU2Hr1G072910	Undescribed protein		-6.03E+13	
HORVU5Hr1G083970	Unplaced genomic scaffold PLICRscaffold_102, whole genome shotgun sequence		-5.18E+13	
HORVU7Hr1G084730	Undescribed protein		-1.66E+13	
HORVU6Hr1G083540	Ubiquitin carboxyl-terminal hydrolase 2		2.58E+14	
HORVU3Hr1G004240	Undescribed protein		3.92E+14	
HORVU1Hr1G056440	Aspartic proteinase A1		7.98E+14	
HORVU3Hr1G033230	Centromere-associated protein E, putative isoform 1			-9.30E+14
HORVU1Hr1G068790	ADP-ribosylation factor 1			-6.87E+14
HORVU7Hr1G122200	Disease resistance protein			-6.68E+14
HORVU2Hr1G038390	Undescribed protein			-6.05E+14
HORVU0Hr1G040120	Undescribed protein			-5.29E+14
HORVU5Hr1G067530	1-aminocyclopropane-1-carboxylate oxidase 1			-4.87E+14
HORVU2Hr1G003640	Cysteine-rich receptor-like protein kinase 41			-4.52E+14
HORVU1Hr1G068640	60S ribosomal protein L30			-4.47E+14
HORVU7Hr1G114850	Disease resistance protein			-4.41E+14
HORVU1Hr1G089380	Subtilisin-like protease			-3.90E+14
HORVU7Hr1G010620	GRAS family transcription factor			-3.78E+14
HORVU5Hr1G088400	Uveal autoantigen with coiled-coil domains and ankyrin repeats isoform 1			-3.39E+14
HORVU7Hr1G043490	Receptor kinase 2			-3.36E+14
HORVU7Hr1G045290	Aluminium-activated malate transporter 9			-3.36E+14
HORVU5Hr1G095250	Kinesin 4			-3.33E+14
HORVU0Hr1G007220	Undescribed protein			-3.31E+14
HORVU4Hr1G063240	Glucan endo-1,3-beta-glucosidase 11			-3.10E+14
HORVU3Hr1G052930	Kinesin 4			-3.08E+14
HORVU7Hr1G025200	Histone superfamily protein			-3.03E+14
HORVU2Hr1G026450	Peroxidase superfamily protein			-2.98E+14
HORVU7Hr1G110110	Transposable element protein, putative			-2.97E+14
HORVU2Hr1G048010	TPX2 (targeting protein for Xklp2) protein family			-2.94E+14
HORVU1Hr1G051050	Chalcone-flavanone isomerase family protein			-2.90E+14
HORVU7Hr1G049860	FASCICLIN-like arabinogalactan-protein 12			-2.85E+14
HORVU4Hr1G068470	TPX2 (targeting protein for Xklp2) protein family			-2.74E+14
HORVU5Hr1G109460	Histone H2A 6			-2.69E+14
HORVU2Hr1G090210	Histone superfamily protein			-2.68E+14
HORVU1Hr1G081770	Early nodulin-like protein 10			-2.66E+14
HORVU7Hr1G101550	Unknown function			-2.66E+14
HORVU6Hr1G055270	Rice-salt sensitive 1-like protein			-2.65E+14
HORVU6Hr1G089000	Kinesin 1			-2.60E+14
HORVU1Hr1G056530	Histone H2B.1			-2.59E+14
HORVU7Hr1G110090	Histone H2B.1			-2.59E+14
HORVU3Hr1G078880	Cyclin family protein			-2.55E+14
HORVU5Hr1G009350	Kinesin 4			-2.48E+14
HORVU6Hr1G013530	Histone superfamily protein			-2.45E+14
HORVU1Hr1G073680	Histone superfamily protein			-2.44E+14
HORVU1Hr1G029540	Myb-related protein 3R-1			-2.42E+14
HORVU2Hr1G085690	Unknown protein			-2.41E+14
HORVU5Hr1G079130	Histone superfamily protein			-2.40E+14
HORVU1Hr1G020040	Histone superfamily protein			-2.39E+14
HORVU5Hr1G023640	Cellulose synthase-like D5			-2.37E+14
HORVU1Hr1G005950	Undescribed protein			-2.34E+14
HORVU7Hr1G121820	Cyclin B2			-2.31E+14
HORVU1Hr1G017830	Histone superfamily protein			-2.31E+14
HORVU6Hr1G018600	Kinesin-like protein 1			-2.28E+14
HORVU2Hr1G097990	Histone superfamily protein			-2.27E+14
HORVU7Hr1G095920	Glycosyltransferase family 61 protein			-2.19E+14
HORVU6Hr1G089250	DNA (cytosine-5)-methyltransferase 3			-2.17E+14
HORVU7Hr1G100400	Histone H2A 7			-2.09E+14
HORVU1Hr1G071190	Histone superfamily protein			-2.05E+14
HORVU4Hr1G086500	Respiratory burst oxidase homolog B			-2.03E+14
HORVU7Hr1G075350	Vacuolar protein sorting-associated protein			-1.93E+14
HORVU1Hr1G035130	Histone H2A 11			-1.91E+14
HORVU2Hr1G085570	Cytochrome b561 and DOMON domain-containing protein			-1.73E+14
HORVU3Hr1G019140	Receptor kinase 1			-1.66E+14
HORVU6Hr1G077400	Unknown protein			-1.63E+14
HORVU4Hr1G055900	Ethylene-overproduction protein 1			-1.36E+14
HORVU7Hr1G096680	Arabinose kinase			-1.32E+14
HORVU7Hr1G047700	Formate dehydrogenase			-1.31E+14
HORVU3Hr1G087430	Interactor of constitutive active ROPs 2, chloroplastic			-1.12E+14
HORVU4Hr1G077420	Receptor kinase 2			-1.05E+14
HORVU4Hr1G083620	Unknown protein			-2.58E+13
HORVU5Hr1G087340	High mobility group B1			-2.33E+13
HORVU1Hr1G058500	Histone H2B.1			-2.05E+13
HORVU4Hr1G088140	Expansin B2			-2.52E+12
HORVU7Hr1G034470	Histone superfamily protein			-2.11E+12
HORVU1Hr1G019590	SAD1/UNC-84 domain protein 2			6.63E-01

Table A14-2 continued

Gene code	Annotation	Log_2 fold change[a] Early	Middle	Late
HORVU7Hr1G114000	Aldehyde oxidase 2			2.46E+13
HORVU4Hr1G068900	Unknown function			3.76E+13
HORVU4Hr1G087390	Nicotianamine synthase 3			1.63E+14
HORVU0Hr1G014030	PLC-like phosphodiesterases superfamily protein			1.67E+14
HORVU2Hr1G087090	Adenine phosphoribosyltransferase 5			1.74E+14
HORVU4Hr1G002130	Dehydrogenase/reductase SDR family member 11			2.01E+14
HORVU6Hr1G092550	Undescribed protein			2.18E+14
HORVU1Hr1G018480	Undescribed protein			2.27E+14
HORVU2Hr1G072750	Protein TERMINAL FLOWER 1			3.38E+14
HORVU2Hr1G124600	Undescribed protein			3.85E+14
HORVU2Hr1G127650	Peroxidase superfamily protein			3.94E+14
HORVU7Hr1G009580	Undescribed protein			3.96E+14
HORVU1Hr1G037270	Chitinase 2			4.31E+14
HORVU2Hr1G102110	Bifunctional inhibitor/lipid-transfer protein/seed storage 2S Albumin superfamily protein			4.59E+14
HORVU4Hr1G081330	Boron transporter 4			7.10E+14
HORVU7Hr1G108160	Undescribed protein			7.93E+14

[a]Positive values indicate higher expression in the inoculated Sloop SA plants. Negative values indicate higher expression in the inoculated Sloop plants.

Table A14-3: Sloop VIC versus Sloop

Gene code	Annotation	Log$_2$ fold change[a] Early	Middle	Late
HORVU4Hr1G001830	Undescribed protein	-9.8E+14	-8.8E+13	-8.6E+06
HORVU3Hr1G009340	ENTH/ANTH/VHS superfamily protein	-7.4E+14	-9.0E+14	-8.1E+06
HORVU4Hr1G050060	PATATIN-like protein 4	6.9E+14	5.3E+14	5.8E+06
HORVU2Hr1G073700	Unknown function	-1.0E+14	-9.8E+14	
HORVU2Hr1G062940	Alpha-glucosidase	-7.4E+14	-9.7E+14	
HORVU2Hr1G036600	Unknown function	-9.1E+14	-9.2E+14	
HORVU2Hr1G061010	Undescribed protein	-8.3E+14	-9.1E+14	
HORVU7Hr1G051900	Unknown function	-4.5E+14	-9.0E+14	
HORVU3Hr1G010450	F-box protein PP2-B1	-9.0E+14	-8.6E+14	
HORVU2Hr1G064860	Undescribed protein	-6.7E+14	-7.7E+14	
HORVU2Hr1G070420	Undescribed protein	-7.2E+14	-7.6E+14	
HORVU7Hr1G028510	Undescribed protein	-9.5E+14	-7.3E+14	
HORVU2Hr1G042830	Chromosome 3B, genomic scaffold, cultivar Chinese Spring	-7.2E+14	-6.8E+14	
HORVU4Hr1G084260	BEST Arabidopsis thaliana protein match is: RPM1 interacting protein 13 .	-5.9E+14	-6.3E+14	
HORVU2Hr1G072370	Unknown function	-5.1E+14	-4.5E+14	
HORVU2Hr1G070390	Undescribed protein	-4.6E+14	-4.5E+14	
HORVU2Hr1G073850	Digalactosyldiacylglycerol synthase 1, chloroplastic	-2.8E+14	-2.2E+14	
HORVU2Hr1G060590	Undescribed protein	-7.7E+14	-1.0E+14	
HORVU2Hr1G096400	CsAtPR5, putative, expressed	8.5E+14	6.8E+13	
HORVU7Hr1G117800	BURP domain-containing protein 11	-4.4E+14	3.4E+14	
HORVU2Hr1G097040	Mitochondrial transcription termination factor family protein	4.4E+14	4.2E+14	
HORVU2Hr1G044460	Glucan endo-1,3-beta-glucosidase 13	3.7E+14	5.0E+14	
HORVU6Hr1G087410	Plant regulator RWP-RK family protein	5.8E+14	6.4E+14	
HORVU2Hr1G043550	Retrotransposon protein, putative, Ty1-copia subclass	6.2E+13	6.8E+14	
HORVU4Hr1G081330	Boron transporter 4	7.1E+14	7.4E+14	
HORVU2Hr1G036610	Undescribed protein	-9.0E+14		
HORVU1Hr1G079280	Late embryogenesis abundant protein 76	-8.9E+14		
HORVU2Hr1G066930	Unknown function	-8.6E+14		
HORVU4Hr1G088990	Undescribed protein	-8.3E+14		
HORVU7Hr1G082040	Late embryogenesis abundant protein D-34	-8.0E+14		
HORVU2Hr1G035130	Undescribed protein	-7.9E+14		
HORVU4Hr1G090630	E3 ubiquitin-protein ligase RFWD3	-7.8E+14		
HORVU1Hr1G089730	Iron-sulfur cluster assembly protein 1	-7.8E+14		
HORVU5Hr1G092120	Dehydrin 7	-7.7E+14		
HORVU5Hr1G125450	AWPM-19-like family protein	-7.6E+14		
HORVU2Hr1G042990	Undescribed protein	-7.2E+14		
HORVU4Hr1G008990	Late embryogenesis abundant protein	-7.2E+14		
HORVU2Hr1G126940	Phosphatidylinositol-4-phosphate 5-kinase family protein	-7.1E+14		
HORVU5Hr1G001750	Undescribed protein	-7.0E+14		
HORVU0Hr1G012340	Undescribed protein	-6.5E+14		
HORVU6Hr1G005600	High affinity nitrate transporter 2.6	-6.4E+14		
HORVU1Hr1G046570	Unknown function	-6.4E+14		
HORVU5Hr1G118100	Transposable element protein, putative	-6.3E+14		
HORVU0Hr1G012330	Undescribed protein	-6.2E+14		
HORVU3Hr1G069590	Heat stress transcription factor C-1b	-5.8E+14		
HORVU3Hr1G030650	Late embryogenesis abundant protein	-5.5E+14		
HORVU7Hr1G040970	Potassium channel SKOR	-5.2E+14		
HORVU2Hr1G058430	Retrotransposon protein, putative, Ty3-gypsy subclass	-5.1E+14		
HORVU3Hr1G030770	ATPase family gene 2 protein	-5.0E+14		
HORVU1Hr1G002100	Defensin-like protein	-4.9E+14		
HORVU3Hr1G049780	Heavy metal transport/detoxification superfamily protein	-4.9E+14		
HORVU3Hr1G077930	Nucleoredoxin	-4.8E+14		
HORVU5Hr1G103460	Dehydrin Rab15	-4.7E+14		
HORVU5Hr1G076730	Chromosome 3B, genomic scaffold, cultivar Chinese Spring	-4.6E+14		
HORVU2Hr1G048290	Thiol protease aleurain	-4.6E+14		
HORVU0Hr1G017570	Inosine-5'-monophosphate dehydrogenase	-4.0E+14		
HORVU6Hr1G070020	Chromosome 3B, genomic scaffold, cultivar Chinese Spring	-4.0E+14		
HORVU2Hr1G013950	Jasmonate-induced protein, putative, expressed	-4.0E+14		
HORVU6Hr1G051860	Loricrin-like protein	-3.7E+14		
HORVU5Hr1G071270	F-box and associated interaction domains-containing protein	-3.5E+14		
HORVU7Hr1G074520	Protein of unknown function (DUF3537)	-3.2E+14		
HORVU4Hr1G090090	Heat stress transcription factor C-2a	-3.1E+14		
HORVU4Hr1G051290	NAC domain protein,	-3.0E+14		
HORVU4Hr1G033510	Chromosome 3B, genomic scaffold, cultivar Chinese Spring	-2.9E+14		
HORVU5Hr1G031210	Undescribed protein	-2.6E+14		
HORVU6Hr1G047560	Calcium-dependent lipid-binding family protein	-1.8E+14		
HORVU5Hr1G088700	Protein phosphatase 2C family protein	-1.8E+14		
HORVU4Hr1G085800	Flowering promoting factor 1	-1.3E+14		
HORVU7Hr1G003170	LEA	-1.1E+14		
HORVU6Hr1G084010	Dehydrin 7	-1.0E+14		
HORVU4Hr1G074710	Undescribed protein	-1.0E+14		
HORVU2Hr1G058670	Undescribed protein	-7.8E+13		
HORVU0Hr1G017490	NAC domain protein,	-5.4E+13		
HORVU4Hr1G090850	Heat stress transcription factor C-2a	-5.0E+12		
HORVU2Hr1G039650	Pol polyprotein	3.7E+13		

Table A14-3 continued

Gene code	Annotation	Log$_2$ fold change[a] Early	Middle	Late
HORVU2Hr1G096410	CsAtPR5, putative, expressed	1.7E+14		
HORVU2Hr1G031400	SPX domain gene 3	2.4E+14		
HORVU0Hr1G017400	Haloacid dehalogenase-like hydrolase (HAD) superfamily protein		-3.4E+14	-4.4E+13
HORVU6Hr1G008780	Cathepsin B-like cysteine proteinase 5		-2.1E+13	-2.1E+06
HORVU1Hr1G001190	Undescribed protein		-5.9E+14	
HORVU5Hr1G065350	Serine/threonine protein kinase 1		-3.6E+14	
HORVU7Hr1G001420	Protein kinase superfamily protein		-3.1E+14	
HORVU1Hr1G061480	Undescribed protein		-3.0E+14	
HORVU2Hr1G110900	Protein kinase superfamily protein		-1.6E+14	
HORVU1Hr1G070890	Undescribed protein		-1.6E+14	
HORVU7Hr1G003460	Glucan synthase-like 8		-1.4E+14	
HORVU2Hr1G041250	Chromosome 3B, genomic scaffold, cultivar Chinese Spring		5.9E+13	
HORVU2Hr1G097030	Serine/threonine dehydratase		2.6E+14	
HORVU0Hr1G040120	Undescribed protein			-6.2E+14
HORVU3Hr1G033230	Centromere-associated protein E, putative isoform 1			-8.0E+06
HORVU3Hr1G030390	Flavin-containing monooxygenase family protein			-7.5E+06
HORVU1Hr1G068790	ADP-ribosylation factor 1			-6.0E+06
HORVU1Hr1G068640	60S ribosomal protein L30			-4.5E+06
HORVU1Hr1G063240	Unknown function			-4.5E+06
HORVU2Hr1G003640	Cysteine-rich receptor-like protein kinase 41			-4.2E+06
HORVU5Hr1G115360	RING/FYVE/PHD zinc finger superfamily protein			-4.1E+06
HORVU7Hr1G085720	Undescribed protein			-3.8E+06
HORVU7Hr1G045290	aluminium-activated malate transporter 9			-3.5E+06
HORVU5Hr1G086610	LysM domain-containing GPI-anchored protein 2			-3.2E+06
HORVU7Hr1G049930	Undescribed protein			-3.0E+06
HORVU2Hr1G106920	Disease resistance protein (CC-NBS-LRR class) family			-2.9E+06
HORVU4Hr1G023830	FRAGILE HISTIDINE TRIAD			-2.0E+06
HORVU5Hr1G054240	Zinc finger (C3HC4-type RING finger) family protein			-1.9E+06
HORVU2Hr1G115640	Beta-D-xylosidase 4			-1.9E+06
HORVU7Hr1G054380	Glutamate-1-semialdehyde-2,1-aminomutase			-1.4E+06
HORVU7Hr1G037420	U-box domain-containing protein 4			-1.4E+06
HORVU2Hr1G106080	WEB family protein At5g16730, chloroplastic			-1.3E+06
HORVU3Hr1G056550	Auxilin-like protein 1			-1.3E+06
HORVU5Hr1G098170	BTB/POZ domain-containing protein			-1.1E+06
HORVU6Hr1G064150	Protein kinase superfamily protein			-1.0E+06
HORVU5Hr1G086780	NAC transcription factor			-3.3E+05
HORVU2Hr1G017650	Receptor-like kinase 902			-1.7E+04
HORVU2Hr1G038480	Time for coffee			8.4E-01
HORVU5Hr1G095570	Chaperone DnaJ-domain superfamily protein			8.9E-01
HORVU1Hr1G052770	Protein phosphatase 2C family protein			9.3E-01
HORVU3Hr1G091350	TRICHOME BIREFRINGENCE-LIKE 7			1.0E+05
HORVU6Hr1G008870	Pentatricopeptide repeat-containing protein			1.0E+06
HORVU6Hr1G083900	E3 ubiquitin-protein ligase BRE1A			1.0E+06
HORVU7Hr1G013600	Transketolase			1.1E+06
HORVU2Hr1G087970	Isocitrate dehydrogenase [NADP]			1.1E+06
HORVU4Hr1G050660	Protein kinase superfamily protein			1.2E+06
HORVU4Hr1G072520	High-affinity nickel-transport family protein			1.2E+06
HORVU1Hr1G078160	P-loop containing nucleoside triphosphate hydrolases superfamily protein			1.2E+06
HORVU7Hr1G007930	Coffea canephora DH200=94 genomic scaffold, scaffold_15			1.3E+06
HORVU6Hr1G020880	Unknown function			1.4E+06
HORVU5Hr1G053370	Ras-related protein Rab-25			1.4E+06
HORVU4Hr1G083210	Anthranilate phosphoribosyltransferase			1.4E+06
HORVU2Hr1G077940	Sequence-specific DNA binding transcription factors			1.5E+06
HORVU7Hr1G031720	Protein kinase superfamily protein			1.5E+06
HORVU3Hr1G088130	PRA1 (Prenylated rab acceptor) family protein			1.9E+06
HORVU6Hr1G077150	Unknown function			2.1E+06
HORVU3Hr1G106370	Aspartic proteinase A1			2.4E+06
HORVU7Hr1G114000	Aldehyde oxidase 2			2.6E+06
HORVU5Hr1G114400	DNA-directed RNA polymerase II subunit 1			2.9E+06
HORVU5Hr1G122060	Basic blue protein			3.1E+06
HORVU3Hr1G117440	23 kDa jasmonate-induced protein			3.1E+06
HORVU5Hr1G063940	Undescribed protein			5.3E+06
HORVU2Hr1G005170	Heat shock protein 90.1			8.4E+06
HORVU0Hr1G025890	GPN-loop GTPase 1			3.4E+14
HORVU0Hr1G006050	Receptor-like protein kinase 4			4.2E+14
HORVU0Hr1G009440	Germin-like protein 2			5.7E+14
HORVU0Hr1G009450	Germin-like protein 2			6.0E+14

[a]Positive values indicate higher expression in the inoculated Sloop VIC plants. Negative values indicate higher expression in the inoculated Sloop plants.

Appendix 15. Genes with significant (p <0.05) differential expression for each time period comparison

List of differentially expressed genes that were differentially expressed between inoculated plants of resistant (Sloop SA or Sloop VIC) cultivars and inoculated plants of the susceptible cultivar Sloop at (a) early (combination of 4 and 8 days after inoculation (DAI), Table A15-1), (b) middle (combination of 12 and 16 DAI, Table A15-2) and (c) late (combination of 20 and 24 DAI, Table A15-3) sampling periods. The numbers represent the $\log_2$ fold change for each individual comparison for the respective genes. The values are in each time period ranked from low to high and shaded from blue (low value) to white to red (high value). The gene list includes the gene code with the respective gene annotation.

Table A15-1: Early time period

Gene code	Annotation	$\log_2$ fold change[a] Sloop SA versus Sloop	Sloop VIC versus Sloop
HORVU4Hr1G001830	Undescribed protein	-9.93E+14	-9.79E+14
HORVU3Hr1G009340	ENTH/ANTH/VHS superfamily protein	-7.53E+14	-7.40E+14
HORVU7Hr1G051900	Unknown function	-9.61E+14	-4.52E+14
HORVU7Hr1G117800	BURP domain-containing protein 11	-3.76E+14	-4.45E+14
HORVU6Hr1G047560	Calcium-dependent lipid-binding family protein	-1.73E+14	-1.82E+14
HORVU6Hr1G087410	Plant regulator RWP-RK family protein	5.64E+14	5.76E+14
HORVU6Hr1G084540	Undescribed protein	-9.92E+14	
HORVU7Hr1G058630	Protein arginine methyltransferase 10	-9.89E+14	
HORVU7Hr1G059690	Undescribed protein	-9.79E+14	
HORVU7Hr1G066170	Galactose mutarotase-like superfamily protein	-9.70E+14	
HORVU6Hr1G084930	Disease resistance protein	-9.62E+14	
HORVU3Hr1G073930	Undescribed protein	-9.54E+14	
HORVU6Hr1G082220	Undescribed protein	-8.61E+14	
HORVU7Hr1G084640	Phosphoethanolamine N-methyltransferase 1	-8.54E+14	
HORVU1Hr1G049000	Subtilisin-like protease	-8.36E+14	
HORVU7Hr1G072620	Receptor-like protein kinase 4	-8.24E+14	
HORVU7Hr1G050920	Undescribed protein	-8.20E+14	
HORVU7Hr1G067200	Undescribed protein	-7.91E+14	
HORVU7Hr1G066450	Isopropylmalate dehydrogenase 1	-7.76E+14	
HORVU7Hr1G084170	Unknown protein	-7.53E+14	
HORVU5Hr1G089790	Receptor kinase 3	-7.31E+14	
HORVU6Hr1G082240	Transcriptional corepressor LEUNIG	-7.30E+14	
HORVU6Hr1G082230	F-box/RNI-like superfamily protein	-7.17E+14	
HORVU3Hr1G069300	Isopropylmalate dehydrogenase 1	-6.92E+14	
HORVU7Hr1G066960	Undescribed protein	-6.74E+14	
HORVU6Hr1G085270	Unknown function	-6.66E+14	
HORVU7Hr1G029190	Histone superfamily protein	-6.61E+14	
HORVU5Hr1G090650	Undescribed protein	-6.58E+14	
HORVU7Hr1G059910	Unknown function	-6.49E+14	
HORVU5Hr1G114960	Pyruvate dehydrogenase E1 component subunit beta	-6.23E+14	
HORVU7Hr1G060480	Tubby-like F-box protein 9	-6.07E+14	
HORVU7Hr1G054890	B12D protein	-5.91E+14	
HORVU7Hr1G108530	Peroxidase superfamily protein	-5.66E+14	
HORVU5Hr1G090640	Histone deacetylase HDT1	-5.38E+14	
HORVU1Hr1G067670	Zinc finger protein 830	-5.37E+14	
HORVU5Hr1G012710	ABC1 family protein	-5.33E+14	
HORVU7Hr1G098110	Peroxidase superfamily protein	-4.95E+14	
HORVU2Hr1G018520	Peroxidase superfamily protein	-4.83E+14	
HORVU7Hr1G089300	Peroxidase superfamily protein	-4.23E+14	
HORVU5Hr1G009840	RAB GDP dissociation inhibitor 2	-4.10E+14	
HORVU3Hr1G036880	Peroxidase superfamily protein	-4.05E+14	
HORVU6Hr1G076270	Unknown function	-3.76E+14	
HORVU7Hr1G075160	ATP-dependent DNA helicase PIF1	-3.74E+14	
HORVU2Hr1G082900	Undescribed protein	-3.67E+14	
HORVU2Hr1G099720	Plant protein of unknown function (DUF247)	-3.35E+14	
HORVU1Hr1G067590	SOSS complex subunit B homolog	-3.16E+14	
HORVU2Hr1G099030	F-box family protein	-2.86E+14	
HORVU2Hr1G082910	Undescribed protein	-2.85E+14	
HORVU3Hr1G003110	Glycosyltransferase	-2.82E+14	
HORVU7Hr1G069420	Structural maintenance of omosomes 5	-2.80E+14	
HORVU7Hr1G068680	Unknown function	-2.71E+14	
HORVU7Hr1G058750	CRIB domain-containing protein RIC1	-2.30E+14	
HORVU2Hr1G121320	Cytochrome P450 superfamily protein	-2.28E+14	

Table A15-1 continued

Gene code	Annotation	Log$_2$ fold change[a] Sloop SA versus Sloop	Sloop VIC versus Sloop
HORVU7Hr1G027520	Flavin-containing monooxygenase family protein	-2.24E+14	
HORVU7Hr1G002370	Glutathione S-transferase family protein	-2.13E+14	
HORVU7Hr1G082180	Undescribed protein	-2.03E+14	
HORVU7Hr1G076680	Non-lysosomal glucosylceramidase	-1.89E+14	
HORVU6Hr1G063860	Tripeptidyl peptidase ii	-1.67E+14	
HORVU7Hr1G078170	Protein kinase superfamily protein	-1.30E+14	
HORVU7Hr1G079220	Undescribed protein	-1.12E+14	
HORVU7Hr1G064420	ENTH/ANTH/VHS superfamily protein	-1.06E+14	
HORVU7Hr1G050930	Undescribed protein	-1.01E+14	
HORVU7Hr1G066970	Cytochrome P450 superfamily protein	-9.37E+13	
HORVU7Hr1G074530	Kelch-like protein 20	-8.78E+13	
HORVU7Hr1G059430	Undescribed protein	-7.92E+13	
HORVU7Hr1G058640	Undescribed protein	-7.87E+13	
HORVU3Hr1G070850	NAD-dependent malic enzyme 2	-5.84E+12	
HORVU5Hr1G125710	Protein kinase superfamily protein	-9.33E-01	
HORVU1Hr1G050130	Mitochondrial substrate carrier family protein	-9.15E-01	
HORVU7Hr1G075590	Undescribed protein	3.29E+12	
HORVU2Hr1G079040	Unknown function	3.40E+13	
HORVU3Hr1G105930	RNA-binding protein 1	1.00E+14	
HORVU4Hr1G075720	Galactosyltransferase family protein	1.31E+14	
HORVU7Hr1G106810	Undescribed protein	1.49E+14	
HORVU7Hr1G074420	BTB-POZ and MATH domain 2	1.67E+14	
HORVU0Hr1G000650	Hexosyltransferase	2.94E+14	
HORVU6Hr1G024170	CRIB domain-containing protein RIC1	2.97E+14	
HORVU4Hr1G059470	Undescribed protein	3.31E+14	
HORVU2Hr1G072950	Tar1p	3.37E+14	
HORVU1Hr1G025060	NADH-ubiquinone oxidoreductase chain 1	3.53E+14	
HORVU6Hr1G085710	Leucine-rich receptor-like protein kinase family protein	3.64E+14	
HORVU1Hr1G083480	Mitochondrial protein, putative	3.74E+14	
HORVU2Hr1G072930	RRNA intron-encoded homing endonuclease	3.76E+14	
HORVU4Hr1G051520	Undescribed protein	3.96E+14	
HORVU2Hr1G039210	RRNA intron-encoded homing endonuclease	4.03E+14	
HORVU1Hr1G026050	Undescribed protein	4.05E+14	
HORVU5Hr1G043850	Chromosome 3B, genomic scaffold, cultivar Chinese Spring	4.05E+14	
HORVU1Hr1G026980	Auxenochlorella protothecoides strain 0710 contig1325, whole genome shotgun sequence	4.23E+14	
HORVU0Hr1G037040	Orf108a	4.27E+14	
HORVU2Hr1G039250	RRNA intron-encoded homing endonuclease	4.36E+14	
HORVU6Hr1G049260	Ribulose bisphosphate carboxylase large chain	4.37E+14	
HORVU7Hr1G020090	Cytochrome C assembly protein	4.41E+14	
HORVU2Hr1G104850	Undescribed protein	4.49E+14	
HORVU0Hr1G000940	Zinc finger protein 830	4.53E+14	
HORVU0Hr1G034160	NADH-ubiquinone oxidoreductase chain 5	4.57E+14	
HORVU2Hr1G121650	S12-like, 30S ribosomal protein S12 subfamily protein	4.67E+14	
HORVU0Hr1G019860	Hypothetical protein M:11918-12241 FORWARD	4.71E+14	
HORVU0Hr1G024560	Ribulose bisphosphate carboxylase large chain	4.74E+14	
HORVU1Hr1G039220	Undescribed protein	4.85E+14	
HORVU4Hr1G016780	Alcohol dehydrogenase 1	4.92E+14	
HORVU0Hr1G023370	Undescribed protein	4.95E+14	
HORVU1Hr1G057550	Undescribed protein	5.14E+14	
HORVU0Hr1G034780	NAD(P)H-quinone oxidoreductase subunit 2 A, chloroplastic	5.28E+14	
HORVU2Hr1G004390	Hypothetical protein M:11918-12241 FORWARD	5.41E+14	
HORVU4Hr1G025470	Senescence-associated protein	5.41E+14	
HORVU2Hr1G082520	DNA, scaffold: scf_mam1_v11112, strain NBRC 6742, whole genome shotgun sequence	5.42E+14	
HORVU7Hr1G002030	Undescribed protein	5.52E+14	
HORVU5Hr1G083980	Senescence-associated protein, putative	5.66E+14	
HORVU3Hr1G084440	Undescribed protein	5.78E+14	
HORVU5Hr1G076970	Senescence-associated protein	5.86E+14	
HORVU0Hr1G023910	Senescence-associated protein	6.00E+14	
HORVU7Hr1G088350	Oxidative stress 3.	6.09E+14	
HORVU2Hr1G053620	Senescence-associated protein, putative	7.50E+14	
HORVU1Hr1G073940	Myb-like transcription factor family protein	7.61E+14	
HORVU7Hr1G028510	Undescribed protein		-9.46E+14
HORVU2Hr1G036600	Unknown function		-9.10E+14
HORVU2Hr1G036610	Undescribed protein		-9.03E+14
HORVU3Hr1G010450	F-box protein PP2-B1		-9.00E+14
HORVU1Hr1G079280	Late embryogenesis abundant protein 76		-8.91E+14
HORVU2Hr1G066930	Unknown function		-8.58E+14
HORVU2Hr1G061010	Undescribed protein		-8.34E+14
HORVU4Hr1G088990	Undescribed protein		-8.28E+14
HORVU7Hr1G082040	Late embryogenesis abundant protein D-34		-8.02E+14
HORVU2Hr1G035130	Undescribed protein		-7.90E+14
HORVU4Hr1G090630	E3 ubiquitin-protein ligase RFWD3		-7.84E+14

Table A15-1: continued

Gene code	Annotation	Log_2 fold change[a] Sloop SA versus Sloop	Sloop VIC versus Sloop
HORVU1Hr1G089730	Iron-sulfur cluster assembly protein 1		-7.81E+14
HORVU5Hr1G092120	Dehydrin 7		-7.70E+14
HORVU2Hr1G060590	Undescribed protein		-7.67E+14
HORVU5Hr1G125450	AWPM-19-like family protein		-7.56E+14
HORVU2Hr1G062940	Alpha-glucosidase		-7.36E+14
HORVU2Hr1G070420	Undescribed protein		-7.24E+14
HORVU2Hr1G042830	Chromosome 3B, genomic scaffold, cultivar Chinese Spring		-7.23E+14
HORVU2Hr1G042990	Undescribed protein		-7.18E+14
HORVU4Hr1G008990	Late embryogenesis abundant protein		-7.15E+14
HORVU2Hr1G126940	Phosphatidylinositol-4-phosphate 5-kinase family protein		-7.07E+14
HORVU5Hr1G001750	Undescribed protein		-7.04E+14
HORVU2Hr1G064860	Undescribed protein		-6.66E+14
HORVU0Hr1G012340	Undescribed protein		-6.45E+14
HORVU6Hr1G005600	High affinity nitrate transporter 2.6		-6.41E+14
HORVU1Hr1G046570	Unknown function		-6.37E+14
HORVU5Hr1G118100	Transposable element protein, putative		-6.32E+14
HORVU0Hr1G012330	Undescribed protein		-6.23E+14
HORVU4Hr1G084260	BEST Arabidopsis thaliana protein match is: RPM1 interacting protein 13 .		-5.90E+14
HORVU3Hr1G069590	Heat stress transcription factor C-1b		-5.85E+14
HORVU3Hr1G030650	Late embryogenesis abundant protein		-5.49E+14
HORVU7Hr1G040970	Potassium channel SKOR		-5.16E+14
HORVU2Hr1G058430	Retrotransposon protein, putative, Ty3-gypsy subclass		-5.10E+14
HORVU2Hr1G072370	Unknown function		-5.09E+14
HORVU3Hr1G030770	ATPase family gene 2 protein		-4.96E+14
HORVU1Hr1G002100	Defensin-like protein		-4.93E+14
HORVU3Hr1G049780	Heavy metal transport/detoxification superfamily protein		-4.89E+14
HORVU3Hr1G077930	Nucleoredoxin		-4.85E+14
HORVU5Hr1G103460	Dehydrin Rab15		-4.68E+14
HORVU5Hr1G076730	Chromosome 3B, genomic scaffold, cultivar Chinese Spring		-4.65E+14
HORVU2Hr1G070390	Undescribed protein		-4.59E+14
HORVU2Hr1G048290	Thiol protease aleurain		-4.56E+14
HORVU0Hr1G017570	Inosine-5'-monophosphate dehydrogenase		-4.04E+14
HORVU6Hr1G070020	Chromosome 3B, genomic scaffold, cultivar Chinese Spring		-4.02E+14
HORVU2Hr1G013950	Jasmonate-induced protein, putative, expressed		-4.02E+14
HORVU6Hr1G051860	Loricrin-like protein		-3.65E+14
HORVU5Hr1G071270	F-box and associated interaction domains-containing protein		-3.49E+14
HORVU7Hr1G074520	Protein of unknown function (DUF3537)		-3.20E+14
HORVU4Hr1G090090	Heat stress transcription factor C-2a		-3.13E+14
HORVU4Hr1G051290	NAC domain protein,		-2.95E+14
HORVU4Hr1G033510	Chromosome 3B, genomic scaffold, cultivar Chinese Spring		-2.95E+14
HORVU2Hr1G073850	Digalactosyldiacylglycerol synthase 1, chloroplastic		-2.77E+14
HORVU5Hr1G031210	Undescribed protein		-2.57E+14
HORVU5Hr1G088700	Protein phosphatase 2C family protein		-1.76E+14
HORVU4Hr1G085800	Flowering promoting factor 1		-1.34E+14
HORVU7Hr1G003170	LEA		-1.07E+14
HORVU6Hr1G084010	Dehydrin 7		-1.05E+14
HORVU4Hr1G074710	Undescribed protein		-1.03E+14
HORVU2Hr1G073700	Unknown function		-1.01E+14
HORVU2Hr1G058670	Undescribed protein		-7.81E+13
HORVU0Hr1G017490	NAC domain protein,		-5.41E+13
HORVU4Hr1G090850	Heat stress transcription factor C-2a		-5.00E+12
HORVU2Hr1G039650	Pol polyprotein		3.71E+13
HORVU2Hr1G043550	Retrotransposon protein, putative, Ty1-copia subclass		6.17E+13
HORVU2Hr1G096410	CsAtPR5, putative, expressed		1.73E+14
HORVU2Hr1G031400	SPX domain gene 3		2.40E+14
HORVU2Hr1G044460	Glucan endo-1,3-beta-glucosidase 13		3.72E+14
HORVU2Hr1G097040	Mitochondrial transcription termination factor family protein		4.44E+14
HORVU4Hr1G085330	Unknown function		6.37E+14
HORVU4Hr1G050060	PATATIN-like protein 4		6.89E+14
HORVU4Hr1G081330	Boron transporter 4		7.12E+14
HORVU2Hr1G096400	CsAtPR5, putative, expressed		8.46E+14

[a]Positive values indicate higher expression in the inoculated resistant plants. Negative values indicate higher expression in the inoculated susceptible plants.

Table A15-2: Middle time period

Gene code	Annotation	Log_2 fold change[a] Sloop SA versus Sloop	Sloop VIC versus Sloop
HORVU7Hr1G051900	Unknown function	-8.88E+14	-9.01E+14
HORVU3Hr1G009340	ENTH/ANTH/VHS superfamily protein	-8.87E+14	-9.00E+14
HORVU0Hr1G017400	Haloacid dehalogenase-like hydrolase (HAD) superfamily protein	-3.44E+14	-3.36E+14
HORVU2Hr1G110900	Protein kinase superfamily protein	-1.53E+14	-1.57E+14
HORVU4Hr1G001830	Undescribed protein	-8.68E+14	-8.81E+13
HORVU6Hr1G087410	Plant regulator RWP-RK family protein	5.80E+14	6.38E+14
HORVU7Hr1G058750	CRIB domain-containing protein RIC1	-9.77E+14	
HORVU7Hr1G066970	Cytochrome P450 superfamily protein	-9.18E+14	
HORVU7Hr1G050930	Undescribed protein	-9.12E+14	
HORVU7Hr1G079220	Undescribed protein	-9.04E+14	
HORVU3Hr1G073930	Undescribed protein	-8.95E+14	
HORVU7Hr1G050920	Undescribed protein	-8.83E+14	
HORVU7Hr1G064420	ENTH/ANTH/VHS superfamily protein	-8.77E+14	
HORVU6Hr1G024220	Cytochrome P450 likeTBP	-8.56E+14	
HORVU5Hr1G083980	Senescence-associated protein, putative	-8.54E+14	
HORVU6Hr1G084540	Undescribed protein	-8.47E+14	
HORVU5Hr1G012990	Protein TAR1	-8.19E+14	
HORVU7Hr1G072620	Receptor-like protein kinase 4	-8.14E+14	
HORVU7Hr1G066960	Undescribed protein	-8.12E+14	
HORVU7Hr1G067200	Undescribed protein	-8.00E+14	
HORVU6Hr1G082220	Undescribed protein	-7.88E+14	
HORVU1Hr1G049000	Subtilisin-like protease	-7.80E+14	
HORVU7Hr1G058630	Protein arginine methyltransferase 10	-7.75E+14	
HORVU6Hr1G053140	Senescence-associated protein, putative	-7.74E+14	
HORVU3Hr1G069300	Isopropylmalate dehydrogenase 1	-7.69E+14	
HORVU6Hr1G084870	Disease resistance protein RPP13	-7.60E+14	
HORVU0Hr1G033370	Protein TAR1	-7.25E+14	
HORVU7Hr1G084640	Phosphoethanolamine N-methyltransferase 1	-7.24E+14	
HORVU3Hr1G084440	Undescribed protein	-7.20E+14	
HORVU5Hr1G058690	RRNA intron-encoded homing endonuclease	-6.98E+14	
HORVU2Hr1G053620	Senescence-associated protein, putative	-6.93E+14	
HORVU6Hr1G084930	Disease resistance protein	-6.83E+14	
HORVU7Hr1G002120	Undescribed protein	-6.46E+14	
HORVU7Hr1G084170	Unknown protein	-6.40E+14	
HORVU6Hr1G082230	F-box/RNI-like superfamily protein	-6.26E+14	
HORVU7Hr1G001980	Undescribed protein	-6.19E+14	
HORVU6Hr1G085270	Unknown function	-6.19E+14	
HORVU5Hr1G012710	ABC1 family protein	-6.03E+14	
HORVU7Hr1G054890	B12D protein	-6.00E+14	
HORVU7Hr1G093830	B12D protein	-5.85E+14	
HORVU2Hr1G053630	RRNA intron-encoded homing endonuclease	-5.63E+14	
HORVU7Hr1G075160	ATP-dependent DNA helicase PIF1	-5.54E+14	
HORVU7Hr1G053600	RRNA intron-encoded homing endonuclease	-5.46E+14	
HORVU6Hr1G024130	Undescribed protein	-5.44E+14	
HORVU5Hr1G024430	Undescribed protein	-5.02E+14	
HORVU3Hr1G082320	Undescribed protein	-4.98E+14	
HORVU0Hr1G011110	Senescence-associated protein	-4.95E+14	
HORVU5Hr1G076970	Senescence-associated protein	-4.86E+14	
HORVU2Hr1G072960	Senescence-associated protein	-4.80E+14	
HORVU1Hr1G067670	Zinc finger protein 830	-4.72E+14	
HORVU5Hr1G024420	Senescence-associated protein, putative	-4.56E+14	
HORVU2Hr1G039250	RRNA intron-encoded homing endonuclease	-4.51E+14	
HORVU5Hr1G073230	Undescribed protein	-4.50E+14	
HORVU3Hr1G056130	Senescence-associated protein	-4.46E+14	
HORVU0Hr1G011140	Macaca fascicularis brain cDNA clone: QflA-19312, similar to human similar to rRNA intron-encoded homing Endonuclease(LOC391446), mRNA, RefSeq: XM_372959.1	-4.44E+14	
HORVU6Hr1G076410	RRNA intron-encoded homing endonuclease	-4.36E+14	
HORVU1Hr1G050020	Senescence-associated protein, putative	-4.35E+14	
HORVU5Hr1G043850	Chromosome 3B, genomic scaffold, cultivar Chinese Spring	-3.99E+14	
HORVU7Hr1G097520	26S proteasome non-ATPase regulatory subunit 2 homolog B	-3.77E+14	
HORVU1Hr1G067590	SOSS complex subunit B homolog	-3.07E+14	
HORVU0Hr1G019870	Hypothetical protein M:11918-12241 FORWARD	-3.03E+14	
HORVU7Hr1G069420	Structural maintenance of chromosomes 5	-3.02E+14	
HORVU7Hr1G094810	Undescribed protein	-2.42E+14	
HORVU7Hr1G082180	Undescribed protein	-2.30E+14	
HORVU7Hr1G082200	Leucine-rich receptor-like protein kinase family protein	-2.04E+14	
HORVU7Hr1G074530	Kelch-like protein 20	-1.19E+14	
HORVU7Hr1G059690	Undescribed protein	-1.17E+14	
HORVU5Hr1G074880	RRNA intron-encoded homing endonuclease	-1.04E+14	
HORVU7Hr1G066450	Isopropylmalate dehydrogenase 1	-9.62E+13	
HORVU7Hr1G053620	Undescribed protein	-9.06E+13	
HORVU7Hr1G066170	Galactose mutarotase-like superfamily protein	-8.36E+13	

Table A15-2 continued

Gene code	Annotation	Log_2 fold change[a] Sloop SA versus Sloop	Sloop VIC versus Sloop
HORVU7Hr1G059430	Undescribed protein	-7.85E+13	
HORVU5Hr1G114960	Pyruvate dehydrogenase E1 component subunit beta	-7.54E+13	
HORVU7Hr1G058640	Undescribed protein	-7.49E+13	
HORVU2Hr1G072910	Undescribed protein	-6.03E+13	
HORVU2Hr1G121320	Cytochrome P450 superfamily protein	-5.89E+13	
HORVU5Hr1G083970	Unplaced genomic scaffold PLICRscaffold_102, whole genome shotgun sequence	-5.18E+13	
HORVU7Hr1G060480	Tubby-like F-box protein 9	-3.84E+13	
HORVU7Hr1G084730	Undescribed protein	-1.66E+13	
HORVU7Hr1G002030	Undescribed protein	-5.75E+12	
HORVU6Hr1G083540	Ubiquitin carboxyl-terminal hydrolase 2	2.58E+14	
HORVU0Hr1G000650	Hexosyltransferase	2.59E+14	
HORVU7Hr1G074420	BTB-POZ and MATH domain 2	2.98E+14	
HORVU3Hr1G004240	Undescribed protein	3.92E+14	
HORVU1Hr1G056440	Aspartic proteinase A1	7.98E+14	
HORVU2Hr1G073700	Unknown function		-9.79E+14
HORVU2Hr1G062940	Alpha-glucosidase		-9.70E+14
HORVU2Hr1G036600	Unknown function		-9.23E+14
HORVU2Hr1G061010	Undescribed protein		-9.12E+14
HORVU3Hr1G010450	F-box protein PP2-B1		-8.57E+14
HORVU2Hr1G064860	Undescribed protein		-7.72E+14
HORVU2Hr1G070420	Undescribed protein		-7.64E+14
HORVU7Hr1G028510	Undescribed protein		-7.35E+14
HORVU2Hr1G042830	Chromosome 3B, genomic scaffold, cultivar Chinese Spring		-6.81E+14
HORVU4Hr1G084260	BEST Arabidopsis thaliana protein match is: RPM1 interacting protein 13 .		-6.34E+14
HORVU1Hr1G001190	Undescribed protein		-5.85E+14
HORVU2Hr1G072370	Unknown function		-4.50E+14
HORVU2Hr1G070390	Undescribed protein		-4.47E+14
HORVU5Hr1G065350	Serine/threonine protein kinase 1		-3.60E+14
HORVU7Hr1G001420	Protein kinase superfamily protein		-3.09E+14
HORVU1Hr1G061480	Undescribed protein		-3.01E+14
HORVU2Hr1G073850	Digalactosyldiacylglycerol synthase 1, chloroplastic		-2.24E+14
HORVU1Hr1G070890	Undescribed protein		-1.57E+14
HORVU7Hr1G003460	Glucan synthase-like 8		-1.40E+14
HORVU2Hr1G060590	Undescribed protein		-1.02E+14
HORVU6Hr1G008780	Cathepsin B-like cysteine proteinase 5		-2.10E+13
HORVU2Hr1G041250	Chromosome 3B, genomic scaffold, cultivar Chinese Spring		5.87E+13
HORVU2Hr1G096400	CsAtPR5, putative, expressed		6.85E+13
HORVU2Hr1G097030	Serine/threonine dehydratase		2.65E+14
HORVU7Hr1G117800	BURP domain-containing protein 11		3.44E+14
HORVU2Hr1G097040	Mitochondrial transcription termination factor family protein		4.23E+14
HORVU2Hr1G044460	Glucan endo-1,3-beta-glucosidase 13		4.96E+14
HORVU4Hr1G050060	PATATIN-like protein 4		5.26E+14
HORVU2Hr1G043550	Retrotransposon protein, putative, Ty1-copia subclass		6.76E+14
HORVU4Hr1G081330	Boron transporter 4		7.35E+14

[a]Positive values indicate higher expression in the inoculated resistant plants. Negative values indicate higher expression in the inoculated susceptible plants.

Table A15-3: Late time period

Gene code	Annotation	Log_2 fold change[a] Sloop SA versus Sloop	Sloop VIC versus Sloop
HORVU0Hr1G040120	Undescribed protein	-5.29E+14	-6.16E+14
HORVU0Hr1G017400	Haloacid dehalogenase-like hydrolase (HAD) superfamily protein	-3.28E+14	-4.43E+13
HORVU4Hr1G001830	Undescribed protein	-9.02E+14	-8.62E+06
HORVU3Hr1G009340	ENTH/ANTH/VHS superfamily protein	-8.52E+14	-8.12E+06
HORVU3Hr1G033230	Centromere-associated protein E, putative isoform 1	-9.30E+14	-7.97E+06
HORVU1Hr1G068790	ADP-ribosylation factor 1	-6.87E+14	-6.02E+06
HORVU1Hr1G068640	60S ribosomal protein L30	-4.47E+14	-4.53E+06
HORVU2Hr1G003640	Cysteine-rich receptor-like protein kinase 41	-4.52E+14	-4.20E+06
HORVU7Hr1G045290	Aluminium-activated malate transporter 9	-3.36E+14	-3.49E+06
HORVU7Hr1G114000	Aldehyde oxidase 2	2.46E+13	2.56E+06
HORVU7Hr1G122200	Disease resistance protein	-6.68E+14	
HORVU2Hr1G038390	Undescribed protein	-6.05E+14	
HORVU5Hr1G067530	1-aminocyclopropane-1-carboxylate oxidase 1	-4.87E+14	
HORVU7Hr1G114850	Disease resistance protein	-4.41E+14	
HORVU1Hr1G089380	Subtilisin-like protease	-3.90E+14	
HORVU7Hr1G010620	GRAS family transcription factor	-3.78E+14	
HORVU5Hr1G088400	Uveal autoantigen with coiled-coil domains and ankyrin repeats isoform 1	-3.39E+14	
HORVU7Hr1G043490	Receptor kinase 2	-3.36E+14	
HORVU5Hr1G095250	Kinesin 4	-3.33E+14	
HORVU0Hr1G007220	Undescribed protein	-3.31E+14	
HORVU4Hr1G063240	Glucan endo-1,3-beta-glucosidase 11	-3.10E+14	
HORVU3Hr1G052930	Kinesin 4	-3.08E+14	
HORVU7Hr1G025200	Histone superfamily protein	-3.03E+14	
HORVU2Hr1G026450	Peroxidase superfamily protein	-2.98E+14	
HORVU7Hr1G110110	Transposable element protein, putative	-2.97E+14	
HORVU2Hr1G048010	TPX2 (targeting protein for Xklp2) protein family	-2.94E+14	
HORVU1Hr1G051050	Chalcone-flavanone isomerase family protein	-2.90E+14	
HORVU7Hr1G049860	FASCICLIN-like arabinogalactan-protein 12	-2.85E+14	
HORVU4Hr1G068470	TPX2 (targeting protein for Xklp2) protein family	-2.74E+14	
HORVU5Hr1G109460	Histone H2A 6	-2.69E+14	
HORVU2Hr1G090210	Histone superfamily protein	-2.68E+14	
HORVU1Hr1G081770	Early nodulin-like protein 10	-2.66E+14	
HORVU7Hr1G101550	Unknown function	-2.66E+14	
HORVU6Hr1G055270	Rice-salt sensitive 1-like protein	-2.65E+14	
HORVU6Hr1G089000	Kinesin 1	-2.60E+14	
HORVU1Hr1G056530	Histone H2B.1	-2.59E+14	
HORVU7Hr1G110090	Histone H2B.1	-2.59E+14	
HORVU3Hr1G078880	Cyclin family protein	-2.55E+14	
HORVU5Hr1G009350	Kinesin 4	-2.48E+14	
HORVU6Hr1G013530	Histone superfamily protein	-2.45E+14	
HORVU1Hr1G073680	Histone superfamily protein	-2.44E+14	
HORVU1Hr1G029540	Myb-related protein 3R-1	-2.42E+14	
HORVU2Hr1G085690	Unknown protein	-2.41E+14	
HORVU5Hr1G079130	Histone superfamily protein	-2.40E+14	
HORVU1Hr1G020040	Histone superfamily protein	-2.39E+14	
HORVU5Hr1G023640	Cellulose synthase-like D5	-2.37E+14	
HORVU1Hr1G005950	Undescribed protein	-2.34E+14	
HORVU7Hr1G121820	Cyclin B2	-2.31E+14	
HORVU1Hr1G017830	Histone superfamily protein	-2.31E+14	
HORVU6Hr1G018600	Kinesin-like protein 1	-2.28E+14	
HORVU2Hr1G097990	Histone superfamily protein	-2.27E+14	
HORVU7Hr1G095920	Glycosyltransferase family 61 protein	-2.19E+14	
HORVU6Hr1G089250	DNA (cytosine-5)-methyltransferase 3	-2.17E+14	
HORVU7Hr1G100400	Histone H2A 7	-2.09E+14	
HORVU1Hr1G071190	Histone superfamily protein	-2.05E+14	
HORVU4Hr1G086500	Respiratory burst oxidase homolog B	-2.03E+14	
HORVU7Hr1G075350	Vacuolar protein sorting-associated protein	-1.93E+14	
HORVU1Hr1G035130	Histone H2A 11	-1.91E+14	
HORVU2Hr1G085570	Cytochrome b561 and DOMON domain-containing protein	-1.73E+14	
HORVU3Hr1G019140	Receptor kinase 1	-1.66E+14	
HORVU6Hr1G047560	Calcium-dependent lipid-binding family protein	-1.66E+14	
HORVU6Hr1G063860	Tripeptidyl peptidase ii	-1.65E+14	
HORVU6Hr1G077400	Unknown protein	-1.63E+14	
HORVU4Hr1G055900	Ethylene-overproduction protein 1	-1.36E+14	
HORVU7Hr1G096680	Arabinose kinase	-1.32E+14	
HORVU7Hr1G047700	Formate dehydrogenase	-1.31E+14	
HORVU3Hr1G087430	Interactor of constitutive active ROPs 2, chloroplastic	-1.12E+14	
HORVU4Hr1G077420	Receptor kinase 2	-1.05E+14	
HORVU4Hr1G083620	Unknown protein	-2.58E+13	
HORVU5Hr1G087340	High mobility group B1	-2.33E+13	
HORVU1Hr1G058500	Histone H2B.1	-2.05E+13	
HORVU4Hr1G088140	Expansin B2	-2.52E+12	

Table A15-3 continued

Gene code	Annotation	Log$_2$ fold change[a] Sloop SA versus Sloop	Sloop VIC versus Sloop
HORVU7Hr1G034470	Histone superfamily protein	-2.11E+12	
HORVU1Hr1G019590	SAD1/UNC-84 domain protein 2	6.63E-01	
HORVU4Hr1G068900	Unknown function	3.76E+13	
HORVU4Hr1G087390	Nicotianamine synthase 3	1.63E+14	
HORVU0Hr1G014030	PLC-like phosphodiesterases superfamily protein	1.67E+14	
HORVU2Hr1G087090	Adenine phosphoribosyltransferase 5	1.74E+14	
HORVU4Hr1G002130	Dehydrogenase/reductase SDR family member 11	2.01E+14	
HORVU6Hr1G092550	Undescribed protein	2.18E+14	
HORVU1Hr1G018480	Undescribed protein	2.27E+14	
HORVU2Hr1G072750	Protein TERMINAL FLOWER 1	3.38E+14	
HORVU2Hr1G124600	Undescribed protein	3.85E+14	
HORVU2Hr1G127650	Peroxidase superfamily protein	3.94E+14	
HORVU7Hr1G009580	Undescribed protein	3.96E+14	
HORVU1Hr1G037270	Chitinase 2	4.31E+14	
HORVU2Hr1G102110	Bifunctional inhibitor/lipid-transfer protein/seed storage 2S albumin superfamily protein	4.59E+14	
HORVU4Hr1G081330	Boron transporter 4	7.10E+14	
HORVU7Hr1G108160	Undescribed protein	7.93E+14	
HORVU3Hr1G030390	Flavin-containing monooxygenase family protein		-7.52E+06
HORVU1Hr1G063240	Unknown function		-4.45E+06
HORVU5Hr1G115360	RING/FYVE/PHD zinc finger superfamily protein		-4.12E+06
HORVU7Hr1G085720	Undescribed protein		-3.82E+06
HORVU5Hr1G086610	LysM domain-containing GPI-anchored protein 2		-3.20E+06
HORVU7Hr1G049930	Undescribed protein		-2.99E+06
HORVU2Hr1G106920	Disease resistance protein (CC-NBS-LRR class) family		-2.94E+06
HORVU6Hr1G008780	Cathepsin B-like cysteine proteinase 5		-2.12E+06
HORVU4Hr1G023830	FRAGILE HISTIDINE TRIAD		-1.96E+06
HORVU5Hr1G054240	Zinc finger (C3HC4-type RING finger) family protein		-1.89E+06
HORVU2Hr1G115640	Beta-D-xylosidase 4		-1.86E+06
HORVU7Hr1G054380	Glutamate-1-semialdehyde-2,1-aminomutase		-1.40E+06
HORVU7Hr1G037420	U-box domain-containing protein 4		-1.38E+06
HORVU2Hr1G106080	WEB family protein At5g16730, chloroplastic		-1.33E+06
HORVU3Hr1G056550	Auxilin-like protein 1		-1.31E+06
HORVU5Hr1G098170	BTB/POZ domain-containing protein		-1.12E+06
HORVU6Hr1G064150	Protein kinase superfamily protein		-1.02E+06
HORVU5Hr1G086780	NAC transcription factor		-3.27E+05
HORVU2Hr1G017650	Receptor-like kinase 902		-1.72E+04
HORVU2Hr1G038480	Time for coffee		8.35E-01
HORVU5Hr1G095570	Chaperone DnaJ-domain superfamily protein		8.86E-01
HORVU1Hr1G052770	Protein phosphatase 2C family protein		9.28E-01
HORVU3Hr1G091350	TRICHOME BIREFRINGENCE-LIKE 7		1.04E+05
HORVU6Hr1G008870	Pentatricopeptide repeat-containing protein		1.04E+06
HORVU6Hr1G083900	E3 ubiquitin-protein ligase BRE1A		1.04E+06
HORVU7Hr1G013600	Transketolase		1.09E+06
HORVU2Hr1G087970	Isocitrate dehydrogenase [NADP]		1.11E+06
HORVU4Hr1G050660	Protein kinase superfamily protein		1.17E+06
HORVU4Hr1G072520	High-affinity nickel-transport family protein		1.19E+06
HORVU1Hr1G078160	P-loop containing nucleoside triphosphate hydrolases superfamily protein		1.24E+06
HORVU7Hr1G007930	Coffea canephora DH200=94 genomic scaffold, scaffold_15		1.32E+06
HORVU6Hr1G020880	Unknown function		1.43E+06
HORVU5Hr1G053370	Ras-related protein Rab-25		1.43E+06
HORVU4Hr1G083210	Anthranilate phosphoribosyltransferase		1.44E+06
HORVU2Hr1G077940	Sequence-specific DNA binding transcription factors		1.47E+06
HORVU7Hr1G031720	Protein kinase superfamily protein		1.52E+06
HORVU3Hr1G088130	PRA1 (Prenylated rab acceptor) family protein		1.86E+06
HORVU6Hr1G077150	Unknown function		2.07E+06
HORVU3Hr1G106370	Aspartic proteinase A1		2.42E+06
HORVU5Hr1G114400	DNA-directed RNA polymerase II subunit 1		2.89E+06
HORVU5Hr1G122060	Basic blue protein		3.08E+06
HORVU3Hr1G117440	23 kDa jasmonate-induced protein		3.14E+06
HORVU5Hr1G063940	Undescribed protein		5.33E+06
HORVU4Hr1G050060	PATATIN-like protein 4		5.83E+06
HORVU2Hr1G005170	Heat shock protein 90.1		8.44E+06
HORVU0Hr1G025890	GPN-loop GTPase 1		3.38E+14
HORVU0Hr1G006050	Receptor-like protein kinase 4		4.16E+14
HORVU0Hr1G009440	Germin-like protein 2		5.66E+14
HORVU0Hr1G009450	Germin-like protein 2		5.96E+14

[a]Positive values indicate higher expression in the inoculated resistant plants. Negative values indicate higher expression in the inoculated susceptible plants.

Appendix 16. Absolute expression values for Figure 4-11

Means and standard errors (among three technical replicates) provided in arbitrary expression units from qPCR analysis of a barley aquaporin gene (HORVU2Hr1G097780) in samples taken from non-inoculated plants of Sloop (control) and inoculated plants of Sloop, Sloop SA and Sloop VIC between 0 and 28 days after inoculation (DAI).

DAI	Sample	Control		Sloop		Sloop SA		Sloop VIC	
		Mean	Standard error	Mean	Standard error	Mean	Standard error	Mean	Standard error
0	1	63332	3846	63332	3846	15967	260	7729	100
	2					8497	292	10351	166
	3					9981	288		
4	1	5603	547	43183	3484	4466	298	1620	187
	2					4255	313		
8	1	10117	673	1376	189	578	66	343	116
	2					387	8		
	3					1899	58		
12	1	12684	326	5492	147	1094	63	3467	58
	2					5806	227	8236	664
	3					1776	258	2121	182
16	1	3079	143	15789	857	2603	610	372	50
	2					3901	204	1183	24
20	1	3315	32	3060	239	4533	550	9	-[a]
	2					789	123	411	50
	3					245	192	175	113
24	1	3484	201	33787	372	1423	176	109	100
28	1	2369	124	2114	88	464	242	86	68
	2					1861	303		

Mean expression values derived of biological replicates (arbitrary expression units) of a barley aquaporin gene (HORVU2Hr1G07780) in samples taken from control, inoculated Sloop, Sloop SA and Sloop VIC. Standard errors among biological replicates are shown for the treatment combinations with biological replicates. These mean values are shown in Figure 4-11.

DAI	Control	Sloop	Sloop SA		Sloop VIC	
	Mean	Mean	Mean	Standard error	Mean	Standard error
0	63332	63332	11481	288	9040	1311
4	5603	43183	4361	105	1620	-
8	10117	1376	955	475	343	-
12	12684	5492	2892	1470	4608	1855
16	3079	15789	3252	649	778	405
20	3315	3060	1856	1348	198	597
24	3484	33787	1423	-[b]	109	-
28	2369	2114	1163	698	86	-

[a]Standard error was not calculated due to technical issues.
[b]Only one replicate was available.

Appendix 17. Abstract of Strock et al. (2019)

Title: Laser Ablation Tomography for Visualization of Root Colonization by Edaphic Organisms

Authors:
Christopher F. Strock[1], Hannah M. Schneider[1], Tania Galindo-Castañeda[1], Benjamin T. Hall[2], Bart Van Gansbeke[3], Diane E. Mather[3], Mitchell G. Roth[4], Martin I. Chilvers[4] , Xiangrong Guo[1], Kathleen Brown[1] and Jonathan P. Lynch[1]*

Institutional Addresses:
[1]Department of Plant Science, Pennsylvania State University, University Park, Pennsylvania 16802 USA.
[2]Lasers for Innovative Solutions, LLC, 200 Innovation Blvd. (Suite 214), State College, PA 16803 USA.
[3]School of Agriculture, Food and Wine, Waite Research Institute, The University of Adelaide, PMB 1, Glen Osmond, SA 5064, Australia.
[4]Department of Plant, Soil, and Microbial Sciences, Michigan State University, East Lansing, MI 48824 USA.

***Corresponding author**: Jonathan P. Lynch, Email: jpl4@psu.edu, Tel.: +1 814863225

Published: 13 June 2019

Abstract:
Soil biota have important effects on crop productivity, but can be difficult to study *in situ*. Laser ablation tomography (LAT) is a novel method that allows for rapid, three-dimensional quantitative and qualitative analysis of root anatomy, providing new opportunities to investigate interactions between roots and edaphic organisms. LAT was used for analysis of maize roots colonized by arbuscular mycorrhizal fungi, maize roots herbivorized by western corn rootworm, barley roots parasitized by cereal cyst nematode, and common bean roots damaged by *Fusarium*. UV excitation of root tissues affected by edaphic organisms resulted in differential autofluorescence emission, facilitating the classification of tissues and anatomical features. Samples were spatially resolved in three dimensions, enabling quantification of the volume and distribution of fungal colonization, western corn rootworm damage, nematode feeding sites, tissue compromised by *Fusarium*, and as well as root anatomical phenotypes. Owing to its capability for high-throughput sample imaging, LAT serves as an excellent tool to conduct large, quantitative screens to characterize genetic control of root anatomy and interactions with edaphic organisms. Additionally, this technology improves interpretation of root–organism interactions in relatively large, opaque root segments, providing opportunities for novel research investigating the effects of root anatomical phenes on associations with edaphic organisms.

Keywords: Cereal Cyst Nematode, *Fusarium*, Mycorrhizae, Root Anatomy, Root Phenotyping, Western Corn Rootworm